Hybrid Structural Biology Studies Reveal a Novel Mechanism by Which Influenza B NS1 Protein Suppresses Host Innate Immune Response

By

Ryan Woltz

A dissertation submitted to the:

School of Graduate Studies

Rutgers, The State University of New Jersey

In partial fulfillments of the requirements

For the degree of

Doctor of Philosophy

Graduate Program in Chemistry and Chemical Biology / Computational Biology and Molecular Biophysics

Written under the direction of

Gaetano T. Montelione

And approved by

_____

_____

_____

_____

New Brunswick, New Jersey

May 2019

Abstract of the Dissertation

Hybrid Structural Biology Studies Reveal a Novel Mechanism by Which Influenza B NS1 Protein Suppresses Host Innate Immune Response

By Ryan Woltz

Dissertation Director:

Gaetano Montelione

Influenza is a highly contagious respiratory disease, which can have severe impacts on human health. Influenza type B is traditionally known as the seasonal flu and is the main source for annually occurring influenza outbreaks. The Non-Structural protein 1 of influenza B (NS1B) is a highly conserved protein that the influenza virus produces post infection. NS1B is hypothesized to inhibit the innate immune system via interactions with the RIG-I activation pathway. NS1B has been known to bind dsRNA via its N-terminal domain (NS1B-NTD) for decades, but recently a second RNA binding site was discovered on the C-terminal domain of NS1B (NS1B-CTD). Due to the high conservation of NS1B, its ability to inhibit the innate immune system, and the recent discovery of a second RNA binding domain, this dissertation research focused on the biological function of this second RNA binding site. We discovered a surprising novel blunt-end binding orientation of the NS1B-CTD by dsRNA. We then looked at the connection between RIG-I's well-known ability to detect and bind triphosphorylated-5' hairpin RNA (3P-5'-hpRNA) with a much higher affinity than OH-5' hairpin RNA (OH-5'-hpRNA). We discovered similar binding affinity changes and characteristics with NS1B-CTD and the 3P-5'-hpRNA/OH-5'-hpRNA. When the second RNA binding site in NS1B was mutated in transgenic influenza B viruses, we observed reduction in the ability of the virus to suppress Rig-I activation, as Rig-I induced phosphorylation of IRF3 was no

longer suppressed flowing virus infection. Our results suggests that the function of the second RNA binding site in the CTD of wildtype NS1B is to outcompete RIG-I for its RNA substrates, typically 5' triphosphorylaed vRNA molecules. Based on these studies we propose that NS1B-CTD acts as a sensory domain with high specificity for vRNA molecules, which form a "panhandle dsRNA duplex structure" with a unique 3P-5' modification not found in host cells. This interaction functions to prevent activation of Rig-I, and the innate host immune response.

Acknowledgments:

We would like to acknowledge Dr. Smita Patel and Brandon Scheiwbenz for intellectual and experimental input with RNA binding. Dr. Joe Marcotrigiano for intellectual input. Patrick Nosker for MD assistance. Dr. John Tainer, Dr. Susan Tsutakawa, Dr. Greg Hura, and the SIBYLS beamline staff for expert advice and experimental assistance. Dr. Richard Gallilan and MacCHESS for onsite training and experimental time. Dr. Jesse Hopkins and the BioCAT facility for experimental assistance. Dr. Robert Krug and Dr. Chen Zhao for intellectual and experimental assistance in virology. Dr. Vikas Nanda, Dr. Eddy Arnold, and Dr. Monica Roth for expert advice. The HADDOCK and FOXS webservers. NIH NIAID for partial funding for this project. Rachel John and Viviane Liao for experimental assistance. Dr. Li Ma and Dr. Swapna Gurla for expert advice and experimental assistance.

Dedicated to Melissa McDowell

Table of Contents

List of Tables

List of Illustrations:

Chapter 1: Introduction and Background

Influenza virus

The United States Center for Disease Control (CDC) estimates that in recent years the influenza virus has caused 12,000-56,000 deaths and infected ~10% of the population annually in the U.S. (30). There has been four influenza pandemics in the last 100 years; 1918 influenza pandemic (H1N1), 1957-1958 influenza pandemic (H2N2), 1968 influenza pandemic (H3N2), 2009 influenza pandemic (H1N1) (50). The 1918 influenza pandemic is still the worst influenza pandemic in recent history with 500 million (1/3 of the population) infected and 50 million reported deaths (51). The influenza 2017-2018 season was the worst in recent years with an infection rate of ~10%. The reported number of influenza-like illnesses was above the epidemic threshold for 16 consecutive weeks, compared to 7-15 weeks over the last 5 years.

Influenza is comprised of four types: A, B, C, and D. Influenza A and B are typically responsible for the seasonal flu. Influenza A has the unique ability to infect a multitude of avian and mammalian species and even jump between species causing pandemics. Influenza B, however, can only infect humans and some primates (32). Influenza type C does cause upper respiratory disease but is not thought to contribute to epidemics and influenza type D primarily infect cattle and are thought to not infect humans (49). Our efforts focus on influenza A and B due to major societal impact.

Natural defenses have evolved and are mounted in host cells against most infections. Influenza is an RNA virus; i.e. its genetic material is RNA. RIG-I is a host protein responsible for detection of RNA viruses and activation of the innate immune system. However, this innate immune response process involves a multitude of proteins. The influenza virus can counter this pathway in many ways. A very well studied influenza

protein that has been known to prevent or suppress the activation of the innate immune system is Non-Structural protein 1 (NS1). However, the mechanism by which influenza B NS1 protein acts is not clear. While influenza A has been more heavily studied due to its association with swine and avian flu, our study is focused on the Influenza B virus due to the lack of understanding and a newly discovered novel second RNA binding site not found in influenza A (2). The discovery of this second RNA binding domain in NS1B is the foundation for this thesis.

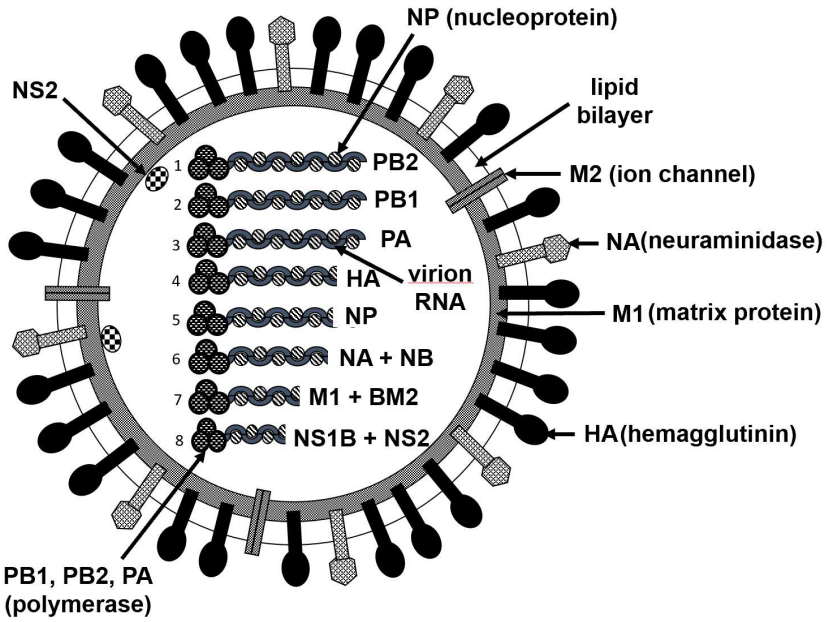

Figure 1.1: Influenza B genome schematic. Influenza B contains 8 chromosomes that encode for all of its proteins. Long S shaped lines represent RNA while small balls represent the NP protein that the virion RNA is wrapped around. The three-ball cluster at the beginning of each chromosome represents the RNA polymerase structure that is essential for virion RNA replication upon infection. This figure is meant to represent relative chromosome length and proteins associated with the virion RNA when enveloped in the virus. Theoretical chromosomal structures are shown in Figure 1.2. The influenza virus is composed of 8 chromosomes and 11 proteins packaged in a viral

particle (Figure 1.1, provided by Dr. Robert Krug). One of the proteins, which is highly conserved throughout all strains of influenza B, is the Non-Structural Protein, NS1. The conservation of this protein throughout all strains of Influenza B makes this a possible drug target that could affect multiple strains at once, and thus is a major interest in the influenza research community. It is also important to note that the first 10/11 nucleotides of the 5' and 3' ends of every gene in all strains of influenza B are conserved. These sequences are complimentary and can form a double-stranded structure, which is referred to as the "panhandle". This panhandle structure has been proposed as early as 1980 (3). In the panhandle theoretical structure (Figure 1.2), the 3' end of each segment of viral RNA (vRNA) comes back around to from a segment of base-paired dsRNA with the 5' end of the genome. This structure also includes a triphosphorylated modification on the 5' end (3P-5' dsRNA) of the stem loop structure. The origin and significance of this triphosphate modification will be explained later in the thesis (Chapter 1: Innate Immune System and RIG-I's Role in its Activation)Another piece of evidence to support the theoretical panhandle RNA structure is the 5' and 3' ends have 8/11 nucleotides base paired with each other, of the already 10/11 conserved nucleotides. If we expand this analysis to include all types of influenza (A/B/C) there are still 7/11 nucleotides that are conserved throughout all influenza types and genes in the 5' and 3' ends. In addition, 4/11 base pairs could possibly form in all genes of influenza types A/B/C (3). This highly conserved base pairing of the ends of the influenza genome must have some function for this level of preservation. It is thought that this conserved 3P-5' dsRNA stem structure is recognized by the innate immune system to identify if it cellular infection (4).

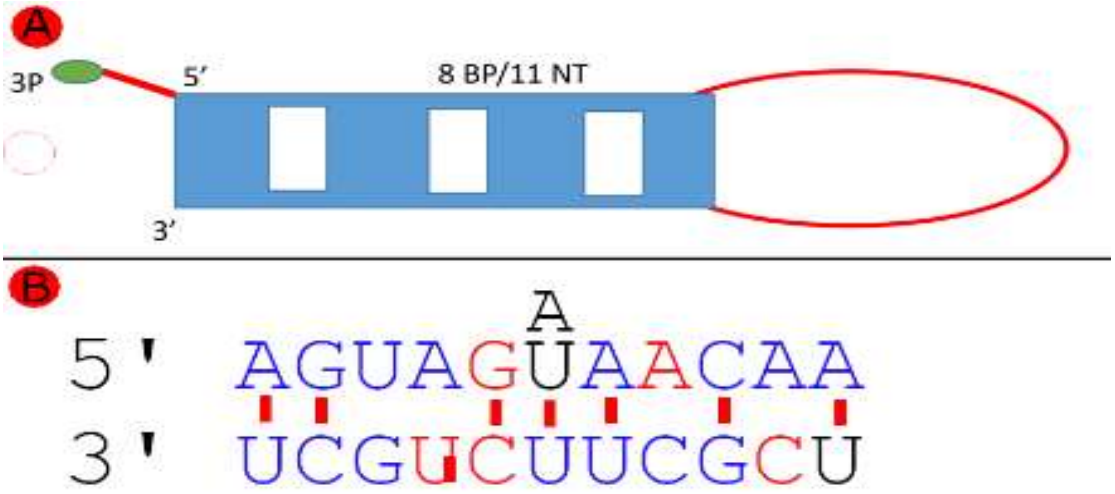

Figure 1.2: Theoretical structure of all influenza B chromosomes. A) The blue box represents the region that would be a base-paired region of the RNA with the white spaces representing mismatches nucleotides. The red loop represents the "pan" section of the chromosomal RNA which would be a large ssRNA loop with the RNA forming various stem loop structures. Inevitably, the 3' end will base pair with the 5' end forming the blunt dsRNA "handle" section of the panhandle. B) Sequence for the first 11 nucleotides on the 5' and 3' end of NS1B gene. Blue letters show conservation through all gene in influenza types A, B, and C. Red letter represent conservation in just influenza type B. Black letter represent conservation is not 100% in influenza type B. It is important to note that even with nucleotide s that are not conserved 100% it is still highly conserved with another letter, sometime up to 90% conserved. Position 6 on the 5' end is either A or U and both nucleotides are around 50% conservation.

Previous NS1B Structural and Biochemical Results:

It is well established that the N-terminal domain (NTD) of NS1B binds RNA (25,26,35). This domain is commonly known as the "RNA binding domain" of NS1. Ma LC, et al. 2016 (2), discovered the C-terminal domain (CTD) of the NS1 protein from

influenza B (NS1B), but not the corresponding C-terminal domain of the NS1 of influenza A (NS1A), also binds RNA (Figure 1.3).

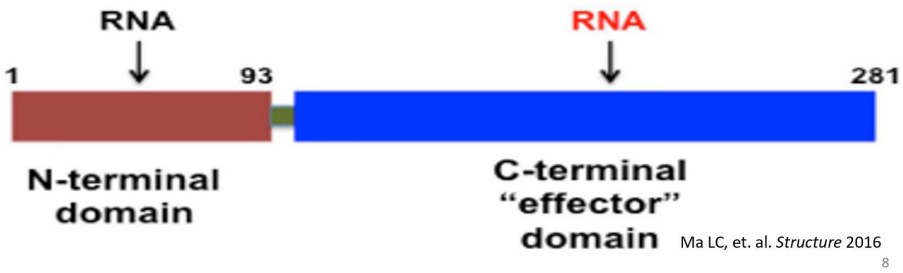

Figure 1.3: Schematic of NS1B denoting domain names and RNA binding activity. Red letters indicate the newly discovered RNA-binding activity in the NS1 protein of influenza B.

In addition, Ma et al. (2)showed that key surface basic residues present in the NS1B-CTD that bind RNA are strictly conserved throughout all strains of NS1B, but is not present in NS1A (Figure 1.4). Thus, this RNA binding function present in NS1B-CTD is specific to Influenza B and not influenza A.

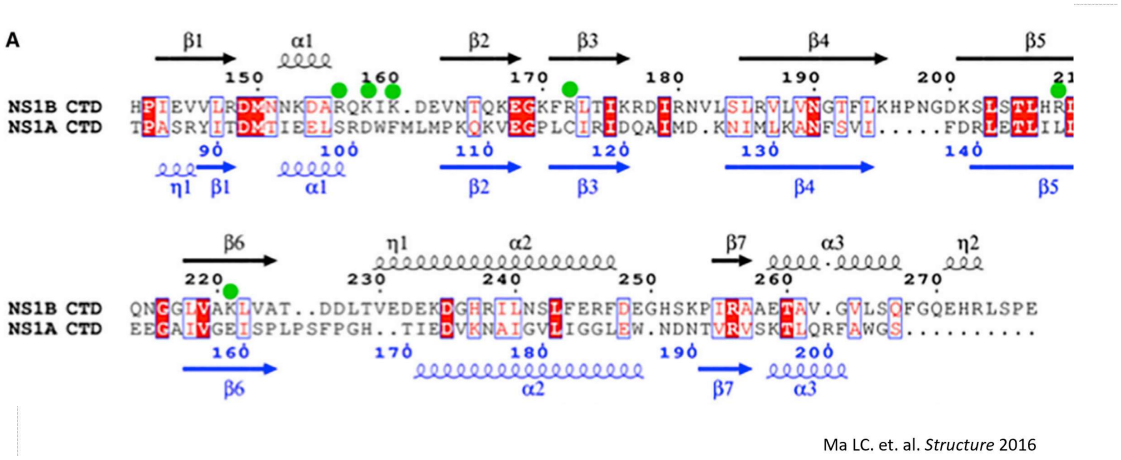

Figure 1.4: Conserved sequence alignment between NS1A and NS1B C-terminal domains. The green dots above the sequence indicate strongly basic residues that are conserved in the NS1B sequences, but are absent in NS1A.

The 1.8 Å X-ray crystal structure of NS1B-CTD (PDB: 5DIL;2) provides the following key observations; 1) the NS1B-CTD has a basic face that is typical of a nucleic acid binding protein, and 2) the protein forms a dimer in the crystal lattice (Figure 1.5A/B). This basic face, and the corresponding basic surface residues, are missing from 3D structure of the NS1A-CTD. None-the-less, the overall structures of NS1A-CTD and NS1B-CTD are very similar (Figure 1.5C), suggesting that any gain in nucleic acid binding activity is the result of the gain of the conserved basic residues. To identify amino acids essential for dsRNA binding, Ma LC. et al. (2) used NMR chemical shift perturbations (CSPs) (Figure 1.6) in the presence of duplex 16-mer dsRNA, along with dsRNA-binding assays based on fluorescent polarization (FP) (Figure 1.7) (2). The amino acid residues exhibiting backbone ^{15}N-^{1}H CSPs in the presence of dsRNA, or when mutated affect the binding affinity for dsRNA (measured by FP), cluster to one face of the protein (figure 1.5D). Another major point was that mutating the basic residue on the dimer interface R238 -> A238, which destabilizes the dimer, has little change in the protein's ability to bind dsRNA (Figure 1.7). This point will be discussed further in Chapter 2 and Chapter 6.

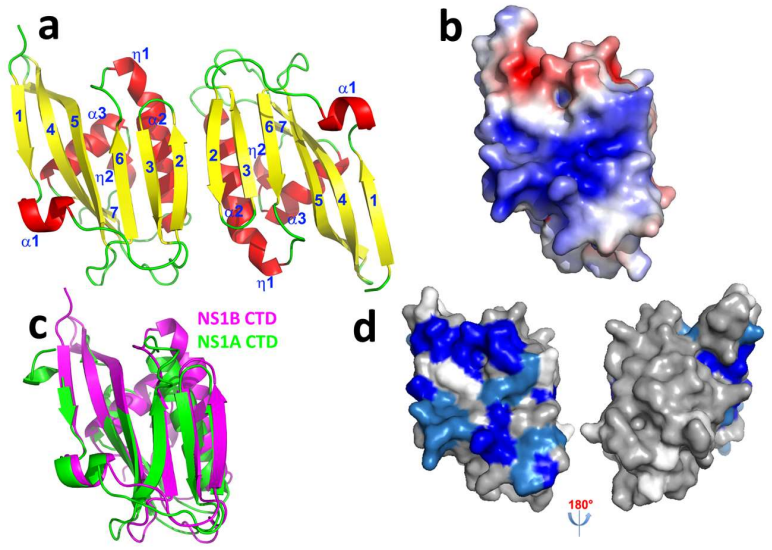

Ma LC, et. al. *Structure* 2016

Figure 1.5: Analysis of the NS1B-CTD crystal structure proposes RNA binding activity. A) NS1B-CTD crystal structure. In the crystal lattice NS1B-CTD appears to be a dimer. B) Surface of NS1B-CTD shows a basic face. The electrostatic potential of the surface is on a sliding scale of Blue -> White -> Red : Basic -> neutral -> acidic. C) Structural comparison of NS1B-CTD compared to NS1A-CTD. Purple is NS1B-CTD, Green is NS1A-CTD. D) CSPs mapped onto the surface of NS1B-CTD. Dark Blue = high CSP, light blue = medium CSP, Grey = little to no CSP, White = could not determine CSP.

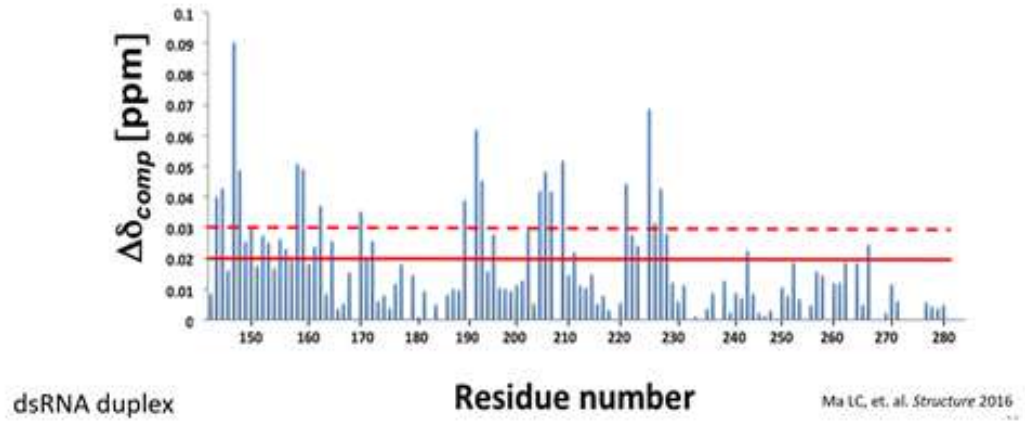

Figure 1.6: Chemical Shift Perturbations (CSPs) of NS1B-CTD with titration of dsRNA. Solid red line represents a minimum threshold for medium CSPs while the dotted red line represents minimum threshold for large CSPs.

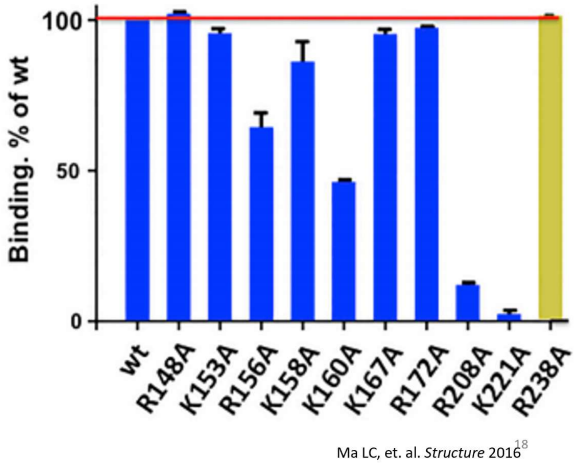

Figure 1.7: Mutation of specific conserved basic residues has a drastic change on the dsRNA binding affinity. The affinity change is measured by FP using the WT dsRNA binding as a 100% baseline. Blue bars are basic residues not involved in dimerization while the yellow bar represents a basic residue that when mutated significantly lowers the dimerization kd.

To support structure-functional analysis of NS1B-CTD bound to dsRNA, we focused on characterizing the 3D structure of the protein-RNA complex. We attempted crystallization of NS1B-CTD with a duplex 16-mer dsRNA molecule. The effort was ultimately unsuccessful, therefore we pursued structural analysis using other biophysical methods in solution. Our crystallization effort did, however, produce a crystal structure of the 16-mer dsRNA used in this study (PDB: 5KVJ, 27). This dsRNA structure was used for generating molecules of the NS1B-CTD / dsRNA complex, by combined analysis of NMR, circular dichroism (CD), and Small Angle X-ray Scattering (SAXS) data, as outline in this thesis.

Innate Immune System and RIG-I's Role in its Activation:

RIG-I is a protein involved in the activation of the innate immune response (4,14,15,48) RigI recognizes, and is activated by, viral RNA (vRNA), which has a 5'-

triphosphate modification (3P-5'). This modification is not removed after synthesis of vRNA (4) (Figure 1.8) and is present in the vRNA that produced during cellular infection, and packaged into the virion. The 3P-5' group has been called the viral Achilles heel because in human cells this triphosphorylation modification is removed (4). Thus the 3P-5' is a clear marker of infection. Upon RIG-I's recognition of the vRNA by binding to the RIG-I CTD domain, a conformational change occurs which exposes its CARD1 and CARD2 domains. These domains of RIG-I will then bind to the CARD domain in the MAVS protein located in the mitochondria (Figure 1.9). This binding, in turn, activates TBK1 and phosphorylation of IRF3. Phosphorylation of IRF3 then activates transcription of IFNα/β, which is then exported outside the cell and binds to the IFN antibody receptor (IFNAR). This binding event has a cascading effect which eventually transcribes interferons (INFs) and interferon-simulated genes (ISGs) which activate programmed cell death in defense of viral infection, (Figure 1.10). In summary RIG-I recognizes 3P-5' vRNAs and uses its ATPase function (Figure 1.11) to initiate a cascading pathway that activates the innate immune response, which can be measured when IRF3 is phosphorylated (Figure 1.10).

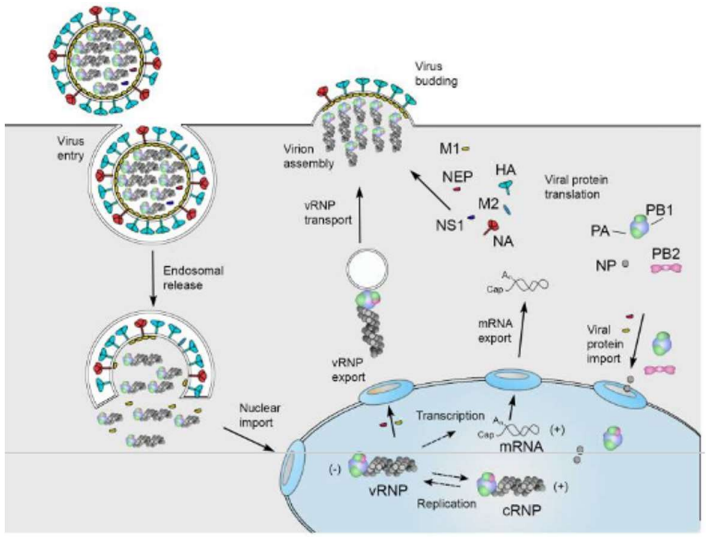

te Velthuis AJ, Fodor E. *Nature Reviews Microbiology.* 2016

Figure 1.8: Influenza life cycle gives insight to where vRNA would be found in the cell. After the virus releases its vRNA and protein complexes into the cell. These complexes travel to the nucleus and begin replication of the vRNA. vRNA is separated into two types, complementary RNA (cRNA) and vRNA that will be converted into mRNA. This conversion takes place when the 5' cap (m^7GpppNm-containing) from newly synthesized host-cell RNA Polymerase II transcripts is cleaved and used to prime vRNA synthesis. In addition, a poly(A) tail will be added to the viral mRNA, producing a 5' capped mRNA that has a poly(A) tail (5, 52).This mRNA then is exported and transcribed to make viral proteins including NS1. The viral proteins travel back to the nucleus and begin mass production of cRNA and vRNA. Viral proteins and RNA is exported to the cytoplasm where viral protein/RNA complexes are assembled, packaged into viral particles, and secreted out of the cell.

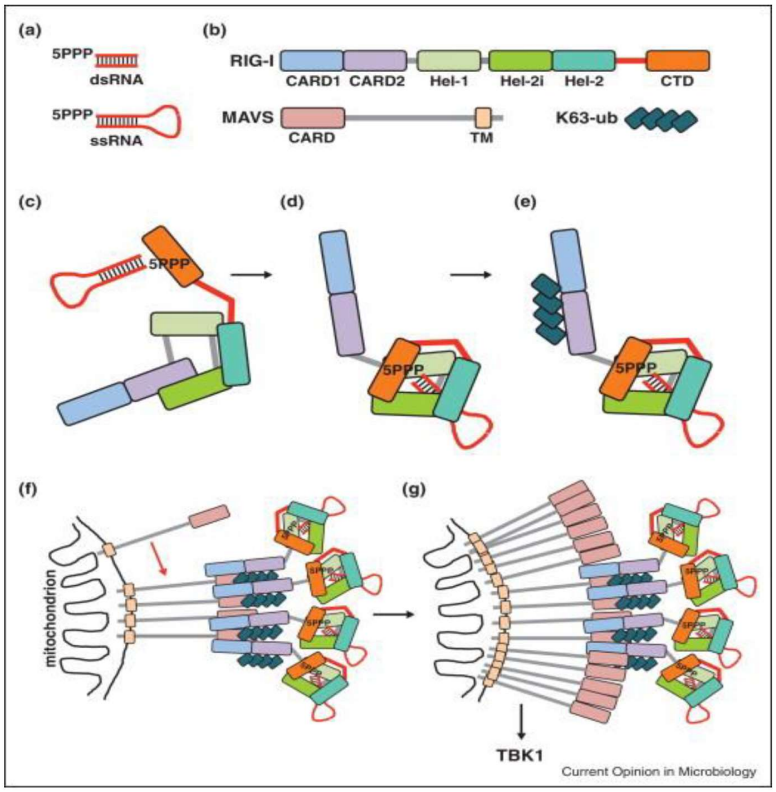

Rehwinkel J, e Sousa CR. *Current opinion in microbiology,* 2016

Figure 1.9: RIG-I's recognition of vRNA and start of the activation of the innate immune system. The CTD of RIG-I binds vRNA (3P-5' modified) which causes a conformational change in RIG-I. This change exposes the CARD1/2 domains of RIG-I which binds to the CARD domain from MAVS proteins in the mitochondria. This binding event will activate TBK1 which continues the activation of the immune system pathways seen in Figure 1.10.

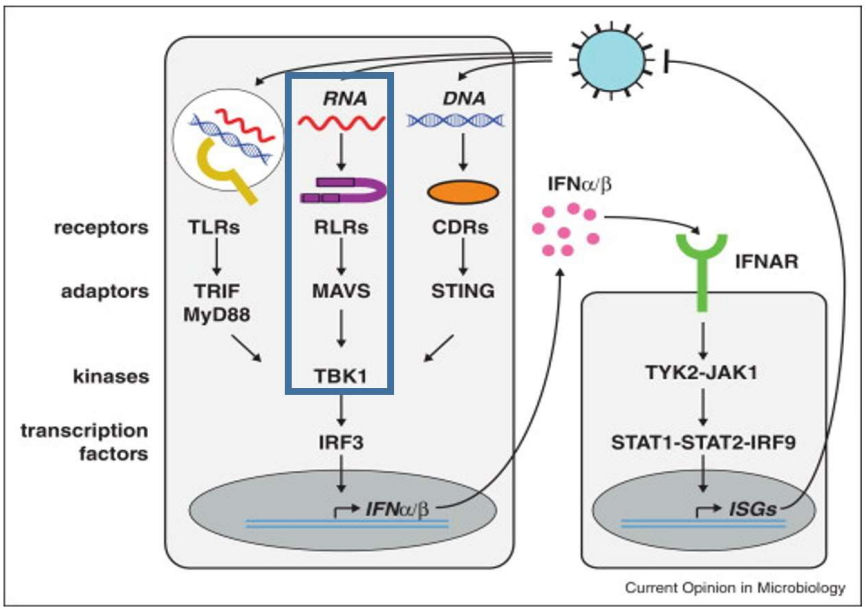

Rehwinkel J, e Sousa CR. *Current opinion in microbiology,* 2016

Figure 1.10: Host cells counter to viral infection. Blue box highlights the host cell's defense pathway against RNA viruses. RIG-I is in the RIG-I Like Receptors (RLRs) group.

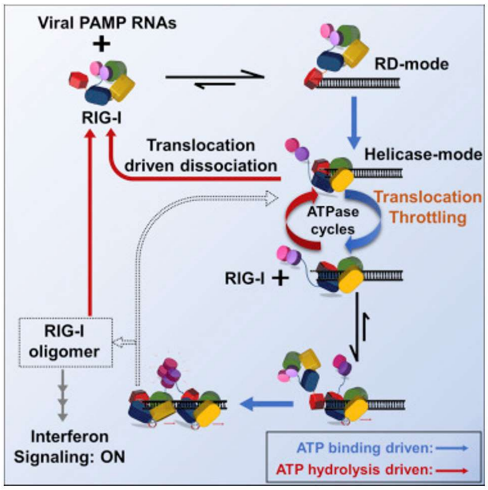

Devarkar SC et. al. *molecular cell* 2018

Figure 1.11: Diagram of RIG-I's ATPase activity. vRNA is recognized by the CTD of RIG-I which causes a conformational change in RIG-I altering it from the RD-mode (Restriction Domain like kinetic phases) to the Helicase mode. The helicase activity consumes ATP. Red arrows indicate a step in which ATP hydrolysis is required. Blue arrows indicate a step in which ATP binding is required.

Structure of RIG-I bound to 3P-5'-hpRNA:

RIG-I has a very interesting mechanism of recognizing the triphosporylated 5' blunt end of RNA (designated 3P-5'). The CTD of RIG-I binds the 3P-5' blunt end of vRNA and has several essential residues involved in the recognition of the triphosphate. In higher eukaryotes the m7G capping reaction also methylates the 2'-O of the first and second ribose, denoted as cap-1 and cap-2. No methylation is denoted as cap-0, vRNA is cap-0. One essential amino acid in RIG-I, according to structural and mutation experiments, is His830. The side chain of His830 is in close proximity with the 5'-end of 3P-5' RNA. However, if the RNA has a cap-1 modification it will clash with His830 (figure 1.12) (15). Mutational experiments show that H830A loses the ability to distinguish between cap-0 and cap-1 modification as cap-1 will no longer clash (15). Another important interaction is the pi-bond stacking between Phe853 and the aromatic rings in

the Gua base group. Additionally, there are several basic residue side chains clustered around the triphosphate. Interestingly there is an acidic Asp872 side chain that is interacting with the side chain of Lys861 and could also be interacting with the slightly charged $P^{\delta+}$ ($^{\delta}$ means partial charge)in the triphosphate group. However, the sidechain carboxylate O^- from Asp872 will also be repulsed by the O^- of the triphosphate due to proximity, so the attraction between O^- of Asp872 and the phosphorus of the triphosphate could be counteracted (PDB: 5F9H)15).

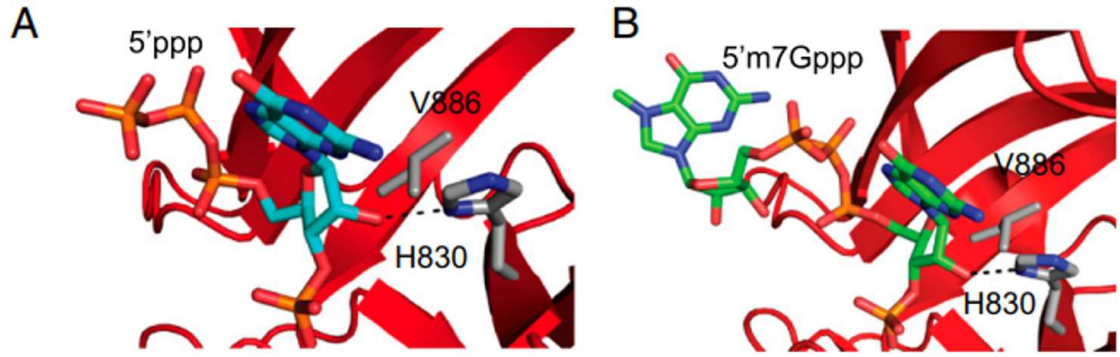

Devarkar SC. et. al. *PNAS* (2016)

Figure 1.12: RNA binds tightly into a cavity of RIG-I with His830 at the center. 3P-5' (5'PPP) (A) and 3P-5'-m7G (5'm7Gppp) (B) modified RNA do not clash with His830.

Differences Between NS1A and NS1B in Inhibiting the RIG-I and Immune System Activation:

It is important to not similarities between NS1A and NS1B. It is known that both NS1B-NTD and NS1A-NTD bind dsRNA along the phosphate backbone of A-form RNA. In addition the secondary structure of NS1A and NS1B NTDs and CTDs are very similar (2. 25, 26). Despite these similarities, NS1A is thought to inhibit the innate immune system through specific mechanisms, whereas NS1B's mechanism(s) are not the same. In fact, very little is known about the mechanisms by which NS1B of inhibits the innate immune system. However, due to the amount of research on Influenza A, the mechanism by which NS1A prevents the activation of

the immune system is better understood (32-38). With the exception of a few strains, NS1A can either inhibit the phosphorylation of IRF3 (this process is not well understood) or bind to the 30k domain of CPSF and prevent the 3'-end processing of IFN pre-mRNA (34) (Figure 1.13, Figure 1.10). Another mechanism which is being currently researched is NS1A interaction with TRIM25 via RNA binding. TRIM25 is essential for the ubiquitin of RIG-I. NS1A is proposed to stop this transfer by binding to TRIM25 with the assistance of RNA. Essentially NS1A does inhibit the immune system but requires protein interaction with a host protein. These results suggest that the NS1A prevention of immune system activation is a protein binding function and restricted to RNA binding. Structures for NS1A-RBD (37), NS1A-ED (2), NS1A-Full Length (38), NS1B-NTD (36), and NS1B-CTD (2) exist and give us insight into the mechanism of inhibition for each Influenza type. While NS1A inhibition can be traced to blocking two steps downstream of RIG-I, NS1B has been proposed to inhibit phosphorylation of IRF3 but does not inhibit RIG-I directly (2). This conclusion was supported because the inhibition appears to be contained in the NS1B-CTD, but not related to the RNA binding activity of NS1B (Figure 1.14) (2). This is clearly seen in Figure 1.14 by comparing the WT, full-length NS1B, panel with the 1-104aa, NS1B-NTD only, panel. It is important at this point to note that K208A, which reduced RNA binding by ~50-fold in the FP experiment, mutation does not fully inhibit this phosphorylation and these experiments were performed with a multiplicity of Infection (M.O.I.) of 5 (2). Since RIG-I is activated by vRNA, it was believed that there is no competition for RNA between the two proteins. Other experiments in literature perform experiments with a M.O.I. of 1 (35) so it is possible that the amount of virus was too high for the cell to counter, and the loss of affinity from the mutations were not strong enough at the experimental M.O.I.

NS1A and NS1B also have one more important difference: they are located differently in the cell and the location changes with time after infection. One reason could be the differences

in the Nuclear Localization Signal (NLS) and Nuclear Export Signal (NES) present in NS1A and NS1B. NS1A contains 2 NLS, one in NS1A-NTD and another in the very C-Terminal tail of NS1A. NS1A also contains NES in the NS1A-CTD. NS1B on the other hand contains an NLS in the NS1B-NTD and a NES in the NS1B-CTD (figure 1.15A) (35). The effect of these signals in the molecular mechanism of action of these two viruses is unknown, but the localization of NS1A and NS1B is very different. First NS1A is present in the nucleus and the cytoplasm during both early and late stages of infection. NS1B, however, is located in the nucleus in a bead formation whereas in late infection NS1B is located in the cytoplasm (35) (Figure 1.15B). This could be because NS1B is binding and being co-transported with some specific macromolecule, whereas, NS1A is not specific to any single macromolecule (35).

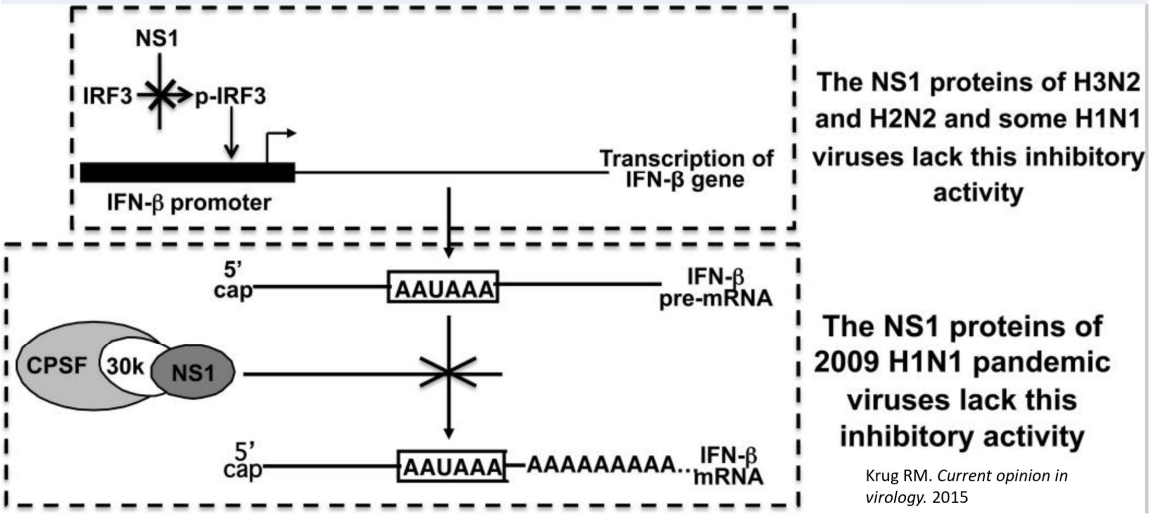

Figure 1.13: With the exception of a few strains, NS1A protein can inhibit the production of IFN-β at multiple steps. NS1A can either prevent the phosphorylation of IRF3 (research being conducted now), or by binding of CPSF-30k domain thus preventing the 3'-end processing, including splicing and polyadenylation, of IFN-β pre-mRNA.

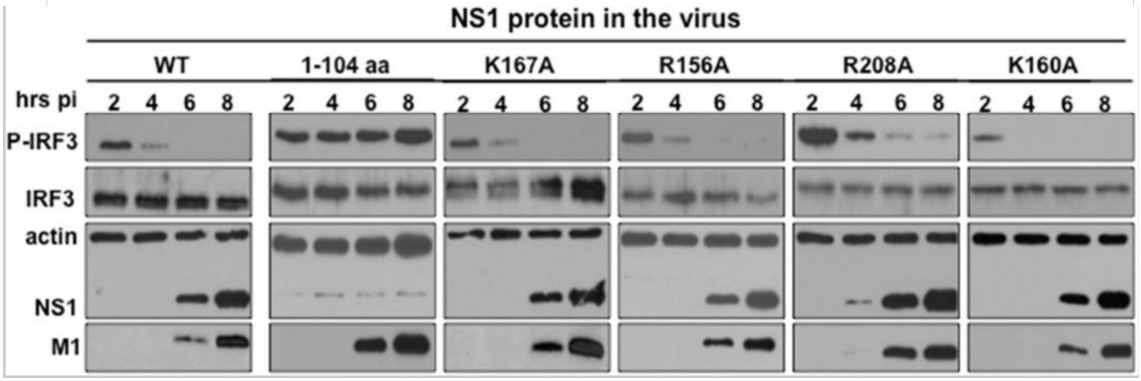

Ma LC. *Structure.* 2016

Figure 1.14: Viral infection of WT and Mutated NS1B shows the NS1B-CTD is essential for prevention of phosphorylation of IRF3. These viruses with point mutations in the RNA binding site of NS1B still resembles WT inhibition activity.

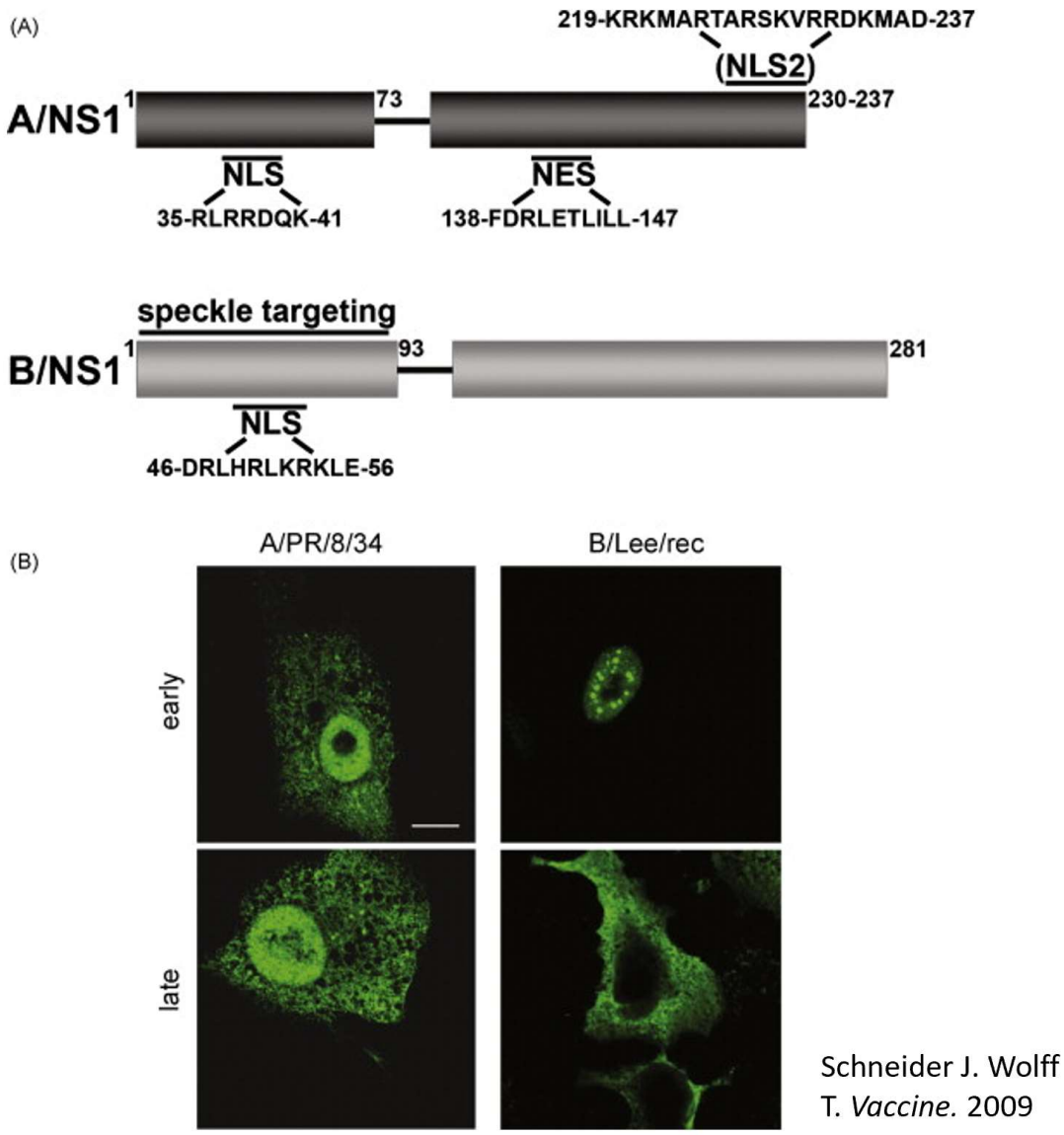

Schneider J. Wolff T. *Vaccine.* 2009

Figure 1.15: NS1A and NS1B localize in the cell differentially. A) NS1A and NS1B localization signals NS1A contains two Nuclear Localization Signals (NLS), one in the NTD and one in the CTD, and 1 Nuclear Export Signal (NES) in the CTD. NS1B only contains 1 NLS in the NTD and 1 NES in the CTD. B) Cellular localization of NS1A at 4 hrs and 16 hrs post viral infection. NS1B cellular localization of NS1B at 8 hrs and 16 hrs post viral infection. Viral infections were performed at a M.O.I. of 1.

Summary of Background Information

1. Influenza A and B inhibit the activation of the immune system
2. Detailed mechanisms for inhibition of the immune system are known for NS1A but very little is known about NS1B.
3. NS1A inhibits the immune system by binding host cell proteins
4. NS1A and NS1B both have an RNA binding domain in their N-terminal dimerization domains (NTD), which binds the polyphosphate backbone of dsRNA
5. NS1B contains a second RNA binding function in its C-terminal domain (CTD), that is not present in NS1A
6. NS1B's second binding domain seems to be important due to high conservation
7. NS1B-CTD is essential for prevention of the activation of the immune system
8. NS1B-CTD's ability to bind RNA does not play a role in the prevention of activating the immune system.
9. RIG-I is activated and starts a cascading pathway resulting in the activation of the immune system
10. RIG-I's activation begins with the binding of vRNA
11. NS1A is located in the nucleus and cytoplasm in early and late stages of infection
12. NS1B is located in the nucleus in early stages of infection and the cytoplasm in late stages of infection.

Hypothesis:

The RNA-binding activity of the C-terminal domain of NS1 from influenza B functions to suppress RNA-induced activation of RIG-I. We set out to obtain the structure of the NS1B-CTD:dsRNA complex, to gain insight into NS1B-CTD's RNA binding function.

Contribution of Thesis:

In this thesis we use hybrid structural techniques, including CD, NMR, SAXS, and molecular modeling, to discover that NS1B-CTD binds dsRNA in blunt-end fashion. This ultimately led us to revisit the theory that NS1B-CTD competes with RIG-I for RNA substrates due to the similarities between RIG-I:RNA complex structures and the NS1B-CTD:dsRNA complex structure. One such major substrate is triphosphorylation modification of a 5' hairpin RNA (3P-5'-hpRNA). We tested this substrate and found that NS1B and RIG-I have similar binding affinities for 3P-5'-hpRNA. RIG-I has a 10-fold affinity change between triphosphorylated and non-triphosphorylated RNA. We found that NS1B has similar differences in affinity between triphosphorylated and non-triphosphorylated RNA. We narrowed the sensitivity of the triphosphate to NS1B-CTD by determining that NS1B-FL and NS1B-CTD have much stronger binding affinities if the substrate RNA has a 5' triphosphate modification, while NS1B-NTD does not.

We then combined CD, NMR, SAXS, and molecular modeling to obtain an RNA blunt-end binding structure of a NS1B-CTD:3P-5'-hpRNA. Using this structure, we produced a theory of function for NS1B and its role in Influenza type B inhibiting innate immune response. We theorized that NS1B would prevent ATPase activity in RIG-I by binding all of the vRNA. We tested this in two ways, first with viral infected cells but with an M.O.I. of 2. This is a lower M.O.I. than was used in Ma LC. et al. and we saw very different results. In Ma et al. (2), using a M.O.I. of 5 it was observed that mutating the RNA binding site in NS1B-CTD had no effect on preventing phosphorylation of IRF3, however, if NS1B-CTD is deleted there is no inhibition of the phosphorylation of IRF3. At the lower M.O.I. of 2 we observed that by mutating the RNA binding site in NS1B-CTD the virus indeed loses the ability to prevent phosphorylation of IRF3. We measured ATPase activity to confirm that the decrease in p-IRF3 is due to the inactivation of RIG-I,

because NS1B competes for RNA substrates. By titrating in NS1B, we found that RIG-I's ATPase activity is significantly decreased.

The hybrid 3D structure model of NS1B bound to the 3P-5'-hpRNA that we developed led to our discovery of a function for NS1B-CTD. The protein acts as a sensory domain and competes for vRNA, thereby preventing the activation of RIG-I and the innate immune system.

Chapter 2: Protein and RNA Sample Production

Introduction:

Structural biology requires a level of care and meticulous sample preparation not needed in other fields. Small changes in salts or contamination can make changes in the environment that are below the minimal detectable threshold for many biochemical experiments. One will always try to minimize contaminations such as aggregation, macromolecules not purified out, or outside particles, but it is impossible to get rid of all contaminations. Thus, it is important to know the homogeneity requirements for a particular sample. A good example of this is how aggregation affects SAXS and NMR. In SAXS you measure scattering intensity vs scattering angle with low angles representing lower resolution, or larger particles. A good rule of thumb for SAXS is that the intensity is proportional to the mass^2; i.e., comparing a monomer and a dimer, the dimer's scattering intensity at a particular scattering angle will increase ~4-fold (43). This will be discussed further in Chapter 5. The relationship between intensity and mass can be affected by shape and size as well so it is not a perfect correlation, but it is a good rule of thumb. In addition, these intensities are additive not averaged. Thus, if we have a 100-mer aggregate it will scatter 10,000 times that of the monomers. This would produce a drastic change in the low angle of our SAXS curve even if the aggregation is present at a level of only 1% of our sample. In contrast, in a similar sample with a low amount of aggregate (~1%), the aggregate has little effect on the NMR spectrum. This is because the rotational correlation time of the aggregate will be so slow that the peaks for the atoms will be broadened below the detection threshold This simple explanation that will be discussed for each technique in the relevant chapters, but it does emphasize that understanding which factors affect the experiment and preparing the samples accordingly is extremely important.

Buffers to prevent aggregation and to keep the protein in a monomer state are essential. NS1B-CTD was sent previously to a buffer screening facility which is when the 2K buffer was developed and used for NMR (2). However, this was never performed for the NS1B-CTD:dsRNA complexes. Because ionic concentrations can affect the polar interactions between positively charged proteins region and negatively charged RNA, it was necessary to adjust the salt concentrations for the complex.

Proteins can be produced either by synthesis or purification from living cells. In the very early days of structural biology, protein was extracted from the tissues they were naturally found in. Due to the massive amount of protein needed for structural biology, purification of proteins was extremely difficult or not possible. Since the understanding and utilization of transformation, we have been able to insert genes into bacteria and force them to overexpress proteins of interest. The amount of protein being produced is not the only problem. In several cases proteins will not be soluble after lysing the cell. Another hurdle is the purification of proteins is difficult. Injecting and flowing a sample through a column filled with resin selecting for specific attributes can be inefficient. To obtain a pure sample, several steps of separation are often required, with significant losses at each step. A big step forward for purification was made with the introduction of protein tags and cleaving enzymes; e.g. 6XHis or MBP tags (1, 53). These tags provide a huge benefit for the quality and quantity of purification. They can increase solubility and be designed to stick to specific purification columns. Tags can also cause unwanted structural changes; therefore, it is advantageous to remove them before obtaining a structure. Introducing a cleavage site, between the protein of interest and a tag, for a cleaving protein is necessary. The method involves transforming a gene of interest into *E. coli* and to produce a protein. This step is followed by purification with the assistance of a tag, cleavage of the tag, then purification of the protein from the tag.

The resulting product could be used for various structural experiments such as crystallization or SAXS. NMR experiments on the other hand, generally detect hydrogen atoms, and requires isotope labeling to detect ^{15}N nitrogen and ^{13}C carbon atoms. This isotope-enrichment is achieved by fermenting the bacteria in minimal media (described in depth in the methods) and introducing ^{15}N-enriched ammonium, or ^{13}C-enriched glucose. The bacteria use these molecules to synthesize protein (1). All other steps could be used on the isotope-enriched proteins at this point (1).

Production of RNA is much easier. The main concerns for structural biology are quantity and quality. While there are a few methods for fermenting and purifying RNA similar to the protein procedure above, they are usually used for large RNA segments and are difficult to purify. For small RNA oligomers we were able to contract a series of companies to synthesize the required RNA substrates. For the large quantities of RNA that could be purchased in this fashion, quality was a major concern. Synthesis is not perfect and for every addition of nucleotide there is chance the reaction can stop. Therefore, it is also required for the RNA to go through a purification process. This was done using High Pressure Liquid Chromatography (HPLC) column. The quality of this can also be verified using Mass Spectrometry. For a 16mer RNA segment this method proved a significant increase in purity. For the NMR experiments performed in this thesis, detected ^{1}H or ^{31}P, isotope labeling of RNA was not necessary since these are naturally occurring isotopes.

Since RNA and protein sample quality is of such importance it is equally important to measure the concentrations accurately. This can be performed in several ways. Standard BCA assays can be performed easily and quickly. These assays, if performed correctly, will give an approximate reading for protein concentrations with RNA concentrations not being detected. Due to this, this reading will not tell you about

other contamination on your sample, for example nucleic acids left over from purification or aggregation. Thus, this method was only used to verify concentrations calculated from absorbance of the protein measured at 280 nm..

An experiment that can give clues to nucleic acid contamination and the presence of aggregation is a UV scan from 240 nm-300 nm. Proteins absorb light at 280 nm but absorb much less at 260 nm; this ratio is estimated to be ~0.57 for 260 nm / 280 nm (55). This information was obtained via a secondary source as primary sources were not easily obtainable or published in 1942 in a non-english language. Despite this fact, using this ratio seemed to be a very good rule of thumb to follow and was replicated in the lab. Nucleic acids on the other hand have a high absorbance at 260 nm. A standard method of detecting nucleic acid contamination is observing the 260 nm to 280 nm ratio; for a pure protein lacking nucleic acid contaminants, this ratio would generally be as close to 0.5 as possible. There is another benefit in observing the UV absorbance as a function of wavelength. Aggregates tend to absorb light at higher wavelengths. Therefore, if the absorbance after 280 nm does not sharply go down to 0 (before reaching 300 nm), then the sample likely contains aggregates.

As mentioned above nucleic acids absorb at 260 nm. Measuring RNA concentration at 260 nm is common, however, sometimes can be inaccurate. This is because the aromatic rings that absorb at 260 nm will absorb less if next to another nucleotide (56). This is called the nearest neighbor effect and can be mathematically corrected for (56). Another way to account for this is to separate the RNA into individual nucleotides using NaOH (54). This method needs no mathematical correction.

All concentrations can be calculated using this equation:

$$Abs = \varepsilon cL$$

Where Abs = absorbance at specified wavelength; ε= extinction coefficient at specific wavelength; c = concentration; L = length of cell

Since all of the proteins in this thesis and RNAs have been produced and used in experiments with, very few pitfalls are expected for fermentation, purification, and synthesis of these macromolecules. Most problems will occur while forming the protein:RNA complexes. One possible pitfall is that concentration might be difficult to measure for NS1B-CTD due to the lack of amino acids that absorb at 280 nm. Unfortunately, the NS1B-CTD construct used in this work contains only 1 Tyr residue, which has an extinction coefficient of 1490 (Abs/(cm*M)). For this reason, concentration estimates for the NS1B-CTD construct are very difficult, and possibly inaccurate at low concentrations. It is important to pay attention to the accuracy range of the Nanodrop (1.0-0.1). Also, due to the hypochromic effect, RNA extinction coefficients will either need to be adjusted or the RNA needs to be broken into individual nucleotides using a protocol developed in the Willamson lab at Scripps University. However, this protocol is not available publicly as of writing of this thesis. The protocol is based off of a chemical reaction mechanism where the hydroxyl will deprotonate the 2'OH of RNA followed by a nucleophilic attack, breaking the Oxygen-Phosphorous bond (54, pg. 85).

Finally, the buffer of the protein:RNA complexes has not been optimized so this task will need to be performed. Buffer optimization has been performed for NS1B-CTD alone which was key in the crystallization of the protein. However, the salt concentration is very high (450 mM) and as discussed in the purification section of this chapter, NS1B-CTD and will elute from a heparin column anywhere between 500 mM NaCl and 700 mM NaCl. This means that the optimized salt concentration for NS1B-CTD will not work for the complex. With a small attempt at trial and error we determined that by decreasing the salt in the optimized NS1B-CTD, RNA and NS1B-CTD complexed seemed more

stable, but we still suffered issues with unbound protein aggregating. I predict, doing a full buffer screen on the NS1B-CTD:dsRNA complex would significantly increase future work needed to be done at concentrations above 1 uM.

Sequences:

NS1B-FL

```
MADNMTTTQIEVGPGATNATINFEAGILECYERLSSQRALDYPGQDRLNRLKRKLESRIK
THNKSEPESKRMSLEERKAIGVKMMKVLLFMNPSAGIEGFEPYCMKNSSNSNCPNCNWTD
YPPTPGKCLDDIEEEPENVDDPTEIVLRDMNNKDARQKIKEEVNTQKEGKFRLTIKRDIR
NVLSLRVLVNGTFLKHPNGYKSLSTLHRLNAYDQSGRLVAKLVATDDLTVEDEEDGHRIL
NSLFERFNEGHSKPIRAAETAVGVLSQFGQEHRLSPEEGDN
```

NS1B-NTD

```
MADNMTTTQIEVGPGATNATINFEAGILECYERLSSQRALDYPGQDRLNRLKRKLESRIK
THNKSEPESKRMSLEERKAIGVKMMKVLLFMNP
```

NS1B-CTD

```
DPTEIVLRDMNNKDARQKIKEEVNTQKEGKFRLTIKRDIR
NVLSLRVLVNGTFLKHPNGYKSLSTLHRLNAYDQSGRLVAKLVATDDLTVEDEEDGHRIL
NSLFERFNEGHSKPIRAAETAVGVLSQFGQEHRLSPEEGDN
```

16-bp dsRNA

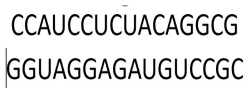

3P-5'-hpRNA

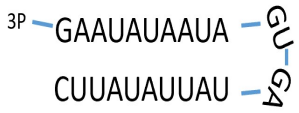

Methods:

Buffers:

While this normally is assumed, we cannot stress enough cleanliness and care while making buffers, especially for SAXS and structural work. For any buffers being used for structural work new sterile filters were always used, and buffers were made fresh before each purification. Salt also plays a very large role in the protein-RNA interactions so paying special attention to these concentrations is essential for replicable experiments. There are eight (8) relevant buffers for this thesis. 1. Ni binding buffer (BB), 2. Ni elution buffer (EB), 3. Low Salt buffer (LS), 4. Heparin buffer A (A), 5 Heparin buffer B (B), 6. NS1B-CTD buffer (2K), 7. NS1B-CTD:RNA binding buffer (1K), 8. NS1B-full length buffer (FL). All buffers are filtered with a 0.1 µm filter to sterilize, however, buffers used for structural work (6-11) should be double filtered by running through an additional 0.02 µm filter to ensure removal of small particles which can seep through the 0.1 µm filter. The recipes for the buffers are summarized in Table 2.1:

Buffer	Components and concentrations
BB	50 mM Tris HCl, pH 7.5, 500 mM NaCl, 1 mM TCEP, 40 mM Imidazole, 0.02% NaN_3
EB	50 mM Tris HCl, pH 7.5, 500 mM NaCl, 1 mM TCEP, 500 mM Imidazole, 0.02% NaN_3
LS	100 mM NaCl, 10 mM Tris HCl, pH 7.5, 0.02% NaN_3

A	50 mM Tris HCl, pH 8.0, 5 mM DTT
B	50 mM Tris HCl, pH 8.0, 1M NaCl, 5 mM DTT
2K	40 mM NH_4OAc, 450 mM NaCl, 5mM $CaCl_2$, 0.02% NaN_3, 50 mM Arginine, pH 5.5
1K	40 mM NH_4OAc, 225 mM NaCl, 5 mM $CaCl_2$, 0.02% NaN_3, 50 mM Arginine, pH 5.5
FL	50 mM Tris HCl, pH 8.0, 300 mM NaCl

Table 2.1: All buffers used in purification and throughout the thesis project.

Protein fermentation and purification:

All protein constructs were produced in *E. coli.* Batches were grown from glycerol stocks currently stored in the Montelione lab. The WT NS1B-CTD was fermented with the method described in previously (2). All mutations, i.e. R238A, were made by point mutating the WT DNA construct. Unlabeled proteins were fermented in standard LB media and labeled proteins being fermented in MJ9 minimal media containing $(^{15}NH_4)_2SO_4$ and D- [$U^{13}C$]-glucose as the sole nitrogen and carbon sources as described elsewhere (1). Cells were first grown at 37 C° until an absorbance of 0.6 at 600 nm. They were then induced by adding isopropyl-β-D-thiogalactoside (IPTG) at a concentration of 1 mM and incubated at 17 C° overnight or 18 hours. They cells were then pelleted by centrifuging at 6000 rpm for 45 mins and the pellet was either prepared for purification or stored at -80 C°. Pellets were suspended in BB, transferred into metal cups, the cups were floated in an ice bath and the samples were sonicated with 10

cycles of 30 seconds on/30 seconds off sonic pulse. Purification of WT NS1B-CTD and mutants were purified using a Ni column, cleavage of the SUMO tag using SUMO protease, Heparin column, Ni column framework procedure. The NS1B full length was purified using a Ni column and buffer exchange framework.

The Ni column was run using the AKTAExpress automated system with a flow rate of 0.5 mL/min of buffer running through the column (for Montelione lab personnel the method name: TEV remove Adam). The column had a loading step followed by 2X volume washing step and finally the elution step. The loading and washing steps were done with the BB buffer described above while the elution was done with EB buffer. There was no gradient transition. A SDS-denaturing gel was run and stained for protein using the wells with a high UV absorbance (read from the chromatogram). All relevant wells were pooled together. 5 mM DTT and a 20-50:1 protein:SUMO protease was added to cleave the SUMO tag from the NS1B-CTD protein variant. Another SDS-denaturing gel was run to assess cleavage. Once the gel confirmed over 90% cleavage the sample was run on a Heparin column using the AKTApure system. This sample was run by loading the sample, washing the column, then increasing salt until over 750 mM NaCl. The washing was done with buffer A and increasing percentage of buffer B was mixed in over a period of ~45 mL until the previously stated concentration was reached (Montelione lab users' protocol on the AKTApure: Hep 2017). Another SDS-denaturing gel was run to assess purity and separation from the tag. It is important to note that at this point the UV absorbance for the protein with no tag is very low due to the low extinction coefficient (1490 Abs/(M*cm), it is recommended to test all samples that eluded in 300 mM-700 mM NaCl, even if no absorbance is detected. Another note is that since the SUMO tag is relatively the same size as the NS1B-CTD, we recommend using good judgement not only for the presence of protein and size, but also the concentration

of salt in the sample. The tag will most likely elute from the column with lower salt concentrations versus NS1B-CTD which elutes at high salt. On occasion we run a very low salt sample next to a high salt sample, to see the slight difference in size, and use this as a guide for all other samples. The samples containing NS1B-CTD were then pooled together and loaded directly back into the Ni column protocol described above. It is vital to collect all samples, including flow through and wash steps, as the protein of interest will no longer have the 6XHis-SUMO tag and will not stick to the column. This last step is to remove an uncleaved sample that was able to stick to the Heparin column. It might take multiple runs to remove all uncleaved sample. Once the sample is pure, assessed by SDS-denaturing gel stained with Coomassie blue, the sample is buffer-exchanged into the appropriate buffer (for WT NS1B-CTD and mutants, this would be the 2K buffer or if used IMMEDIATELY 1K buffer) using a Bio-Rad desalting column (#7322010).

The NS1B full length protein was purified using the same methods, however, it was only subjected to a Ni-column until pure by SDS-denaturing gel, followed by the buffer exchange into FL buffer for storage.

NS1B-CTD Quality Assessment:

If the protein was not in the appropriate buffer (i.e. 2K buffer is for storage and 1K buffer is for RNA binding studies) a buffer exchange must be done. Once in the appropriate buffer, and immediately before adding RNA, a nanodrop scan is performed paying special attention to the 260 nm / 280 nm ratio, and if the spectrum goes to absorbance of 0 before reaching 300 nm. The sample is then centrifuged at 10,000 rpm for 10-20 minutes. The supernatant is next transferred to another tube, being careful not to mix the sample or disturb the nearly invisible to the human eye pellet. The nanodrop spectrum is taken again and compared to spectrum previous to centrifuging. This is

repeated until the sample records a suitable spectrum. The sample is put on ice and the concentration is calculated from the absorbance at 280 nm, using the extinction coefficient above. The appropriate amount of RNA will be added as quickly as possible to stabilize the protein.

RNA concentration:

RNA was diluted to 1 mM stock solution based off of the manufacturer's stated number of moles. If an RNA concentration is uncertain and needs to be double checked, it is recommended to use a method which will break apart the individual nucleotides. Absorbance measured by either a nanodrop or a spectrometer is preferred. This hydrolysis protocol is highly recommended, because it is difficult to properly calculate the hypochromic effect due to base pair and the nearest neighbor effect present in single stranded RNA/DNA. We incubated a dilute sample for 1 hour in 1 M NaOH at 37°C. The pH was then neutralized by adding equal amount of 1 M HCl. Water was used to blank and the absorbance was taken. The extinction coefficient was calculated by adding the individual nucleic acids present extinction coefficients.

Results:

Protein quality control:

The three most important steps added onto the protocols in place in the Montelione lab was the addition of the quality control steps for protein, a protocol to correctly calculate RNA concentration, and the repeated use of 1K buffer for binding studies. When all three of these steps were implemented the experimental results had decreased noise/error and were easier to reproduce.

As mentioned previously NS1B-CTD has a very low extinction coefficient. This is due to the lack of aromatics (NS1B-CTD has 1 Tyr and 5 Phe). A Tyr has a main

absorbance peak at 280 nm with an extinction coefficient of 1490 abs/(M*cm). However, Phe has a main peak at 260n m with an extinction coefficient of 140 abs/(M*cm) giving the protein an extinction coefficient of 700 abs/(M*cm) at 260 nm. Because of this composition the standard nucleic acid contamination method of measuring 260nm/280nm does not work well.

For proteins with more aromatics the normal expected ratio to indicate 0% nucleic acid contamination = 0.51, for 5% contamination = 0.95, and 10% contamination = 1.02. Note that Tyr also has an extinction coefficient at 260 nm, but the literature only lists the extinction coefficient at 260 nm in free Tyr but in the context of Tyr in a folded protein this number is inaccurate. There were many attempts to calculate an accurate extinction coefficient and all estimations gave an optimal 260nm/280nm between 0.95-1.10. It was later determined experimentally that the optimum 260nm/280nm ratio for a WT NS1B-CTD and mutant samples over 50 μM in concentration is ~1.00.

This was a very useful tool not only to determine whether the heparin column used in the purification had removed any nucleic acids from the sample but this detailed analysis also gave rise to identifying whether a sample is aggregated which is shown in Figure 2.1. We observed that aggregates can be removed from the NS1B-CTD samples by centrifuging. Centrifugation was done at 14,000 RPM for 10 minutes at 4°C. There are two qualitative observations while comparing the before centrifuging scan and after centrifuging. Scanning from 200 nm and up the UV absorbance has a slow decline around 240 nm and before reaching 260 nm in the before sample. However, in the after sample the curve has a much more rapid drop before 260 nm where it plateaus until after 280 nm. The second observation is the rapid absorbance drop to 0 after 280 nm in the after sample where the before sample has a very slow decline and, in most cases, still had absorbance at 300 nm. These two observations with quantitative 260 nm / 280

nm absorbance target stated above produced a dramatic improvement in the reproducibility and error of the results.

A) B)

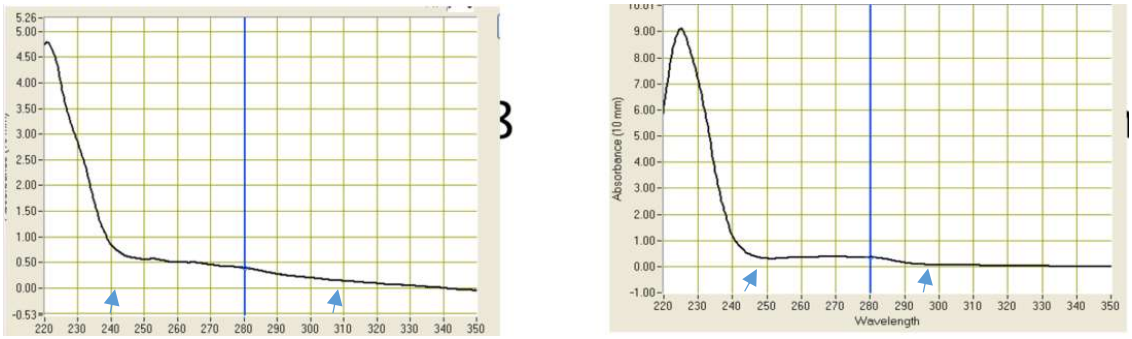

Figure 2.1: UV absorbance scan provides quantitative and qualitative evidence for sample quality and presence of aggregates. A) UV absorbance scan before centrifugation. Arrows indicate regions where the scan qualitatively differs from panel B. B) UV absorbance scan after centrifugation.

Method	Expected Abs based on trilink data sheet and extinction coefficient	Expected concentration based on Trilink data sheet (uM)	Measured absorbance	**Calculated concentration (uM)**
Nanodrop	26.74	100	15	56

Heating to 85 C for 5 mins – nanodrop	26.74	100	16.8	62.8
Incubate with 1M NaOH for 1 hour - nanodrop	.0.411	1.54	0.42	1.57

Table 2.2: Comparison of RNA concentration techniques.

RNA concentrations:

Directly measuring absorbance with a nanodrop at 260 nm gave RNA concentrations that were off by 50%+. This problem was amplified with hpRNA vs ssRNA, as the hpRNA could become double stranded and gain inaccuracies due to the hypochromic effect. For the ssRNA we attempted to correct the extinction coefficient by using the nearest neighbor effect adjustment. However, this proved to be inaccurate as well. For hpRNA we attempted to make double stranded by heating, then adjusting the extinction coefficient for the nearest neighbor effect. Again, the result was inaccurate. Finally, we broke the RNA into individual nucleotides by incubating with NaOH for 1 hour (original protocol was found at this discontinued URL: https://www.scripps.edu/california/research/dna-protein-research/forms/biopolymercalc2.html). Using this method, we routinely got within 5% of the expected concentration (Table 2.2).

Discussion:

Most of the protocol was in place in the laboratory and used for most of the experiments such as the SAXS data collection of the protein by itself and the 16-mer

dsRNA. The additional optimization of salt in buffers, buffer filtration, protein aggregation assessment and proper RNA concentrations was critical for reproducible results. For example, the data represented in this thesis that did not include the additional steps in sample preparation and characterization, as outlined above, were only successful because we used expected concentrations. At some point we needed to measure a concentration and noticed we were off from the expected value. We assumed the measured value as the most accurate, however, without implementation of the described steps before the measurements were taken. This resulted in inaccurate concentrations and thus the data was not reproducible. After a major effort to make our measurements accurate again our data became reliable and an extremely high quality SAXS sample was collect using the 3P-10HP RNA. It is also important to note where the 2K buffer and the 1K buffer came from. The 2K buffer was created during the crystallization of NS1B-CTD on its own. This buffer was a result from buffer screenings to optimize buffer for the protein (2). Unfortunately, late in the project it was discovered that the 2K buffer was not a good buffer to do the RNA binding studies because of the high salt. The salt was reduced by half resulting in the 1K buffer. The binding affinity of NS1B-CTD to RNA increased and most RNA binding studies were either run/repeated with this buffer with the exception of the 16-bp dsRNA SAXS result. It is recognized that there may be an even better buffer for the complex of NS1B-CTD:RNA, and buffer screening is in future plans to optimize the complex system even further.

Supplemental Material:

RNA Concentration Protocol Adapted from Williamson Website:

Purpose: To accurately measure the concentration of an RNA sample. RNA secondary structure inuces hyperchromicity in the UV absorption of nucleotides. This procedure hydrolyzes the RNA to nucleotides to remove the hyperchromicity and allows for

repeated measurements to reduce the inaccuracy associated with this procedure (mostly pipetting error). This procedure hydrolyzes your RNA so it is probably not worth doing unless you are doing at least a 1 mL transcription.

1. Aliquot 2 uL of your RNA sample into each of the three 0.5 mL Eppendorf tubes
2. Aliquot 2 uL of ddH2O each into three more tubes.
3. Add 8 uL of 1M NaOH into each tube
4. Incubate the tubes at 37 C for at least one hour
5. Add 8 uL of 1 M HCl to each tube.
6. Add 282 uL of ddH2O (make sure to invert the tube, or spin it down in the ventrifuge quicklyto get any condensation from the top of the tube)
7. Using the wate tubes as blanks, and the microquartes cuvettes (300 uL), take the absorbance of each solution at 260 nm. (*could also be taken by nanodrop if microquartes cuvette spectrometer reader is not available but the nanodrop is not preferred).
8. Average the three readings and use the value to determine the concentration, (make sure you use specific RNA sequence *to calculate extinction co-efficient).using the programs installed on the website (Extinction Coefficient Calculator). *this can also be done by simply googiing extinction coefficients of RNA nucleotides and adding all values for you sequence.

   Notes: depending on how accurately you desire to know your concentration, three readings may not be enough. You should make sure that your RNA is at least 100 uL so that your assay doesn't use up too much RNA. *Absorbance is only accurate between 0.1-1 (2 is still accurate but it is a maximum value). Therefore if your concentration is estimated (i.e. synthesized RNA from a manufacturer and you need to confirm). This can be done in 2 ways, i) take a

small RNA sample and dilute so that after performing this experiment your absorbance in this range (see formula in this chapter for concentration calculations). Ii) perform this experiment on the RNA stock. Due to the high RNA concentration of the RNA you should have a very high absorbance. From the resulting 300 uL sample take further aliquotes and dilute in a serial way so that you get absorbance above, within, and below this range. The sample that falls into the 0.1-1 abs range is your true concentration, back calculate the concentration of your stock depending on the dilution factor.

*my additions/notes/tips for this protocol

Chapter 3: Studies of Protein-RNA Interactions using Circular Dichroism Spectroscopy (CD)

Introduction:

Modeling of the protein complex requires docking the two molecules: NS1B-CTD with either 16-bp dsRNA or 3P-5'-hpRNA. There are two major docking methods, rigid and flexible. Rigid docking simply takes structures as an input and finds all orientations in which the two molecules can interact without changing the structure. It is always more accurate to dock the structures rigidly. If either one of the molecules goes through a conformational change it significantly adds degrees of freedom as you also have to model the flexible regions with docking orientations. To determine whether we can use rigid docking, we used Circular Dichroism Spectroscopy (CD) to determine the initial secondary structure, and to identify if there were any major changes to the structure upon binding.

CD uses circularly-polarized light to determine secondary structures of protein and nucleic acids. All biological molecules have chiral centers that force them to either right handed or left-handed conformations. In CD, the absorbance of left or right rotating circular light is measured by a detector (Figure 3.1). Alpha helices and beta strands from protein will give unique signatures in a CD scan in the wavelength range 180 nm-260 nm (Figure 3.2A). Since NS1B-CTD is a mixture of α-helix, β-strand, and coil-coil, we expect a mixture of the three signatures in Figure 3.2A. RNA also will give unique signatures in the CD spectrum from 200 nm-300 nm (Figure 3.2B). For dsRNA we expect to see a signal similar to the dsRNA signal in Figure 3.2B where the maximum degree is at 260 nm. hpRNA has a dsRNA stem and ssRNA in the loop. This usually produces a signal that is not typical of dsRNA or ssRNA and cannot be predicted (Figure 3.3) (44).

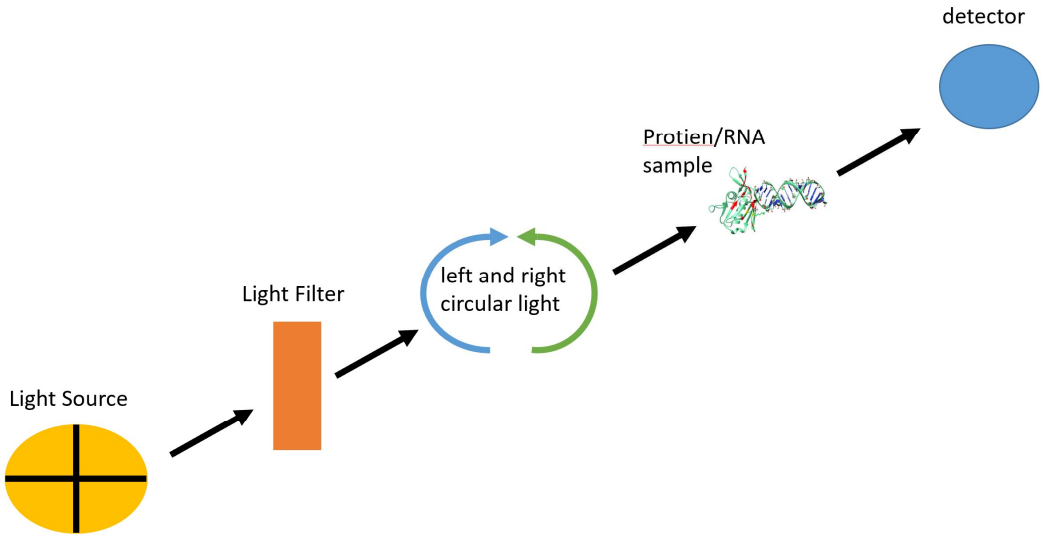

Figure 3.1: Diagram of the theory of CD. Light source emits light which passes through a filter only allowing circular light. The protein/RNA/complex samples will absorb some amount of either left or right rotating light which will then be detected.

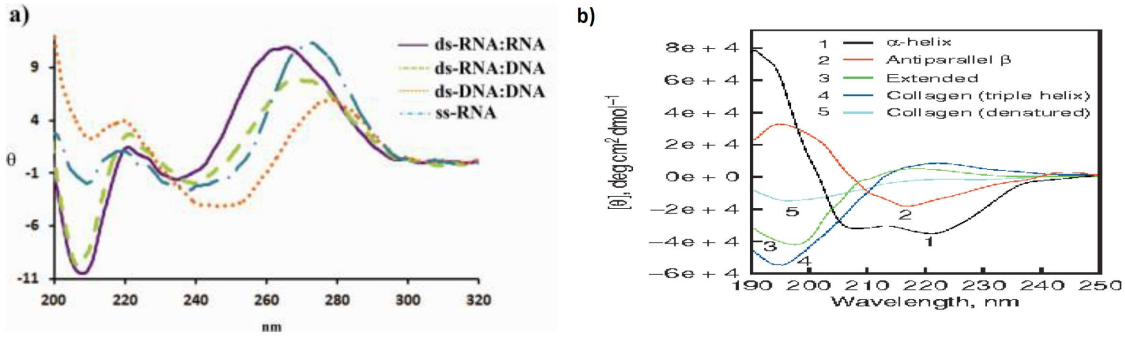

Baker ES, *Journal of the American Society for Mass Spectrometry*. 2007

Greenfeild NJ *Nature protocols*. 2006

Figure 3.2: Example spectrum for various RNA structures (A) and proteins conforming to a single secondary structure (B).

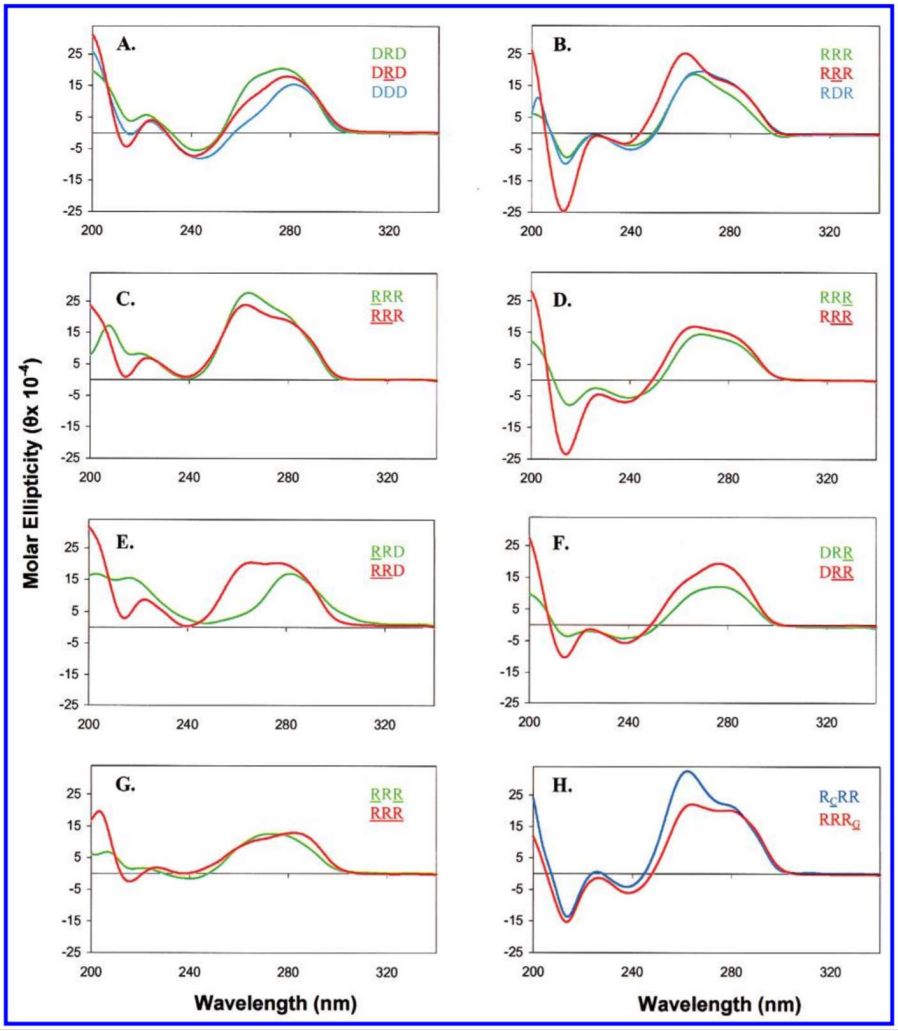

Hannoush RN. et. al. *JACS*. 2001

Figure 3.3: CD spectra of various RNA/DNA hairpins. Segment (1) is the 5' end (2) is the loop (3) is the 3' end that base pairs with the 5' end to form a stem. R signifies RNA segment and D represents DNA segment. Hairpin RNA/DNA contain various sequences and stabilities.

Methods:

The CD samples were prepared by buffer exchanging protein into 1K buffer (40 mM NH_4OAc, 225 mM NaCl, 5 mM $CaCl_2$, 0.02% NaN_3, 50 mM Arginine, pH 5.5) and immediately adding RNA (see chapter 2) and storing on ice until measurements could be made. All CD measurements were made with a concentration between 0.1 - 1mg / mL of

protein and RNA at a 1:1 ratio. CD scan was completed using the AVIV CD spectrometer. The scan was started at 310 nm and ended at 185 nm, taking measurements at every 2 nm. Each reading was measured for a total of 10 secs. For all samples the CD dynode was monitored to assess whether a measurement had high error. All data shown had a dynode recording between 100 mA and 600 mA. The reported data is in molar ellipticity (mdegree / molar). Most CD for protein is reported in molar ellipticity/residue, however, because we are adding RNA to the sample this unit is not appropriate. A blank of the same buffer stock used for the buffer exchange was subtracted from the sample to give final reported values.

Sample CD signal – Buffer CD signal)/ molarity = normalized sample CD signal

To get the signal of the predicted structure we made one major assumption that the two molecules would not interact. In this case the two signals of the individual components can be added

Normalized signal of NS1B-CTD + Normalized signal of RNA substrate = predicted signal of non-interacting components.

NS1B-CTD was then mixed with the appropriate RNA substrate and compared to the predicted.

Results:

NS1B-CTD gives a protein CD profile that was expected as a mixture of α-helix, β-strand, random-coil (7). The 16-bp dsRNA also gave a typical A-form RNA:RNA duplex CD signal with the (+) signal peaking at 260 nm (6,8). We then mixed NS1B-CTD and with 16-bp dsRNA and compared this measurement to the predicted signal if the two molecules do not interact. The signal of the measured and the predicted deviate slightly which can indicate binding but the amount of change is minor enough to assume the

molecules are not going through a conformational change and can be docked rigidly (Figure 3.4 A/B). In order to confirm complex formation in this sample, we then measured a 1D proton NMR spectrum and saw that it was similar to a complexed RNA, These NMR studies are discussed further in Chapter 4.

A) B)

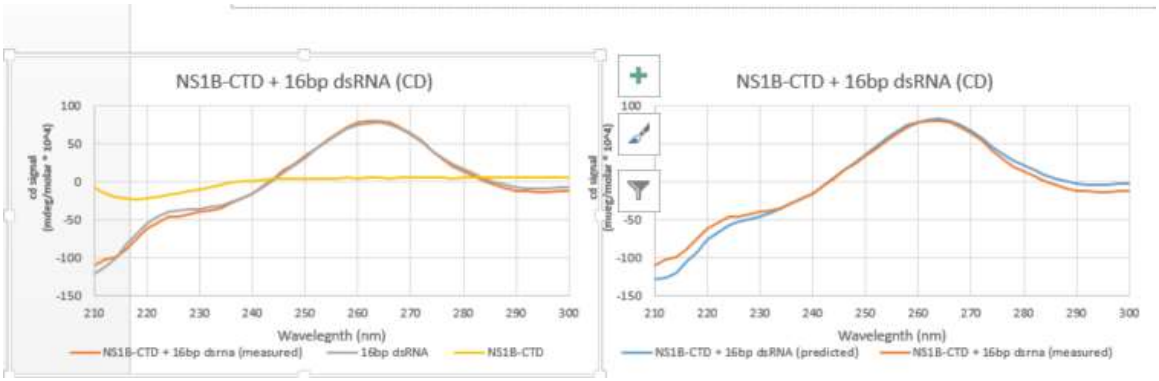

Figure 3.4: CD spectrum for NS1B-CTD complexed with 16-bp dsRNA shows limited structural changes upon binding. A) CD scans for NS1B alone, 16-bp dsRNA alone, and complexed NS1B-CTD with 16-bp dsRNA. B) Measured NS1B-CTD complexed with 16-bp dsRNA and predicted CD of NS1B-CTD and 16-bp dsRNA if they were not interacting.

The same experiment was repeated for the NS1B-CTD : 3P-5'-hpRNA complex, with similar results. It is worth noting that the free 3P-5'-hpRNA has a very unique CD signature with not only a maximum peak at 260 nm which is predicted but also a second bump in the curve around 280 nm. It is unclear what this bump is attributed to as it could be because of the loop of the hairpin, ssRNA has a peak at 280 nm, or it could be the triphosphate group. Whatever the case the main peak of the spectrum is at 260 nm which is typical of A-form dsRNA (Figure 3.5 A/B). This is very important because it lets

us know that the hairpin is folded and annealed together, and not single stranded. Again, 1D proton NMR experiments were performed to confirm that the RNA was indeed bound and that it is in a double stranded state.

A) B)

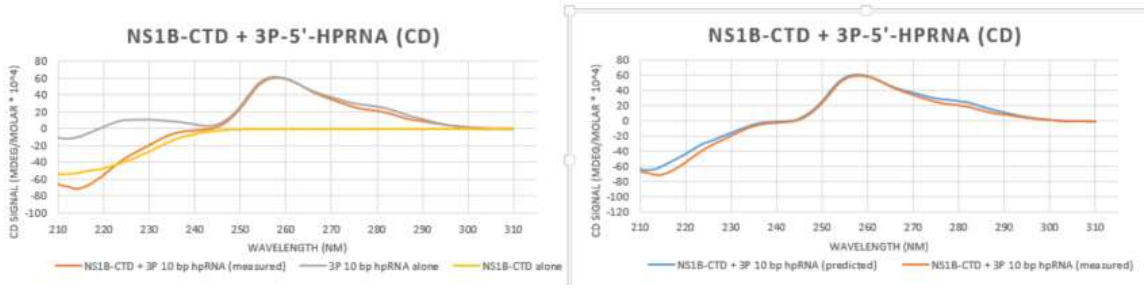

Figure 3.5: CD spectrum for NS1B-CTD complexed with 3P-5'-hpRNA shows limited structural changes upon binding. A) CD scans for NS1B alone, 3P-5'-hpRNA alone, and complexed NS1B-CTD with 3P-5'-hpRNA. B) Measured NS1B-CTD complexed with 3P-5'-hpRNA and predicted CD of NS1B-CTD and 3P-5'-hpRNA if they were not interacting.

Discussion:

NS1B-CTD is shown to bind both RNA substrates by the results presented in this chapter, as well as chapters 4, 5, and 6. In addition to this these results show that there are no major secondary structural changes in either the RNA or NS1B-CTD. It is very curious the 3P-5'-hpRNA CD spectrum has a second peak at 280 nm. After reviewing, we were able to find other hpRNA spectra (8) which concluded that because of the mixture of double stranded and single stranded RNA in a hairpin structure, hpRNA does not conform to expected RNA CD results and each one has a unique profile. It would be interesting to really examine what part of the RNA is causing the 280 nm second peak, but it is out of the scope of this study. To study this one could do a melting CD scan to see if the peak increases/decreases/or stays the same as the RNA unfolds. Doing this

experiment would tell us whether that second peak is in the double stranded part of the RNA or elsewhere. Since this is a part of the CD spectrum that changes the most on the RNA side versus the predicted spectrum, it would be worth understanding what is causing this feature for our study as well as providing the community with a unique CD result. Regardless the ultimate conclusion that the molecules do not have changes in secondary structure and can be docked rigidly stands.

Chapter 4: Studies of Protein-RNA Interactions using Nuclear Magnetic Resonance Spectroscopy (NMR)

Introduction:

Nuclear Magnetic Resonance (NMR) works by observing magnetic fields surrounding atomic nuclei in a sample. Upon pulsing with a radio frequency a nucleus will be excited to a certain angle to the magnetic field. The nuclei will then relax to the ground state.. The frequency at which a radio frequency pulse can energizes a nuclei to certain angle and the rate at which the nuclei returns to the ground state can give a lot of information about which types of atoms are bound to it and the environment the nuclei is in.

NMR is used in structural biology to obtain information about protein and nucleic acids structures. In fact, as of 2016, 39% of protein-RNA complexes are solved by NMR (40). The process for determining protein structures by NMR is very straight forward, for a high-quality protein sample, since the technology has been around for several decades (45). $^{15}N/^{13}C$ labeled protein sample is required. ^{15}N is necessary for detection of the backbone nitrogen and ^{13}C are required to determine environments around amino acids as well as assignments of the Nitrogen. Collection of 1D, 2D, and 3D, and Nuclear Overhauser Effect (NOE) experiments measure the change in integrated intensity by transfer of nuclear spin polarization from another atom when it is saturated by irradiation. Based on these experiments, distance and dihedral angle restraints can be defined, then the 3D protein structure is generated from these restraints and refined (Figure 4.1). Similar methods can be used for RNA structure calculations (38-42). For our study, however, we know the X-ray crystal structure of the RNA and secondary structure was confirmed by CD.

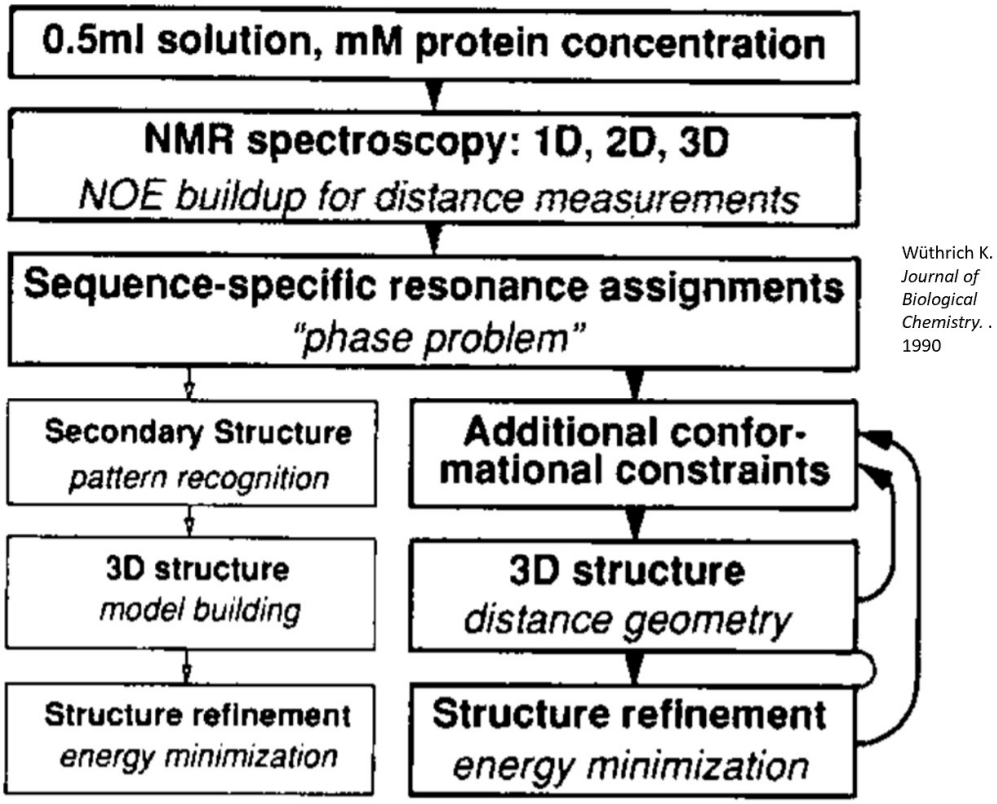

Figure 4.1: Flow chart of a typical 3D structural calculation for protein using NMR.

NMR was used to verify and refine the initial model in a variety of ways. Since the crystal structure of NS1B-CTD was missing the last 5 amino acids, MD modeling was performed to predict flexibility of these amino acids. The ^{15}N-^{1}H Heteronuclear NOE (HETNOE) NMR experiment provides information about the motion of the N-H bond. If the N-H is moving faster than the tumbling time of the protein, we can infer these atoms are flexible. To perform this experiment, we collected an Heteronuclear Single Quantum Coherence (HSQC). Conveniently we were able to match this HSQC to the one submitted to the BMRB entry (BMRB ID: 25462, 2) and assign the peaks needed.. This also served as a way to confirm that we could replicate the NH-HSQC for our experiments. For proper modeling of NS1B-CTD bound to RNA we needed to obtain

information on which residues are affected by the presence of RNA and which nucleotides on the RNA are affected by the presence of NS1B-CTD. To do this we replicated Chemical Shift Perturbations (CSP)s performed in Ma L.C. et. at. but with the 16bp dsRNA and 3P-5'-hpRNA substrates (sequences shown in Chapter 2 introduction) . By using the assignments verified for the HSQC in the HETNOE experiment, we collected ^{15}N-^{1}HHSQC spectra with varying amounts of RNA. Since atoms have different magnetic properties depending on the environment surrounding them, if the environment changes the assigned peak will shift in the spectra. By observing these shifts, we can determine which regions of the protein structure are environmentally altered by binding to RNA, providing evidence for the location of the binding site on the surface of the protein.

Upon initial modeling of NS1B-CTD bound to 16-bp dsRNA using chemical shift perturbation on the protein due to RNA binding, it became clear that without any information from the RNA side of the complex the RNA was free to rotate and bind in a variety of orientations during modeling. To minimize possibilities in the RNA orientation and degrees of freedom, information about which nucleic acids were active in the binding of NS1B-CTD needed to be acquired. Since crystal structures of the RNA are available, structural determination of the RNA were not required, however, secondary structure identification became very useful. Table 4.1 list useful experiments in identifying RNA secondary structure and structural determination (42) The guanine and uracil have imine and imide groups that are unique in their magnetic resonance (Figure 4.2A). Since the imine and imide NHs are involved in hydrogen-bonded base pairing, it is also easy to distinguish between non-base paired and base paired nucleotides. Additionally, if there is base pairing non-Watson-Crick base pairing can be determined by collecting an NOESY and linking the imine/imide H^N protons to the protons on the

paired base (Figure 4.2B, Figure 4.7). Each imine / imide group only contains a single $^{1}H^{N}$, so in the NMR experiment a single resonance peak is observed per base pair (42). In addition to determining the whether a nucleotide is base paired or not, it is also possible to determine adjacent bases (42). This can be done by using the NOESY experiment and observing the cross peaks between imine/imide H^{1} (figure 4.2). This makes it very convenient for determining which nucleic acid is involved in binding, using chemical shift perturbations of resonances of the RNA. The proposed NMR experiments generate sufficient data to determine protein-RNA interfacial atoms. These binding sites can then be used as input for HADDOCK protein-RNA docking calculations.

Experiment	Information
1D ^{1}H spectrum	Peak count; buffer conditions; solvent exchanging peaks
2D ^{1}H-^{1}H NOESY[a]	
Mix Time[b]	
25–75 ms	Base pair type from strong cross-peaks
100–300 ms	Find adjacent base pairs from imino–imino walk
2D ^{1}H-^{15}N HSQC	Assign imino protons as G or U (base pair type)
2D HNN-COSY	Identify imino hydrogen-bonding by correlation to two ^{15}N (base pair type)
2D/3D ^{13}C HMQC-NOESY[a]	Identify strong imino NOEs as H2, H6/H8, or NH_2 (base pair type)

[a]NOESY experiments should use water-suppression readout pulses optimized for excitation of the imino proton region (9–15 ppm)
[b]Within each range of mixing times, the shorter times are more appropriate for large RNAs (>~60 nts), while the longer times of the range are more appropriate for small RNAs (<~25 nts)

ırner DH. *Springer ature.* 2016

Table 4.1: Useful NMR experiments in RNA secondary structure identification

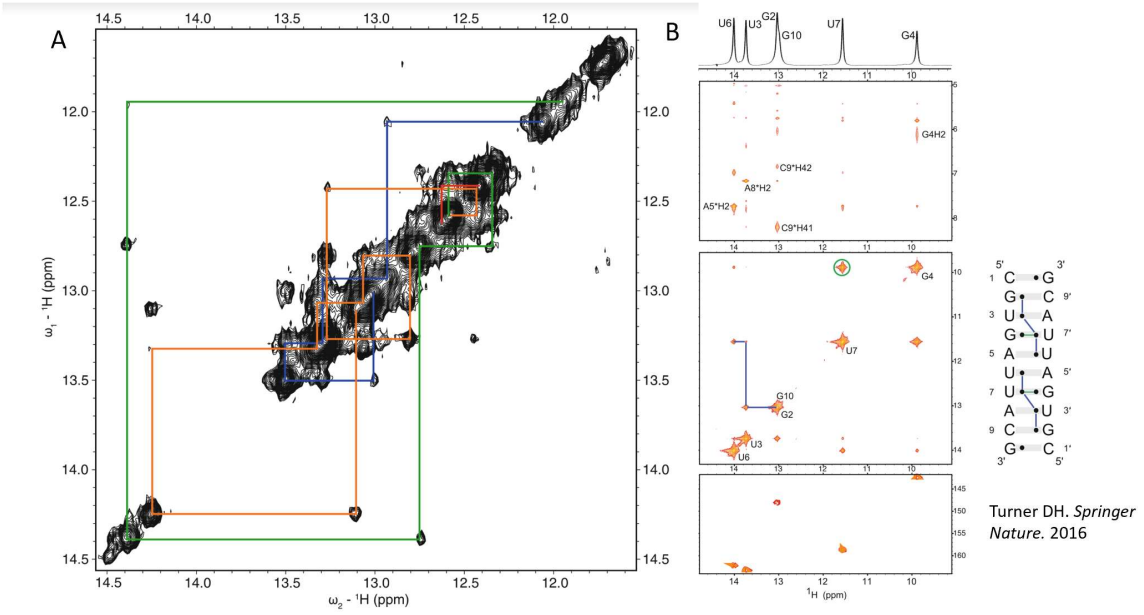

Figure 4.2: Literature data showing how NOESY cross peaks provide information for determining base pair and base pair sequence. A) NOESY for a 72-nt base paired dsRNA. Lines link cross peaks for sequence walking. B) NMR on the RNA duplex $(CGUGAUUACG)_2$, Top spectra shows the 1D proton NMR spectrum for dsRNA, Top panel shows GC base pairs identified by NOESY cross peak signatures. C*42H is the Hydrogen involved in base pairing from the cytidine. Middle identifies a GU base pair. Bottom is the NH HSQC.

Methods:

NMR sample preparation:

HetNOE samples were prepared in 2K buffer at 100 μM with 10% DSS/D_2O. These samples were then transferred to a micro tube (1.7 mm) and run on a Bruker 800 MHz magnet. Measurements of NH-HSQC peak intensities in unsaturated and saturated hydrogen exchange conditions was taken. The peak intensities ratio of unsaturated/saturated was then graphed on a per residue basis.

NS1B-CTD NH/CH HSQC samples were prepared using the protocol outlined in chapter 2 for a ^{15}N / ^{13}C - enriched labeled sample. NS1B-CTD was then transferred into 1K buffer, concentrated to 100 μM and 10% DSS / D_2O was added. The appropriate amount of RNA was then added. RNA was also transferred into 1K buffer before addition if it was not in this buffer previously. Samples were then transferred to a Shigemi 4-mm tube and standard NH/CH HSQC spectra were recorded.

1D Hydrogen and 2D Hydrogen NOESY experiments were performed on RNA. The RNA samples were exchanged into 1K buffer if it was not in this buffer previously. The RNA was then brought to 100 μM. For samples with NS1B-CTD, an equal number of moles of NS1B-CTD (unless otherwise stated) and 10% DSS / D_2O was added. Samples were transferred into a Shigemi 4-mm NMR tube. Samples were then run on the Bruker 600 MHz magnet with standard 1D/2D Hydrogen NOESY protocols with the exception of an increased sweep width ranging from 5-18 ppm to include the imine/imide hydrogens of RNA.

NMR data collection:

Samples of ^{13}C , ^{15}N enriched NS1B-CTD, ^{1}H 16-bp dsRNA, ^{1}H 3P-5'-hpRNA and the complexes described in this chapter, were prepared at a concentration of 0.03-0.25 mM (initial concentration was always at 0.1 mM and then adjusted to improve data collection quality) in 90% buffer/10% DSS D_2O (refer to buffer chart in Chapter 2 for description of each buffer used in each experiment). 2D ^{1}H, ^{15}N HetNOE experiment was acquired at 20 °C whereas data for RNA, RNA:protein complexes, and HSQCs of protein were acquired at 10 °C on a Bruker Avance III HD 600 MHz NMR spectrometer equipped with a 5 mm triple resonance TCI cryogenic probe. Time-domain NMR data was converted to frequency domain using San NMRPipe 2.1 (28), and analyzed using SPARKY 3.106 (29). Proton chemical shifts were referenced to DSS, while ^{13}C and ^{15}N

chemical shifts were referenced indirectly using the gyromagnetic ratios of ^{13}C:^{1}H (0.251449530) and ^{15}N:^{1}H (0.101329118), respectively. Backbone (H-N) resonance assignments were made using assignments for NS1B-CTD from the BMRB (BMRB # 25462, 2). C-H assignments were not made as they were not available, however, ^{13}C-^{1}H HSQC spectrum was recorded and discussed in this Chapter in the context of no assignments. 1D ^{1}H, ^{15}N HetNOE spectrum was used to optimize the recycle delay in order to avoid misinterpretation of data due to solvent saturation. Proton saturation was done with a time of 3.0 secs with a recycle delay of 12.0 seconds. Final 2D ^{1}H, ^{15}N HetNOE data was processed and analyzed using the assignments from ^{1}H, ^{15}N HSQC spectrum and the ratio of intensities of the cross-peaks from spectra with and without proton saturation were plotted (Figure 4.3), as described elsewhere (58). The 2D ^{1}H, ^{15}N HSQC and ^{1}H, ^{13}C HSQC were standard collection parameters described (57)^{1}H-1D and 2D ^{1}H-1H NOESY spectra for the RNA samples were acquired using a ^{1}H with a sweep width of 28 ppm with the center on water at 4.70 ppm. The 2D NOESY data was acquired using 32 scans with 300 complex points in the indirect proton dimension for each 4096 complex points in the acquisition dimension. A NOESY mixing time of 300 ms and a recycle delay of 1.5 s was used.

Data processing:

1D Hydrogen experiments were processed, analyzed, and figures were created using Topspin. 2D experiments were processed with NMRPipe software (28) and analyzed with Sparky software (29). HetNOE graph was created by taking the intensity of the peaks for each residue in the saturated and unsaturated conditions and plotted using Microsoft Excel.

Results:

In order to have a complete model of NS1B-CTD we needed to assess the flexibility of the residues in NS1B-CTD. HET-NOE ratio ranges for flexibility were defined as +0.25 = not flexible, 0.0-0.25 = mildly flexible, -0.0 (negative ratios) = highly flexible. Using HET-NOE experiments we were able to see that the majority of NS1B-CTD is not flexible, however, the last 5 amino acids were found to be flexible figure 4.3 A. This was not a surprising result since the electron density for these amino acids was missing in the crystal structure (one factor leading to this is flexibility), MD simulations predicted a higher RMSF for the last 5 amino acids vs the rest of NS1B-CTD (data not shown), and TALOS+ predicted these last 5 amino acids were non-structured. The HET-NOE ratios were mapped on the structure resulting from the MD simulations to see if there were any other highly flexible regions, but only mild flexible residues were found (Fgure 4.3 B). In addition, we used the HSQC that the HET-NOE experiment produced to confirm we could replicate data provided on the BMRB website (figure 4.3 C). ’

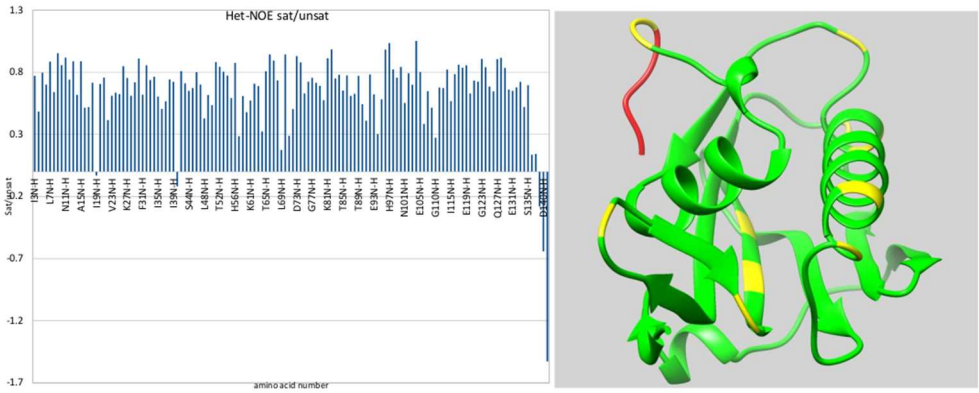

Figure 4.3: HET-NOE confirms the last 5 amino acids are flexible and the majority of NS1B-CTD is highly structure. A) HET-NOE ratios are on the Y-axis, sequence of NS1B-CTD is on X-axis. Number is relative to only NS1B-CTD and not the full length NS1B protein. Ratios with negative values implying highly flexible amino acids. B) ratios

from panel A mapped onto the NS1B-CTD model from the MD simulation. Red = highly flixible, yellow = mild flexiblitity, green = not flexible. C) HSQC of NS1B-CTD with the peaks from the BMRB database confirm correct NS1B-CTD folding and structure.

Generation of CSPs for NS1B-CTD bound to 3P-5'-hpRNA:

CSPs on NS1B-CTD bound to 16-bp dsRNA was taken from Ma LC. et al. (2). A table with the CSPs is provided below. CSPs for the 3P-5'-hpRNA needed to be generated as this is a different RNA substrate. NH/CH HSQCs on NS1B-CTD were taken with and without 3P-5'-hpRNA. CSPs were observed in the NH-HSQC (Figure 4.4), the aromatic region of the CH-HSQC (figure 4.5), and the aliphatic region of the CH-HSQC (figure 4.6). However, it was decided to use 1K buffer for this experiment since it was shown to increase NS1B-CTD's affinity for RNA Since the original NH-HSQC on the BMRB was taken in 2K buffer, the peaks for NS1B-CTD in 1K buffer did not match the peak list, thus assignments for these peaks are not available for this thesis. It was recognized that the overall pattern of the peaks in 1K buffer was similar to that in 2K buffer. Because of this we conclude that the protein fold is similar, however, due to environmental changes in salt the assignment of the residues in 2K buffer cannot be used for the NH-HSQC in 1K buffer. There are no assignments available for CH peaks in an HSQC.

Res+A1:H121idue(s)	Shift H (unbound)(ppm)	Shift H (RNA bound)(ppm)	CSP H (ppm)	Shift N (unbound)(ppm)	Shift N (RNA bound)(ppm)	CSP N (ppm)	CSP Sum
143Ile	8.3912	8.38866	-0.00249	120.91816	120.86961	-0.04855	0.01059
144Glu	8.4232	8.39707	-0.02608	124.70973	124.52698	-0.18275	0.05654

145Val	9.4193	9.40106	-0.01823	120.56458	120.33209	-0.23249	0.05698
146Val	8.7883	8.78023	-0.00802	127.35619	127.27231	-0.08389	0.022
147Leu	8.9924	8.90393	-0.08849	129.84847	129.7403	-0.10817	0.10652
148Arg	8.4613	8.43483	-0.02646	119.3527	119.1065	-0.2462	0.06749
149Asp	8.8155	8.79044	-0.02503	122.57314	122.54413	-0.02902	0.02987
150Met	9.2872	9.26475	-0.02246	118.70594	118.8271	0.12116	0.04266
151Asn	9.1114	9.09395	-0.01747	120.38862	120.40046	0.01184	0.01945
152Asn	8.4735	8.49143	0.01795	116.74515	116.86961	0.12447	0.03869
153Lys	8.0409	8.05263	0.01177	120.30514	120.43874	0.1336	0.03404
154Asp	8.5476	8.54678	-7.82E-04	121.67019	121.56914	-0.10104	0.01762
155Ala	7.934	7.91841	-0.01555	120.03173	120.15835	0.12662	0.03665
156Arg	7.2371	7.25966	0.02256	112.8757	112.84553	-0.03017	0.02759
157Gln	7.2621	7.24641	-0.01571	122.52808	122.59407	0.06598	0.02671
158Lys	8.4847	8.52586	0.04112	123.55664	123.73449	0.17785	0.07076
159Ile	8.6361	8.63367	-0.00239	123.49002	123.19601	-0.294	0.05139
160Lys	8.6353	8.6419	0.00665	128.54441	128.44245	-0.10196	0.02364

161Asp	7.6102	7.58848	-0.0217	117.3012	117.36104	0.05984	0.03167
162Glu	8.5811	8.61684	0.03577	117.80238	117.86294	0.06056	0.04586
163Val	8.5318	8.53522	0.00337	114.35945	114.40616	0.04671	0.01116
164Asn	9.1311	9.12335	-0.0077	118.40474	118.55099	0.14625	0.03208
165Thr	8.5574	8.55424	-0.00311	113.22519	113.23675	0.01156	0.00504
166Gln	8.9852	8.98079	-0.00442	122.98506	123.00292	0.01786	0.00739
168Glu	8.1151	8.13016	0.01509	123.27937	123.30035	0.02098	0.01859
169Gly	8.9916	8.99159	0	115.97802	115.97802	0	0
170Lys	9.6205	9.58553	-0.03496	128.06096	128.03172	-0.02924	0.03983
171Phe	8.5158	8.4978	-0.01796	115.46541	115.41253	-0.05288	0.02677
172Arg	8.9134	8.93899	0.02561	120.84212	120.8274	-0.01472	0.02807
173Leu	9.3878	9.38191	-0.00592	130.74383	130.73391	-0.00992	0.00757
174Thr	9.2504	9.24248	-0.00788	124.53086	124.53859	0.00774	0.00917
175Ile	9.0688	9.07126	0.00246	123.80176	123.81986	0.0181	0.00547
176Lys	8.5299	8.52852	-0.00137	126.52612	126.45593	-0.07019	0.01307
177Arg	8.4212	8.42067	-5.31E-04	123.88689	123.77813	-0.10876	0.01866
178Asp	8.4161	8.41608	0	117.2582	117.2582	0	0
179Ile	7.7373	7.72465	-0.0126	119.44381	119.39981	-0.044	0.01993

180Arg	8.2824	8.28297	5.63E-04	122.18238	122.17786	-0.00451	0.00132
181Asn	8.218	8.20866	-0.00938	113.95832	113.9616	0.00328	0.00993
182Val	7.8178	7.81775	0	121.98854	121.98854	0	0
184Ser	7.7533	7.74901	-0.00428	110.52707	110.54198	0.01491	0.00676
185Leu	8.0875	8.08751	0	117.03365	117.03365	0	0
186Arg	8.9632	8.95587	-0.00731	124.96206	124.93927	-0.02279	0.01111
187Val	9.0709	9.06097	-0.00996	126.34877	126.34341	-0.00536	0.01085
188Leu	9.0698	9.06187	-0.00789	127.24854	127.28203	0.03349	0.01347
189Val	10.379	10.3407	-0.03794	122.51189	122.45992	-0.05197	0.04661
190Asn	8.5138	8.51377	0	122.88976	122.88976	0	0
192Thr	9.0461	8.98453	-0.06155	116.82669	116.78828	-0.03841	0.06795
193Phe	9.891	9.88646	-0.00449	126.33898	126.6095	0.27052	0.04958
194Leu	9.1345	9.12129	-0.01321	121.65696	121.6044	-0.05256	0.02197
195Lys	9.052	9.02421	-0.02777	124.8637	124.85006	-0.01364	0.03005
196His	9.0216	9.01343	-0.00819	126.08113	126.04254	-0.03859	0.01462
198Asn	8.1168	8.10671	-0.0101	114.17456	114.16522	-0.00933	0.01166

199Gly	8.3977	8.38834	-0.00934	109.15035	109.1463	-0.00405	0.01001
200Asp	8.0936	8.08246	-0.01109	122.22836	122.21632	-0.01204	0.0131
201Lys	8.6497	8.63693	-0.01275	119.09926	119.09446	-0.0048	0.01355
202Ser	8.8739	8.84614	-0.02772	115.68614	115.6299	-0.05624	0.0371
203Leu	9.3702	9.37543	0.00529	127.56482	127.56278	-0.00205	0.00563
204Ser	8.9606	8.92083	-0.03979	124.15277	124.2313	0.07853	0.05288
205Thr	7.7825	7.75759	-0.02494	115.71775	115.96575	0.248	0.06627
206Leu	9.2787	9.30409	0.02541	128.8592	129.05743	0.19823	0.05845
208Arg	7.8429	7.84293	0	112.74015	112.74015	0	0
209Leu	8.5932	8.55048	-0.04275	128.57747	128.40267	-0.17481	0.07188
210Asn	9.2828	9.2769	-0.00585	125.97568	125.89521	-0.08047	0.01926
211Ala	8.4111	8.39147	-0.01967	121.75304	121.69356	-0.05948	0.02958
212Tyr	9.4596	9.45142	-0.00817	122.20412	122.15789	-0.04623	0.01587
213Asp	9.2021	9.19437	-0.00775	119.75975	119.71753	-0.04221	0.01479
214Gln	8.8453	8.83099	-0.0143	117.14457	117.16679	0.02222	0.018
215Asn	8.77	8.76475	-0.00521	119.90686	119.90307	-0.00379	0.00584

216Gly	8.2266	8.21894	-0.00762	109.13152	109.12039	-0.01113	0.00948
217Gly	9.2629	9.25976	-0.00313	112.54528	112.54108	-0.00421	0.00383
218Leu	8.7523	8.75233	0	127.24273	127.24273	0	0
220Ala	7.6282	7.62263	-0.00561	119.24532	119.25056	0.00524	0.00649
221Lys	9.0397	9.03117	-0.00856	117.98854	117.72826	-0.26028	0.05194
222Leu	9.4627	9.44198	-0.02073	126.16738	126.05751	-0.10987	0.03904
223Val	8.3865	8.3639	-0.02262	118.64921	118.59777	-0.05144	0.03119
224Ala	8.499	8.49901	0	120.83312	120.83312	0	0
225Thr	9.2933	9.27042	-0.02292	112.02219	111.63473	-0.38746	0.08749
226Asp	7.2947	7.29906	0.00437	117.80217	117.61402	-0.18815	0.03573
227Asp	8.64	8.67491	0.03494	120.59223	120.73949	0.14726	0.05948
228Leu	9.0679	9.05803	-0.00983	120.60647	120.44876	-0.15771	0.03611
229Thr	9.7959	9.78806	-0.00782	113.13255	113.18846	0.05591	0.01714
230Val	8.8221	8.8172	-0.00485	121.03581	121.05672	0.02092	0.00834
231Glu	8.2666	8.25643	-0.01019	119.79232	119.76207	-0.03024	0.01523
232Asp	8.0402	8.04016	0	116.99156	116.99156	0	0
233Glu	7.8301	7.8292	-9.34E-04	120.69666	120.69951	0.00285	0.00141

234Lys	8.2291	8.22907	0	118.95532	118.95532	0	0
235Asp	8.1939	8.19654	0.00261	121.80242	121.81779	0.01537	0.00517
236Gly	8.1361	8.14467	0.00861	108.30961	108.31737	0.00777	0.00991
237His	8.692	8.69195	0	119.86487	119.86487	0	0
238Arg	8.1365	8.14751	0.011	118.70849	118.74675	0.03825	0.01738
239Ile	8.5706	8.56919	-0.00142	120.97368	120.98548	0.0118	0.00339
240Leu	7.381	7.37391	-0.00711	121.94731	121.91629	-0.03103	0.01228
241Asn	7.8562	7.84994	-0.00629	119.37966	119.3996	0.01993	0.00961
242Ser	7.7043	7.7082	0.00393	113.3775	113.50998	0.13248	0.02601
243Leu	7.3294	7.3289	-4.50E-04	120.56347	120.51226	-0.05121	0.00899
244Phe	7.936	7.93473	-0.00124	114.81926	114.8081	-0.01116	0.0031
245Glu	9.0392	9.03921	-3.22E-05	120.07005	120.07788	0.00783	0.00134
247Phe	7.4644	7.46359	-8.24E-04	117.43559	117.41794	-0.01765	0.00376
248Asp	8.2073	8.20729	0	118.89046	118.89046	0	0
250Gly	8.3098	8.30007	-0.00976	108.9584	108.98255	0.02415	0.01378
251His	8.0603	8.05441	-0.00591	118.69796	118.66731	-0.03064	0.01101
252Ser	9.0017	9.02029	0.01859	116.85732	116.84688	-0.01044	0.02033
253Lys	8.5627	8.55593	-0.00679	125.89371	125.88879	-0.00492	0.00761

255Ile	8.2366	8.2366	0	121.58664	121.58664	0	0
256Arg	8.7316	8.72878	-0.00278	125.33483	125.31126	-0.02358	0.00671
257Ala	8.7447	8.73189	-0.01281	122.70139	122.64605	-0.05535	0.02203
258Ala	7.8256	7.81113	-0.01448	123.78266	123.78625	0.00359	0.01508
259Glu	8.4908	8.49083	0	117.26674	117.26674	0	0
260Thr	11.012	11.00061	-0.01172	122.04288	122.0562	0.01331	0.01394
261Ala	8.7232	8.71123	-0.01193	126.29296	126.30283	0.00987	0.01358
262Val	8.6856	8.66748	-0.01812	119.58849	119.56214	-0.02634	0.02251
263Gly	7.3327	7.33266	0	106.20685	106.20685	0	0
264Val	7.5319	7.51397	-0.01791	122.72209	122.74909	0.027	0.02241
265Leu	8.935	8.93	-0.00497	118.85334	118.85309	########	0.00501
266Ser	8.3715	8.34733	-0.02421	113.99367	114.01623	0.02256	0.02797
267Gln	8.0209	8.02088	0	124.47528	124.47528	0	0
268Phe	7.4739	7.47393	0	112.20027	112.20027	0	0
269Gly	7.9134	7.91214	-0.00121	109.60425	109.61565	0.0114	0.00311
270Gln	8.6731	8.66166	-0.01148	114.04152	114.03379	-0.00773	0.01277
271Glu	9.3435	9.33743	-0.00603	123.20269	123.19676	-0.00593	0.00702

272His	8.4569	8.4569	0	117.29663	117.29663	0	0
273Arg	7.1542	7.15421	0	117.39012	117.39012	0	0
274Leu	7.1097	7.10974	0	115.83452	115.83452	0	0
275Ser	8.5512	8.55116	0	118.33944	118.33944	0	0
277Glu	8.6302	8.62474	-0.00546	121.49912	121.48994	-0.00918	0.00699
278Glu	8.6106	8.60692	-0.00369	122.31683	122.30298	-0.01385	0.006
279Gly	8.4316	8.42791	-0.00373	110.23886	110.23764	-0.00121	0.00394
280Asp	8.2908	8.28598	-0.00482	120.83972	120.83412	-0.0056	0.00575
281Asn	8.0196	8.01957	0	124.01416	124.01416	0	0
							0.0196822

Table 4.2: CSPs on NS1B-CTD with the titration of 16bp dsRNA.

Yellow highlighted boxes indicate a significant shift, >0.02 ppm. Refer to Figure 1.5 for CSPs mapped onto the NS1B-CTD structure.

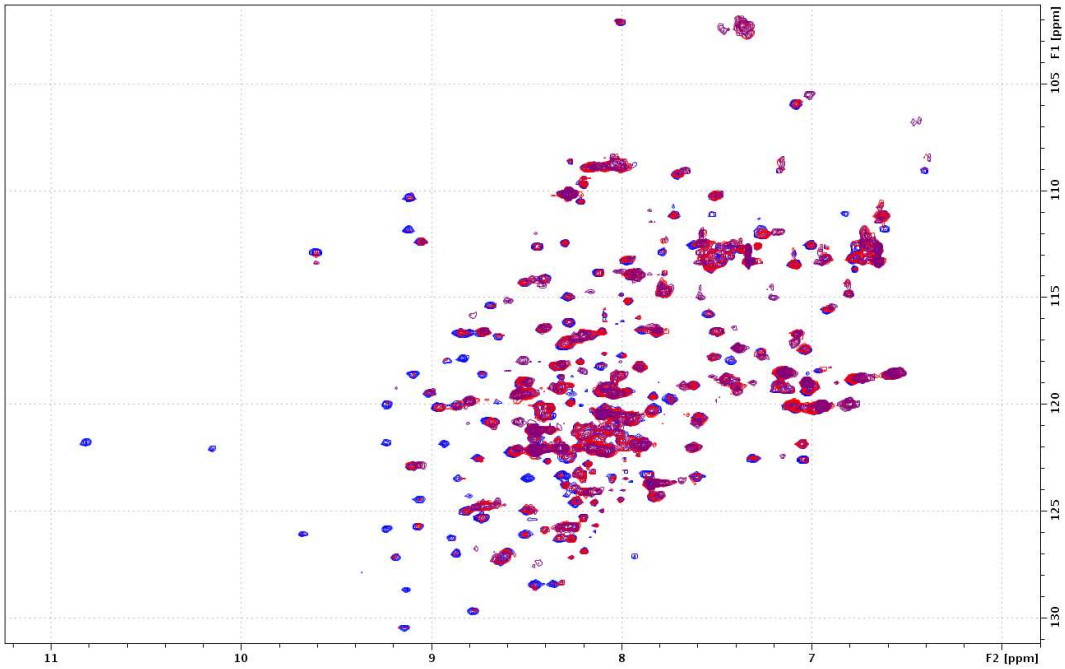

Figure 4.4: NH-HSQC of NS1B-CTD with (red) and without (blue) 3P-5'-hpRNA

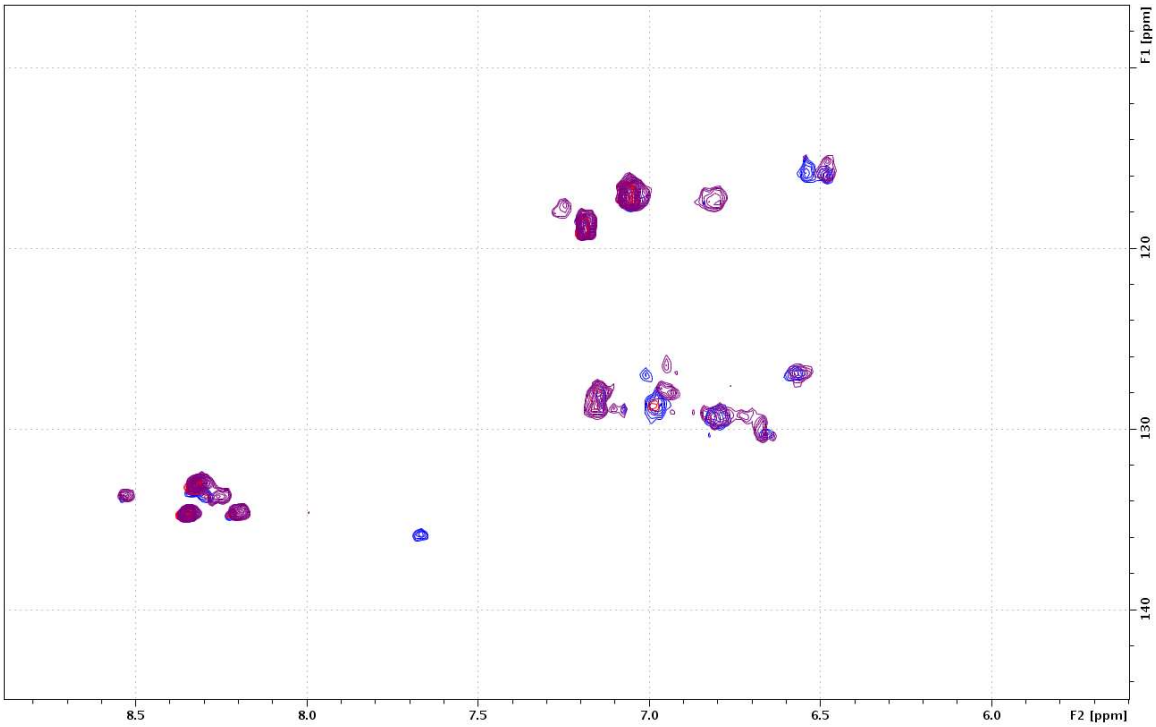

Figure 4.5: CH-HSQC of NS1B-CTD aromatic region with (red) and without (blue) 3P-5'-hpRNA

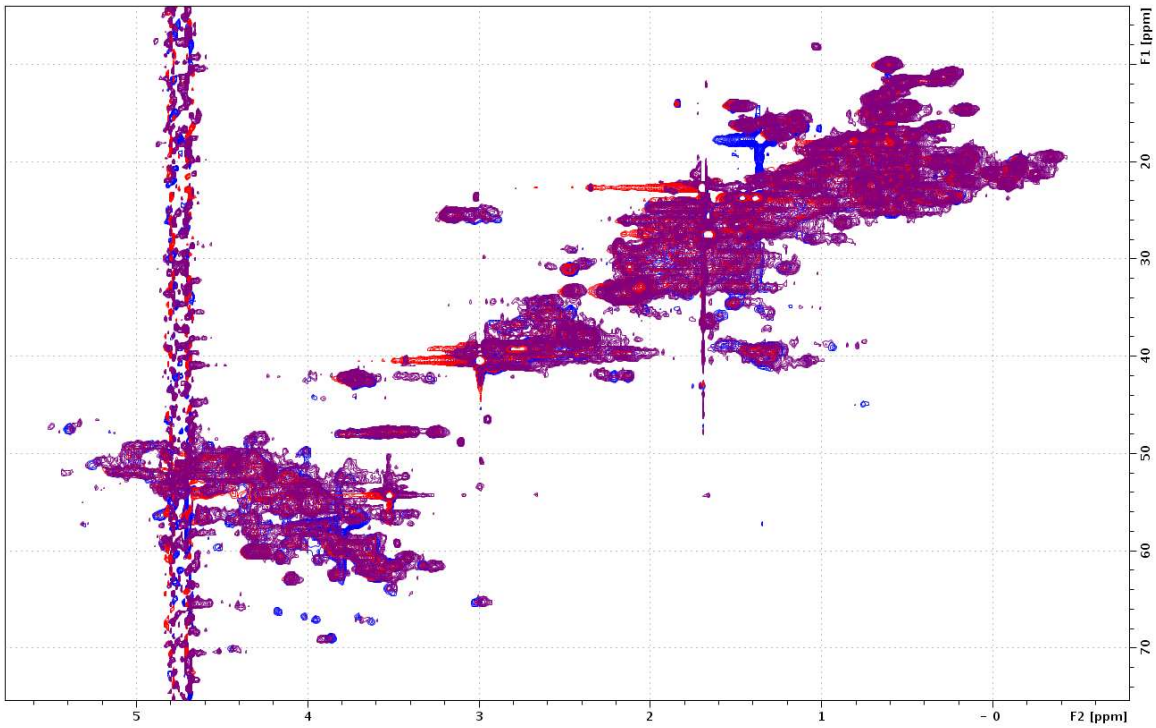

Figure 4.6: CH-HSQC of NS1B-CTD alaphatic region with (red) and without (blue) 3P-5'-hpRNA

Theory and expectations of RNA NMR:

Imide and imine hydrogen from guanine and uracil nucleotide have a unique magnetic field when base paired (12-15 ppm). Conviently, because there is only 1 hydrogen that is on this functional group in a 1D hydrogen spectrum we should only see 1 imide/imine resonance per base pair. It is also noted that if an imide/imine hydrogen is not base paired, it will exchange with water at a rate that broadens the peak to a point of not being obserable. Non-base paired hydrogens also have a unique range (10-15 ppm) but must be protected from exchange with water in order for them to be observable. In addition a 2D NOESY of the imide/imine hyrdogens will also show crosspeaks with hydrogens on the base that it is hydrogen bonded to (i.e. guanine imine has a cross

peak with cytidine H41 when base paired figure 4.7/4.8). This allows for quick and easy identification of either a G-C base pari of a U-A base pair. After identifying a peak as a G-C base pair of a U-A base pair the imine/imide hydrogens can also have crosspeaks with a sequently adjacent imine/imide hydrogen. By linking these peaks together one can start sequencing along the RNA, to determine the sequential order of G-C or A-U base pairs and establish their sequence-specific resonance assignments.

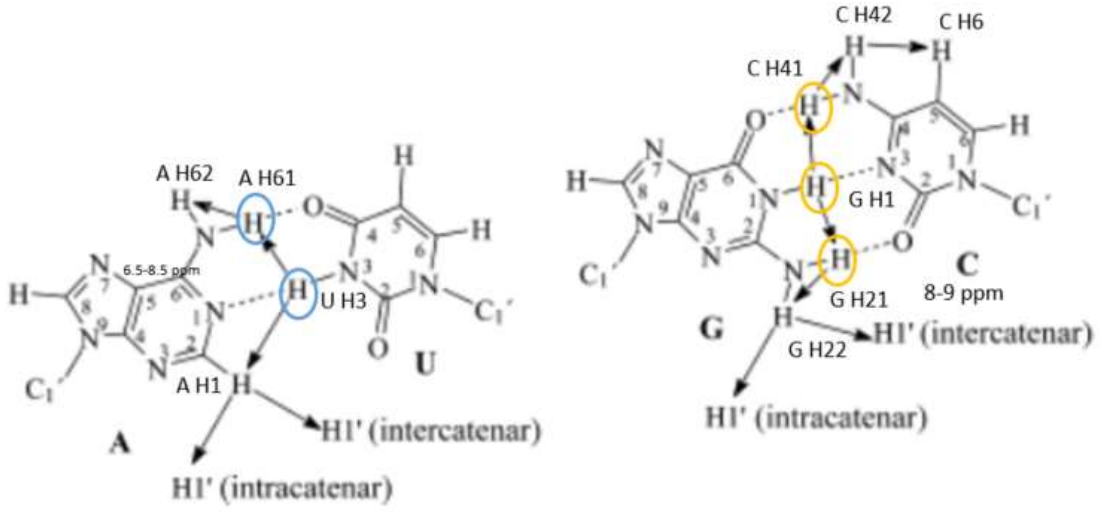

Figure 4.7: the location of imine/imide hydrogens when base paired and inter/intramolecular hydrogens that would produce a cross peak. Hydrogen naming

is per the BMRB website.

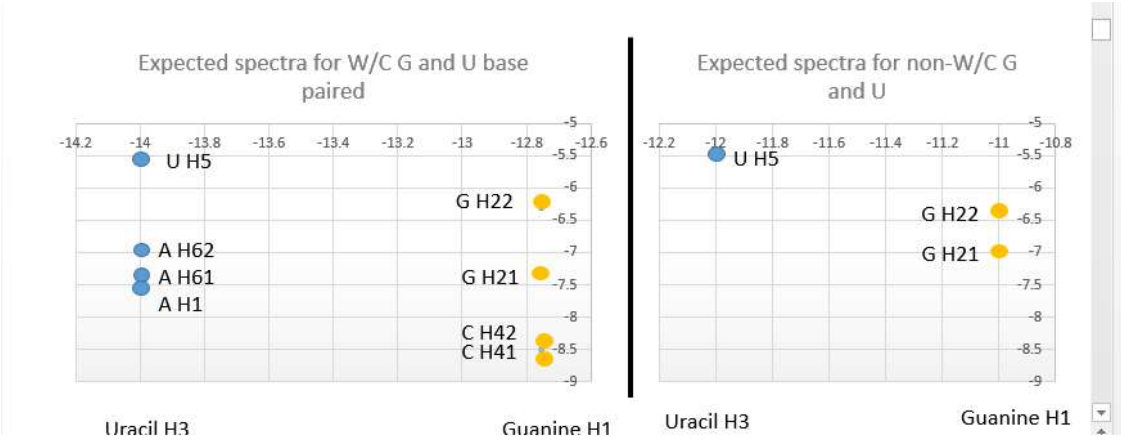

Figure 4.8: expected 2D NOESY cross peaks that can identify either a base paired or a non-base paired imine/imide. Hydrogen names and average ppm shifts are from the BMRB.

1D proton NMR was performed on the 16-bp dsRNA with and without NS1B-CTD to see if we could identify complex formation (Figure 4.9). We were able to clearly see a difference between the 1D spectra. We then used these spectra to confirm complex formation in other experiments, such as CD where complex formation could not be easily identified.

NMR data was also used to identify specific nucleic acids that are active in binding to NS1B-CTD. Looking at the structure and sequence of the 16-bp dsRNA we see that there are several G-C and U-A base pairs with 6/10 G-C base pairs near the end of the RNA (Figure 4.10). In the 2D NOESY it was clear which peak was a G-C base pair or a U-A base pair due to the pressence of a cross peak at between 12-13.5 ppm (Imide) and 8.0-9.0 ppm (C-H41)(Figure 4.11). This matches the theoretical NOESY results described above and shown in Figure 4.8. However, sequencing the RNA proved to be difficult and with the success of the 3P-5'-hpRNA NMR and SAXS experiments

resources were dedicated to that project with intentions of completeing the sequencing at a later time.

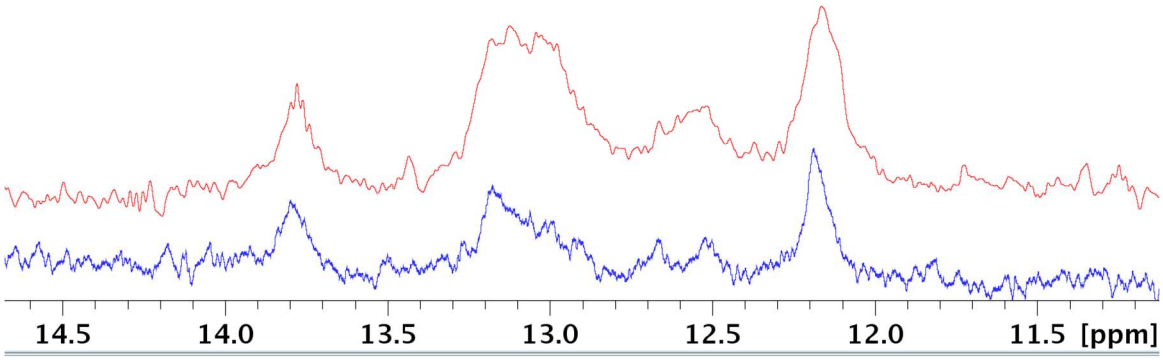

Figure 4.9. 1D Hydrogen NMR experiment focusing on the range RNA imine/imide hydrogens are visible. Experiment was performed with (red) and without (blue) NS1B-CTD. The experiment clearly shows binding due to changes in the spectra but peak identification was not possible due to weak peak-peak NOEs (Figure 4.11).

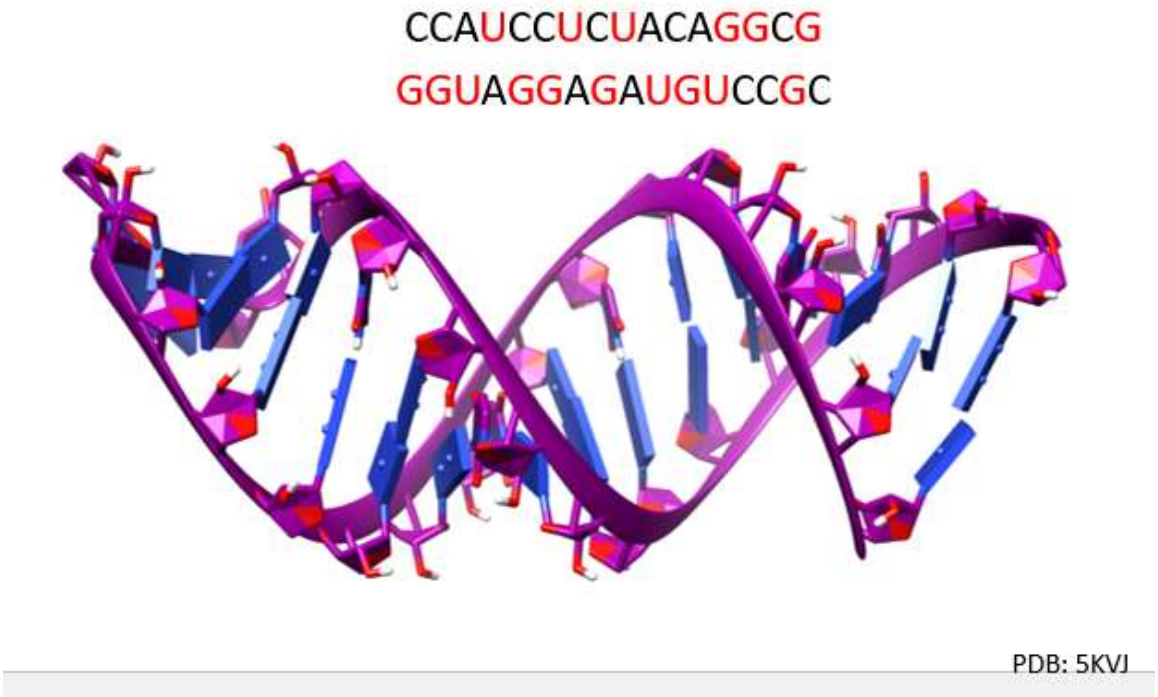

Figure 4.10: Structure and sequence of 16-bp dsRNA. Red letters signify an expected peak from an imine/imide hydrogen.

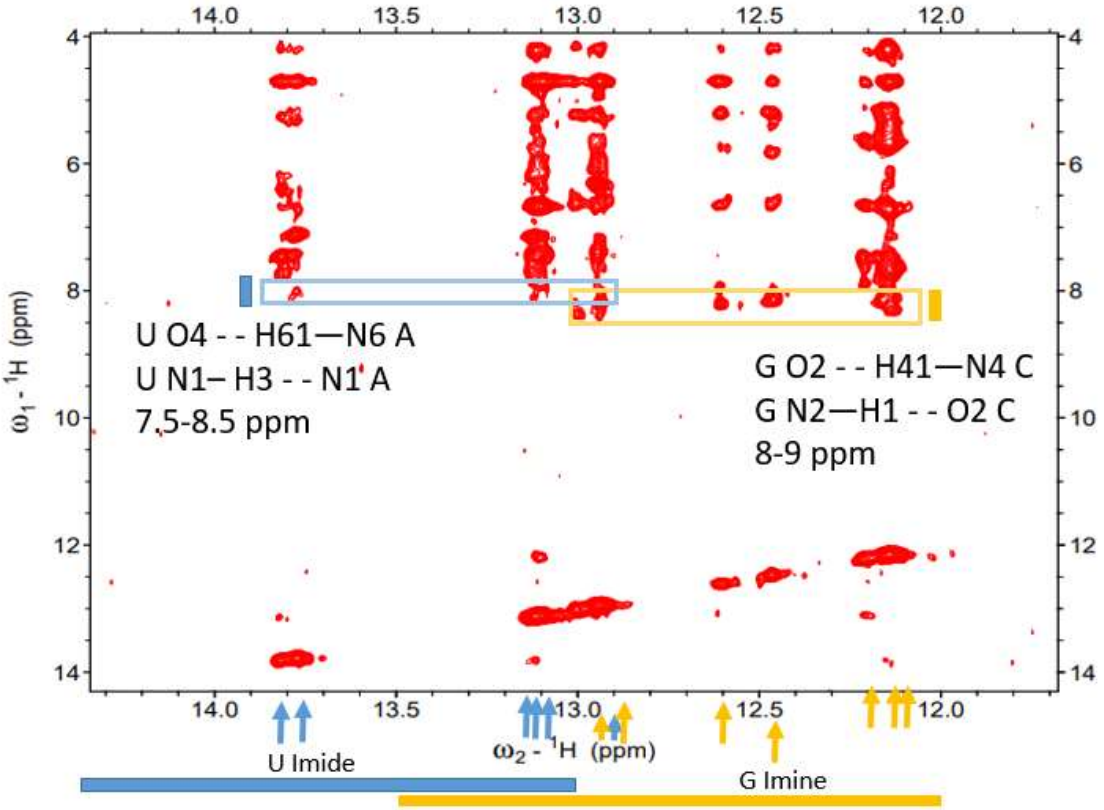

Figure 4.11: 2D NOESY of 16-bp dsRNA. Blue bar and arrows indicate regions to expect a U-A base paired imide, blue box indicates and expected cross peak between the U-imide hydrogen and H61 from Adenosine. Yellow bar and arrows indicate regions to expect a G-C base paired imine, yellow box indicates and expected cross peak between the G-imine hydrogen and H41 from Cytidine.

3P-5'-hpRNA NMR

1D Hydrogen NMR was first performed in similar conditions as the 16-bp dsRNA. Clear changes are observed in the spectrum but most noteworthy is the rise of at least 2

peaks that would belong to non-base paired imine/imides (figure 4.12). Comparing this to the structure and sequence in Figure 4.13 we see that there are 3 possible non-base paired RNA nucleotides which are located in the loop region of the hpRNA. Identification of these imine/imide hydrogens was attempted in the 2D NOESY, however, these peaks were only observable in the 1D spectrum. In the 2D NOESY, however, we see 1 G-C base pair, identified by arrow, and this peak shifts with the addition of NS1B-CTD (Figure 4.14), this shift is ~0.25 ppm. Comparing this to the structure and sequence of the 3P-5'-hpRNA we see that there is only 1 G-C base pair and it is located at the blunt end of the RNA.

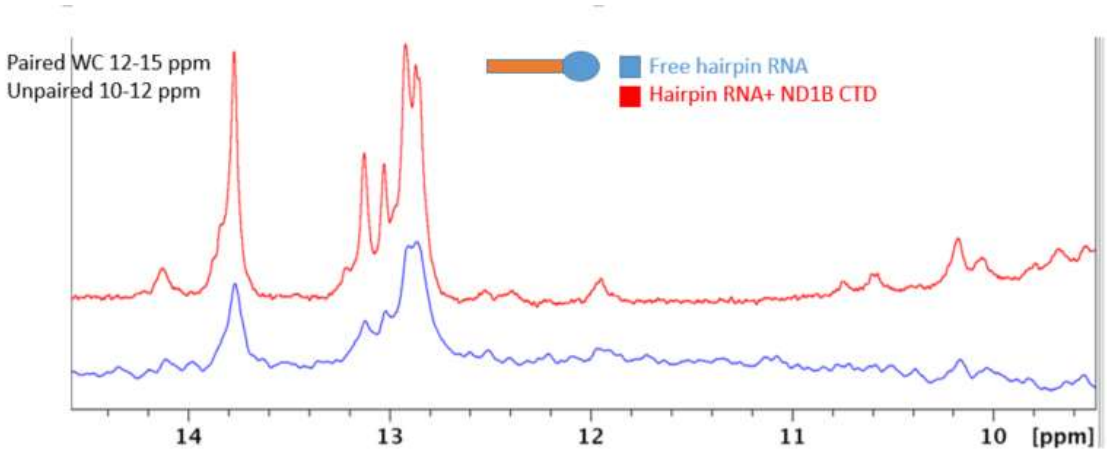

Figure 4.12: 1D Hydrogen NMR of 3P-5'-hpRNA with (red) and without (blue) NS1B-CTD. Ranges for expected Watson-Crick base paired nucleotides and non-base paired nucleotides are indicated in the upper left. With this range in mind it is interesting to see peaks rise in the non-base paired region of the spectrum

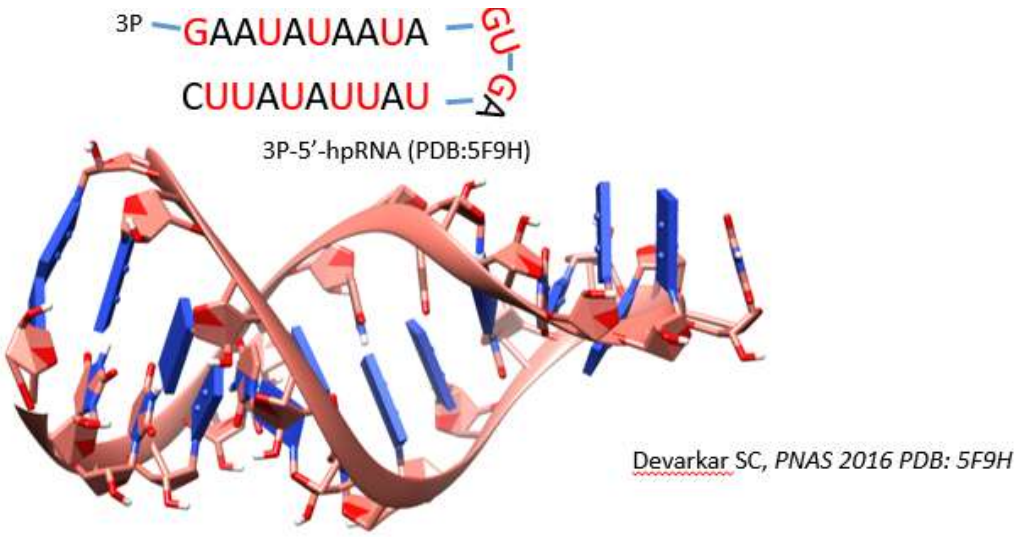

Figure 4.13: Structure and sequence of 3P-5'- hpRNA. Red letters signify an expected peak from an imine/imide hydrogen.

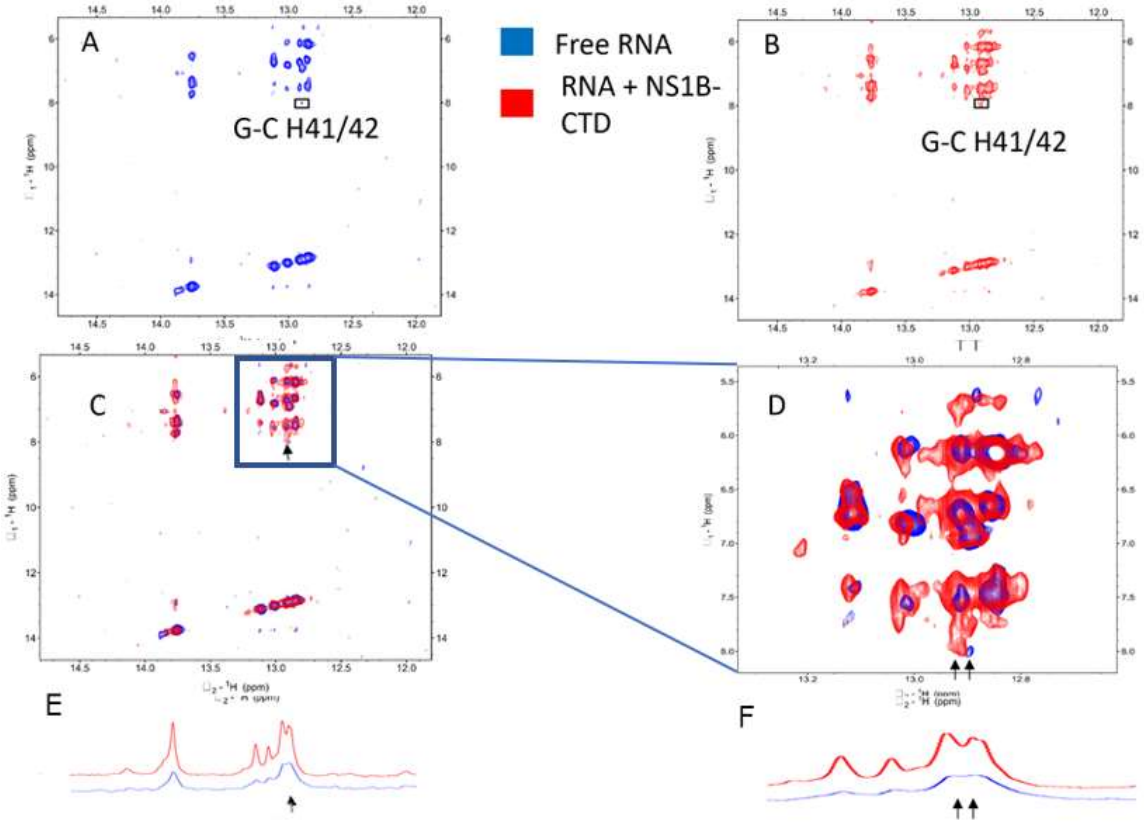

Figure 4.14: 2D NOESY of 3P-5'-hpRNA with (red) and without (blue) NS1B-CTD. A) RNA alone, box indicates G-C base pair. B) RNA with NS1B-CTD, box indicates G-C base pair. C) Full spectrum of RNA alone overlaid by RNA + NS1B-CTD spectrum. Arrow points to G-C base pair. D) Zoomed in of C to focus on the G-C base pair and to show the drastic shift of the G-C base paired peak. E-F) 1D proton NMR spectrum from Figure 4.12. E and F are on the same X-axis scale as C and D respectively.

Discussion:

While the NMR studies in this chapter leave a few open-ended questions and experiments to do, they do confirm the blunt end binding for the 3P-5'-hpRNA by the shift in the G-C base pair. We have plans to do complete peak assignments in NS1B-CTD in 1K buffer, measure chemical shifts in the NH/CH HSQC spectra with and with

3P-5'-hpRNA/16bp dsRNA, sequencing of in the 2D NOESY 16-bp dsRNA, and a 2D NOESY of the 16bp dsRNA with NS1B-CTD. These experiments were not completed due to reagent availability and untimely NMR magnet repairs. When resources are available again the protocols are in place to make these experiments fairly routine. The sequencing of the 16-bp dsRNA and comparison of the 2D NOESY with NS1B-CTD is a matter of completeness and we do not expect major surprises as we were able to obtain the SAXS structure assuming all nucleotides were active in binding. Gaining this information on the RNA side will greatly help in the confidence of our structure. However, it is of note that the blunt end binding model served the purpose of giving us the idea to test the 3P-5'-hpRNA. If this model is incorrect it will not affect the biological evidence, interpretation of the 3P-5'-hpRNA experiments, and interpretation of the virology experiments.

The NMR requires more work in the future. C-H and N-H NMR spectra need to be assigned in 1K buffer in order to really identify CSPs with the addition of 3P-5'-hpRNA. The CSPs for the 16-bp dsRNA also needs to be completed in the 1K buffer for completeness of the project. The NMR on 3P-5'-hpRNA did help improve the HADDOCK modeling results. There are two main conclusions we can draw from these experiments. First the G-C base pair at the blunt end is active in the binding shown in the 2D NOESY. The G-C base pair peak has a predicted shift of ~0.25 ppm, although this needs to be confirmed by titrating RNA and tracking the peak movement. Regardless if the peak shifted or disappeared there is a clear change to this peak. Secondly, the loop might play a role in NS1B-CTD binding. This conclusion is supported by the rise of the peaks between 10-12 ppm (non-base paired imine/imide region) in the 1D proton NMR spectrum. This rise in peaks could be observed for a few reasons; first the protein binds at this site and thus protects the hydrogens from exchanging with water narrowing the

peak and making it observable. Second, the event of NS1B-CTD at another location than the loop could make a structural change that would now protect the imine/imide hydrogens from exchanging. For this reason, when we identified active 3P-5'-hpRNA nucleotides we cannot exclude the possibility that the loop is active in binding.

Additionally, we attempted ^{31}P NMR to see if we could identify changes in the triphosphate environment, however, no conclusions can be made because the free RNA spectrum is well distributed but the NS1B-CTD + 3P-5'-hpRNA is a single peak large peak. Because the spectrums are so different, identifying a specific phosphorus atom that shifts is not possible. Carefully reviewing the literature and careful planning of this experiment will need to be done before it is attempted again.

Chapter 5: Studies of Protein-RNA Interactions by Combining Molecular Modeling and Small Angle X-ray Scattering (SAXS)

INTRODUCTION

MD Simulations:

Small Angle X-ray Scattering (SAXS) data provides a density envelope. A protein complex can be assembled by fitting each component into the envelope, or more specifically by fitting structure of the complex to provide a predicted scattering curve that best-fits the experimental scattering curve. However, this approach can be quite challenging without having significant restraints on the potential structure of the complex. A simple metaphor would be trying to predict a 3-dimensional shape from a 1-dimensional line. There are many 3D shapes that are equally consistent with the 1D data. However, a given 3D shape will correspond to only a single 1D line. Hence, given a reasonably accurate model of the complex, the 1D line from this model can be compared with 1D line from the data set.

In this study, we generated many 3D models consistent with experimental data available for individual components of protein-RNA complexes and data for the complex itself, and predicted their 1D small angle X-ray scattering (SAXS) curves. The predicted SAXS curves were then compared with the experimental SAXS curves, and the models (or distributions of models) which best fit the experimental SAXS data were selected for further refinement.

Fortunately, the NS1B-CTD protein (2), the 16-bp dsRNA (PDB: 5VKJ), and the 3P-5'-hpRNA (15) all have crystal structures. The crystal structures of the RNAs were used without alterations to model the corresponding RNA components of the complexes. However, the X-ray crystal structure of NS1B-CTD was missing the electron density of

the last five-residue polypeptide segment (276-281), which needed to be modeled. MD simulations were performed to estimate the conformational distribution these disordered C-terminal amino acid residues.

HADDOCK:

High Ambiguity Driven protein-protein DOCKing (HADDOCK) is a very successful molecular modeling program which takes biochemical or spectroscopic data as an input and computes constrained docking of biomolecules (16, 17). Despite its name HADDOCK has also proven to also be a reliable docking program for modeling protein-nucleic acid complexes (17). To model the complex, we used the CD and NMR data described in Chapters 3 and 4, together with X-ray crystal structures of NS1B-CTD, 16-bp-dsRNA or the 3P-5'-hpRNA, with the HADDOCK webserver (expert level access was required) to create models of NS1B-CTD bound to the two RNAs. HADDOCK uses these experimental data to constrain and generate a small set of models. However, there are still a significant number of models that can fit the data (as shown in Figure 5.1). SAXS was then used to filter out the incorrect models, and identify the subset of models consistent with these scattering data.

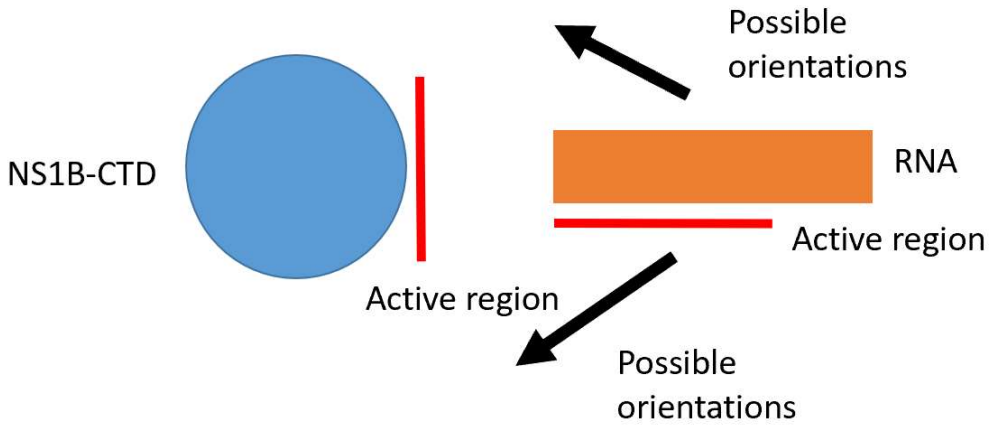

Figure 5.1: Diagram demonstrating many solutions can fit the docking data driving HADDOCK. Input data into HADDOCK, red bars represent a theoretical active binding residues and sites determined by biochemical or biophysical methods. Using NS1B-CTD as a stationary object for reference the RNA can still pivot and bind at several different angles (shown by arrows) in relation to NS1B-CTD. Despite narrowing down the binding site to a small region on NS1B-CTD and the RNA substrate HADDOCK will still produce several models that will be incorrect, thus a need for filtering.

Small Angle X-ray Scattering (SAXS):

SAXS is an extremely important tool for determining orientations of molecular components in a complex. In SAXS, the sample is exposed to high intensity X-ray light. A large portion of the X-rays pass through the sample unaffected, some X-rays are absorbed by the sample, and a small percentage of the X-rays interact with the electron field of the atoms in the sample and scatter over a range of scattering angles. The pattern of the scattered light is recorded on a detector. The data are plotted as a function of the sum of all light at a certain radius (I) vs. the radius or distance from the center of the beam (q). The main difference between SAXS and X-ray crystallography is that SAXS is performed on molecules in solution. While SAXS gives the benefit of taking measurements in biologically relevant environments, resolution is lost due to movement of the molecule. A good metaphor is taking a long exposure picture of someone who is posing for the camera vs. that same person doing their normal daily activities. If they are posing you can get high resolution of their features and face. The picture of them moving will give a better idea of what they look like every day, but it will be lower resolution.

SAXS is an experiment of differences. This means that the scattering data from buffers must be first be collected. Then biomolecules are added to the exact same buffer, and the difference in scattering by the buffer alone and the buffer plus

biomolecule is analyzed (23, 43, 46, 47). SAXS essentially measures the change in the scattering by the buffer due to the introduction of biomolecules. Depending on the polar dispersion on the biomolecule, flexibility of the biomolecule, and ionic strength in the buffer, the scattering from the solvent/buffer itself can drastically change. This is important in the interpretation of the SAXS data. A common mistake arises when scientists expect the biomolecule to fit tightly within the resulting electron density envelope. However, water and other solvent molecules will often reorient to accommodate for the biomolecule. This reorientation is a difference in structure of the solvent and is detected by SAXS and included in the electron envelope. This is called the hydration layer. Thus, the electron density envelope will generally be slightly larger than the atomic coordinates of the biomolecule. It is also important to keep in mind this hydration layer will change in size depending on the ionic strength of buffers (47).

While both protein and RNA structures can be studied with SAXS, it is important to also keep in mind that there are differences in their intrinsic scattering. RNA tends to scatter X-rays more strongly than protein. Thus, the mass and $I(_0)$ of protein and RNA are estimated slightly differently. $I(_0)$ is an estimate of where the scattering plot will intercept the Y-axis and is directly affected by mass. $I(_0)$ is an estimate because in a SAXS experiment it cannot be directly measured due to the presence of a beamstop. Since RNA $I(_0)$ is higher than protein $I(_0)$, the mass of the RNA will be estimated to be higher than protein for the same $I(_0)$. For a protein:RNA complex the mass is usually estimated to be somewhere between the estimated masses of the RNA alone and protein alone. While this method has inaccuracies, it is very convenient because is it does not require knowledge of the exact concentrations of RNA and protein (43). This is the primary, but critical, difference and difficulty when developing SAXS structures of protein:RNA complexes (46).

Due to the ambiguous nature of the input restraints, HADDOCK often produces many models (e.g. in this study, more than 10 clusters of ~ 4 models each, or more than 40 models). SAXS data can be used to determine the overall shape of the complex and filter out molecule models with protein-RNA orientations that do not fit the experimental X-ray scattering data. This is done by creating a calculated "predicted" SAXS curve from each individual model and comparing these curves with the SAXS data that is collected. The point at which the SAXS curve diverges from the model calculated curve is the resolution at which the two models no longer match. This matching is quantified by χ^2. $\chi$is affected by a multitude of factors including noise of data (which, in turn, can be affected by sample quality) and whether the molecular system is flexible and if that flexibility is modeled correctly (46, 47). The best optimized system will have a $\chi^2 = 1$, however, the acceptable χ^2 will change depending on sample quality, for example, SAXS data that is not noisy will inherently have a low χ^2 because the trend line will be more difficult to fit. Noisy data will have a low χ^2 because the "fitting region" will be much wider. That being said the cutoffs we used to determine and "acceptable model" was $\chi^2 < 3.00$ (this is regardless of sample/data quality). Despite the absolute maximum χ^2 cutoff we also would adjust the "good" model cutoff depending on the sample/data quality and relative matching of the group of models that were being submitted (11). In addition to matching the SAXS data to a model's calculated SAXS curve we also compared the model's calculated P(r) and the sample's P(r) The P(r) is a distribution of the distances between every atom and all other atoms in the structure and is determined by Indirect Fourier Transformation (IFT). There is a monodispersed system, for which the explicit connection between the particle form factor $F^2(S)$ and scattering intensities I(s) can be obtained. However, due to the inherent complications in modeling inhomogeneous particle shape (flexibility of proteins) and dispersion there are a few

methods to solve the P(r) function. One function that accurately describes the method used here is given by:

$$\langle F^2(s)\rangle = \int_0^\infty \langle F_0^2(s,R)\rangle m^2(R) D_N(R) dR$$

Where $F^2(s)$ is the average form factor for the system, $F^2_0(s,R)$ is the averaged, normalized form factor of the particles of size R {$F_0(0,R) = 1$}. m(R) connects the chosen effective size with the full scattering length of a particle. Finally $D_N(R)dR$ corresponds to the number of particles that fall within the interval (R,R + dR).

Because we are calculating distances of the atoms this method is much more sensitive to small changes in the model versus comparing the SAXS curves. We choose to look at the P(r) if there were multiple acceptable models that were functionally different (46).

Modeling for full length NS1B bound to dsRNA:

The model of NS1B-CTD binding to the blunt end of dsRNA was a very surprising result in terms of energetics because interface surface area contacts is typically maximized. Due to replication of the results we decided to try to make sense of why it would bind in this fashion. To understand this highly focused interaction we decided to take a step back and look at this interaction in terms of the full-length NS1 molecule (NS1B-FL).

Hybrid Methods for Modeling Protein Nucleic Acid Complexes:

Using NMR to drive a molecular modeling which then would be filtered by SAXS is a technique in its early stages, however, one prime example of how powerful this technique can be is seen in Belorusova AY. et al. (46). While we are exploring a protein:RNA complex, the structural analysis by Belorusova AY. et al. (46) is a

protein:DNA complex. However, the methodology we would use is very similar (NMR drives modeling, modeling generates a large pool of possible modes, SAXS filters out bad models to optimize final solution). Belorusova AY. et al. (46) provided the structure of the

complex between Retinoid X receptor (RXR) and dsDNA. The N-terminal domain (NTD) of these receptors is an intrinsically disordered domain and highly variable. The NTD is also close to the DNA binding site. Belorusova AY et al. (46) used NMR to determine the amino acid residues bind to the DNA segment by looking at the ^{15}N-^{1}H HSQC of the NTD with and without DNA. It is important to note that the NTD is not completely intrinsically disordered and contains 130 amino acids. The folded amino acids that are folded in the NTD are the ones that can be observed in the HSQC. In the HSQC spectrum, they noticed observed only 7 peaks which exhibited small chemical shift perturbations (CSPs) (Figure 5.2). They then used this information, together with X-ray crystal structures of dsDNA bound to ΔNTD RXR, and Isothermal Titration Calorimetry (ITC) to piece together a full-length structure bound to dsDNA. SAXS data was then used to screen the various assemblies (Figure 5.3; notice the differences in the P(r) curves of the various modeled assemblies). Because the NTD is intrinsically disordered even in the complex formed with dsDNA bound, this region has to be modeled as ensembles. They used Ensemble Optimization Method EOM. This method selects randomly selected ensembles from a large pool of models and fits to SAXS data to minimize discrepancies. Based on this analysis Belorusova et al. propose a final model of the complex with the NTD adopting a dynamic ensemble modeled from the EOM calculations by conformational selection (Figure 5.4). In this study, Belorusova AY. et al. used SAXS and NMR to gain insights into the hydrodynamics of RXR NTD and

region with and without dsDNA. They were able to show that the NTD is dynamic even in the presence of dsDNA, and that the SAXS data confirm this conclusion. CSPs helped explain change in RXR's affinity to DNA with and without the NTDs. With this data they were able to generate an ensemble of structures for the full-length RXR protein, both dsDNA-free and bound to dsDNA.

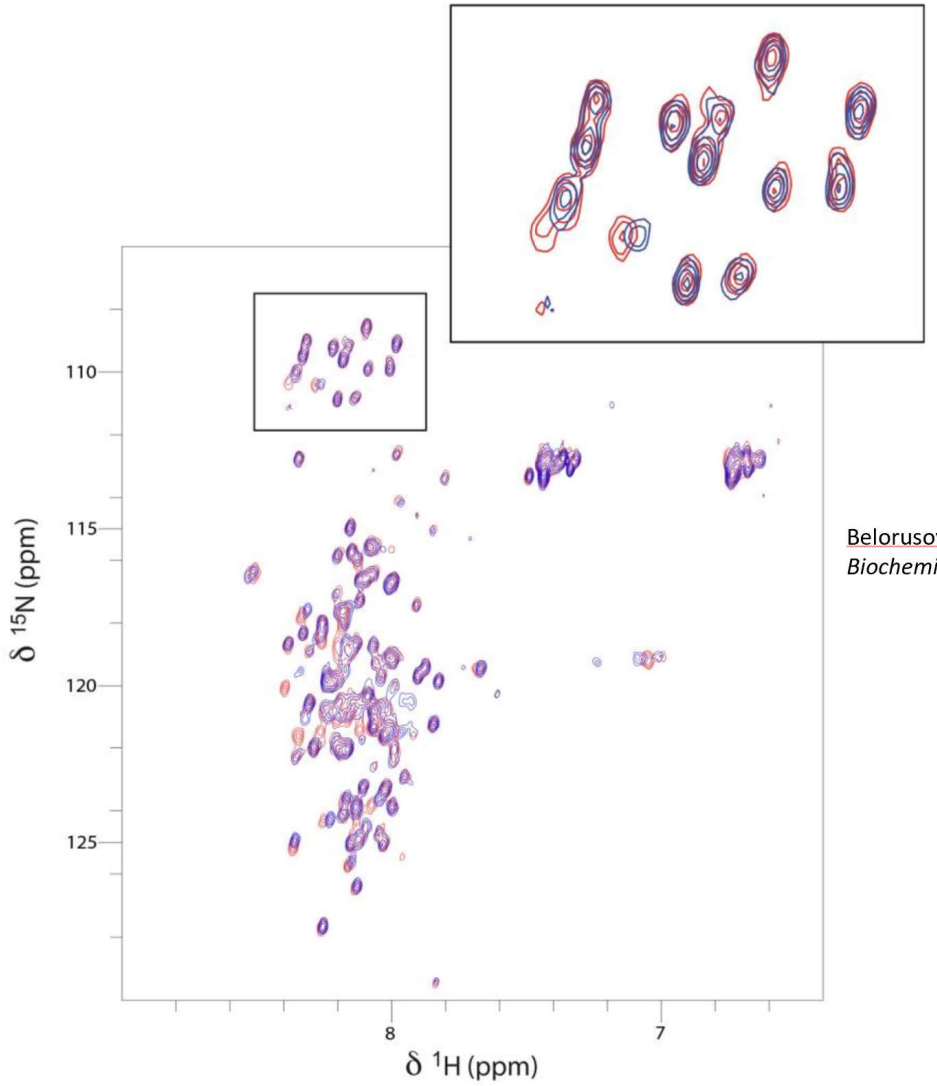

Belorusova A. et. al. *Biochemistry.* 2016

Figure 5.2: HSQC of Retinoid X receptor (RXR) N-terminal domain (NTD) free of DNA (blue) and with DNA (red)

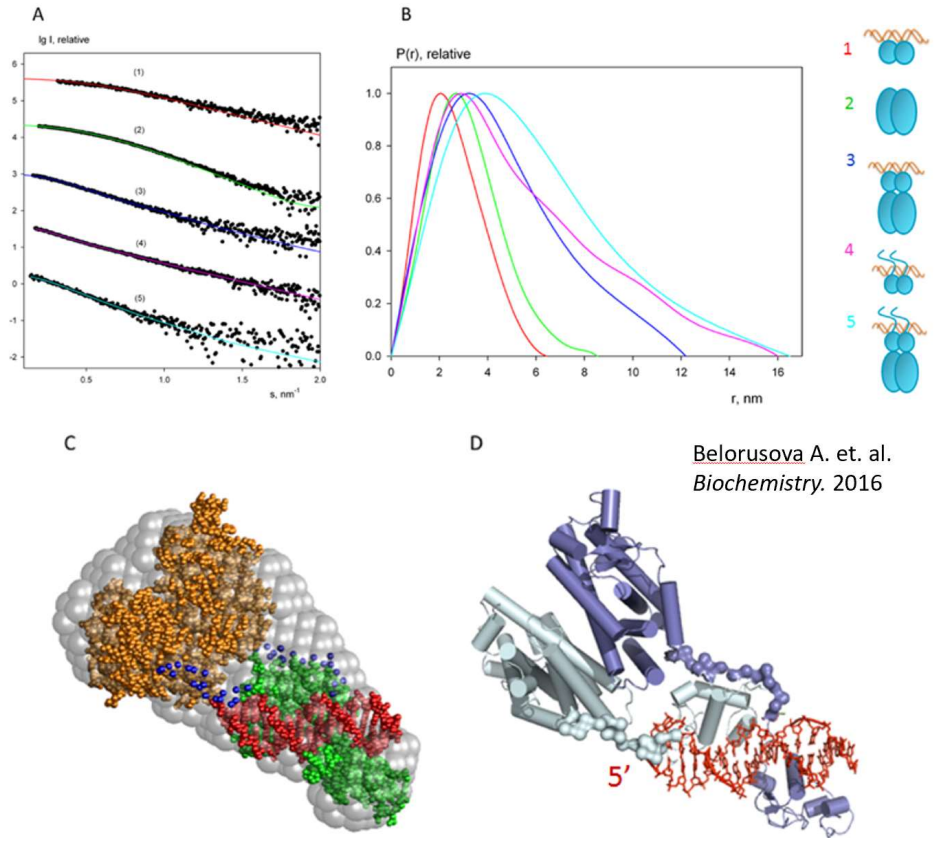

Figure 5.3: SAXS data compared to various complexes with DNA. A) SAXS data matched with predicted SAXS curve from models. Black dots represent the raw SAXS data while colored lines match the number coloring for the cartoon models on the right. B) P(r) curves for models. C) Predicted envelope for ΔNTD RXR bound to DNA. D) ribbon cartoon model of ΔNTD RXR.

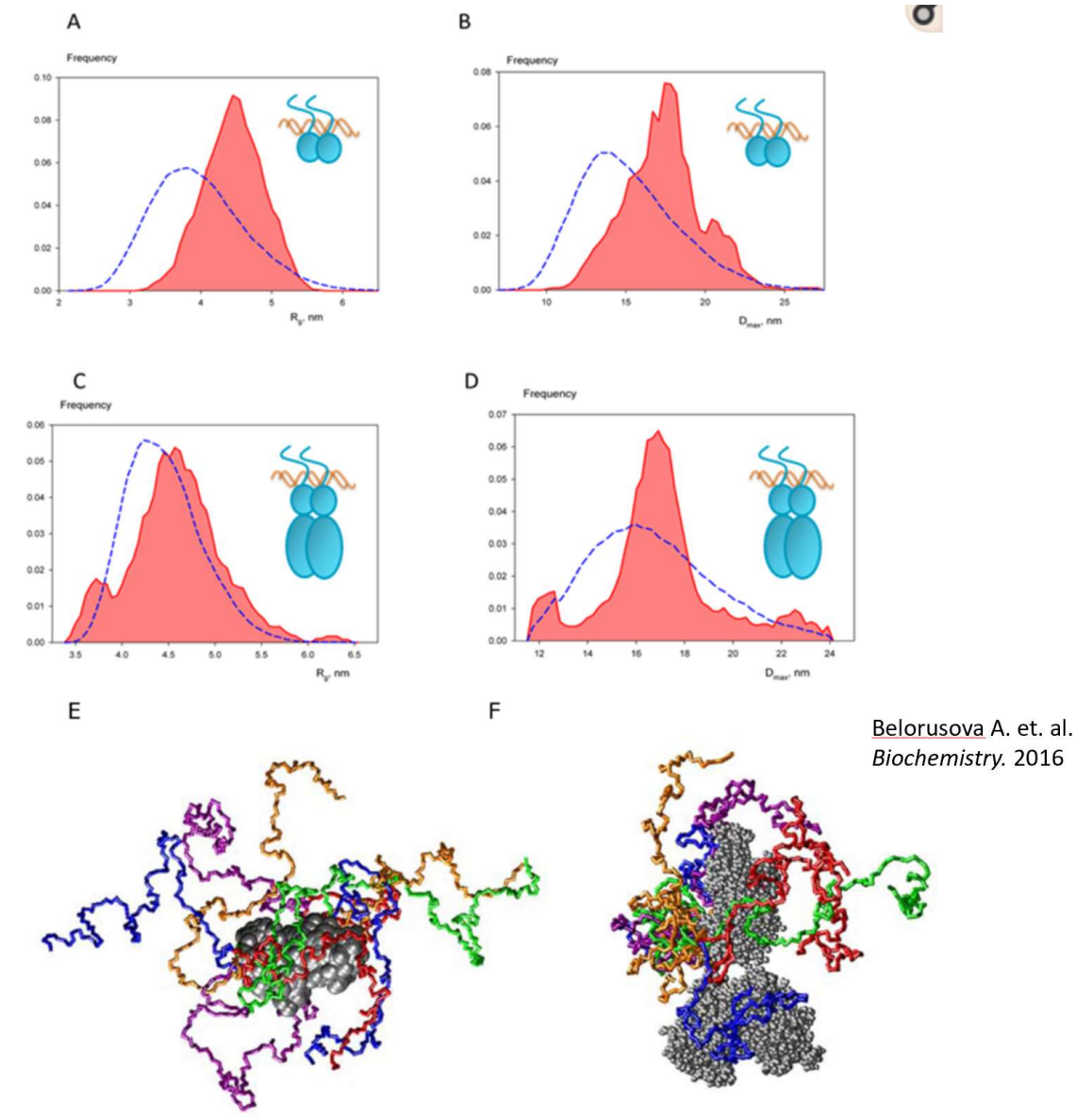

Figure 5.4: Modeling of the NTD with RXR and DNA. A-D: Size and shape distribution. R(g) (A and C) and D_{max} (B and D) of NTD-DBD bound to DNA (A and B) and full length RXR bound to DNA (C and D). Distributions are calculated from selected structures (red lines) compared to random pools generated by EOM (blue lines) E) ensemble of NTD-DBD, DNA is not shown for clarity. F) ensemble full length RXR bound to DNA complex.

METHODS

MD simulations:

Molecular dynamics simulation was carried out with AMBER 14 force fields (59). The run plateaued in the RMSF graph after 25 nsecs; however, the entire run was run for 300 nsecs. During the plateau a decoy was created every 10,000 steps which took 2 fsecs (decoy every 20 psecs). The lowest scored 10% of all decoys were then subjected to Rosetta clustering, as described previously (10). The clustering was limited to 10 clusters. Each cluster was plotted by RMSD from each other and the center of each cluster was chosen as the representative model. The model that was used in all of the following modeling was the center of the best ranked cluster. Ranking was determined by lowest energy and largest cluster size.

HADDOCK docking:

The details of methods for using the HADDOCK server for docking protein and RNA molecules has been described previously (16,17).HADDOCK takes inputs such as structures, active and passive amino acids/nucleotides (referred to as residues just for this specific application), and distance constraints to drive the docking. Active and passive residues are determined by biophysically or biochemically. Active residues are defined as essential residues involved in binding, these residues are manually defined by the user. Passive residues are defined as residues that may or may not be involved in binding and can be manually or automatically defined. If passive residues are defined by automation the server will choose residues immediately surrounding the active residues. The large CSPs from NS1B-CTD (2) were used to define active residues on NS1B-CTD, which drove the docking of both the 16-bp dsRNA and the 3P-5'-hpRNA models. In the 16-bp dsRNA model, every nucleotide was assumed to be a possible active nucleotide because we had no data of specific nucleotides involved in binding. In the 3P-5'-hpRNA

HADDOCK special modifications to the RNA file were made. HADDOCK cleans the PDB files it is given by removing any atoms it does not recognize, except for HETATMs. In the PDB file it was necessary to remove the bond between the triphosphate and the RNA. However, now that the triphosphate was no longer tethered to the RNA it is free to “float away” in the docking calculations. To overcome this, we also submitted a constraint file that constrained the triphosphate within 3.5 Å +/- 0.5 Å.

Constraints file in CNS format

ASSIGN (resid 0 and atomtype PG) (resid 1 and atomtype O5’) 3.5 3.0 4.0

This provides for an effective chemical bond between the triphosphate and the RNA. From the 2D NMR studies we were able to see the first and only GC base pair had a significant CSP. In addition, the 1D hydrogen experiment had peaks rising in the range of non-base paired imines/imides. While this is not definitive of binding to the ssRNA loop region of the 3P-5’-hpRNA, in the model we assumed it was possible. Therefore, the blunt end and the loop were active in the docking.

The resulting files were then zipped into one file and compared to the SAXS data using the FOXS server (11). The analysis of these results is described in much more detail in the SAXS section in Chapter 5. All graphical analysis and PDB figures were created using UCSF Chimera (9).

SAXS:

Beamline choice:

Beamlines used:

BioCAT: 18ID at the Advanced Photon Source, Chicago, IL

SIBYLS: beamline 12.3.1 at the Advanced Light Source – Lawrence Berkeley National Laboratory, Berkeley CA

MacCHESS: 161 Synchrotron drive, Ithaca NY – Cornell University

The beamlines that were chosen were done so on the basis of available time. The data shown is a representation of the best data collected and is from several different beamlines. Despite this all observations and conclusions were first identified at the SIBYLS beamline. However, due to the novel binding, replication and optimization of the samples was necessary.

NS1B-CTD:

NS1B-CTD was prepared in 2K buffer in a 96-well plate and shipped to SIBYLS following the HT-SAXS protocol and SAXS was performed with previously described methods (20, 21, 22, 23). A concentration dependent SAXS run (10 mg/ml, 6 mg/ml, 4 mg/ml, 3 mg/ml, 2 mg/ml, and 1mg/ml) determined that the optimum concentration for NS1B-CTD is 4 mg/ml (250 uM). All future experiments at SIBYLS and other beamlines were performed at this concentration. The SAXS data was analyzed using a combination of Scatter (24) (for general SAXS curve viewing and envelope calculations) and PRIMUS (13) (for Guinier calculations, P(r), R_g, D_{max}).

NS1B-CTD bound to 16-bp dsRNA:

Sample concentration dependence was performed prior to this particular run. Optimum concentration was determined at 250 μM (4 mg/mL of NS1B-CTD) and RNA was added to make a 1:1 NS1B-CTD:16bp dsRNA ratio. SAXS data was collected on CHESS beamline G1 at 9.924 keV (1.249 Å) at 7.7×1011 photons/s. The X-ray beam was collimated to 250 × 250 μm^2 diameter and centered on a capillary sample cell with

1.5 mm path length and 25 μm thick quartz glass walls (Charles Supper Company, Natik, MA). The sample cell and full X-ray flight path, including beamstop, were kept *in vacuo* (< 1×10-3 Torr) to eliminate air scatter. Temperature was maintained at 4 °C. Images were collected on a dual Pilatus 100K-S detector system (Dectris, Baden, Switzerland). Sample-to-detector distance was calibrated using silver behenate powder (The Gem Dugout, State College, PA). The useful q-space range (4πSinθ/λ with 2θ being the scattering angle) was generally from q_{min}= 0.01 $Å^{-1}$ to q_{max}= 0.27 $Å^{-1}$. Image integration, normalization, and subtraction was carried out using the BioXTAS RAW program (12). Radiation damage was assessed using the CORMAP criterion as implemented in RAW's built-in averaging function (19). Sample and buffer solutions were normalized to equivalent exposure before subtraction, using beamstop photodiode counts. Sample plugs of approximately 20-30 μl were delivered from a 96-well plate to the capillary using a Hudson SOLO single-channel pipetting robot (Hudson Robotics Inc. Springfield, New Jersey). To reduce radiation damage, sample plugs were oscillated in the X-ray beam using a computer-controlled syringe pump. Typically, 10-20 undamaged 1s exposures were averaged to produce buffer and sample profiles. Scattering intensities were placed on an absolute scale using water as a standard. These methods are summarized in **Table 5.1:**

SAXS Data Collection	
Instrument	BioSAXS facility at the Cornell High Energy Synchrotron Source beamline G1 with dual Pilatus 100k (Dectris) detector
Wavelength, energy	1.249 Å , 9.924 keV
Flux	7.7×1011 ph/s
Beam size	250 μm × 250 μm
q-measurement range	0.01-0.28 Å-1 (SAXS)
Absolute scaling method	water standard

Basis for normalization	transmitted intensity via beamstop photodiode
Method of monitoring radiation damage	comparison of sequential exposures via CORMAP statistic
Exposure time, number of exposures	1 s × 10 exposures
Sample configuration	1.5 mm OD quartzglass capillary with 10 μm thick walls in vacuuo; Robot: oscillating 30 μl sample
Data processing	
SAXS data reduction	Radial averaging, frame comparison, and subtraction using BioXTAS RAW 1.4.1 (12)
Basic analysis	Guinier fit, P(r) using PRIMUS (13)

Table 5.1 MacCHESS Data Collection Parameters

NS1B-CTD bound to 3P-5'-hpRNA:

SAXS was performed at BioCAT (beamline 18ID at the Advanced Photon Source, Chicago). Sample was measured in a SAXS flow cell which consists of a 1.5 mm ID quartz capillary with 10 μm walls held at 20 ^{o}C using 12 keV incident x-rays. Scattering intensity was recorded using a Pilatus3 X 1M (Dectris) detector which was placed 3.44 m from the sample, giving us access to a q-range of 0.012 $Å^{-1}$ to 0.3 $Å^{-1}$. During exposure sample was flowed through the beam in a single direction, and 0.5 s exposures were acquired every 2 seconds during flow. Data was reduced using BioXTAS RAW 1.4.1 (12). Buffer blanks were created by recording SAXS data from a matched buffer and subtracted from exposures from the sample to create the I(q) vs q curves used for subsequent analyses. All sets of nominally identical measured profiles were automatically compared using the CorMap method (18) to test for radiation damage or other changes.

Data analysis:

As mentioned previously a combination of RAW, Scatter, and PRIMUS was used for the data analysis. In addition, comparison of SAXS data curves and model calculated

curves was done using FOXS webserver (11). The resulting calculated SAXS curve for the model was then downloaded and P(r), R_g, and D_{max} were calculated using PRIMUS. To compare the P(r) plots it was required to export the data points from the GNOM file that is created when calculating the P(r), into an Excel spreadsheet, and create a plot within Excel. Visualization of models and SAXS envelopes was done using UCSF Chimera modeling software (9).

Modeling of full length NS1B in complex with dsRNA:

Crystal structure of NS1B-NTD was used (25) for the structure of the NTD. There is no NS1B-NTD bound to RNA crystal structure however, there is a NS1A-NTD crystal structure bound to RNA (26). Using matchmaker tool inside of UCSF Chimera the NS1B-NTD crystal structure was aligned onto the NS1A-NTD bound to RNA crystal structure to give us a model of NS1B-NTD bound to RNA. We can do this with confidence due to structural similarities between NS1A-NTD and NS1B-NTD. The RNA in the resulting model was replaced by the 16-bp dsRNA crystal structure (PDB: 5KVJ, 27). The selected NS1B-CTD bound to 16-bp dsRNA model from the SAXS experiments was aligned using the matchmaker tool and the dsRNA as the template. Because the NS1B-NTD binds as a dimer there will be two NS1B-CTD molecules, so this last step was repeated but for the opposite side of the RNA to give two molecules of NS1B-CTD bound to 16-bp dsRNA. Slight manual adjustments in the positioning of the domains was necessary because the 16-bp dsRNA was not perfectly symmetrical.

Results:

MD based modeling of NS1-B:

MD calculations were performed to provide a model of the N-terminal 5 residues of NS1B. The top cluster that the MD produced had a large number of models (Figure 5.5). The center of this cluster was chosen and eventually compared to the SAXS data which

gave us a reasonable χ^2 (Figure 5.11 A/B). Because the SAXS of NS1B-CTD matched the model it was decided that is was not necessary to revisit the modeling. This protein model was then used for all future HADDOCK docking and modeling.

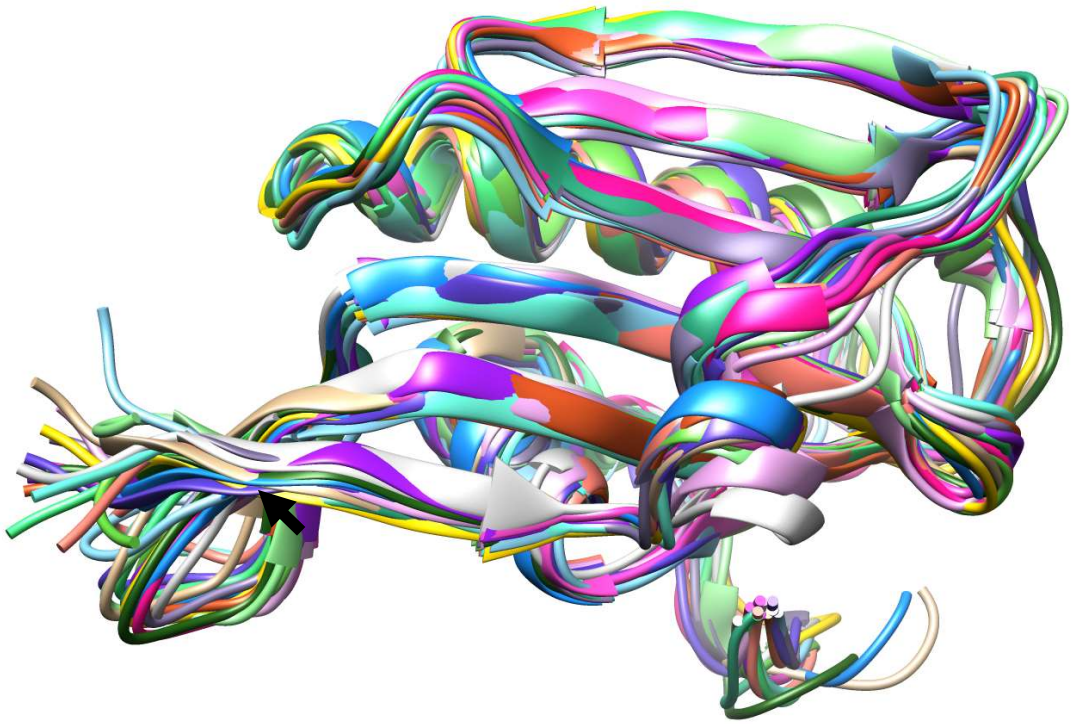

Figure 5.5: All models of the top cluster from the MD are all very close in RMSD. Arrow is pointing to the modeled 5 amino acids that were missing in the crystal structure.

Hybrid modeling of NS1B – dsRNA complex using HADDOCK:

The resulting MD model of NS1B-CTD and the 16-bp dsRNA (PDB: 5KVJ) was cleaned (all solvents removed) and prepped (residue IDs converted to a HADDOCK accepted format, see 16, 17) for HADDOCK. While the CSPs were available for NS1B-CTD to help drive the docking (2), no data was available on specific nucleotides from the RNA that afre involved in binding. We therefore gave all nucleotides equal weight in the

HADDOCK docking by making all nucleotides active. In the resulting ensemble of models, the RNA is bound to a specific site on NS1B-CTD, but in a wide range of orientations (Figure 5.6). While the 40 different models that HADDOCK produces gives little insight at this point, the overwhelming number of models coupled with SAXS data will turn out to be extremely helpful into furthering the project which will be discussed in the next chapter.

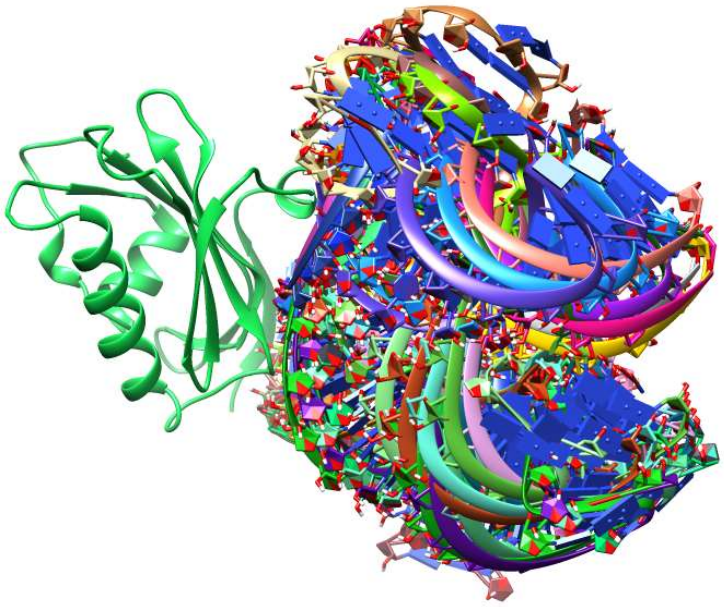

Figure 5.6 All possible orientations of 16-bp dsRNA provides limited insight due to the number of possibilities.

While the docking of the 16-bp dsRNA had no data involving the nucleotides involved in binding from the RNA side, for the corresponding docking of the 3P-5'-hpRNA substrate, I was able to limit the active nucleotides of the 3P-5'-hpRNA, based on the NMR data discussed in Chapter 4, to either the blunt end or the hairpin loop. In

these HADDOCK docking calculations, the first three base pairs on the blunt end and the entire loop together with the first base pair of the loop were defined as active binding residues.

16-bp dsRNA sequence:

CCAUCCUCUACAGGCG
GGUAGGAGAUGUCCGC

3P-5'-hpRNA:

3P GAAUAUAAUA GU
CUUAUAUUAU GA

In this docking experiment, we used the CSPs on NS1B-CTD observed in binding to the 16-bp dsRNA, in place of those for the 3P-5'-hpRNA (these were not available at this time, and this work is in progress in the Montelione lab). The variety of resulting complex structures include models with NS1B-CTD binding to the blunt end, the loop, and a small number where the RNA is oriented parallel to NS1B-CTD (Figure 5.7 A/B/C). The resulting models were then zipped and compared to the SAXS data which is discussed in Chapter 5. The best models that were selected form SAXS had 2 clusters of blunt end binding models and 1 cluster of loop binding models.

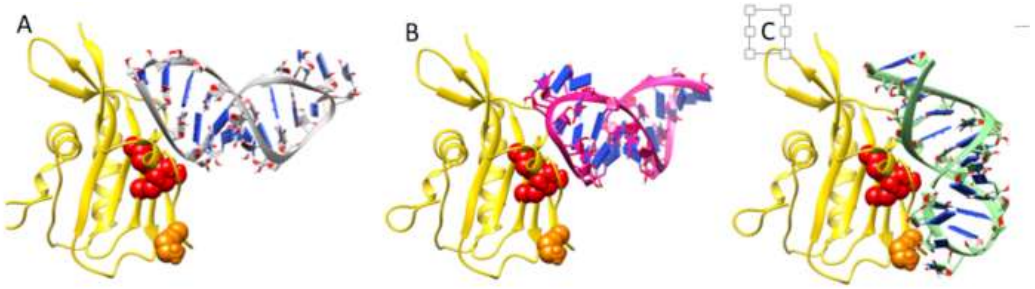

Figure 5.7: Resulting orientations of the docking. A) blunt end binding orientation. B) loop binding orientation. C) 0 degree binding orientation. Red balls signify atoms in residues R208/K221 orange balls represent atoms in residue K160

Comparisons of models to RIG-I structure:

A key function of RIG-I is to recognize 3P-5' RNAs. Similarly, the NS1B-CTD:3P-5'-hpRNA top models from the HADDOCK and that were selected by SAXS have the triphosphate group buried in the basic ridge in NS1B-CTD (Figure 5.8). In addition, all acceptable models have the triphosphate interacting with R208/K221 (Figure 5.9). In addition to this the RIG-I structure has Phe853 stacking with the blunt end of 3P-5' RNA (15). The model we are reporting as the top model also has a His (His207) parallel to the aromatic rings of the blunt end nucleotides of the 3P-5'-hpRNA thus giving evidence that this residue participates in pi stacking with the RNA (Figure 5.10). Also, interestingly this residue is next to R208, one of the most important residues for RNA binding according to FP results.

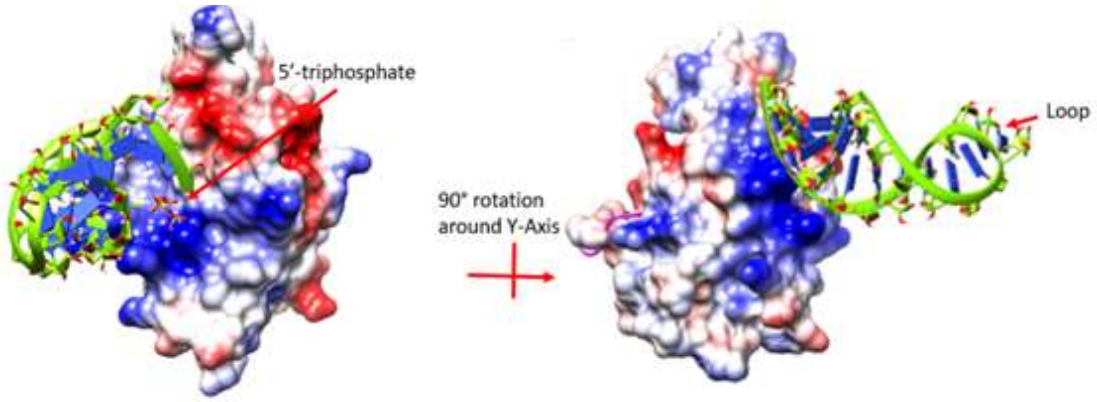

Figure 5.8: 3P-5'-hpRNA bound to NS1B-CTD represented in electrostatic surface. Two orientations of the top model which shows the triphosphate of the RNA fitted deep within a basic pocket. Color scheme: Red -> White -> Blue : Acidic -> Neutral -> Basic.

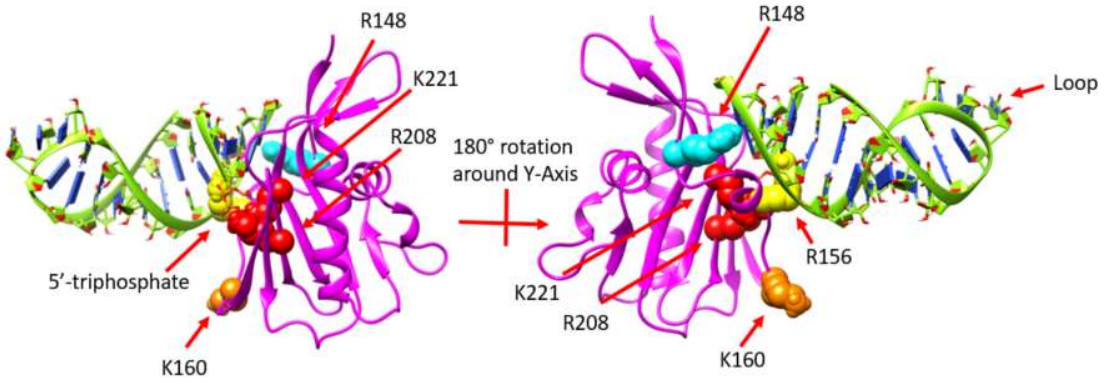

Figure 5.9: 3P-5'-hpRNA bound to NS1B-CTD with essential RNA binding amino acids for binding shown. Red = high affinity loss when mutated (R208/K221), orange = medium affinity loss when mutated (K160), yellow = low/medium affinity loss when mutated (R156), Blue = no affinity loss when mutated (R148).

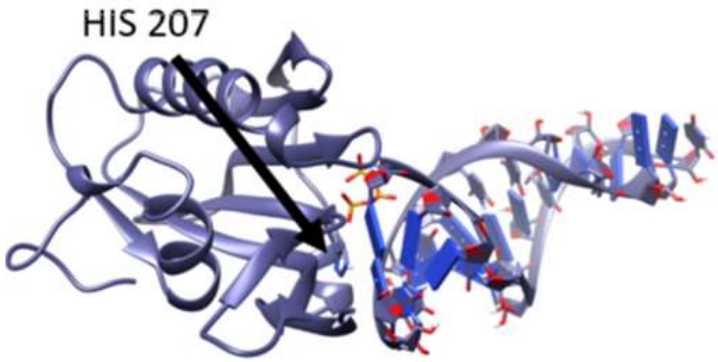

Figure 5.10: His207 pi stacking with the blunt end nucleic acids from 3P-5'-hpRNA

SAXS:

SAXS was performed on NS1B-CTD which served multiple purposes. First, we wanted to compare the MD model to see if this model could fit the SAXS data which it

did with an acceptable $\chi^2 = 2.41$ (Figure 5.11). If it did not fit with a reasonable χ^2, then more complicated experiments would not work. The second purpose was to determine which protein construct to use, at which concentration, and optimization of other conditions such as buffers. At the time of the SAXS experiments there were a few assumptions that needed to be investigated. First it was assumed that NS1B-CTD bound RNA on the backbone and that is bound as a dimer. At the time we only knew that NS1B-CTD bound dsRNA and that it was a dimer in the crystal structure so, this assumption seemed valid. The SAXS experiments gave hints that if a mutation that prevented dimerization, R238A, the SAXS curves for the WT and R238A were similar, albeit the WT also had dimerized NS1B-CTD along with NS1B-CTD:dsRNA complex so the curves did not match exactly. The data quality of the SAXS curves were not great due to early stages in protocol development/optimization so hard conclusions could not be drawn from this result. Simultaneous to the experiment though, FP from Ma LC. et al. (2) showed that the R238A mutation did not affect dsRNA binding significantly. Thus it was determined that R238A was the optimum construct to use for SAXS since A) we would have an easier time getting a homogeneous sample (dimer interface mutated). B) the R238A mutation had very little effect on dsRNA binding if any.

(χ^2 = 2.41)

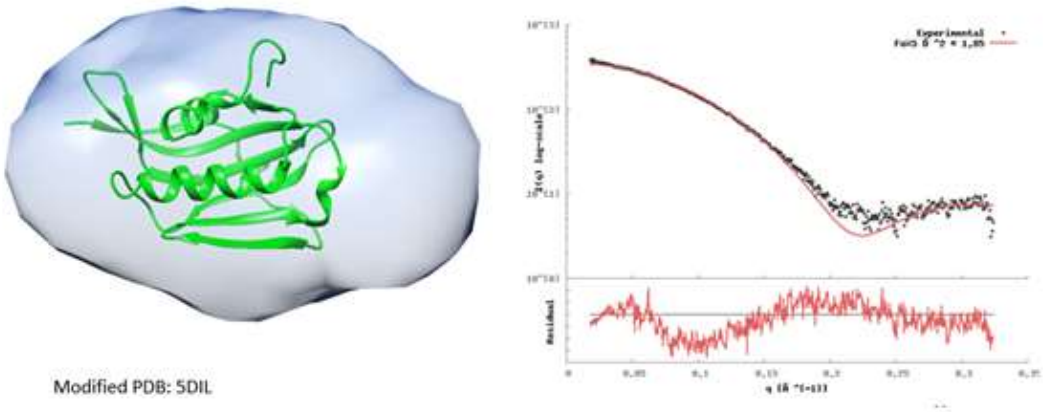

Figure 5.11: SAXS matching between NS1B-CTD and MD model confirms the MD model is accurate. Model fit inside the SAXS envelope (left) and model's calculated SAXS curve fit into the SAXS data (right)

Conditions were then optimized for R238A bound to 16-bp dsRNA and SAXS data collected was compared to the various models created in HADDOCK (Figure 5.6). We routinely collected data that selected and preferred the blunt end binding model from HADDOCK. However, the data quality was not optimum due to aggregation in the sample and various logicstical issues with shipping the sample. An oppurtunity to record the SAXS in person was taken at the MacCHESS beamline at Cornell. Samples were prepared fresh and instantly run on the beamline. The data the was collected was of high quality (Figure 5.12) and again the blunt end binding model was selected. While initially were skeptical of this result, but it became clear through replication that the result

was correct.

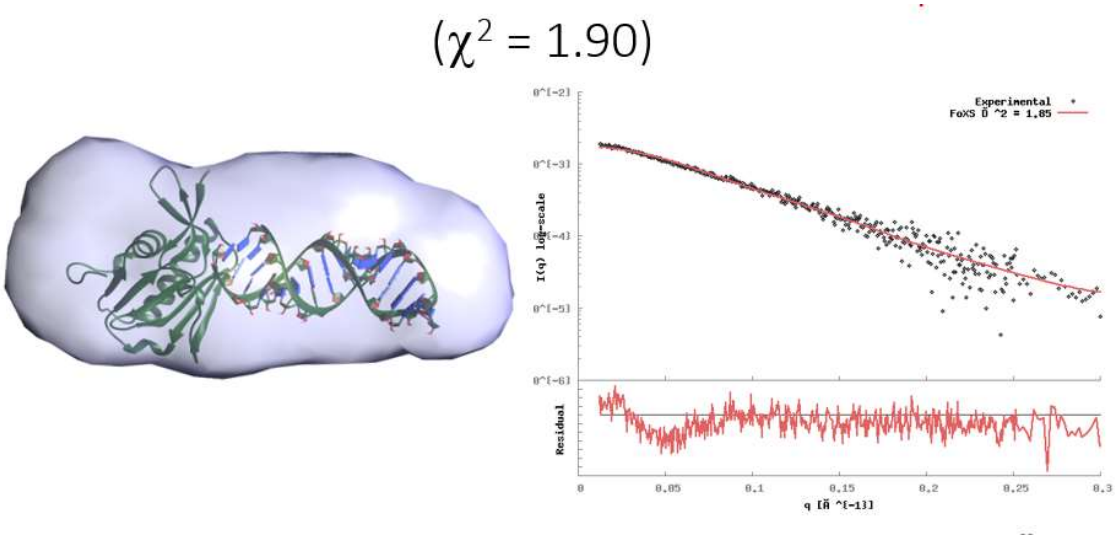

Figure 5.12: SAXS data collected at Cornell selected a blunt end binding model. Model fit inside the SAXS envelope (left) and model's calculated SAXS curve fit into the SAXS data (right) .

Due to the unusual result of blunt end binding we then tried a 5'-triphosphorylated hpRNA for the biological implications. The SAXS was collected at the BioCAT beamline due to collect very high-quality data. The data selected both blunt-end binding models and loop models with an optimum χ^2 (1.02-1.19). To confirm that R238A was binding in a blunt-end or loop fashion and not along the backbone (0 degree model) SAXS curves were first calculated for all 3 scenarios and compared (figure 5.13A). When comparing multiple models, it is clearly seen at what angle the SAXS curve can differentiate models which can then be translated to a resolution at which the models deviate. While comparing the calculated SAXS curves it can be seen that the 0 degree model deviates from the loop binding model and the blunt-end binding model between q = 0.1-0.15. When looking for similar deviation between the 0 degree model and the

SAXS data a large deviation occurs between q = 0.05-0.15 confirming that this model is not valid (figure 5.13B). It is also noteworthy that due to the relative shape of the envelopes the SAXS curves for the blunt-end binding and loop binding cannot be differentiated. To try to see if there is a preference for the blunt-end or the loop model we looked at the P(r) distribution, which can be more sensitive.

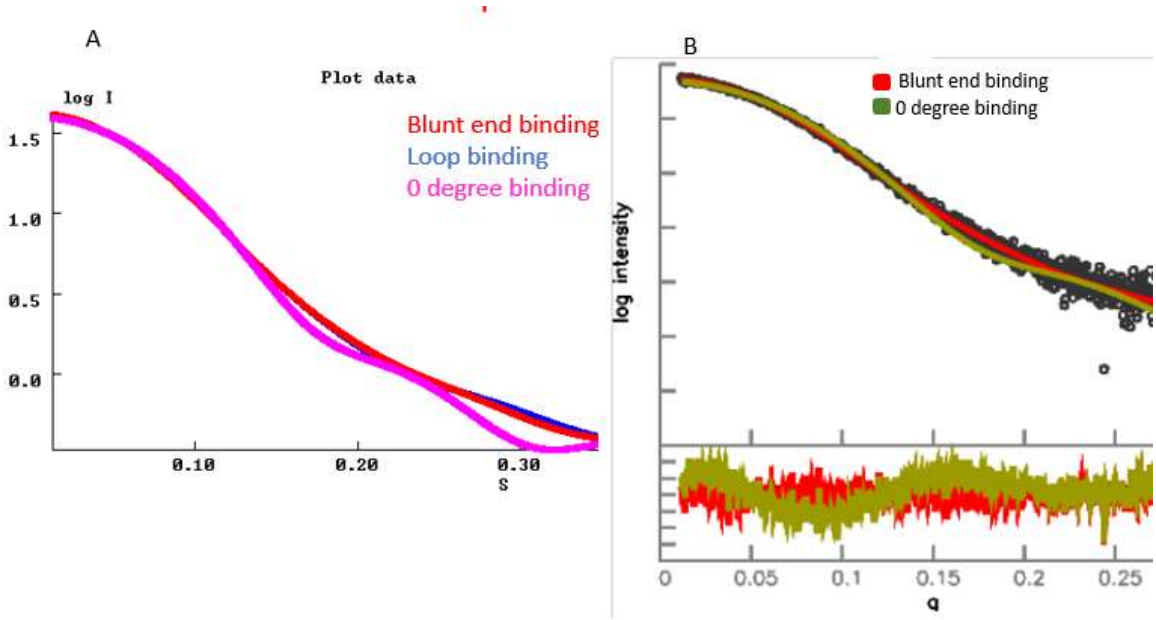

Figure 5.13. Comparison of calculated SAXS to the data collection rules out 0 degree binding. A) calculated SAXS curves for R238A binding 3P-5'-hpRNA in blunt-end binding (blue), loop binding (red), and 0 degree binding (magenta). B) SAXS data

compared to blunt-end binding (red) and 0 degree binding (green).

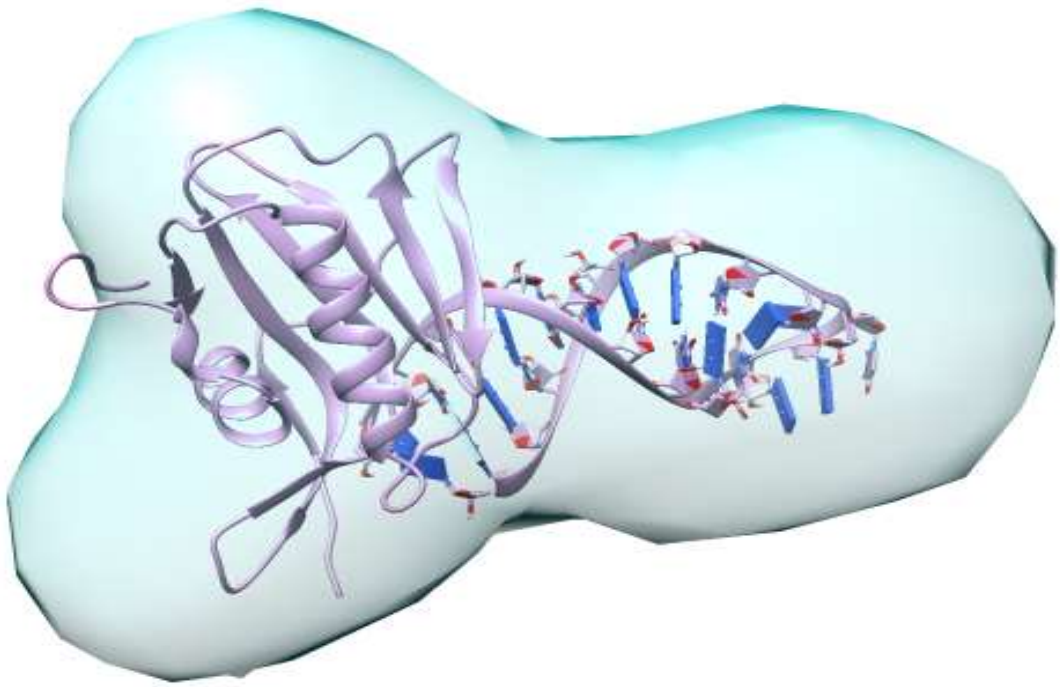

Figure 5.14: SAXS envelope of NS1B-CTD bound to 3P-5'-hpRNA

As a result of the P(r) calculation we are able to compare all models χ^2 selected models to the SAXS data (Table 5.2). While the radius of gyration (R_g) does not seem to prefer any binding type, the maximum diameter (Dmax) from the raw data is closer on average to the blunt-end binding models. In addition to this we looked at the P(r) curves for the top models in each cluster (selected by χ^2) to the P(r) from the raw data (Figure 5.15). Visually we can see that the loop binding model deviates the most especially at the peak of the curve which signifies the largest number of atoms at that distance. Thus, the loop model would have its largest number of atoms at a specific distance different from the raw data. Methods are currently being discussed on the best way to quantify this and determine the significance of this deviation. At this point it would appear that the

blunt end binding models are the more likely model but loop binding models cannot be ruled out.

Model	**Rg**	**dmax**	**SAXS Curve χ^2**
Model loop 1	20.3	67	1.02
Model loop 2	20.2	66	1.08
Model loop 3	20.2	65	1.09
Model blunt 1.1	20.3	69	1.17
Model blunt 1.2	20.4	68	1.19
Model blunt 1.3	20.2	68	1.06
Model blunt 2.1	20.3	69	1.15
Model blunt 2.2	20.2	66	1.09
Model blunt 2.3	20.3	69	1.18
Raw SAXS data	20.0	69	

Table 5.2: values calculated by the P(r) curve generation process

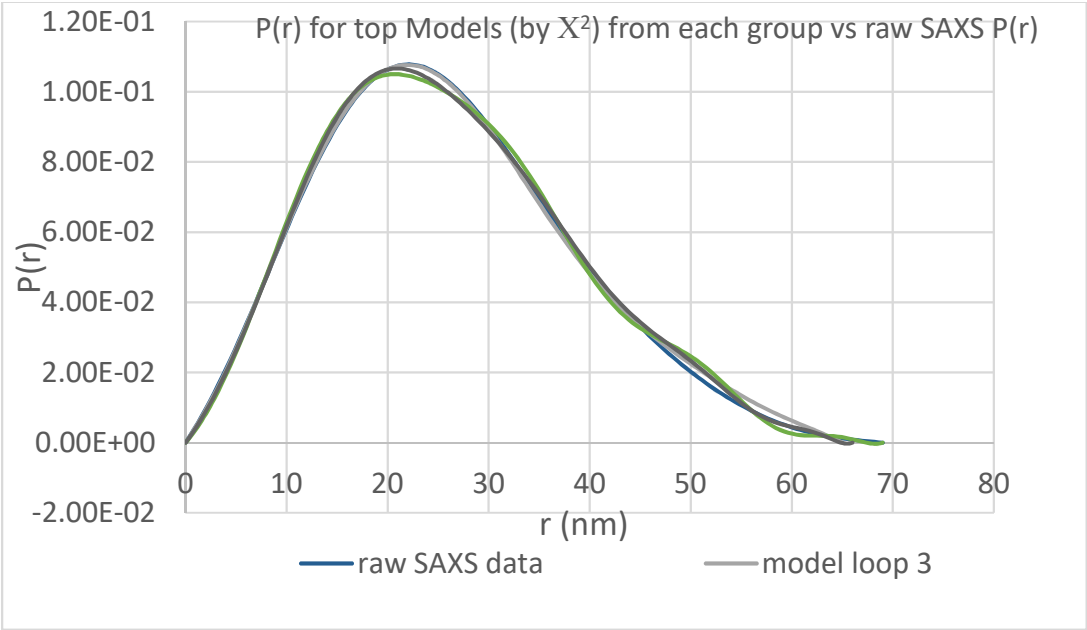

Figure 5.15: P(r) distribution for top models from the 3 clusters compared to raw SAXS data

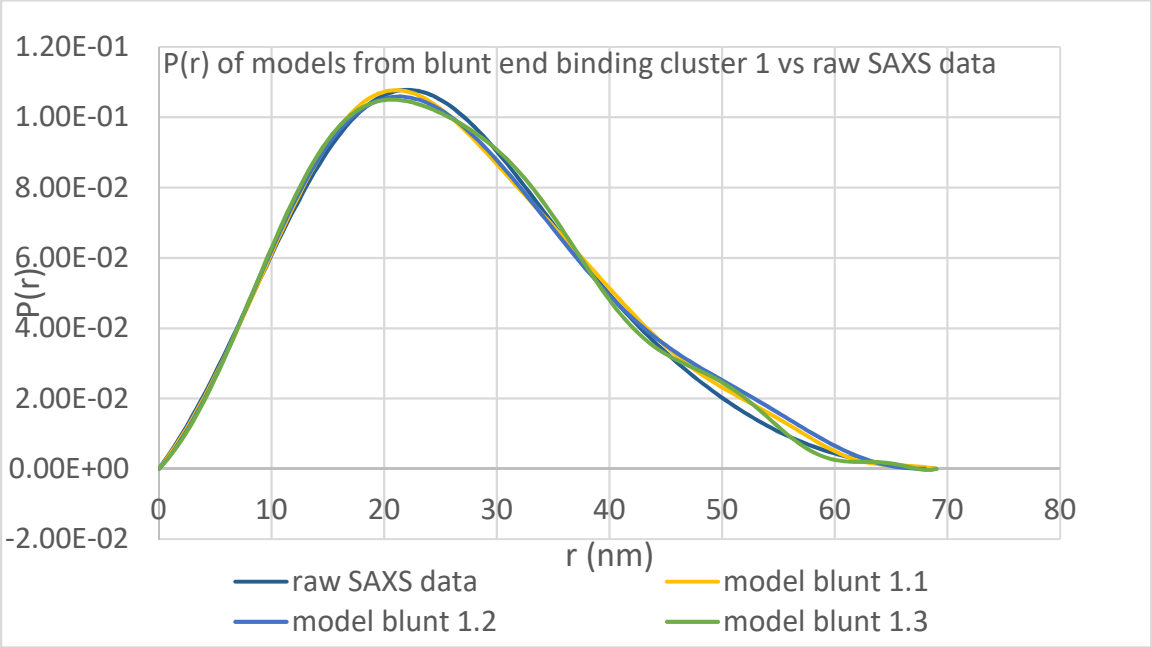

Figure 5.16: P(r) distribution for all models in the blunt-end cluster 1 vs raw SAXS data

To gain a better understanding of the sensitivity of the P(r) curve we set out to determine if it could select for models that are very close in RMSD, or the 3 top models of the top bluster. Again, statistical methods are not available at this time but we can see that the blunt-end model 1.3 is the closest which also agrees with the relative χ^2 value. This suggest that this method is very accurate and sensitive, especially at the peak of the distribution.

Model of full length NS1B in complex with dsRNA:

The NS1B-FL bound to dsRNA connects and makes sense of all the previous data (figure 5.17). While this model was created simply to understand why NS1B-CTD bound the blunt end of dsRNA, it also made sense of newly acquired data and was the foundation for comparing NS1B-FL to RIG-I.

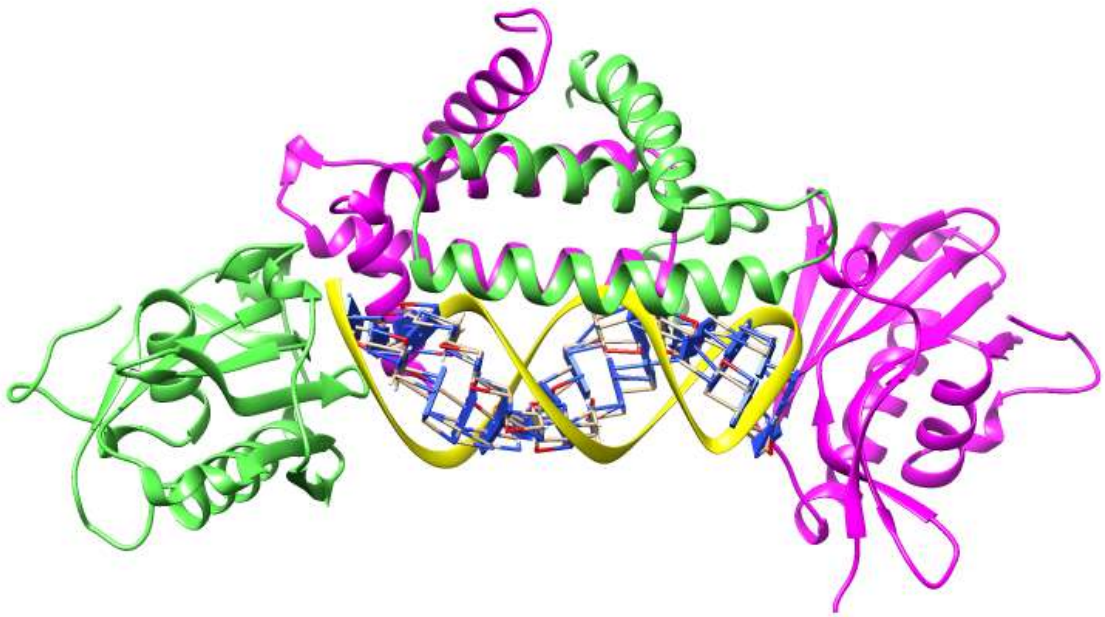

Figure 5.17. Hypothetical model of a dimerized NS1B-FL bound to a 16-bp dsRNA that is consistent with the structural data outlined in this paper.

Discussion:

There are several interesting feature and similarities that can be observed between the RIG-I and the NS1B-CTD modeled structure. First in the RIG-I structure, is the pi-bond stacking of Phe853 with the aromatic rings in the base of Gua on the blunt end of the RNA. In the NS1B-CTD His207 would be pi-bond stacking in a very similar fashion. In the RIG-I structure His830 is used as a residue that can recognize the triphosphate by direct interaction. The importance of the His830 is emphasized by mutational experiments, which then prevents RIG-I's ability to recognize triphosphorylated RNA substrates. However, the His207 in the NS1B-CTD model is directed away from the triphosphate group, suggesting that this His207 main purpose is for affinity not specify. It is recognized that this is a SAXS model which at best has a resolution of 10 Å so a definitive conclusion about the orientation of the sidechain is not possible. That being said it is known that R208 plays a large role in RNA binding and therefore by proximity His207 should have some role in this interaction. Future mutational experiments should be done to see what the true purpose of His207 is. Another not surprising commonality between the RIG-I structure and the NS1B-CTD model is the presence of basic residues around the triphosphate. The model for NS1B-CTD has the triphosphate buried very deeply inside a basic pocket and is the closest in proximity to R208/K221, the two residues that when mutated showed the largest change in affinity for RNA. Again, this is a SAXS model, but it is worth mentioning that all models that fit within the χ^2 cutoff that had a blunt end binding had the triphosphate interacting with R208/K221. The next commonality and a slight concern on first inspection was the

presence of CSPs on acidic residues in NS1B-CTD. The negatively charged amino acids should be repulsing the negatively charged RNA. Close inspection of the RIG-I structure shows acidic residues interacting with other basic residues of RIG-I, but they are also in close proximity to a partially positively charged phosphorus atom in the triphosphate. Taking this into consideration, the CSPs in the acidic amino acids of NS1B-CTD make more sense as they are positioned similarly to RIG-I's acidic amino acids. While the NS1B-CTD models gave insights into the orientation and type of interaction that NS1B-CTD has with RNA and the role of the interaction, hard conclusions and in-depth analysis of the atomic interactions cannot be made. Crystallization experiments will need to be performed to make hard conclusions. That being said the modeling work did give us a lot of information about the structure of the complex, and why previous crystallization did not work. We also learned how to adjust the system to give us a better chance at successful crystallization on the second attempt.

SAXS was an essential tool for identifying the blunt-end binding mechanism. It is also of note that the data collected early on the R238A alone and R238A bound to 16bp dsRNA was performed with the unoptimized SAXS data collection protocol. While the χ^2 did improve from the R238A alone to the R238A 16bp dsRNA complex this improvement was most likely due to noise in the data. The 3P-5'-hpRNA on the other hand was prepared with the new optimized protocol (described in Chapter 2). The data for 3P-5'-hpRNA was of the highest quality (determined by Guinier region and general noise) collected during this study. It is unclear whether the improvement in data quality is due to the protocol being optimized or the tighter binding of the RNA substrate; it is most likely a combination of both, sample preparation and correct substrate selection cannot be emphasized enough. Theoretically, the χ^2 should get worse with the increasing components and molecular size. Because our χ^2 improved with the addition of the 3P-5'-

hpRNA, we have more confidence in the reported structure. SAXS was able to completely rule out the possibility of a 0 degree binding model, although, it was not able to discriminate between blunt-end binding and loop binding. While it could not rule out the possibility of loop binding model it does appear that the P(r) curve is much closer at the peak to the blunt-end binding model vs the loop binding model.

We did notice, and have concerns, that the SAXS envelope shape of NS1B-CTD:16-bp dsRNA and NS1B-CTD:3P-5'-hpRNA is very different, with the latter having a butterfly shape to it. There are two main differences between these samples which is the buffer and the RNA substrate. However, the RNA substrates are fairly similar in shape (elongated oval), thus we predict this difference to be due to the buffer. It is noted in Chapter 2 that the 2K buffer was optimized for the protein alone but NS1B-CTD:RNA complexes seemed to behave better in the 1K buffer. Another major difference is the 1K buffer has half of the salt that 2K buffer does. This is important because as discussed in the introduction of Chapter 5, SAXS detects differences. This means that if the solvent acts differently around a molecule than when it is far away, that difference will be measured. This is called the hydration layer and the hydration layer can drastically change in size depending on the amount of salt in the buffer. To show that the buffer will change to shape of a molecule we obtained a SAXS sample of the NS1B-CTD protein alone and calculated the envelope (Figure 5.18). This sample also has a butterfly shape, suggesting that the change in shape is due to either the protein being less stable or being in another buffer. This exercise gives further proof to the argument that fitting to a shape for SAXS is less important that fitting to the SAXS curve, which we have excellent matching for the NS1B-CTD:RNA complexes.

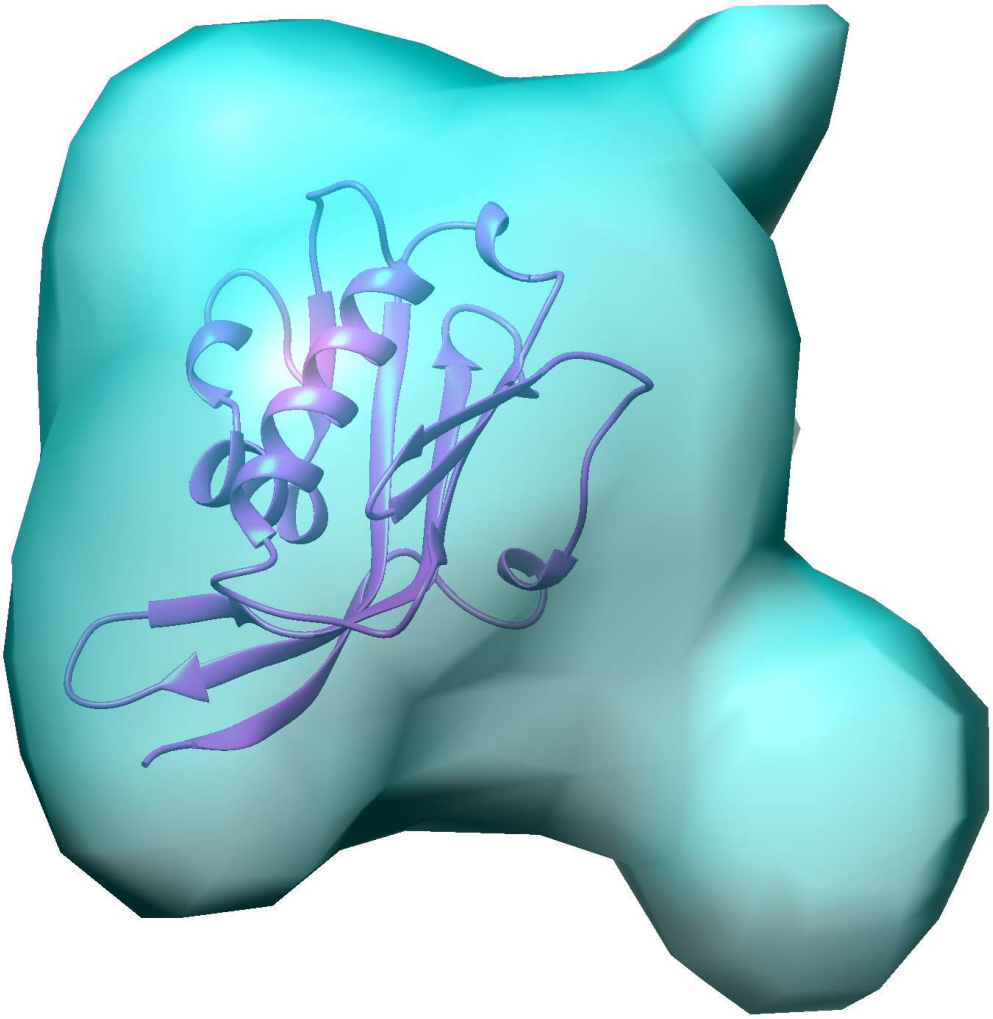

Figure: 5.18: NS1B-CTD fitted into the SAXS envelope which has a butterfly shape.

Model of full length NS1B in complex with dsRNA:

The model proposed in this chapter was the foundation for comparing NS1B-FL RNA binding to RIG-I. It is important to recognize that the model has confidence within the individual domains and their interactions with RNA but very little confidence between domain interactions. Despite this the model has a few important conclusions. First the RNA that is bound is a 16bp dsRNA substrate, however, when all the domains are tightly fit onto the RNA there are clashes between the NS1B-NTDs and the NS1B-CTDs, implying that the RNA substrate must be longer than 16bp in order to fit all the domains.

This is supported by the binding results shown in this chapter. NS1B-FL bound a 10bp-hpRNA much weaker that the NS1B-CTD suggesting that this substrate is optimum for the NS1B-CTD but not for the NS1B-FL. It is therefore suggested in order to properly test binding for NS1B-FL to use longer RNA substrates. Another important conclusion that can be made is that the NS1B-NTD is not affected by 5' modifications but NS1B-CTD is. This conclusion is supported by the binding results in this chapter. Additionally, this suggests that NS1B-CTD has an important biological role as the NS1B-CTD would act as a sensory domain.

Supplemental Material:

HADDOCK input files:

NS1B-CTD active residues (field input):

16-bp-dsRNA active residues (field input):

1,2,3,4,5,6,7,8,9,10,11,12,13,14,15,16,17,18,19,20,21,22,23,24,25,26,27,28,29,30,31,32

3P-5'-hpRNA active residues (entire active molecule) (field input):

1,2,3,4,5,6,7,8,9,10,11,12,13,14,15,16,17,18,19,20,21,22,23,24

3P-5'-hpRNA active residues (loop active molecule) (field input):

9,10,11,12,13,14,15,16

3P-5'-hpRNA active residues (blunt-end active molecule) (field input):

1,2,3,4,21,22,23,24

NS1B-CTD PDB file:

```
REMARK FILENAME="complex_23w.pdb0"
REMARK ==============================================================
REMARK HADDOCK run for complex
REMARK initial structure: complex_23.pdb
REMARK final NOE weights: unambig 50 amb: 50
```

```
REMARK ==============================================================
REMARK            total,bonds,angles,improper,dihe,vdw,elec,air,cdih,coup,rdcs,vean,dani,xpcs,rg
REMARK energies: -260.141, 0, 0, 0, 0, -59.6506, -611.123, 384.428, 0, 0, 0, 0, 0, 0, 0
REMARK ==============================================================
REMARK            bonds,angles,impropers,dihe,air,cdih,coup,rdcs,vean,dani,xpcs
REMARK rms-dev.: 0,0,0,0,0.751414,0.176396,0, 0, 0, 0, 0
REMARK ==============================================================
REMARK               air,cdih,coup,rdcs,vean,dani,xpcs
REMARK               >0.3,>5,>1,>0,>5,>0.2,>0.2
REMARK violations.: 12, 0, 0, 0, 0, 0, 0
REMARK ==============================================================
REMARK                        CVpartition#,violations,rms
REMARK AIRs cross-validation: 2, 21, 1.6631
REMARK ==============================================================
REMARK NCS energy: 0
REMARK ==============================================================
REMARK Symmetry energy: 0
REMARK ==============================================================
REMARK Desolvation energy: 29.6873
REMARK Internal energy free molecules: -2123.61
REMARK Internal energy complex: -7275.23
REMARK Binding energy: -5792.7
REMARK ==============================================================
REMARK buried surface area: 1710.83
REMARK ==============================================================
REMARK water - chain1: 0 0 0
REMARK water - chain2: 0 0 0
REMARK water - chain3: 0 0 0
REMARK water - chain4: 0 0 0
REMARK water - chain5: 0 0 0
REMARK water - chain6: 0 0 0
REMARK ==============================================================
REMARK water - water: 0 0 0
REMARK ==============================================================
REMARK DATE:11-Nov-2018  02:00:34       created by user: enm009
REMARK VERSION:1.3U
HELIX    1   1 ASN A   12  ALA A   15  1                                   4
HELIX    2   2 VAL A   90  PHE A  107  1                                  18
HELIX    3   3 GLU A  119  PHE A  128  1                                  10
HELIX    4   4 GLU A  131  ARG A  133  1                                   3
SHEET    1   1 1 ILE A   3  ARG A   8  0
SHEET    2   2 1 ASN A  24  GLU A  28  0
SHEET    3   3 1 PHE A  31  ILE A  35  0
SHEET    4   4 1 LEU A  45  LYS A  55  0
SHEET    5   5 1 LYS A  61  LEU A  63  0
SHEET    6   6 1 THR A  65  ASP A  73  0
SHEET    7   7 1 LEU A  78  ALA A  84  0
SHEET    8   8 1 ILE A 115  ALA A 117  0
ATOM      1  N   HIS A   1      20.675 -20.569  -6.307  1.00 10.00      A    N
ATOM      2  HN  HIS A   1      21.088 -20.869  -5.467  1.00 10.00      A    H
ATOM      3  CA  HIS A   1      19.536 -19.666  -6.243  1.00 10.00      A    C
ATOM      4  CB  HIS A   1      18.214 -20.438  -6.400  1.00 10.00      A    C
ATOM      5  CG  HIS A   1      17.907 -21.410  -5.298  1.00 10.00      A    C
ATOM      6  ND1 HIS A   1      18.120 -22.762  -5.448  1.00 10.00      A    N
ATOM      7  CD2 HIS A   1      17.390 -21.177  -4.068  1.00 10.00      A    C
ATOM      8  CE1 HIS A   1      17.730 -23.319  -4.315  1.00 10.00      A    C
ATOM      9  NE2 HIS A   1      17.284 -22.397  -3.455  1.00 10.00      A    N
ATOM     10  HE2 HIS A   1      16.940 -22.563  -2.550  1.00 10.00      A    H
ATOM     11  C   HIS A   1      19.554 -18.857  -4.946  1.00 10.00      A    C
ATOM     12  O   HIS A   1      20.188 -19.261  -3.966  1.00 10.00      A    O
ATOM     13  N   PRO A   2      18.887 -17.695  -4.935  1.00 10.00      A    N
ATOM     14  CA  PRO A   2      18.818 -16.831  -3.754  1.00 10.00      A    C
ATOM     15  CB  PRO A   2      18.256 -15.525  -4.314  1.00 10.00      A    C
ATOM     16  CG  PRO A   2      17.436 -15.951  -5.482  1.00 10.00      A    C
ATOM     17  CD  PRO A   2      18.157 -17.122  -6.081  1.00 10.00      A    C
ATOM     18  C   PRO A   2      17.876 -17.393  -2.692  1.00 10.00      A    C
ATOM     19  O   PRO A   2      16.862 -18.020  -3.013  1.00 10.00      A    O
ATOM     20  N   ILE A   3      18.213 -17.162  -1.433  1.00 10.00      A    N
ATOM     21  HN  ILE A   3      19.025 -16.644  -1.242  1.00 10.00      A    H
ATOM     22  CA  ILE A   3      17.398 -17.646  -0.327  1.00 10.00      A    C
ATOM     23  CB  ILE A   3      18.266 -18.059   0.886  1.00 10.00      A    C
ATOM     24  CG1 ILE A   3      19.264 -19.151   0.481  1.00 10.00      A    C
ATOM     25  CG2 ILE A   3      17.391 -18.538   2.037  1.00 10.00      A    C
ATOM     26  CD1 ILE A   3      18.620 -20.376  -0.134  1.00 10.00      A    C
ATOM     27  C   ILE A   3      16.385 -16.590   0.099  1.00 10.00      A    C
ATOM     28  O   ILE A   3      16.732 -15.420   0.279  1.00 10.00      A    O
ATOM     29  N   GLU A   4      15.135 -17.003   0.237  1.00 10.00      A    N
ATOM     30  HN  GLU A   4      14.917 -17.953   0.061  1.00 10.00      A    H
ATOM     31  CA  GLU A   4      14.074 -16.103   0.646  1.00 10.00      A    C
ATOM     32  CB  GLU A   4      12.695 -16.706   0.341  1.00 10.00      A    C
ATOM     33  CG  GLU A   4      12.460 -18.089   0.936  1.00 10.00      A    C
ATOM     34  CD  GLU A   4      12.844 -19.215  -0.003  1.00 10.00      A    C
ATOM     35  OE1 GLU A   4      11.948 -19.974  -0.421  1.00 10.00      A    O
ATOM     36  OE2 GLU A   4      14.043 -19.350  -0.331  1.00 10.00      A    O
ATOM     37  C   GLU A   4      14.204 -15.757   2.128  1.00 10.00      A    C
ATOM     38  O   GLU A   4      14.294 -16.643   2.979  1.00 10.00      A    O
ATOM     39  N   VAL A   5      14.237 -14.471   2.425  1.00 10.00      A    N
ATOM     40  HN  VAL A   5      14.176 -13.810   1.696  1.00 10.00      A    H
ATOM     41  CA  VAL A   5      14.352 -14.002   3.798  1.00 10.00      A    C
ATOM     42  CB  VAL A   5      15.764 -13.439   4.103  1.00 10.00      A    C
ATOM     43  CG1 VAL A   5      16.161 -12.354   3.112  1.00 10.00      A    C
ATOM     44  CG2 VAL A   5      15.867 -12.933   5.536  1.00 10.00      A    C
ATOM     45  C   VAL A   5      13.278 -12.958   4.084  1.00 10.00      A    C
ATOM     46  O   VAL A   5      13.076 -12.029   3.303  1.00 10.00      A    O
ATOM     47  N   VAL A   6      12.578 -13.121   5.193  1.00 10.00      A    N
```

ATOM	48	HN	VAL	A	6	12.788	-13.870	5.789	1.00	10.00	A	H
ATOM	49	CA	VAL	A	6	11.519	-12.195	5.557	1.00	10.00	A	C
ATOM	50	CB	VAL	A	6	10.366	-12.896	6.312	1.00	10.00	A	C
ATOM	51	CG1	VAL	A	6	9.183	-11.952	6.479	1.00	10.00	A	C
ATOM	52	CG2	VAL	A	6	9.934	-14.164	5.586	1.00	10.00	A	C
ATOM	53	C	VAL	A	6	12.058	-11.036	6.395	1.00	10.00	A	C
ATOM	54	O	VAL	A	6	12.577	-11.231	7.497	1.00	10.00	A	O
ATOM	55	N	LEU	A	7	11.933	-9.832	5.865	1.00	10.00	A	N
ATOM	56	HN	LEU	A	7	11.493	-9.734	4.990	1.00	10.00	A	H
ATOM	57	CA	LEU	A	7	12.393	-8.638	6.557	1.00	10.00	A	C
ATOM	58	CB	LEU	A	7	13.377	-7.853	5.689	1.00	10.00	A	C
ATOM	59	CG	LEU	A	7	14.711	-8.547	5.386	1.00	10.00	A	C
ATOM	60	CD1	LEU	A	7	15.549	-7.699	4.443	1.00	10.00	A	C
ATOM	61	CD2	LEU	A	7	15.479	-8.833	6.670	1.00	10.00	A	C
ATOM	62	C	LEU	A	7	11.194	-7.780	6.931	1.00	10.00	A	C
ATOM	63	O	LEU	A	7	10.319	-7.526	6.100	1.00	10.00	A	O
ATOM	64	N	ARG	A	8	11.142	-7.343	8.176	1.00	10.00	A	N
ATOM	65	HN	ARG	A	8	11.877	-7.551	8.795	1.00	10.00	A	H
ATOM	66	CA	ARG	A	8	10.020	-6.548	8.644	1.00	10.00	A	C
ATOM	67	CB	ARG	A	8	9.073	-7.426	9.472	1.00	10.00	A	C
ATOM	68	CG	ARG	A	8	9.781	-8.410	10.395	1.00	10.00	A	C
ATOM	69	CD	ARG	A	8	8.804	-9.163	11.282	1.00	10.00	A	C
ATOM	70	NE	ARG	A	8	8.026	-10.158	10.547	1.00	10.00	A	N
ATOM	71	HE	ARG	A	8	8.505	-10.702	9.876	1.00	10.00	A	H
ATOM	72	CZ	ARG	A	8	6.723	-10.372	10.751	1.00	10.00	A	C
ATOM	73	NH1	ARG	A	8	6.072	-9.660	11.667	1.00	10.00	A	N
ATOM	74	HH11	ARG	A	8	6.575	-8.941	12.227	1.00	10.00	A	H
ATOM	75	HH12	ARG	A	8	5.047	-9.822	11.832	1.00	10.00	A	H
ATOM	76	NH2	ARG	A	8	6.079	-11.305	10.055	1.00	10.00	A	N
ATOM	77	HH21	ARG	A	8	6.587	-11.879	9.347	1.00	10.00	A	H
ATOM	78	HH22	ARG	A	8	5.056	-11.470	10.218	1.00	10.00	A	H
ATOM	79	C	ARG	A	8	10.457	-5.329	9.453	1.00	10.00	A	C
ATOM	80	O	ARG	A	8	11.108	-5.458	10.491	1.00	10.00	A	O
ATOM	81	N	ASP	A	9	10.087	-4.148	8.970	1.00	10.00	A	N
ATOM	82	HN	ASP	A	9	9.580	-4.113	8.128	1.00	10.00	A	H
ATOM	83	CA	ASP	A	9	10.410	-2.898	9.652	1.00	10.00	A	C
ATOM	84	CB	ASP	A	9	10.350	-1.717	8.673	1.00	10.00	A	C
ATOM	85	CG	ASP	A	9	11.662	-1.439	7.969	1.00	10.00	A	C
ATOM	86	OD1	ASP	A	9	12.719	-1.888	8.467	1.00	10.00	A	O
ATOM	87	OD2	ASP	A	9	11.645	-0.771	6.914	1.00	10.00	A	O
ATOM	88	C	ASP	A	9	9.402	-2.661	10.768	1.00	10.00	A	C
ATOM	89	O	ASP	A	9	9.740	-2.140	11.832	1.00	10.00	A	O
ATOM	90	N	MET	A	10	8.161	-3.058	10.506	1.00	10.00	A	N
ATOM	91	HN	MET	A	10	7.973	-3.480	9.637	1.00	10.00	A	H
ATOM	92	CA	MET	A	10	7.069	-2.897	11.456	1.00	10.00	A	C
ATOM	93	CB	MET	A	10	5.914	-2.133	10.798	1.00	10.00	A	C
ATOM	94	CG	MET	A	10	6.278	-0.757	10.273	1.00	10.00	A	C
ATOM	95	SD	MET	A	10	5.088	-0.155	9.060	1.00	10.00	A	S
ATOM	96	CE	MET	A	10	5.333	-1.346	7.743	1.00	10.00	A	C
ATOM	97	C	MET	A	10	6.549	-4.254	11.918	1.00	10.00	A	C
ATOM	98	O	MET	A	10	6.975	-5.302	11.420	1.00	10.00	A	O
ATOM	99	N	ASN	A	11	5.616	-4.229	12.861	1.00	10.00	A	N
ATOM	100	HN	ASN	A	11	5.313	-3.360	13.209	1.00	10.00	A	H
ATOM	101	CA	ASN	A	11	5.014	-5.447	13.386	1.00	10.00	A	C
ATOM	102	CB	ASN	A	11	4.643	-5.246	14.862	1.00	10.00	A	C
ATOM	103	CG	ASN	A	11	4.234	-6.528	15.564	1.00	10.00	A	C
ATOM	104	OD1	ASN	A	11	3.063	-6.913	15.551	1.00	10.00	A	O
ATOM	105	ND2	ASN	A	11	5.193	-7.197	16.184	1.00	10.00	A	N
ATOM	106	HD21	ASN	A	11	6.105	-6.834	16.160	1.00	10.00	A	H
ATOM	107	HD22	ASN	A	11	4.958	-8.031	16.642	1.00	10.00	A	H
ATOM	108	C	ASN	A	11	3.771	-5.779	12.563	1.00	10.00	A	C
ATOM	109	O	ASN	A	11	3.259	-4.919	11.844	1.00	10.00	A	O
ATOM	110	N	ASN	A	12	3.283	-7.011	12.669	1.00	10.00	A	N
ATOM	111	HN	ASN	A	12	3.722	-7.648	13.271	1.00	10.00	A	H
ATOM	112	CA	ASN	A	12	2.098	-7.438	11.917	1.00	10.00	A	C
ATOM	113	CB	ASN	A	12	1.809	-8.926	12.108	1.00	10.00	A	C
ATOM	114	CG	ASN	A	12	2.365	-9.774	10.984	1.00	10.00	A	C
ATOM	115	OD1	ASN	A	12	3.490	-10.265	11.063	1.00	10.00	A	O
ATOM	116	ND2	ASN	A	12	1.585	-9.958	9.935	1.00	10.00	A	N
ATOM	117	HD21	ASN	A	12	0.692	-9.543	9.937	1.00	10.00	A	H
ATOM	118	HD22	ASN	A	12	1.922	-10.503	9.197	1.00	10.00	A	H
ATOM	119	C	ASN	A	12	0.871	-6.618	12.290	1.00	10.00	A	C
ATOM	120	O	ASN	A	12	-0.035	-6.442	11.481	1.00	10.00	A	O
ATOM	121	N	LYS	A	13	0.855	-6.112	13.517	1.00	10.00	A	N
ATOM	122	HN	LYS	A	13	1.607	-6.305	14.121	1.00	10.00	A	H
ATOM	123	CA	LYS	A	13	-0.260	-5.296	14.001	1.00	10.00	A	C
ATOM	124	CB	LYS	A	13	-0.037	-4.901	15.463	1.00	10.00	A	C
ATOM	125	CG	LYS	A	13	1.242	-4.114	15.697	1.00	10.00	A	C
ATOM	126	CD	LYS	A	13	1.407	-3.736	17.157	1.00	10.00	A	C
ATOM	127	CE	LYS	A	13	2.471	-2.666	17.327	1.00	10.00	A	C
ATOM	128	NZ	LYS	A	13	2.150	-1.437	16.553	1.00	10.00	A	N
ATOM	129	HZ1	LYS	A	13	1.131	-1.236	16.607	1.00	10.00	A	H
ATOM	130	HZ2	LYS	A	13	2.414	-1.566	15.549	1.00	10.00	A	H
ATOM	131	HZ3	LYS	A	13	2.674	-0.625	16.935	1.00	10.00	A	H
ATOM	132	C	LYS	A	13	-0.455	-4.045	13.138	1.00	10.00	A	C
ATOM	133	O	LYS	A	13	-1.565	-3.531	13.011	1.00	10.00	A	O
ATOM	134	N	ASP	A	14	0.627	-3.568	12.539	1.00	10.00	A	N
ATOM	135	HN	ASP	A	14	1.489	-4.022	12.675	1.00	10.00	A	H
ATOM	136	CA	ASP	A	14	0.574	-2.383	11.689	1.00	10.00	A	C
ATOM	137	CB	ASP	A	14	1.815	-1.511	11.900	1.00	10.00	A	C
ATOM	138	CG	ASP	A	14	2.041	-1.146	13.352	1.00	10.00	A	C
ATOM	139	OD1	ASP	A	14	1.339	-0.253	13.872	1.00	10.00	A	O
ATOM	140	OD2	ASP	A	14	2.928	-1.755	13.990	1.00	10.00	A	O
ATOM	141	C	ASP	A	14	0.461	-2.784	10.224	1.00	10.00	A	C
ATOM	142	O	ASP	A	14	0.268	-1.947	9.343	1.00	10.00	A	O

ATOM	143	N	ALA	A	15	0.568	-4.080	9.975	1.00	10.00	A	N
ATOM	144	HN	ALA	A	15	0.703	-4.697	10.725	1.00	10.00	A	H
ATOM	145	CA	ALA	A	15	0.484	-4.615	8.624	1.00	10.00	A	C
ATOM	146	CB	ALA	A	15	1.361	-5.849	8.480	1.00	10.00	A	C
ATOM	147	C	ALA	A	15	-0.960	-4.928	8.251	1.00	10.00	A	C
ATOM	148	O	ALA	A	15	-1.279	-5.124	7.083	1.00	10.00	A	O
ATOM	149	N	ARG	A	16	-1.831	-4.965	9.247	1.00	10.00	A	N
ATOM	150	HN	ARG	A	16	-1.518	-4.798	10.161	1.00	10.00	A	H
ATOM	151	CA	ARG	A	16	-3.239	-5.247	9.018	1.00	10.00	A	C
ATOM	152	CB	ARG	A	16	-3.682	-6.450	9.860	1.00	10.00	A	C
ATOM	153	CG	ARG	A	16	-5.059	-7.000	9.509	1.00	10.00	A	C
ATOM	154	CD	ARG	A	16	-5.079	-7.629	8.128	1.00	10.00	A	C
ATOM	155	NE	ARG	A	16	-4.325	-8.875	8.094	1.00	10.00	A	N
ATOM	156	HE	ARG	A	16	-3.859	-9.156	8.925	1.00	10.00	A	H
ATOM	157	CZ	ARG	A	16	-4.224	-9.655	7.029	1.00	10.00	A	C
ATOM	158	NH1	ARG	A	16	-4.832	-9.326	5.897	1.00	10.00	A	N
ATOM	159	HH11	ARG	A	16	-5.386	-8.447	5.841	1.00	10.00	A	H
ATOM	160	HH12	ARG	A	16	-4.753	-9.938	5.060	1.00	10.00	A	H
ATOM	161	NH2	ARG	A	16	-3.495	-10.757	7.104	1.00	10.00	A	N
ATOM	162	HH21	ARG	A	16	-3.007	-10.993	8.011	1.00	10.00	A	H
ATOM	163	HH22	ARG	A	16	-3.401	-11.391	6.286	1.00	10.00	A	H
ATOM	164	C	ARG	A	16	-4.077	-4.016	9.360	1.00	10.00	A	C
ATOM	165	O	ARG	A	16	-5.303	-4.075	9.425	1.00	10.00	A	O
ATOM	166	N	GLN	A	17	-3.400	-2.895	9.579	1.00	10.00	A	N
ATOM	167	HN	GLN	A	17	-2.423	-2.904	9.497	1.00	10.00	A	H
ATOM	168	CA	GLN	A	17	-4.077	-1.649	9.923	1.00	10.00	A	C
ATOM	169	CB	GLN	A	17	-3.093	-0.653	10.549	1.00	10.00	A	C
ATOM	170	CG	GLN	A	17	-3.746	0.613	11.077	1.00	10.00	A	C
ATOM	171	CD	GLN	A	17	-4.692	0.347	12.235	1.00	10.00	A	C
ATOM	172	OE1	GLN	A	17	-4.466	-0.549	13.048	1.00	10.00	A	O
ATOM	173	NE2	GLN	A	17	-5.760	1.123	12.318	1.00	10.00	A	N
ATOM	174	HE21	GLN	A	17	-5.884	1.819	11.639	1.00	10.00	A	H
ATOM	175	HE22	GLN	A	17	-6.390	0.969	13.056	1.00	10.00	A	H
ATOM	176	C	GLN	A	17	-4.749	-1.032	8.697	1.00	10.00	A	C
ATOM	177	O	GLN	A	17	-4.122	-0.892	7.642	1.00	10.00	A	O
ATOM	178	N	LYS	A	18	-6.028	-0.688	8.837	1.00	10.00	A	N
ATOM	179	HN	LYS	A	18	-6.471	-0.838	9.699	1.00	10.00	A	H
ATOM	180	CA	LYS	A	18	-6.789	-0.073	7.751	1.00	10.00	A	C
ATOM	181	CB	LYS	A	18	-8.263	-0.506	7.797	1.00	10.00	A	C
ATOM	182	CG	LYS	A	18	-8.495	-1.990	7.544	1.00	10.00	A	C
ATOM	183	CD	LYS	A	18	-9.979	-2.341	7.585	1.00	10.00	A	C
ATOM	184	CE	LYS	A	18	-10.224	-3.796	7.202	1.00	10.00	A	C
ATOM	185	NZ	LYS	A	18	-11.674	-4.094	7.027	1.00	10.00	A	N
ATOM	186	HZ1	LYS	A	18	-12.041	-3.592	6.194	1.00	10.00	A	H
ATOM	187	HZ2	LYS	A	18	-12.210	-3.788	7.868	1.00	10.00	A	H
ATOM	188	HZ3	LYS	A	18	-11.818	-5.120	6.891	1.00	10.00	A	H
ATOM	189	C	LYS	A	18	-6.685	1.447	7.848	1.00	10.00	A	C
ATOM	190	O	LYS	A	18	-6.318	1.982	8.897	1.00	10.00	A	O
ATOM	191	N	ILE	A	19	-7.009	2.137	6.763	1.00	10.00	A	N
ATOM	192	HN	ILE	A	19	-7.322	1.655	5.965	1.00	10.00	A	H
ATOM	193	CA	ILE	A	19	-6.936	3.597	6.733	1.00	10.00	A	C
ATOM	194	CB	ILE	A	19	-6.135	4.101	5.517	1.00	10.00	A	C
ATOM	195	CG1	ILE	A	19	-4.822	3.324	5.395	1.00	10.00	A	C
ATOM	196	CG2	ILE	A	19	-5.859	5.594	5.649	1.00	10.00	A	C
ATOM	197	CD1	ILE	A	19	-4.100	3.540	4.087	1.00	10.00	A	C
ATOM	198	C	ILE	A	19	-8.330	4.212	6.716	1.00	10.00	A	C
ATOM	199	O	ILE	A	19	-9.109	3.979	5.797	1.00	10.00	A	O
ATOM	200	N	LYS	A	20	-8.619	5.017	7.731	1.00	10.00	A	N
ATOM	201	HN	LYS	A	20	-7.928	5.203	8.398	1.00	10.00	A	H
ATOM	202	CA	LYS	A	20	-9.925	5.651	7.871	1.00	10.00	A	C
ATOM	203	CB	LYS	A	20	-10.127	6.152	9.304	1.00	10.00	A	C
ATOM	204	CG	LYS	A	20	-10.260	5.055	10.345	1.00	10.00	A	C
ATOM	205	CD	LYS	A	20	-10.630	5.629	11.703	1.00	10.00	A	C
ATOM	206	CE	LYS	A	20	-11.962	6.357	11.646	1.00	10.00	A	C
ATOM	207	NZ	LYS	A	20	-12.327	6.941	12.962	1.00	10.00	A	N
ATOM	208	HZ1	LYS	A	20	-11.575	7.579	13.288	1.00	10.00	A	H
ATOM	209	HZ2	LYS	A	20	-12.453	6.184	13.664	1.00	10.00	A	H
ATOM	210	HZ3	LYS	A	20	-13.213	7.478	12.882	1.00	10.00	A	H
ATOM	211	C	LYS	A	20	-10.127	6.810	6.899	1.00	10.00	A	C
ATOM	212	O	LYS	A	20	-9.165	7.329	6.322	1.00	10.00	A	O
ATOM	213	N	ASP	A	21	-11.398	7.202	6.747	1.00	10.00	A	N
ATOM	214	HN	ASP	A	21	-12.092	6.709	7.233	1.00	10.00	A	H
ATOM	215	CA	ASP	A	21	-11.820	8.310	5.879	1.00	10.00	A	C
ATOM	216	CB	ASP	A	21	-10.943	9.559	6.047	1.00	10.00	A	C
ATOM	217	CG	ASP	A	21	-11.699	10.840	5.777	1.00	10.00	A	C
ATOM	218	OD1	ASP	A	21	-11.314	11.584	4.854	1.00	10.00	A	O
ATOM	219	OD2	ASP	A	21	-12.688	11.111	6.491	1.00	10.00	A	O
ATOM	220	C	ASP	A	21	-11.942	7.896	4.412	1.00	10.00	A	C
ATOM	221	O	ASP	A	21	-11.551	6.792	4.033	1.00	10.00	A	O
ATOM	222	N	GLU	A	22	-12.526	8.771	3.599	1.00	10.00	A	N
ATOM	223	HN	GLU	A	22	-12.844	9.625	3.965	1.00	10.00	A	H
ATOM	224	CA	GLU	A	22	-12.700	8.505	2.179	1.00	10.00	A	C
ATOM	225	CB	GLU	A	22	-13.811	9.383	1.597	1.00	10.00	A	C
ATOM	226	CG	GLU	A	22	-15.135	9.290	2.341	1.00	10.00	A	C
ATOM	227	CD	GLU	A	22	-16.260	10.007	1.621	1.00	10.00	A	C
ATOM	228	OE1	GLU	A	22	-16.131	11.222	1.362	1.00	10.00	A	O
ATOM	229	OE2	GLU	A	22	-17.285	9.356	1.318	1.00	10.00	A	O
ATOM	230	C	GLU	A	22	-11.394	8.769	1.443	1.00	10.00	A	C
ATOM	231	O	GLU	A	22	-11.042	9.920	1.171	1.00	10.00	A	O
ATOM	232	N	VAL	A	23	-10.672	7.704	1.139	1.00	10.00	A	N
ATOM	233	HN	VAL	A	23	-11.004	6.812	1.387	1.00	10.00	A	H
ATOM	234	CA	VAL	A	23	-9.396	7.821	0.449	1.00	10.00	A	C
ATOM	235	CB	VAL	A	23	-8.305	6.965	1.131	1.00	10.00	A	C
ATOM	236	CG1	VAL	A	23	-8.100	7.416	2.571	1.00	10.00	A	C
ATOM	237	CG2	VAL	A	23	-8.666	5.489	1.088	1.00	10.00	A	C

ATOM	238	C	VAL	A	23	-9.523	7.435	-1.023	1.00	10.00	A	C
ATOM	239	O	VAL	A	23	-10.577	6.970	-1.464	1.00	10.00	A	O
ATOM	240	N	ASN	A	24	-8.459	7.643	-1.784	1.00	10.00	A	N
ATOM	241	HN	ASN	A	24	-7.642	8.017	-1.379	1.00	10.00	A	H
ATOM	242	CA	ASN	A	24	-8.464	7.309	-3.203	1.00	10.00	A	C
ATOM	243	CB	ASN	A	24	-8.230	8.552	-4.074	1.00	10.00	A	C
ATOM	244	CG	ASN	A	24	-8.969	8.486	-5.406	1.00	10.00	A	C
ATOM	245	OD1	ASN	A	24	-9.099	7.420	-6.010	1.00	10.00	A	O
ATOM	246	ND2	ASN	A	24	-9.458	9.628	-5.872	1.00	10.00	A	N
ATOM	247	HD21	ASN	A	24	-9.318	10.443	-5.343	1.00	10.00	A	H
ATOM	248	HD22	ASN	A	24	-9.946	9.611	-6.724	1.00	10.00	A	H
ATOM	249	C	ASN	A	24	-7.428	6.228	-3.491	1.00	10.00	A	C
ATOM	250	O	ASN	A	24	-6.566	5.950	-2.656	1.00	10.00	A	O
ATOM	251	N	THR	A	25	-7.509	5.624	-4.663	1.00	10.00	A	N
ATOM	252	HN	THR	A	25	-8.194	5.909	-5.306	1.00	10.00	A	H
ATOM	253	CA	THR	A	25	-6.598	4.560	-5.030	1.00	10.00	A	C
ATOM	254	CB	THR	A	25	-7.322	3.198	-5.003	1.00	10.00	A	C
ATOM	255	OG1	THR	A	25	-6.393	2.133	-5.236	1.00	10.00	A	O
ATOM	256	HG1	THR	A	25	-6.878	1.326	-5.450	1.00	10.00	A	H
ATOM	257	CG2	THR	A	25	-8.420	3.151	-6.053	1.00	10.00	A	C
ATOM	258	C	THR	A	25	-5.977	4.791	-6.407	1.00	10.00	A	C
ATOM	259	O	THR	A	25	-6.469	5.597	-7.206	1.00	10.00	A	O
ATOM	260	N	GLN	A	26	-4.883	4.092	-6.657	1.00	10.00	A	N
ATOM	261	HN	GLN	A	26	-4.543	3.485	-5.960	1.00	10.00	A	H
ATOM	262	CA	GLN	A	26	-4.171	4.167	-7.919	1.00	10.00	A	C
ATOM	263	CB	GLN	A	26	-3.191	5.342	-7.920	1.00	10.00	A	C
ATOM	264	CG	GLN	A	26	-2.323	5.428	-9.164	1.00	10.00	A	C
ATOM	265	CD	GLN	A	26	-1.599	6.752	-9.277	1.00	10.00	A	C
ATOM	266	OE1	GLN	A	26	-1.316	7.407	-8.275	1.00	10.00	A	O
ATOM	267	NE2	GLN	A	26	-1.303	7.159	-10.496	1.00	10.00	A	N
ATOM	268	HE21	GLN	A	26	-1.568	6.590	-11.253	1.00	10.00	A	H
ATOM	269	HE22	GLN	A	26	-0.826	8.009	-10.599	1.00	10.00	A	H
ATOM	270	C	GLN	A	26	-3.429	2.857	-8.136	1.00	10.00	A	C
ATOM	271	O	GLN	A	26	-2.632	2.448	-7.290	1.00	10.00	A	O
ATOM	272	N	LYS	A	27	-3.714	2.192	-9.247	1.00	10.00	A	N
ATOM	273	HN	LYS	A	27	-4.362	2.568	-9.878	1.00	10.00	A	H
ATOM	274	CA	LYS	A	27	-3.080	0.920	-9.555	1.00	10.00	A	C
ATOM	275	CB	LYS	A	27	-4.117	-0.206	-9.610	1.00	10.00	A	C
ATOM	276	CG	LYS	A	27	-5.137	-0.083	-10.736	1.00	10.00	A	C
ATOM	277	CD	LYS	A	27	-6.132	-1.231	-10.711	1.00	10.00	A	C
ATOM	278	CE	LYS	A	27	-6.961	-1.266	-11.985	1.00	10.00	A	C
ATOM	279	NZ	LYS	A	27	-7.872	-2.442	-12.017	1.00	10.00	A	N
ATOM	280	HZ1	LYS	A	27	-8.373	-2.481	-12.925	1.00	10.00	A	H
ATOM	281	HZ2	LYS	A	27	-8.573	-2.371	-11.253	1.00	10.00	A	H
ATOM	282	HZ3	LYS	A	27	-7.332	-3.322	-11.893	1.00	10.00	A	H
ATOM	283	C	LYS	A	27	-2.281	0.973	-10.852	1.00	10.00	A	C
ATOM	284	O	LYS	A	27	-2.666	1.647	-11.812	1.00	10.00	A	O
ATOM	285	N	GLU	A	28	-1.164	0.269	-10.855	1.00	10.00	A	N
ATOM	286	HN	GLU	A	28	-0.914	-0.221	-10.036	1.00	10.00	A	H
ATOM	287	CA	GLU	A	28	-0.288	0.186	-12.012	1.00	10.00	A	C
ATOM	288	CB	GLU	A	28	0.865	1.182	-11.889	1.00	10.00	A	C
ATOM	289	CG	GLU	A	28	0.542	2.573	-12.409	1.00	10.00	A	C
ATOM	290	CD	GLU	A	28	0.819	2.723	-13.891	1.00	10.00	A	C
ATOM	291	OE1	GLU	A	28	1.317	3.791	-14.302	1.00	10.00	A	O
ATOM	292	OE2	GLU	A	28	0.571	1.767	-14.651	1.00	10.00	A	O
ATOM	293	C	GLU	A	28	0.260	-1.227	-12.127	1.00	10.00	A	C
ATOM	294	O	GLU	A	28	1.139	-1.624	-11.358	1.00	10.00	A	O
ATOM	295	N	GLY	A	29	-0.274	-1.987	-13.069	1.00	10.00	A	N
ATOM	296	HN	GLY	A	29	-0.980	-1.616	-13.642	1.00	10.00	A	H
ATOM	297	CA	GLY	A	29	0.167	-3.356	-13.261	1.00	10.00	A	C
ATOM	298	C	GLY	A	29	-0.364	-4.279	-12.181	1.00	10.00	A	C
ATOM	299	O	GLY	A	29	-1.497	-4.762	-12.270	1.00	10.00	A	O
ATOM	300	N	LYS	A	30	0.451	-4.514	-11.158	1.00	10.00	A	N
ATOM	301	HN	LYS	A	30	1.335	-4.087	-11.150	1.00	10.00	A	H
ATOM	302	CA	LYS	A	30	0.073	-5.378	-10.047	1.00	10.00	A	C
ATOM	303	CB	LYS	A	30	0.923	-6.650	-10.038	1.00	10.00	A	C
ATOM	304	CG	LYS	A	30	0.554	-7.668	-11.109	1.00	10.00	A	C
ATOM	305	CD	LYS	A	30	1.384	-8.936	-10.973	1.00	10.00	A	C
ATOM	306	CE	LYS	A	30	2.859	-8.660	-11.220	1.00	10.00	A	C
ATOM	307	NZ	LYS	A	30	3.727	-9.662	-10.549	1.00	10.00	A	N
ATOM	308	HZ1	LYS	A	30	3.762	-10.539	-11.109	1.00	10.00	A	H
ATOM	309	HZ2	LYS	A	30	3.356	-9.880	-9.603	1.00	10.00	A	H
ATOM	310	HZ3	LYS	A	30	4.697	-9.285	-10.449	1.00	10.00	A	H
ATOM	311	C	LYS	A	30	0.229	-4.649	-8.717	1.00	10.00	A	C
ATOM	312	O	LYS	A	30	0.069	-5.242	-7.650	1.00	10.00	A	O
ATOM	313	N	PHE	A	31	0.530	-3.361	-8.781	1.00	10.00	A	N
ATOM	314	HN	PHE	A	31	0.606	-2.928	-9.657	1.00	10.00	A	H
ATOM	315	CA	PHE	A	31	0.722	-2.565	-7.579	1.00	10.00	A	C
ATOM	316	CB	PHE	A	31	2.086	-1.872	-7.614	1.00	10.00	A	C
ATOM	317	CG	PHE	A	31	3.255	-2.814	-7.615	1.00	10.00	A	C
ATOM	318	CD1	PHE	A	31	3.836	-3.215	-6.424	1.00	10.00	A	C
ATOM	319	CD2	PHE	A	31	3.775	-3.296	-8.805	1.00	10.00	A	C
ATOM	320	CE1	PHE	A	31	4.913	-4.078	-6.419	1.00	10.00	A	C
ATOM	321	CE2	PHE	A	31	4.852	-4.159	-8.806	1.00	10.00	A	C
ATOM	322	CZ	PHE	A	31	5.422	-4.551	-7.611	1.00	10.00	A	C
ATOM	323	C	PHE	A	31	-0.374	-1.521	-7.435	1.00	10.00	A	C
ATOM	324	O	PHE	A	31	-0.670	-0.787	-8.378	1.00	10.00	A	O
ATOM	325	N	ARG	A	32	-0.974	-1.456	-6.255	1.00	10.00	A	N
ATOM	326	HN	ARG	A	32	-0.698	-2.071	-5.540	1.00	10.00	A	H
ATOM	327	CA	ARG	A	32	-2.026	-0.487	-5.990	1.00	10.00	A	C
ATOM	328	CB	ARG	A	32	-3.405	-1.152	-5.944	1.00	10.00	A	C
ATOM	329	CG	ARG	A	32	-3.525	-2.291	-4.951	1.00	10.00	A	C
ATOM	330	CD	ARG	A	32	-4.869	-2.986	-5.074	1.00	10.00	A	C
ATOM	331	NE	ARG	A	32	-4.867	-4.309	-4.455	1.00	10.00	A	N
ATOM	332	HE	ARG	A	32	-3.997	-4.675	-4.179	1.00	10.00	A	H

ATOM	333	CZ	ARG	A	32	-5.963	-5.038	-4.256	1.00	10.00	A	C
ATOM	334	NH1	ARG	A	32	-7.149	-4.572	-4.621	1.00	10.00	A	N
ATOM	335	HH11	ARG	A	32	-8.008	-5.140	-4.461	1.00	10.00	A	H
ATOM	336	HH12	ARG	A	32	-7.228	-3.636	-5.070	1.00	10.00	A	H
ATOM	337	NH2	ARG	A	32	-5.871	-6.236	-3.699	1.00	10.00	A	N
ATOM	338	HH21	ARG	A	32	-6.731	-6.809	-3.543	1.00	10.00	A	H
ATOM	339	HH22	ARG	A	32	-4.938	-6.612	-3.413	1.00	10.00	A	H
ATOM	340	C	ARG	A	32	-1.736	0.266	-4.698	1.00	10.00	A	C
ATOM	341	O	ARG	A	32	-1.329	-0.334	-3.699	1.00	10.00	A	O
ATOM	342	N	LEU	A	33	-1.913	1.578	-4.729	1.00	10.00	A	N
ATOM	343	HN	LEU	A	33	-2.225	2.001	-5.559	1.00	10.00	A	H
ATOM	344	CA	LEU	A	33	-1.661	2.404	-3.562	1.00	10.00	A	C
ATOM	345	CB	LEU	A	33	-0.558	3.438	-3.851	1.00	10.00	A	C
ATOM	346	CG	LEU	A	33	-0.949	4.655	-4.704	1.00	10.00	A	C
ATOM	347	CD1	LEU	A	33	-1.245	5.864	-3.828	1.00	10.00	A	C
ATOM	348	CD2	LEU	A	33	0.140	4.986	-5.709	1.00	10.00	A	C
ATOM	349	C	LEU	A	33	-2.934	3.096	-3.090	1.00	10.00	A	C
ATOM	350	O	LEU	A	33	-3.724	3.586	-3.898	1.00	10.00	A	O
ATOM	351	N	THR	A	34	-3.138	3.105	-1.785	1.00	10.00	A	N
ATOM	352	HN	THR	A	34	-2.487	2.655	-1.196	1.00	10.00	A	H
ATOM	353	CA	THR	A	34	-4.290	3.757	-1.188	1.00	10.00	A	C
ATOM	354	CB	THR	A	34	-5.017	2.799	-0.224	1.00	10.00	A	C
ATOM	355	OG1	THR	A	34	-4.720	1.440	-0.585	1.00	10.00	A	O
ATOM	356	HG1	THR	A	34	-4.792	1.336	-1.545	1.00	10.00	A	H
ATOM	357	CG2	THR	A	34	-6.519	3.012	-0.305	1.00	10.00	A	C
ATOM	358	C	THR	A	34	-3.803	4.983	-0.422	1.00	10.00	A	C
ATOM	359	O	THR	A	34	-3.140	4.854	0.608	1.00	10.00	A	O
ATOM	360	N	ILE	A	35	-4.119	6.167	-0.922	1.00	10.00	A	N
ATOM	361	HN	ILE	A	35	-4.682	6.219	-1.729	1.00	10.00	A	H
ATOM	362	CA	ILE	A	35	-3.664	7.399	-0.285	1.00	10.00	A	C
ATOM	363	CB	ILE	A	35	-2.775	8.225	-1.244	1.00	10.00	A	C
ATOM	364	CG1	ILE	A	35	-1.966	9.277	-0.480	1.00	10.00	A	C
ATOM	365	CG2	ILE	A	35	-3.604	8.866	-2.350	1.00	10.00	A	C
ATOM	366	CD1	ILE	A	35	-0.808	9.844	-1.273	1.00	10.00	A	C
ATOM	367	C	ILE	A	35	-4.826	8.243	0.227	1.00	10.00	A	C
ATOM	368	O	ILE	A	35	-5.911	8.251	-0.363	1.00	10.00	A	O
ATOM	369	N	LYS	A	36	-4.595	8.926	1.343	1.00	10.00	A	N
ATOM	370	HN	LYS	A	36	-3.717	8.841	1.779	1.00	10.00	A	H
ATOM	371	CA	LYS	A	36	-5.599	9.785	1.951	1.00	10.00	A	C
ATOM	372	CB	LYS	A	36	-5.129	10.236	3.336	1.00	10.00	A	C
ATOM	373	CG	LYS	A	36	-6.215	10.866	4.192	1.00	10.00	A	C
ATOM	374	CD	LYS	A	36	-5.717	11.137	5.602	1.00	10.00	A	C
ATOM	375	CE	LYS	A	36	-6.792	11.798	6.453	1.00	10.00	A	C
ATOM	376	NZ	LYS	A	36	-6.352	11.979	7.862	1.00	10.00	A	N
ATOM	377	HZ1	LYS	A	36	-6.198	11.053	8.311	1.00	10.00	A	H
ATOM	378	HZ2	LYS	A	36	-7.074	12.496	8.400	1.00	10.00	A	H
ATOM	379	HZ3	LYS	A	36	-5.463	12.518	7.894	1.00	10.00	A	H
ATOM	380	C	LYS	A	36	-5.868	10.994	1.061	1.00	10.00	A	C
ATOM	381	O	LYS	A	36	-4.963	11.487	0.386	1.00	10.00	A	O
ATOM	382	N	ARG	A	37	-7.113	11.461	1.060	1.00	10.00	A	N
ATOM	383	HN	ARG	A	37	-7.788	11.024	1.620	1.00	10.00	A	H
ATOM	384	CA	ARG	A	37	-7.503	12.603	0.250	1.00	10.00	A	C
ATOM	385	CB	ARG	A	37	-9.017	12.812	0.320	1.00	10.00	A	C
ATOM	386	CG	ARG	A	37	-9.548	13.866	-0.641	1.00	10.00	A	C
ATOM	387	CD	ARG	A	37	-10.848	14.467	-0.133	1.00	10.00	A	C
ATOM	388	NE	ARG	A	37	-10.684	15.060	1.189	1.00	10.00	A	N
ATOM	389	HE	ARG	A	37	-9.876	15.609	1.341	1.00	10.00	A	H
ATOM	390	CZ	ARG	A	37	-11.549	14.908	2.186	1.00	10.00	A	C
ATOM	391	NH1	ARG	A	37	-12.655	14.191	2.021	1.00	10.00	A	N
ATOM	392	HH11	ARG	A	37	-12.857	13.740	1.103	1.00	10.00	A	H
ATOM	393	HH12	ARG	A	37	-13.328	14.074	2.814	1.00	10.00	A	H
ATOM	394	NH2	ARG	A	37	-11.294	15.467	3.354	1.00	10.00	A	N
ATOM	395	HH21	ARG	A	37	-10.411	16.026	3.486	1.00	10.00	A	H
ATOM	396	HH22	ARG	A	37	-11.963	15.354	4.146	1.00	10.00	A	H
ATOM	397	C	ARG	A	37	-6.779	13.863	0.708	1.00	10.00	A	C
ATOM	398	O	ARG	A	37	-6.392	14.699	-0.109	1.00	10.00	A	O
ATOM	399	N	ASP	A	38	-6.601	13.997	2.014	1.00	10.00	A	N
ATOM	400	HN	ASP	A	38	-6.936	13.302	2.617	1.00	10.00	A	H
ATOM	401	CA	ASP	A	38	-5.916	15.156	2.569	1.00	10.00	A	C
ATOM	402	CB	ASP	A	38	-6.733	15.817	3.685	1.00	10.00	A	C
ATOM	403	CG	ASP	A	38	-7.666	16.890	3.159	1.00	10.00	A	C
ATOM	404	OD1	ASP	A	38	-8.901	16.684	3.188	1.00	10.00	A	O
ATOM	405	OD2	ASP	A	38	-7.171	17.948	2.708	1.00	10.00	A	O
ATOM	406	C	ASP	A	38	-4.520	14.789	3.052	1.00	10.00	A	C
ATOM	407	O	ASP	A	38	-4.320	14.434	4.215	1.00	10.00	A	O
ATOM	408	N	ILE	A	39	-3.559	14.853	2.144	1.00	10.00	A	N
ATOM	409	HN	ILE	A	39	-3.787	15.114	1.230	1.00	10.00	A	H
ATOM	410	CA	ILE	A	39	-2.179	14.531	2.468	1.00	10.00	A	C
ATOM	411	CB	ILE	A	39	-1.747	13.182	1.847	1.00	10.00	A	C
ATOM	412	CG1	ILE	A	39	-0.402	12.723	2.422	1.00	10.00	A	C
ATOM	413	CG2	ILE	A	39	-1.697	13.269	0.327	1.00	10.00	A	C
ATOM	414	CD1	ILE	A	39	0.020	11.339	1.976	1.00	10.00	A	C
ATOM	415	C	ILE	A	39	-1.230	15.651	2.033	1.00	10.00	A	C
ATOM	416	O	ILE	A	39	-0.096	15.742	2.507	1.00	10.00	A	O
ATOM	417	N	ARG	A	40	-1.710	16.530	1.158	1.00	10.00	A	N
ATOM	418	HN	ARG	A	40	-2.632	16.432	0.836	1.00	10.00	A	H
ATOM	419	CA	ARG	A	40	-0.895	17.642	0.671	1.00	10.00	A	C
ATOM	420	CB	ARG	A	40	-1.597	18.384	-0.466	1.00	10.00	A	C
ATOM	421	CG	ARG	A	40	-1.601	17.652	-1.795	1.00	10.00	A	C
ATOM	422	CD	ARG	A	40	-2.060	18.568	-2.918	1.00	10.00	A	C
ATOM	423	NE	ARG	A	40	-0.961	19.375	-3.453	1.00	10.00	A	N
ATOM	424	HE	ARG	A	40	-0.229	18.891	-3.915	1.00	10.00	A	H
ATOM	425	CZ	ARG	A	40	-0.895	20.706	-3.375	1.00	10.00	A	C
ATOM	426	NH1	ARG	A	40	-1.863	21.399	-2.785	1.00	10.00	A	N
ATOM	427	HH11	ARG	A	40	-2.684	20.907	-2.374	1.00	10.00	A	H

ATOM	428	HH12	ARG	A	40	-1.803	22.440	-2.732	1.00	10.00	A	H
ATOM	429	NH2	ARG	A	40	0.149	21.344	-3.884	1.00	10.00	A	N
ATOM	430	HH21	ARG	A	40	0.918	20.803	-4.343	1.00	10.00	A	H
ATOM	431	HH22	ARG	A	40	0.205	22.386	-3.833	1.00	10.00	A	H
ATOM	432	C	ARG	A	40	-0.584	18.620	1.795	1.00	10.00	A	C
ATOM	433	O	ARG	A	40	0.310	19.453	1.673	1.00	10.00	A	O
ATOM	434	N	ASN	A	41	-1.326	18.502	2.886	1.00	10.00	A	N
ATOM	435	HN	ASN	A	41	-2.020	17.812	2.911	1.00	10.00	A	H
ATOM	436	CA	ASN	A	41	-1.151	19.367	4.046	1.00	10.00	A	C
ATOM	437	CB	ASN	A	41	-2.393	19.292	4.936	1.00	10.00	A	C
ATOM	438	CG	ASN	A	41	-3.197	20.577	4.941	1.00	10.00	A	C
ATOM	439	OD1	ASN	A	41	-3.126	21.375	4.005	1.00	10.00	A	O
ATOM	440	ND2	ASN	A	41	-3.972	20.784	5.993	1.00	10.00	A	N
ATOM	441	HD21	ASN	A	41	-3.983	20.104	6.701	1.00	10.00	A	H
ATOM	442	HD22	ASN	A	41	-4.506	21.608	6.023	1.00	10.00	A	H
ATOM	443	C	ASN	A	41	0.085	18.985	4.857	1.00	10.00	A	C
ATOM	444	O	ASN	A	41	0.588	19.785	5.645	1.00	10.00	A	O
ATOM	445	N	VAL	A	42	0.583	17.772	4.642	1.00	10.00	A	N
ATOM	446	HN	VAL	A	42	0.169	17.198	3.963	1.00	10.00	A	H
ATOM	447	CA	VAL	A	42	1.748	17.278	5.371	1.00	10.00	A	C
ATOM	448	CB	VAL	A	42	1.726	15.738	5.493	1.00	10.00	A	C
ATOM	449	CG1	VAL	A	42	2.708	15.270	6.555	1.00	10.00	A	C
ATOM	450	CG2	VAL	A	42	0.318	15.242	5.807	1.00	10.00	A	C
ATOM	451	C	VAL	A	42	3.048	17.725	4.699	1.00	10.00	A	C
ATOM	452	O	VAL	A	42	3.132	17.786	3.471	1.00	10.00	A	O
ATOM	453	N	LEU	A	43	4.058	18.033	5.507	1.00	10.00	A	N
ATOM	454	HN	LEU	A	43	3.925	17.968	6.479	1.00	10.00	A	H
ATOM	455	CA	LEU	A	43	5.350	18.488	4.991	1.00	10.00	A	C
ATOM	456	CB	LEU	A	43	5.768	19.793	5.675	1.00	10.00	A	C
ATOM	457	CG	LEU	A	43	5.070	21.065	5.185	1.00	10.00	A	C
ATOM	458	CD1	LEU	A	43	5.480	22.261	6.030	1.00	10.00	A	C
ATOM	459	CD2	LEU	A	43	5.387	21.317	3.718	1.00	10.00	A	C
ATOM	460	C	LEU	A	43	6.457	17.441	5.138	1.00	10.00	A	C
ATOM	461	O	LEU	A	43	7.552	17.611	4.598	1.00	10.00	A	O
ATOM	462	N	SER	A	44	6.190	16.369	5.872	1.00	10.00	A	N
ATOM	463	HN	SER	A	44	5.306	16.276	6.292	1.00	10.00	A	H
ATOM	464	CA	SER	A	44	7.194	15.325	6.066	1.00	10.00	A	C
ATOM	465	CB	SER	A	44	8.042	15.619	7.308	1.00	10.00	A	C
ATOM	466	OG	SER	A	44	9.402	15.271	7.105	1.00	10.00	A	O
ATOM	467	HG	SER	A	44	9.912	16.070	6.914	1.00	10.00	A	H
ATOM	468	C	SER	A	44	6.548	13.944	6.156	1.00	10.00	A	C
ATOM	469	O	SER	A	44	5.501	13.778	6.790	1.00	10.00	A	O
ATOM	470	N	LEU	A	45	7.176	12.958	5.518	1.00	10.00	A	N
ATOM	471	HN	LEU	A	45	8.012	13.153	5.041	1.00	10.00	A	H
ATOM	472	CA	LEU	A	45	6.660	11.597	5.503	1.00	10.00	A	C
ATOM	473	CB	LEU	A	45	6.125	11.276	4.103	1.00	10.00	A	C
ATOM	474	CG	LEU	A	45	5.495	9.897	3.901	1.00	10.00	A	C
ATOM	475	CD1	LEU	A	45	4.057	9.887	4.390	1.00	10.00	A	C
ATOM	476	CD2	LEU	A	45	5.567	9.489	2.441	1.00	10.00	A	C
ATOM	477	C	LEU	A	45	7.739	10.579	5.888	1.00	10.00	A	C
ATOM	478	O	LEU	A	45	8.923	10.760	5.584	1.00	10.00	A	O
ATOM	479	N	ARG	A	46	7.317	9.514	6.559	1.00	10.00	A	N
ATOM	480	HN	ARG	A	46	6.355	9.442	6.780	1.00	10.00	A	H
ATOM	481	CA	ARG	A	46	8.212	8.440	6.980	1.00	10.00	A	C
ATOM	482	CB	ARG	A	46	8.176	8.289	8.502	1.00	10.00	A	C
ATOM	483	CG	ARG	A	46	8.640	9.521	9.262	1.00	10.00	A	C
ATOM	484	CD	ARG	A	46	8.377	9.376	10.752	1.00	10.00	A	C
ATOM	485	NE	ARG	A	46	9.111	8.249	11.326	1.00	10.00	A	N
ATOM	486	HE	ARG	A	46	10.096	8.250	11.223	1.00	10.00	A	H
ATOM	487	CZ	ARG	A	46	8.536	7.239	11.986	1.00	10.00	A	C
ATOM	488	NH1	ARG	A	46	7.215	7.220	12.169	1.00	10.00	A	N
ATOM	489	HH11	ARG	A	46	6.768	6.428	12.682	1.00	10.00	A	H
ATOM	490	HH12	ARG	A	46	6.619	7.999	11.811	1.00	10.00	A	H
ATOM	491	NH2	ARG	A	46	9.283	6.247	12.456	1.00	10.00	A	N
ATOM	492	HH21	ARG	A	46	10.320	6.255	12.312	1.00	10.00	A	H
ATOM	493	HH22	ARG	A	46	8.840	5.455	12.973	1.00	10.00	A	H
ATOM	494	C	ARG	A	46	7.762	7.137	6.327	1.00	10.00	A	C
ATOM	495	O	ARG	A	46	6.574	6.812	6.366	1.00	10.00	A	O
ATOM	496	N	VAL	A	47	8.696	6.397	5.732	1.00	10.00	A	N
ATOM	497	HN	VAL	A	47	9.635	6.692	5.751	1.00	10.00	A	H
ATOM	498	CA	VAL	A	47	8.359	5.148	5.052	1.00	10.00	A	C
ATOM	499	CB	VAL	A	47	8.755	5.190	3.553	1.00	10.00	A	C
ATOM	500	CG1	VAL	A	47	8.644	3.813	2.909	1.00	10.00	A	C
ATOM	501	CG2	VAL	A	47	7.888	6.191	2.803	1.00	10.00	A	C
ATOM	502	C	VAL	A	47	8.988	3.925	5.717	1.00	10.00	A	C
ATOM	503	O	VAL	A	47	10.175	3.914	6.046	1.00	10.00	A	O
ATOM	504	N	LEU	A	48	8.163	2.903	5.910	1.00	10.00	A	N
ATOM	505	HN	LEU	A	48	7.227	3.001	5.633	1.00	10.00	A	H
ATOM	506	CA	LEU	A	48	8.583	1.634	6.498	1.00	10.00	A	C
ATOM	507	CB	LEU	A	48	8.128	1.524	7.959	1.00	10.00	A	C
ATOM	508	CG	LEU	A	48	8.806	2.466	8.962	1.00	10.00	A	C
ATOM	509	CD1	LEU	A	48	7.972	3.720	9.181	1.00	10.00	A	C
ATOM	510	CD2	LEU	A	48	9.058	1.758	10.283	1.00	10.00	A	C
ATOM	511	C	LEU	A	48	7.979	0.502	5.669	1.00	10.00	A	C
ATOM	512	O	LEU	A	48	6.800	0.562	5.298	1.00	10.00	A	O
ATOM	513	N	VAL	A	49	8.766	-0.525	5.364	1.00	10.00	A	N
ATOM	514	HN	VAL	A	49	9.687	-0.561	5.717	1.00	10.00	A	H
ATOM	515	CA	VAL	A	49	8.267	-1.617	4.535	1.00	10.00	A	C
ATOM	516	CB	VAL	A	49	8.892	-1.606	3.114	1.00	10.00	A	C
ATOM	517	CG1	VAL	A	49	8.137	-2.533	2.171	1.00	10.00	A	C
ATOM	518	CG2	VAL	A	49	8.944	-0.198	2.542	1.00	10.00	A	C
ATOM	519	C	VAL	A	49	8.481	-2.991	5.168	1.00	10.00	A	C
ATOM	520	O	VAL	A	49	9.473	-3.236	5.852	1.00	10.00	A	O
ATOM	521	N	ASN	A	50	7.521	-3.877	4.931	1.00	10.00	A	N
ATOM	522	HN	ASN	A	50	6.743	-3.595	4.401	1.00	10.00	A	H

ATOM	523	CA	ASN	A	50	7.569	-5.249	5.420	1.00	10.00	A	C
ATOM	524	CB	ASN	A	50	6.415	-5.510	6.401	1.00	10.00	A	C
ATOM	525	CG	ASN	A	50	6.718	-5.091	7.824	1.00	10.00	A	C
ATOM	526	OD1	ASN	A	50	7.436	-4.127	8.063	1.00	10.00	A	O
ATOM	527	ND2	ASN	A	50	6.161	-5.812	8.786	1.00	10.00	A	N
ATOM	528	HD21	ASN	A	50	5.588	-6.565	8.529	1.00	10.00	A	H
ATOM	529	HD22	ASN	A	50	6.354	-5.568	9.722	1.00	10.00	A	H
ATOM	530	C	ASN	A	50	7.402	-6.178	4.227	1.00	10.00	A	C
ATOM	531	O	ASN	A	50	6.534	-5.942	3.383	1.00	10.00	A	O
ATOM	532	N	GLY	A	51	8.219	-7.217	4.136	1.00	10.00	A	N
ATOM	533	HN	GLY	A	51	8.912	-7.362	4.823	1.00	10.00	A	H
ATOM	534	CA	GLY	A	51	8.099	-8.132	3.022	1.00	10.00	A	C
ATOM	535	C	GLY	A	51	9.141	-9.228	3.023	1.00	10.00	A	C
ATOM	536	O	GLY	A	51	9.790	-9.488	4.034	1.00	10.00	A	O
ATOM	537	N	THR	A	52	9.287	-9.878	1.885	1.00	10.00	A	N
ATOM	538	HN	THR	A	52	8.736	-9.614	1.113	1.00	10.00	A	H
ATOM	539	CA	THR	A	52	10.248	-10.952	1.723	1.00	10.00	A	C
ATOM	540	CB	THR	A	52	9.545	-12.259	1.307	1.00	10.00	A	C
ATOM	541	OG1	THR	A	52	8.370	-12.435	2.113	1.00	10.00	A	O
ATOM	542	HG1	THR	A	52	8.197	-11.620	2.595	1.00	10.00	A	H
ATOM	543	CG2	THR	A	52	10.466	-13.454	1.500	1.00	10.00	A	C
ATOM	544	C	THR	A	52	11.284	-10.566	0.671	1.00	10.00	A	C
ATOM	545	O	THR	A	52	10.940	-10.012	-0.377	1.00	10.00	A	O
ATOM	546	N	PHE	A	53	12.543	-10.835	0.973	1.00	10.00	A	N
ATOM	547	HN	PHE	A	53	12.744	-11.265	1.834	1.00	10.00	A	H
ATOM	548	CA	PHE	A	53	13.642	-10.527	0.074	1.00	10.00	A	C
ATOM	549	CB	PHE	A	53	14.652	-9.605	0.765	1.00	10.00	A	C
ATOM	550	CG	PHE	A	53	14.318	-8.140	0.693	1.00	10.00	A	C
ATOM	551	CD1	PHE	A	53	14.984	-7.307	-0.190	1.00	10.00	A	C
ATOM	552	CD2	PHE	A	53	13.346	-7.595	1.515	1.00	10.00	A	C
ATOM	553	CE1	PHE	A	53	14.688	-5.960	-0.252	1.00	10.00	A	C
ATOM	554	CE2	PHE	A	53	13.044	-6.250	1.457	1.00	10.00	A	C
ATOM	555	CZ	PHE	A	53	13.715	-5.430	0.573	1.00	10.00	A	C
ATOM	556	C	PHE	A	53	14.350	-11.804	-0.366	1.00	10.00	A	C
ATOM	557	O	PHE	A	53	14.136	-12.876	0.203	1.00	10.00	A	O
ATOM	558	N	LEU	A	54	15.176	-11.680	-1.389	1.00	10.00	A	N
ATOM	559	HN	LEU	A	54	15.268	-10.796	-1.817	1.00	10.00	A	H
ATOM	560	CA	LEU	A	54	15.946	-12.795	-1.908	1.00	10.00	A	C
ATOM	561	CB	LEU	A	54	15.644	-13.009	-3.392	1.00	10.00	A	C
ATOM	562	CG	LEU	A	54	14.255	-13.557	-3.727	1.00	10.00	A	C
ATOM	563	CD1	LEU	A	54	14.009	-13.504	-5.226	1.00	10.00	A	C
ATOM	564	CD2	LEU	A	54	14.097	-14.980	-3.207	1.00	10.00	A	C
ATOM	565	C	LEU	A	54	17.425	-12.510	-1.719	1.00	10.00	A	C
ATOM	566	O	LEU	A	54	17.990	-11.655	-2.403	1.00	10.00	A	O
ATOM	567	N	LYS	A	55	18.039	-13.210	-0.777	1.00	10.00	A	N
ATOM	568	HN	LYS	A	55	17.529	-13.879	-0.265	1.00	10.00	A	H
ATOM	569	CA	LYS	A	55	19.450	-13.023	-0.486	1.00	10.00	A	C
ATOM	570	CB	LYS	A	55	19.766	-13.439	0.954	1.00	10.00	A	C
ATOM	571	CG	LYS	A	55	21.166	-13.065	1.421	1.00	10.00	A	C
ATOM	572	CD	LYS	A	55	21.362	-11.556	1.425	1.00	10.00	A	C
ATOM	573	CE	LYS	A	55	22.723	-11.182	1.987	1.00	10.00	A	C
ATOM	574	NZ	LYS	A	55	22.869	-9.711	2.145	1.00	10.00	A	N
ATOM	575	HZ1	LYS	A	55	22.901	-9.245	1.211	1.00	10.00	A	H
ATOM	576	HZ2	LYS	A	55	23.747	-9.488	2.655	1.00	10.00	A	H
ATOM	577	HZ3	LYS	A	55	22.065	-9.328	2.682	1.00	10.00	A	H
ATOM	578	C	LYS	A	55	20.316	-13.799	-1.467	1.00	10.00	A	C
ATOM	579	O	LYS	A	55	20.295	-15.034	-1.498	1.00	10.00	A	O
ATOM	580	N	HIS	A	56	21.067	-13.065	-2.271	1.00	10.00	A	N
ATOM	581	HN	HIS	A	56	21.024	-12.082	-2.198	1.00	10.00	A	H
ATOM	582	CA	HIS	A	56	21.954	-13.665	-3.259	1.00	10.00	A	C
ATOM	583	CB	HIS	A	56	22.141	-12.720	-4.451	1.00	10.00	A	C
ATOM	584	CG	HIS	A	56	21.068	-12.811	-5.492	1.00	10.00	A	C
ATOM	585	ND1	HIS	A	56	21.294	-13.207	-6.790	1.00	10.00	A	N
ATOM	586	HD1	HIS	A	56	22.160	-13.469	-7.175	1.00	10.00	A	H
ATOM	587	CD2	HIS	A	56	19.742	-12.542	-5.409	1.00	10.00	A	C
ATOM	588	CE1	HIS	A	56	20.127	-13.166	-7.443	1.00	10.00	A	C
ATOM	589	NE2	HIS	A	56	19.149	-12.771	-6.648	1.00	10.00	A	N
ATOM	590	C	HIS	A	56	23.309	-13.991	-2.638	1.00	10.00	A	C
ATOM	591	O	HIS	A	56	23.720	-13.354	-1.663	1.00	10.00	A	O
ATOM	592	N	PRO	A	57	24.020	-14.996	-3.184	1.00	10.00	A	N
ATOM	593	CA	PRO	A	57	25.340	-15.401	-2.689	1.00	10.00	A	C
ATOM	594	CB	PRO	A	57	25.752	-16.543	-3.627	1.00	10.00	A	C
ATOM	595	CG	PRO	A	57	24.472	-17.039	-4.197	1.00	10.00	A	C
ATOM	596	CD	PRO	A	57	23.584	-15.836	-4.312	1.00	10.00	A	C
ATOM	597	C	PRO	A	57	26.360	-14.263	-2.757	1.00	10.00	A	C
ATOM	598	O	PRO	A	57	27.337	-14.246	-2.002	1.00	10.00	A	O
ATOM	599	N	ASN	A	58	26.126	-13.305	-3.650	1.00	10.00	A	N
ATOM	600	HN	ASN	A	58	25.331	-13.363	-4.223	1.00	10.00	A	H
ATOM	601	CA	ASN	A	58	27.027	-12.168	-3.805	1.00	10.00	A	C
ATOM	602	CB	ASN	A	58	26.882	-11.526	-5.193	1.00	10.00	A	C
ATOM	603	CG	ASN	A	58	25.613	-10.706	-5.353	1.00	10.00	A	C
ATOM	604	OD1	ASN	A	58	24.597	-10.970	-4.715	1.00	10.00	A	O
ATOM	605	ND2	ASN	A	58	25.666	-9.700	-6.207	1.00	10.00	A	N
ATOM	606	HD21	ASN	A	58	26.512	-9.539	-6.680	1.00	10.00	A	H
ATOM	607	HD22	ASN	A	58	24.856	-9.164	-6.344	1.00	10.00	A	H
ATOM	608	C	ASN	A	58	26.804	-11.133	-2.704	1.00	10.00	A	C
ATOM	609	O	ASN	A	58	27.655	-10.277	-2.455	1.00	10.00	A	O
ATOM	610	N	GLY	A	59	25.658	-11.222	-2.043	1.00	10.00	A	N
ATOM	611	HN	GLY	A	59	25.020	-11.931	-2.276	1.00	10.00	A	H
ATOM	612	CA	GLY	A	59	25.343	-10.293	-0.978	1.00	10.00	A	C
ATOM	613	C	GLY	A	59	24.153	-9.408	-1.286	1.00	10.00	A	C
ATOM	614	O	GLY	A	59	23.608	-8.773	-0.385	1.00	10.00	A	O
ATOM	615	N	ASP	A	60	23.733	-9.387	-2.546	1.00	10.00	A	N
ATOM	616	HN	ASP	A	60	24.180	-9.957	-3.209	1.00	10.00	A	H
ATOM	617	CA	ASP	A	60	22.607	-8.557	-2.967	1.00	10.00	A	C

ATOM	618	CB	ASP	A	60	22.530	-8.483	-4.494	1.00	10.00	A	C
ATOM	619	CG	ASP	A	60	22.036	-7.140	-4.998	1.00	10.00	A	C
ATOM	620	OD1	ASP	A	60	22.537	-6.669	-6.044	1.00	10.00	A	O
ATOM	621	OD2	ASP	A	60	21.154	-6.538	-4.349	1.00	10.00	A	O
ATOM	622	C	ASP	A	60	21.291	-9.089	-2.406	1.00	10.00	A	C
ATOM	623	O	ASP	A	60	21.211	-10.237	-1.955	1.00	10.00	A	O
ATOM	624	N	LYS	A	61	20.263	-8.254	-2.449	1.00	10.00	A	N
ATOM	625	HN	LYS	A	61	20.388	-7.359	-2.851	1.00	10.00	A	H
ATOM	626	CA	LYS	A	61	18.952	-8.623	-1.941	1.00	10.00	A	C
ATOM	627	CB	LYS	A	61	18.780	-8.124	-0.503	1.00	10.00	A	C
ATOM	628	CG	LYS	A	61	19.145	-6.659	-0.304	1.00	10.00	A	C
ATOM	629	CD	LYS	A	61	18.859	-6.199	1.118	1.00	10.00	A	C
ATOM	630	CE	LYS	A	61	19.097	-4.705	1.271	1.00	10.00	A	C
ATOM	631	NZ	LYS	A	61	18.955	-4.261	2.682	1.00	10.00	A	N
ATOM	632	HZ1	LYS	A	61	18.028	-4.541	3.059	1.00	10.00	A	H
ATOM	633	HZ2	LYS	A	61	19.041	-3.227	2.744	1.00	10.00	A	H
ATOM	634	HZ3	LYS	A	61	19.697	-4.690	3.270	1.00	10.00	A	H
ATOM	635	C	LYS	A	61	17.839	-8.068	-2.830	1.00	10.00	A	C
ATOM	636	O	LYS	A	61	17.663	-6.855	-2.940	1.00	10.00	A	O
ATOM	637	N	SER	A	62	17.092	-8.959	-3.463	1.00	10.00	A	N
ATOM	638	HN	SER	A	62	17.280	-9.914	-3.337	1.00	10.00	A	H
ATOM	639	CA	SER	A	62	15.998	-8.560	-4.342	1.00	10.00	A	C
ATOM	640	CB	SER	A	62	16.067	-9.374	-5.632	1.00	10.00	A	C
ATOM	641	OG	SER	A	62	17.414	-9.555	-6.020	1.00	10.00	A	O
ATOM	642	HG	SER	A	62	17.928	-8.792	-5.736	1.00	10.00	A	H
ATOM	643	C	SER	A	62	14.655	-8.775	-3.650	1.00	10.00	A	C
ATOM	644	O	SER	A	62	14.600	-9.368	-2.579	1.00	10.00	A	O
ATOM	645	N	LEU	A	63	13.579	-8.297	-4.256	1.00	10.00	A	N
ATOM	646	HN	LEU	A	63	13.676	-7.834	-5.118	1.00	10.00	A	H
ATOM	647	CA	LEU	A	63	12.250	-8.447	-3.674	1.00	10.00	A	C
ATOM	648	CB	LEU	A	63	11.393	-7.225	-4.004	1.00	10.00	A	C
ATOM	649	CG	LEU	A	63	11.621	-5.979	-3.143	1.00	10.00	A	C
ATOM	650	CD1	LEU	A	63	10.961	-4.767	-3.782	1.00	10.00	A	C
ATOM	651	CD2	LEU	A	63	11.077	-6.194	-1.739	1.00	10.00	A	C
ATOM	652	C	LEU	A	63	11.567	-9.714	-4.189	1.00	10.00	A	C
ATOM	653	O	LEU	A	63	11.682	-10.047	-5.368	1.00	10.00	A	O
ATOM	654	N	SER	A	64	10.859	-10.420	-3.310	1.00	10.00	A	N
ATOM	655	HN	SER	A	64	10.805	-10.118	-2.377	1.00	10.00	A	H
ATOM	656	CA	SER	A	64	10.166	-11.645	-3.700	1.00	10.00	A	C
ATOM	657	CB	SER	A	64	10.828	-12.867	-3.063	1.00	10.00	A	C
ATOM	658	OG	SER	A	64	11.305	-12.566	-1.761	1.00	10.00	A	O
ATOM	659	HG	SER	A	64	12.012	-13.176	-1.531	1.00	10.00	A	H
ATOM	660	C	SER	A	64	8.682	-11.600	-3.344	1.00	10.00	A	C
ATOM	661	O	SER	A	64	7.835	-12.034	-4.119	1.00	10.00	A	O
ATOM	662	N	THR	A	65	8.367	-11.078	-2.168	1.00	10.00	A	N
ATOM	663	HN	THR	A	65	9.080	-10.749	-1.581	1.00	10.00	A	H
ATOM	664	CA	THR	A	65	6.982	-10.987	-1.727	1.00	10.00	A	C
ATOM	665	CB	THR	A	65	6.595	-12.200	-0.855	1.00	10.00	A	C
ATOM	666	OG1	THR	A	65	7.013	-13.420	-1.488	1.00	10.00	A	O
ATOM	667	HG1	THR	A	65	6.512	-13.545	-2.317	1.00	10.00	A	H
ATOM	668	CG2	THR	A	65	5.093	-12.242	-0.632	1.00	10.00	A	C
ATOM	669	C	THR	A	65	6.771	-9.705	-0.926	1.00	10.00	A	C
ATOM	670	O	THR	A	65	7.643	-9.299	-0.160	1.00	10.00	A	O
ATOM	671	N	LEU	A	66	5.624	-9.065	-1.106	1.00	10.00	A	N
ATOM	672	HN	LEU	A	66	4.955	-9.436	-1.724	1.00	10.00	A	H
ATOM	673	CA	LEU	A	66	5.324	-7.837	-0.388	1.00	10.00	A	C
ATOM	674	CB	LEU	A	66	4.768	-6.766	-1.334	1.00	10.00	A	C
ATOM	675	CG	LEU	A	66	4.472	-5.398	-0.705	1.00	10.00	A	C
ATOM	676	CD1	LEU	A	66	5.748	-4.756	-0.178	1.00	10.00	A	C
ATOM	677	CD2	LEU	A	66	3.789	-4.485	-1.708	1.00	10.00	A	C
ATOM	678	C	LEU	A	66	4.339	-8.103	0.739	1.00	10.00	A	C
ATOM	679	O	LEU	A	66	3.245	-8.629	0.515	1.00	10.00	A	O
ATOM	680	N	HIS	A	67	4.732	-7.751	1.952	1.00	10.00	A	N
ATOM	681	HN	HIS	A	67	5.613	-7.334	2.073	1.00	10.00	A	H
ATOM	682	CA	HIS	A	67	3.876	-7.952	3.106	1.00	10.00	A	C
ATOM	683	CB	HIS	A	67	4.691	-8.313	4.352	1.00	10.00	A	C
ATOM	684	CG	HIS	A	67	4.913	-9.784	4.539	1.00	10.00	A	C
ATOM	685	ND1	HIS	A	67	4.747	-10.379	5.767	1.00	10.00	A	N
ATOM	686	CD2	HIS	A	67	5.283	-10.727	3.634	1.00	10.00	A	C
ATOM	687	CE1	HIS	A	67	5.013	-11.660	5.590	1.00	10.00	A	C
ATOM	688	NE2	HIS	A	67	5.343	-11.914	4.317	1.00	10.00	A	N
ATOM	689	HE2	HIS	A	67	5.572	-12.792	3.940	1.00	10.00	A	H
ATOM	690	C	HIS	A	67	3.024	-6.720	3.364	1.00	10.00	A	C
ATOM	691	O	HIS	A	67	1.806	-6.812	3.427	1.00	10.00	A	O
ATOM	692	N	ARG	A	68	3.668	-5.564	3.500	1.00	10.00	A	N
ATOM	693	HN	ARG	A	68	4.651	-5.545	3.424	1.00	10.00	A	H
ATOM	694	CA	ARG	A	68	2.945	-4.322	3.754	1.00	10.00	A	C
ATOM	695	CB	ARG	A	68	2.220	-4.383	5.111	1.00	10.00	A	C
ATOM	696	CG	ARG	A	68	1.790	-3.033	5.672	1.00	10.00	A	C
ATOM	697	CD	ARG	A	68	0.688	-2.393	4.840	1.00	10.00	A	C
ATOM	698	NE	ARG	A	68	-0.639	-2.912	5.175	1.00	10.00	A	N
ATOM	699	HE	ARG	A	68	-0.836	-3.850	4.922	1.00	10.00	A	H
ATOM	700	CZ	ARG	A	68	-1.589	-2.207	5.795	1.00	10.00	A	C
ATOM	701	NH1	ARG	A	68	-1.371	-0.947	6.157	1.00	10.00	A	N
ATOM	702	HH11	ARG	A	68	-2.124	-0.405	6.640	1.00	10.00	A	H
ATOM	703	HH12	ARG	A	68	-0.448	-0.489	5.962	1.00	10.00	A	H
ATOM	704	NH2	ARG	A	68	-2.764	-2.758	6.045	1.00	10.00	A	N
ATOM	705	HH21	ARG	A	68	-2.952	-3.749	5.762	1.00	10.00	A	H
ATOM	706	HH22	ARG	A	68	-3.509	-2.207	6.534	1.00	10.00	A	H
ATOM	707	C	ARG	A	68	3.876	-3.116	3.718	1.00	10.00	A	C
ATOM	708	O	ARG	A	68	4.912	-3.098	4.376	1.00	10.00	A	O
ATOM	709	N	LEU	A	69	3.505	-2.125	2.929	1.00	10.00	A	N
ATOM	710	HN	LEU	A	69	2.693	-2.223	2.388	1.00	10.00	A	H
ATOM	711	CA	LEU	A	69	4.271	-0.895	2.830	1.00	10.00	A	C
ATOM	712	CB	LEU	A	69	4.566	-0.576	1.360	1.00	10.00	A	C

ATOM	713	CG	LEU	A	69	5.815	0.269	1.076	1.00	10.00	A	C
ATOM	714	CD1	LEU	A	69	6.355	-0.024	-0.316	1.00	10.00	A	C
ATOM	715	CD2	LEU	A	69	5.523	1.756	1.237	1.00	10.00	A	C
ATOM	716	C	LEU	A	69	3.441	0.214	3.458	1.00	10.00	A	C
ATOM	717	O	LEU	A	69	2.323	0.477	3.009	1.00	10.00	A	O
ATOM	718	N	ASN	A	70	3.973	0.850	4.494	1.00	10.00	A	N
ATOM	719	HN	ASN	A	70	4.883	0.622	4.788	1.00	10.00	A	H
ATOM	720	CA	ASN	A	70	3.246	1.901	5.187	1.00	10.00	A	C
ATOM	721	CB	ASN	A	70	3.068	1.552	6.668	1.00	10.00	A	C
ATOM	722	CG	ASN	A	70	1.910	0.611	6.938	1.00	10.00	A	C
ATOM	723	OD1	ASN	A	70	0.997	0.474	6.123	1.00	10.00	A	O
ATOM	724	ND2	ASN	A	70	1.932	-0.034	8.094	1.00	10.00	A	N
ATOM	725	HD21	ASN	A	70	2.690	0.131	8.703	1.00	10.00	A	H
ATOM	726	HD22	ASN	A	70	1.190	-0.642	8.306	1.00	10.00	A	H
ATOM	727	C	ASN	A	70	3.938	3.248	5.078	1.00	10.00	A	C
ATOM	728	O	ASN	A	70	5.169	3.336	5.058	1.00	10.00	A	O
ATOM	729	N	ALA	A	71	3.129	4.293	5.005	1.00	10.00	A	N
ATOM	730	HN	ALA	A	71	2.162	4.141	4.997	1.00	10.00	A	H
ATOM	731	CA	ALA	A	71	3.620	5.656	4.934	1.00	10.00	A	C
ATOM	732	CB	ALA	A	71	3.287	6.270	3.584	1.00	10.00	A	C
ATOM	733	C	ALA	A	71	2.994	6.467	6.063	1.00	10.00	A	C
ATOM	734	O	ALA	A	71	1.789	6.739	6.056	1.00	10.00	A	O
ATOM	735	N	TYR	A	72	3.810	6.828	7.041	1.00	10.00	A	N
ATOM	736	HN	TYR	A	72	4.765	6.593	6.980	1.00	10.00	A	H
ATOM	737	CA	TYR	A	72	3.341	7.588	8.189	1.00	10.00	A	C
ATOM	738	CB	TYR	A	72	3.906	7.000	9.486	1.00	10.00	A	C
ATOM	739	CG	TYR	A	72	3.520	5.566	9.765	1.00	10.00	A	C
ATOM	740	CD1	TYR	A	72	2.264	5.249	10.266	1.00	10.00	A	C
ATOM	741	CD2	TYR	A	72	4.417	4.531	9.546	1.00	10.00	A	C
ATOM	742	CE1	TYR	A	72	1.914	3.940	10.539	1.00	10.00	A	C
ATOM	743	CE2	TYR	A	72	4.077	3.220	9.813	1.00	10.00	A	C
ATOM	744	CZ	TYR	A	72	2.823	2.930	10.309	1.00	10.00	A	C
ATOM	745	OH	TYR	A	72	2.482	1.626	10.582	1.00	10.00	A	O
ATOM	746	HH	TYR	A	72	3.101	1.267	11.225	1.00	10.00	A	H
ATOM	747	C	TYR	A	72	3.784	9.034	8.090	1.00	10.00	A	C
ATOM	748	O	TYR	A	72	4.834	9.330	7.525	1.00	10.00	A	O
ATOM	749	N	ASP	A	73	2.985	9.931	8.633	1.00	10.00	A	N
ATOM	750	HN	ASP	A	73	2.142	9.638	9.047	1.00	10.00	A	H
ATOM	751	CA	ASP	A	73	3.331	11.342	8.631	1.00	10.00	A	C
ATOM	752	CB	ASP	A	73	2.073	12.215	8.739	1.00	10.00	A	C
ATOM	753	CG	ASP	A	73	2.062	13.126	9.950	1.00	10.00	A	C
ATOM	754	OD1	ASP	A	73	2.579	14.262	9.858	1.00	10.00	A	O
ATOM	755	OD2	ASP	A	73	1.537	12.713	10.996	1.00	10.00	A	O
ATOM	756	C	ASP	A	73	4.321	11.612	9.764	1.00	10.00	A	C
ATOM	757	O	ASP	A	73	4.405	10.831	10.715	1.00	10.00	A	O
ATOM	758	N	GLN	A	74	5.081	12.694	9.650	1.00	10.00	A	N
ATOM	759	HN	GLN	A	74	4.966	13.275	8.867	1.00	10.00	A	H
ATOM	760	CA	GLN	A	74	6.082	13.047	10.657	1.00	10.00	A	C
ATOM	761	CB	GLN	A	74	6.799	14.341	10.276	1.00	10.00	A	C
ATOM	762	CG	GLN	A	74	8.115	14.549	11.009	1.00	10.00	A	C
ATOM	763	CD	GLN	A	74	9.142	13.483	10.673	1.00	10.00	A	C
ATOM	764	OE1	GLN	A	74	9.207	12.434	11.315	1.00	10.00	A	O
ATOM	765	NE2	GLN	A	74	9.947	13.740	9.659	1.00	10.00	A	N
ATOM	766	HE21	GLN	A	74	9.838	14.595	9.186	1.00	10.00	A	H
ATOM	767	HE22	GLN	A	74	10.624	13.074	9.426	1.00	10.00	A	H
ATOM	768	C	GLN	A	74	5.490	13.174	12.064	1.00	10.00	A	C
ATOM	769	O	GLN	A	74	6.139	12.819	13.053	1.00	10.00	A	O
ATOM	770	N	ASN	A	75	4.260	13.666	12.149	1.00	10.00	A	N
ATOM	771	HN	ASN	A	75	3.776	13.905	11.324	1.00	10.00	A	H
ATOM	772	CA	ASN	A	75	3.601	13.846	13.436	1.00	10.00	A	C
ATOM	773	CB	ASN	A	75	2.383	14.764	13.297	1.00	10.00	A	C
ATOM	774	CG	ASN	A	75	2.749	16.157	12.834	1.00	10.00	A	C
ATOM	775	OD1	ASN	A	75	3.047	17.038	13.644	1.00	10.00	A	O
ATOM	776	ND2	ASN	A	75	2.739	16.373	11.528	1.00	10.00	A	N
ATOM	777	HD21	ASN	A	75	2.500	15.620	10.930	1.00	10.00	A	H
ATOM	778	HD22	ASN	A	75	2.964	17.270	11.206	1.00	10.00	A	H
ATOM	779	C	ASN	A	75	3.189	12.507	14.034	1.00	10.00	A	C
ATOM	780	O	ASN	A	75	3.365	12.269	15.227	1.00	10.00	A	O
ATOM	781	N	GLY	A	76	2.633	11.642	13.205	1.00	10.00	A	N
ATOM	782	HN	GLY	A	76	2.482	11.903	12.267	1.00	10.00	A	H
ATOM	783	CA	GLY	A	76	2.212	10.337	13.662	1.00	10.00	A	C
ATOM	784	C	GLY	A	76	0.854	9.965	13.108	1.00	10.00	A	C
ATOM	785	O	GLY	A	76	-0.153	10.596	13.443	1.00	10.00	A	O
ATOM	786	N	GLY	A	77	0.823	8.951	12.257	1.00	10.00	A	N
ATOM	787	HN	GLY	A	77	1.656	8.483	12.037	1.00	10.00	A	H
ATOM	788	CA	GLY	A	77	-0.424	8.516	11.664	1.00	10.00	A	C
ATOM	789	C	GLY	A	77	-0.243	7.992	10.254	1.00	10.00	A	C
ATOM	790	O	GLY	A	77	0.547	8.538	9.478	1.00	10.00	A	O
ATOM	791	N	LEU	A	78	-0.968	6.928	9.931	1.00	10.00	A	N
ATOM	792	HN	LEU	A	78	-1.574	6.542	10.605	1.00	10.00	A	H
ATOM	793	CA	LEU	A	78	-0.900	6.315	8.612	1.00	10.00	A	C
ATOM	794	CB	LEU	A	78	-1.434	4.881	8.676	1.00	10.00	A	C
ATOM	795	CG	LEU	A	78	-1.235	4.024	7.426	1.00	10.00	A	C
ATOM	796	CD1	LEU	A	78	0.243	3.903	7.097	1.00	10.00	A	C
ATOM	797	CD2	LEU	A	78	-1.855	2.650	7.620	1.00	10.00	A	C
ATOM	798	C	LEU	A	78	-1.708	7.130	7.606	1.00	10.00	A	C
ATOM	799	O	LEU	A	78	-2.868	7.468	7.858	1.00	10.00	A	O
ATOM	800	N	VAL	A	79	-1.090	7.459	6.477	1.00	10.00	A	N
ATOM	801	HN	VAL	A	79	-0.157	7.184	6.342	1.00	10.00	A	H
ATOM	802	CA	VAL	A	79	-1.762	8.245	5.444	1.00	10.00	A	C
ATOM	803	CB	VAL	A	79	-1.211	9.685	5.367	1.00	10.00	A	C
ATOM	804	CG1	VAL	A	79	-1.763	10.531	6.502	1.00	10.00	A	C
ATOM	805	CG2	VAL	A	79	0.311	9.691	5.385	1.00	10.00	A	C
ATOM	806	C	VAL	A	79	-1.678	7.595	4.061	1.00	10.00	A	C
ATOM	807	O	VAL	A	79	-2.230	8.118	3.092	1.00	10.00	A	O

ATOM	808	N	ALA	A	80	-0.993	6.462	3.966	1.00	10.00	A	N
ATOM	809	HN	ALA	A	80	-0.574	6.087	4.763	1.00	10.00	A	H
ATOM	810	CA	ALA	A	80	-0.853	5.766	2.688	1.00	10.00	A	C
ATOM	811	CB	ALA	A	80	0.169	6.468	1.806	1.00	10.00	A	C
ATOM	812	C	ALA	A	80	-0.475	4.295	2.876	1.00	10.00	A	C
ATOM	813	O	ALA	A	80	0.293	3.955	3.779	1.00	10.00	A	O
ATOM	814	N	LYS	A	81	-1.017	3.436	2.013	1.00	10.00	A	N
ATOM	815	HN	LYS	A	81	-1.617	3.781	1.315	1.00	10.00	A	H
ATOM	816	CA	LYS	A	81	-0.751	1.998	2.058	1.00	10.00	A	C
ATOM	817	CB	LYS	A	81	-1.974	1.270	2.633	1.00	10.00	A	C
ATOM	818	CG	LYS	A	81	-1.973	-0.241	2.469	1.00	10.00	A	C
ATOM	819	CD	LYS	A	81	-3.319	-0.827	2.862	1.00	10.00	A	C
ATOM	820	CE	LYS	A	81	-3.446	-2.275	2.420	1.00	10.00	A	C
ATOM	821	NZ	LYS	A	81	-4.819	-2.803	2.631	1.00	10.00	A	N
ATOM	822	HZ1	LYS	A	81	-5.018	-2.894	3.648	1.00	10.00	A	H
ATOM	823	HZ2	LYS	A	81	-4.916	-3.739	2.186	1.00	10.00	A	H
ATOM	824	HZ3	LYS	A	81	-5.522	-2.159	2.210	1.00	10.00	A	H
ATOM	825	C	LYS	A	81	-0.433	1.470	0.655	1.00	10.00	A	C
ATOM	826	O	LYS	A	81	-1.013	1.926	-0.333	1.00	10.00	A	O
ATOM	827	N	LEU	A	82	0.489	0.516	0.576	1.00	10.00	A	N
ATOM	828	HN	LEU	A	82	0.927	0.204	1.396	1.00	10.00	A	H
ATOM	829	CA	LEU	A	82	0.879	-0.071	-0.698	1.00	10.00	A	C
ATOM	830	CB	LEU	A	82	2.295	0.380	-1.056	1.00	10.00	A	C
ATOM	831	CG	LEU	A	82	2.489	1.018	-2.432	1.00	10.00	A	C
ATOM	832	CD1	LEU	A	82	3.914	1.525	-2.569	1.00	10.00	A	C
ATOM	833	CD2	LEU	A	82	2.169	0.024	-3.539	1.00	10.00	A	C
ATOM	834	C	LEU	A	82	0.838	-1.592	-0.614	1.00	10.00	A	C
ATOM	835	O	LEU	A	82	1.286	-2.172	0.382	1.00	10.00	A	O
ATOM	836	N	VAL	A	83	0.300	-2.231	-1.658	1.00	10.00	A	N
ATOM	837	HN	VAL	A	83	-0.042	-1.706	-2.417	1.00	10.00	A	H
ATOM	838	CA	VAL	A	83	0.201	-3.688	-1.713	1.00	10.00	A	C
ATOM	839	CB	VAL	A	83	-1.140	-4.200	-1.137	1.00	10.00	A	C
ATOM	840	CG1	VAL	A	83	-1.077	-4.272	0.379	1.00	10.00	A	C
ATOM	841	CG2	VAL	A	83	-2.300	-3.320	-1.584	1.00	10.00	A	C
ATOM	842	C	VAL	A	83	0.355	-4.202	-3.145	1.00	10.00	A	C
ATOM	843	O	VAL	A	83	0.167	-3.452	-4.110	1.00	10.00	A	O
ATOM	844	N	ALA	A	84	0.694	-5.481	-3.275	1.00	10.00	A	N
ATOM	845	HN	ALA	A	84	0.822	-6.024	-2.465	1.00	10.00	A	H
ATOM	846	CA	ALA	A	84	0.865	-6.122	-4.580	1.00	10.00	A	C
ATOM	847	CB	ALA	A	84	2.288	-6.634	-4.744	1.00	10.00	A	C
ATOM	848	C	ALA	A	84	-0.135	-7.268	-4.723	1.00	10.00	A	C
ATOM	849	O	ALA	A	84	-0.349	-8.025	-3.780	1.00	10.00	A	O
ATOM	850	N	THR	A	85	-0.730	-7.409	-5.908	1.00	10.00	A	N
ATOM	851	HN	THR	A	85	-0.484	-6.802	-6.645	1.00	10.00	A	H
ATOM	852	CA	THR	A	85	-1.737	-8.442	-6.147	1.00	10.00	A	C
ATOM	853	CB	THR	A	85	-2.669	-8.065	-7.312	1.00	10.00	A	C
ATOM	854	OG1	THR	A	85	-1.971	-7.211	-8.230	1.00	10.00	A	O
ATOM	855	HG1	THR	A	85	-2.016	-6.299	-7.915	1.00	10.00	A	H
ATOM	856	CG2	THR	A	85	-3.890	-7.334	-6.785	1.00	10.00	A	C
ATOM	857	C	THR	A	85	-1.154	-9.842	-6.360	1.00	10.00	A	C
ATOM	858	O	THR	A	85	-1.869	-10.772	-6.737	1.00	10.00	A	O
ATOM	859	N	ASP	A	86	0.131	-9.996	-6.083	1.00	10.00	A	N
ATOM	860	HN	ASP	A	86	0.639	-9.231	-5.743	1.00	10.00	A	H
ATOM	861	CA	ASP	A	86	0.808	-11.279	-6.250	1.00	10.00	A	C
ATOM	862	CB	ASP	A	86	0.848	-11.670	-7.734	1.00	10.00	A	C
ATOM	863	CG	ASP	A	86	0.913	-13.170	-7.953	1.00	10.00	A	C
ATOM	864	OD1	ASP	A	86	-0.141	-13.782	-8.217	1.00	10.00	A	O
ATOM	865	OD2	ASP	A	86	2.018	-13.746	-7.870	1.00	10.00	A	O
ATOM	866	C	ASP	A	86	2.226	-11.166	-5.704	1.00	10.00	A	C
ATOM	867	O	ASP	A	86	2.511	-10.269	-4.912	1.00	10.00	A	O
ATOM	868	N	ASP	A	87	3.109	-12.061	-6.127	1.00	10.00	A	N
ATOM	869	HN	ASP	A	87	2.821	-12.756	-6.764	1.00	10.00	A	H
ATOM	870	CA	ASP	A	87	4.497	-12.038	-5.685	1.00	10.00	A	C
ATOM	871	CB	ASP	A	87	5.145	-13.417	-5.829	1.00	10.00	A	C
ATOM	872	CG	ASP	A	87	4.888	-14.313	-4.633	1.00	10.00	A	C
ATOM	873	OD1	ASP	A	87	5.561	-14.141	-3.596	1.00	10.00	A	O
ATOM	874	OD2	ASP	A	87	4.013	-15.204	-4.732	1.00	10.00	A	O
ATOM	875	C	ASP	A	87	5.287	-11.000	-6.476	1.00	10.00	A	C
ATOM	876	O	ASP	A	87	4.766	-10.399	-7.418	1.00	10.00	A	O
ATOM	877	N	LEU	A	88	6.543	-10.805	-6.114	1.00	10.00	A	N
ATOM	878	HN	LEU	A	88	6.924	-11.346	-5.382	1.00	10.00	A	H
ATOM	879	CA	LEU	A	88	7.385	-9.824	-6.784	1.00	10.00	A	C
ATOM	880	CB	LEU	A	88	8.023	-8.878	-5.763	1.00	10.00	A	C
ATOM	881	CG	LEU	A	88	7.069	-8.242	-4.751	1.00	10.00	A	C
ATOM	882	CD1	LEU	A	88	7.835	-7.416	-3.733	1.00	10.00	A	C
ATOM	883	CD2	LEU	A	88	6.028	-7.390	-5.456	1.00	10.00	A	C
ATOM	884	C	LEU	A	88	8.465	-10.497	-7.620	1.00	10.00	A	C
ATOM	885	O	LEU	A	88	9.018	-11.525	-7.233	1.00	10.00	A	O
ATOM	886	N	THR	A	89	8.746	-9.912	-8.772	1.00	10.00	A	N
ATOM	887	HN	THR	A	89	8.247	-9.107	-9.029	1.00	10.00	A	H
ATOM	888	CA	THR	A	89	9.758	-10.428	-9.684	1.00	10.00	A	C
ATOM	889	CB	THR	A	89	9.108	-11.290	-10.783	1.00	10.00	A	C
ATOM	890	OG1	THR	A	89	7.682	-11.294	-10.611	1.00	10.00	A	O
ATOM	891	HG1	THR	A	89	7.381	-10.393	-10.387	1.00	10.00	A	H
ATOM	892	CG2	THR	A	89	9.624	-12.718	-10.717	1.00	10.00	A	C
ATOM	893	C	THR	A	89	10.519	-9.263	-10.328	1.00	10.00	A	C
ATOM	894	O	THR	A	89	10.255	-8.103	-10.007	1.00	10.00	A	O
ATOM	895	N	VAL	A	90	11.442	-9.562	-11.243	1.00	10.00	A	N
ATOM	896	HN	VAL	A	90	11.603	-10.502	-11.476	1.00	10.00	A	H
ATOM	897	CA	VAL	A	90	12.224	-8.516	-11.906	1.00	10.00	A	C
ATOM	898	CB	VAL	A	90	13.399	-9.089	-12.738	1.00	10.00	A	C
ATOM	899	CG1	VAL	A	90	12.914	-9.720	-14.034	1.00	10.00	A	C
ATOM	900	CG2	VAL	A	90	14.448	-8.022	-13.014	1.00	10.00	A	C
ATOM	901	C	VAL	A	90	11.337	-7.605	-12.764	1.00	10.00	A	C
ATOM	902	O	VAL	A	90	11.650	-6.430	-12.972	1.00	10.00	A	O

ATOM	903	N	GLU	A	91	10.226	-8.151	-13.253	1.00	10.00	A	N
ATOM	904	HN	GLU	A	91	10.046	-9.099	-13.072	1.00	10.00	A	H
ATOM	905	CA	GLU	A	91	9.284	-7.393	-14.072	1.00	10.00	A	C
ATOM	906	CB	GLU	A	91	8.312	-8.343	-14.787	1.00	10.00	A	C
ATOM	907	CG	GLU	A	91	7.303	-7.656	-15.701	1.00	10.00	A	C
ATOM	908	CD	GLU	A	91	7.927	-7.069	-16.955	1.00	10.00	A	C
ATOM	909	OE1	GLU	A	91	9.118	-6.704	-16.926	1.00	10.00	A	O
ATOM	910	OE2	GLU	A	91	7.220	-6.953	-17.977	1.00	10.00	A	O
ATOM	911	C	GLU	A	91	8.509	-6.399	-13.211	1.00	10.00	A	C
ATOM	912	O	GLU	A	91	8.104	-5.333	-13.677	1.00	10.00	A	O
ATOM	913	N	ASP	A	92	8.330	-6.752	-11.945	1.00	10.00	A	N
ATOM	914	HN	ASP	A	92	8.698	-7.607	-11.635	1.00	10.00	A	H
ATOM	915	CA	ASP	A	92	7.601	-5.914	-11.000	1.00	10.00	A	C
ATOM	916	CB	ASP	A	92	7.343	-6.680	-9.697	1.00	10.00	A	C
ATOM	917	CG	ASP	A	92	6.307	-7.778	-9.837	1.00	10.00	A	C
ATOM	918	OD1	ASP	A	92	5.140	-7.547	-9.476	1.00	10.00	A	O
ATOM	919	OD2	ASP	A	92	6.662	-8.884	-10.300	1.00	10.00	A	O
ATOM	920	C	ASP	A	92	8.368	-4.635	-10.691	1.00	10.00	A	C
ATOM	921	O	ASP	A	92	7.777	-3.621	-10.322	1.00	10.00	A	O
ATOM	922	N	GLU	A	93	9.685	-4.680	-10.869	1.00	10.00	A	N
ATOM	923	HN	GLU	A	93	10.092	-5.509	-11.199	1.00	10.00	A	H
ATOM	924	CA	GLU	A	93	10.541	-3.532	-10.589	1.00	10.00	A	C
ATOM	925	CB	GLU	A	93	12.011	-3.875	-10.822	1.00	10.00	A	C
ATOM	926	CG	GLU	A	93	12.547	-4.958	-9.904	1.00	10.00	A	C
ATOM	927	CD	GLU	A	93	14.014	-5.256	-10.136	1.00	10.00	A	C
ATOM	928	OE1	GLU	A	93	14.615	-4.653	-11.048	1.00	10.00	A	O
ATOM	929	OE2	GLU	A	93	14.573	-6.100	-9.401	1.00	10.00	A	O
ATOM	930	C	GLU	A	93	10.155	-2.293	-11.394	1.00	10.00	A	C
ATOM	931	O	GLU	A	93	10.113	-1.185	-10.854	1.00	10.00	A	O
ATOM	932	N	LYS	A	94	9.855	-2.478	-12.677	1.00	10.00	A	N
ATOM	933	HN	LYS	A	94	9.863	-3.385	-13.046	1.00	10.00	A	H
ATOM	934	CA	LYS	A	94	9.494	-1.362	-13.545	1.00	10.00	A	C
ATOM	935	CB	LYS	A	94	9.525	-1.763	-15.027	1.00	10.00	A	C
ATOM	936	CG	LYS	A	94	8.335	-2.580	-15.507	1.00	10.00	A	C
ATOM	937	CD	LYS	A	94	8.592	-3.153	-16.890	1.00	10.00	A	C
ATOM	938	CE	LYS	A	94	7.303	-3.582	-17.570	1.00	10.00	A	C
ATOM	939	NZ	LYS	A	94	7.568	-4.429	-18.764	1.00	10.00	A	N
ATOM	940	HZ1	LYS	A	94	6.763	-4.384	-19.418	1.00	10.00	A	H
ATOM	941	HZ2	LYS	A	94	7.706	-5.427	-18.476	1.00	10.00	A	H
ATOM	942	HZ3	LYS	A	94	8.421	-4.103	-19.257	1.00	10.00	A	H
ATOM	943	C	LYS	A	94	8.156	-0.738	-13.157	1.00	10.00	A	C
ATOM	944	O	LYS	A	94	7.966	0.470	-13.297	1.00	10.00	A	O
ATOM	945	N	ASP	A	95	7.241	-1.561	-12.656	1.00	10.00	A	N
ATOM	946	HN	ASP	A	95	7.459	-2.512	-12.554	1.00	10.00	A	H
ATOM	947	CA	ASP	A	95	5.922	-1.083	-12.249	1.00	10.00	A	C
ATOM	948	CB	ASP	A	95	4.883	-2.206	-12.324	1.00	10.00	A	C
ATOM	949	CG	ASP	A	95	4.370	-2.435	-13.731	1.00	10.00	A	C
ATOM	950	OD1	ASP	A	95	4.879	-1.787	-14.672	1.00	10.00	A	O
ATOM	951	OD2	ASP	A	95	3.456	-3.263	-13.906	1.00	10.00	A	O
ATOM	952	C	ASP	A	95	5.978	-0.493	-10.846	1.00	10.00	A	C
ATOM	953	O	ASP	A	95	5.362	0.539	-10.568	1.00	10.00	A	O
ATOM	954	N	GLY	A	96	6.732	-1.148	-9.967	1.00	10.00	A	N
ATOM	955	HN	GLY	A	96	7.191	-1.976	-10.246	1.00	10.00	A	H
ATOM	956	CA	GLY	A	96	6.873	-0.674	-8.607	1.00	10.00	A	C
ATOM	957	C	GLY	A	96	7.536	0.684	-8.560	1.00	10.00	A	C
ATOM	958	O	GLY	A	96	7.161	1.541	-7.765	1.00	10.00	A	O
ATOM	959	N	HIS	A	97	8.526	0.883	-9.417	1.00	10.00	A	N
ATOM	960	HN	HIS	A	97	8.793	0.152	-10.019	1.00	10.00	A	H
ATOM	961	CA	HIS	A	97	9.234	2.154	-9.481	1.00	10.00	A	C
ATOM	962	CB	HIS	A	97	10.413	2.048	-10.453	1.00	10.00	A	C
ATOM	963	CG	HIS	A	97	11.222	3.302	-10.579	1.00	10.00	A	C
ATOM	964	ND1	HIS	A	97	11.489	3.859	-11.808	1.00	10.00	A	N
ATOM	965	CD2	HIS	A	97	11.809	4.047	-9.613	1.00	10.00	A	C
ATOM	966	CE1	HIS	A	97	12.231	4.925	-11.567	1.00	10.00	A	C
ATOM	967	NE2	HIS	A	97	12.449	5.076	-10.254	1.00	10.00	A	N
ATOM	968	HE2	HIS	A	97	12.978	5.785	-9.828	1.00	10.00	A	H
ATOM	969	C	HIS	A	97	8.288	3.261	-9.926	1.00	10.00	A	C
ATOM	970	O	HIS	A	97	8.321	4.374	-9.403	1.00	10.00	A	O
ATOM	971	N	ARG	A	98	7.434	2.931	-10.882	1.00	10.00	A	N
ATOM	972	HN	ARG	A	98	7.446	2.013	-11.231	1.00	10.00	A	H
ATOM	973	CA	ARG	A	98	6.471	3.877	-11.422	1.00	10.00	A	C
ATOM	974	CB	ARG	A	98	5.809	3.272	-12.660	1.00	10.00	A	C
ATOM	975	CG	ARG	A	98	5.223	4.283	-13.630	1.00	10.00	A	C
ATOM	976	CD	ARG	A	98	4.955	3.651	-14.989	1.00	10.00	A	C
ATOM	977	NE	ARG	A	98	3.853	2.687	-14.949	1.00	10.00	A	N
ATOM	978	HE	ARG	A	98	2.934	3.055	-14.894	1.00	10.00	A	H
ATOM	979	CZ	ARG	A	98	4.010	1.360	-14.968	1.00	10.00	A	C
ATOM	980	NH1	ARG	A	98	5.221	0.822	-15.016	1.00	10.00	A	N
ATOM	981	HH11	ARG	A	98	5.328	-0.225	-15.025	1.00	10.00	A	H
ATOM	982	HH12	ARG	A	98	6.072	1.427	-15.039	1.00	10.00	A	H
ATOM	983	NH2	ARG	A	98	2.949	0.563	-14.943	1.00	10.00	A	N
ATOM	984	HH21	ARG	A	98	3.073	-0.475	-14.957	1.00	10.00	A	H
ATOM	985	HH22	ARG	A	98	1.978	0.972	-14.907	1.00	10.00	A	H
ATOM	986	C	ARG	A	98	5.418	4.239	-10.377	1.00	10.00	A	C
ATOM	987	O	ARG	A	98	5.159	5.417	-10.134	1.00	10.00	A	O
ATOM	988	N	ILE	A	99	4.830	3.221	-9.757	1.00	10.00	A	N
ATOM	989	HN	ILE	A	99	5.085	2.302	-9.999	1.00	10.00	A	H
ATOM	990	CA	ILE	A	99	3.801	3.426	-8.740	1.00	10.00	A	C
ATOM	991	CB	ILE	A	99	3.088	2.104	-8.339	1.00	10.00	A	C
ATOM	992	CG1	ILE	A	99	1.725	2.379	-7.699	1.00	10.00	A	C
ATOM	993	CG2	ILE	A	99	3.944	1.243	-7.420	1.00	10.00	A	C
ATOM	994	CD1	ILE	A	99	0.700	2.932	-8.660	1.00	10.00	A	C
ATOM	995	C	ILE	A	99	4.361	4.147	-7.510	1.00	10.00	A	C
ATOM	996	O	ILE	A	99	3.660	4.924	-6.864	1.00	10.00	A	O
ATOM	997	N	LEU	A	100	5.626	3.899	-7.197	1.00	10.00	A	N

ATOM	998	HN	LEU	A	100	6.141	3.267	-7.744	1.00	10.00	A	H
ATOM	999	CA	LEU	A	100	6.267	4.534	-6.053	1.00	10.00	A	C
ATOM	1000	CB	LEU	A	100	7.635	3.905	-5.787	1.00	10.00	A	C
ATOM	1001	CG	LEU	A	100	8.213	4.096	-4.384	1.00	10.00	A	C
ATOM	1002	CD1	LEU	A	100	7.241	3.587	-3.329	1.00	10.00	A	C
ATOM	1003	CD2	LEU	A	100	9.552	3.387	-4.265	1.00	10.00	A	C
ATOM	1004	C	LEU	A	100	6.402	6.035	-6.292	1.00	10.00	A	C
ATOM	1005	O	LEU	A	100	6.234	6.841	-5.375	1.00	10.00	A	O
ATOM	1006	N	ASN	A	101	6.688	6.406	-7.534	1.00	10.00	A	N
ATOM	1007	HN	ASN	A	101	6.809	5.720	-8.227	1.00	10.00	A	H
ATOM	1008	CA	ASN	A	101	6.824	7.810	-7.894	1.00	10.00	A	C
ATOM	1009	CB	ASN	A	101	7.272	7.950	-9.348	1.00	10.00	A	C
ATOM	1010	CG	ASN	A	101	7.486	9.394	-9.764	1.00	10.00	A	C
ATOM	1011	OD1	ASN	A	101	8.104	10.179	-9.047	1.00	10.00	A	O
ATOM	1012	ND2	ASN	A	101	6.977	9.747	-10.930	1.00	10.00	A	N
ATOM	1013	HD21	ASN	A	101	6.495	9.066	-11.448	1.00	10.00	A	H
ATOM	1014	HD22	ASN	A	101	7.104	10.670	-11.233	1.00	10.00	A	H
ATOM	1015	C	ASN	A	101	5.491	8.523	-7.703	1.00	10.00	A	C
ATOM	1016	O	ASN	A	101	5.438	9.626	-7.159	1.00	10.00	A	O
ATOM	1017	N	SER	A	102	4.413	7.865	-8.132	1.00	10.00	A	N
ATOM	1018	HN	SER	A	102	4.527	6.981	-8.544	1.00	10.00	A	H
ATOM	1019	CA	SER	A	102	3.068	8.416	-8.016	1.00	10.00	A	C
ATOM	1020	CB	SER	A	102	2.071	7.481	-8.699	1.00	10.00	A	C
ATOM	1021	OG	SER	A	102	2.591	7.027	-9.938	1.00	10.00	A	O
ATOM	1022	HG	SER	A	102	3.047	7.754	-10.377	1.00	10.00	A	H
ATOM	1023	C	SER	A	102	2.685	8.625	-6.553	1.00	10.00	A	C
ATOM	1024	O	SER	A	102	1.969	9.571	-6.216	1.00	10.00	A	O
ATOM	1025	N	LEU	A	103	3.185	7.748	-5.688	1.00	10.00	A	N
ATOM	1026	HN	LEU	A	103	3.751	7.016	-6.022	1.00	10.00	A	H
ATOM	1027	CA	LEU	A	103	2.912	7.838	-4.258	1.00	10.00	A	C
ATOM	1028	CB	LEU	A	103	3.523	6.634	-3.531	1.00	10.00	A	C
ATOM	1029	CG	LEU	A	103	3.335	6.580	-2.012	1.00	10.00	A	C
ATOM	1030	CD1	LEU	A	103	1.879	6.324	-1.652	1.00	10.00	A	C
ATOM	1031	CD2	LEU	A	103	4.241	5.523	-1.397	1.00	10.00	A	C
ATOM	1032	C	LEU	A	103	3.495	9.136	-3.702	1.00	10.00	A	C
ATOM	1033	O	LEU	A	103	2.851	9.841	-2.923	1.00	10.00	A	O
ATOM	1034	N	PHE	A	104	4.709	9.453	-4.129	1.00	10.00	A	N
ATOM	1035	HN	PHE	A	104	5.169	8.851	-4.756	1.00	10.00	A	H
ATOM	1036	CA	PHE	A	104	5.383	10.667	-3.686	1.00	10.00	A	C
ATOM	1037	CB	PHE	A	104	6.892	10.563	-3.935	1.00	10.00	A	C
ATOM	1038	CG	PHE	A	104	7.551	9.386	-3.266	1.00	10.00	A	C
ATOM	1039	CD1	PHE	A	104	7.148	8.967	-2.008	1.00	10.00	A	C
ATOM	1040	CD2	PHE	A	104	8.578	8.704	-3.896	1.00	10.00	A	C
ATOM	1041	CE1	PHE	A	104	7.754	7.890	-1.392	1.00	10.00	A	C
ATOM	1042	CE2	PHE	A	104	9.189	7.624	-3.287	1.00	10.00	A	C
ATOM	1043	CZ	PHE	A	104	8.777	7.217	-2.033	1.00	10.00	A	C
ATOM	1044	C	PHE	A	104	4.815	11.887	-4.402	1.00	10.00	A	C
ATOM	1045	O	PHE	A	104	4.729	12.972	-3.831	1.00	10.00	A	O
ATOM	1046	N	GLU	A	105	4.412	11.689	-5.651	1.00	10.00	A	N
ATOM	1047	HN	GLU	A	105	4.514	10.794	-6.047	1.00	10.00	A	H
ATOM	1048	CA	GLU	A	105	3.843	12.757	-6.468	1.00	10.00	A	C
ATOM	1049	CB	GLU	A	105	3.551	12.238	-7.881	1.00	10.00	A	C
ATOM	1050	CG	GLU	A	105	3.127	13.313	-8.867	1.00	10.00	A	C
ATOM	1051	CD	GLU	A	105	2.555	12.733	-10.143	1.00	10.00	A	C
ATOM	1052	OE1	GLU	A	105	1.373	12.333	-10.134	1.00	10.00	A	O
ATOM	1053	OE2	GLU	A	105	3.280	12.678	-11.162	1.00	10.00	A	O
ATOM	1054	C	GLU	A	105	2.573	13.323	-5.831	1.00	10.00	A	C
ATOM	1055	O	GLU	A	105	2.300	14.520	-5.911	1.00	10.00	A	O
ATOM	1056	N	ARG	A	106	1.799	12.456	-5.196	1.00	10.00	A	N
ATOM	1057	HN	ARG	A	106	2.055	11.507	-5.179	1.00	10.00	A	H
ATOM	1058	CA	ARG	A	106	0.567	12.884	-4.544	1.00	10.00	A	C
ATOM	1059	CB	ARG	A	106	-0.363	11.700	-4.303	1.00	10.00	A	C
ATOM	1060	CG	ARG	A	106	-0.923	11.101	-5.579	1.00	10.00	A	C
ATOM	1061	CD	ARG	A	106	-1.898	9.977	-5.281	1.00	10.00	A	C
ATOM	1062	NE	ARG	A	106	-2.382	9.342	-6.507	1.00	10.00	A	N
ATOM	1063	HE	ARG	A	106	-1.718	8.857	-7.055	1.00	10.00	A	H
ATOM	1064	CZ	ARG	A	106	-3.648	9.390	-6.927	1.00	10.00	A	C
ATOM	1065	NH1	ARG	A	106	-4.572	10.044	-6.229	1.00	10.00	A	N
ATOM	1066	HH11	ARG	A	106	-4.316	10.535	-5.341	1.00	10.00	A	H
ATOM	1067	HH12	ARG	A	106	-5.560	10.073	-6.567	1.00	10.00	A	H
ATOM	1068	NH2	ARG	A	106	-3.991	8.793	-8.060	1.00	10.00	A	N
ATOM	1069	HH21	ARG	A	106	-4.979	8.829	-8.395	1.00	10.00	A	H
ATOM	1070	HH22	ARG	A	106	-3.275	8.289	-8.625	1.00	10.00	A	H
ATOM	1071	C	ARG	A	106	0.859	13.619	-3.241	1.00	10.00	A	C
ATOM	1072	O	ARG	A	106	0.091	14.482	-2.817	1.00	10.00	A	O
ATOM	1073	N	PHE	A	107	1.979	13.278	-2.626	1.00	10.00	A	N
ATOM	1074	HN	PHE	A	107	2.546	12.590	-3.030	1.00	10.00	A	H
ATOM	1075	CA	PHE	A	107	2.405	13.903	-1.377	1.00	10.00	A	C
ATOM	1076	CB	PHE	A	107	3.477	13.026	-0.709	1.00	10.00	A	C
ATOM	1077	CG	PHE	A	107	4.146	13.636	0.493	1.00	10.00	A	C
ATOM	1078	CD1	PHE	A	107	5.520	13.826	0.511	1.00	10.00	A	C
ATOM	1079	CD2	PHE	A	107	3.411	14.011	1.604	1.00	10.00	A	C
ATOM	1080	CE1	PHE	A	107	6.148	14.380	1.610	1.00	10.00	A	C
ATOM	1081	CE2	PHE	A	107	4.035	14.565	2.707	1.00	10.00	A	C
ATOM	1082	CZ	PHE	A	107	5.404	14.751	2.709	1.00	10.00	A	C
ATOM	1083	C	PHE	A	107	2.947	15.303	-1.675	1.00	10.00	A	C
ATOM	1084	O	PHE	A	107	2.732	16.256	-0.914	1.00	10.00	A	O
ATOM	1085	N	ASP	A	108	3.644	15.407	-2.796	1.00	10.00	A	N
ATOM	1086	HN	ASP	A	108	3.786	14.604	-3.341	1.00	10.00	A	H
ATOM	1087	CA	ASP	A	108	4.216	16.662	-3.254	1.00	10.00	A	C
ATOM	1088	CB	ASP	A	108	5.503	16.987	-2.496	1.00	10.00	A	C
ATOM	1089	CG	ASP	A	108	6.081	18.337	-2.872	1.00	10.00	A	C
ATOM	1090	OD1	ASP	A	108	5.363	19.151	-3.489	1.00	10.00	A	O
ATOM	1091	OD2	ASP	A	108	7.258	18.591	-2.546	1.00	10.00	A	O
ATOM	1092	C	ASP	A	108	4.504	16.575	-4.746	1.00	10.00	A	C

ATOM	1093	O	ASP	A	108	5.464	15.931	-5.166	1.00	10.00	A	O
ATOM	1094	N	GLU	A	109	3.670	17.233	-5.538	1.00	10.00	A	N
ATOM	1095	HN	GLU	A	109	2.937	17.750	-5.134	1.00	10.00	A	H
ATOM	1096	CA	GLU	A	109	3.817	17.222	-6.988	1.00	10.00	A	C
ATOM	1097	CB	GLU	A	109	2.536	17.699	-7.690	1.00	10.00	A	C
ATOM	1098	CG	GLU	A	109	1.921	18.971	-7.123	1.00	10.00	A	C
ATOM	1099	CD	GLU	A	109	1.169	18.737	-5.832	1.00	10.00	A	C
ATOM	1100	OE1	GLU	A	109	1.654	19.183	-4.770	1.00	10.00	A	O
ATOM	1101	OE2	GLU	A	109	0.098	18.102	-5.864	1.00	10.00	A	O
ATOM	1102	C	GLU	A	109	5.028	18.035	-7.436	1.00	10.00	A	C
ATOM	1103	O	GLU	A	109	5.509	17.886	-8.561	1.00	10.00	A	O
ATOM	1104	N	GLY	A	110	5.532	18.877	-6.544	1.00	10.00	A	N
ATOM	1105	HN	GLY	A	110	5.120	18.941	-5.653	1.00	10.00	A	H
ATOM	1106	CA	GLY	A	110	6.686	19.693	-6.865	1.00	10.00	A	C
ATOM	1107	C	GLY	A	110	7.984	19.006	-6.504	1.00	10.00	A	C
ATOM	1108	O	GLY	A	110	9.065	19.501	-6.832	1.00	10.00	A	O
ATOM	1109	N	HIS	A	111	7.870	17.861	-5.832	1.00	10.00	A	N
ATOM	1110	HN	HIS	A	111	6.971	17.527	-5.616	1.00	10.00	A	H
ATOM	1111	CA	HIS	A	111	9.034	17.080	-5.408	1.00	10.00	A	C
ATOM	1112	CB	HIS	A	111	9.659	16.306	-6.574	1.00	10.00	A	C
ATOM	1113	CG	HIS	A	111	8.958	15.017	-6.893	1.00	10.00	A	C
ATOM	1114	ND1	HIS	A	111	8.077	14.439	-6.007	1.00	10.00	A	N
ATOM	1115	CD2	HIS	A	111	9.047	14.242	-8.002	1.00	10.00	A	C
ATOM	1116	CE1	HIS	A	111	7.647	13.333	-6.592	1.00	10.00	A	C
ATOM	1117	NE2	HIS	A	111	8.210	13.173	-7.796	1.00	10.00	A	N
ATOM	1118	HE2	HIS	A	111	8.060	12.423	-8.414	1.00	10.00	A	H
ATOM	1119	C	HIS	A	111	10.064	17.943	-4.685	1.00	10.00	A	C
ATOM	1120	O	HIS	A	111	11.207	18.078	-5.121	1.00	10.00	A	O
ATOM	1121	N	SER	A	112	9.632	18.538	-3.589	1.00	10.00	A	N
ATOM	1122	HN	SER	A	112	8.693	18.404	-3.315	1.00	10.00	A	H
ATOM	1123	CA	SER	A	112	10.483	19.394	-2.779	1.00	10.00	A	C
ATOM	1124	CB	SER	A	112	9.962	20.832	-2.827	1.00	10.00	A	C
ATOM	1125	OG	SER	A	112	8.594	20.870	-3.222	1.00	10.00	A	O
ATOM	1126	HG	SER	A	112	8.139	20.071	-2.902	1.00	10.00	A	H
ATOM	1127	C	SER	A	112	10.543	18.900	-1.332	1.00	10.00	A	C
ATOM	1128	O	SER	A	112	11.566	19.039	-0.661	1.00	10.00	A	O
ATOM	1129	N	LYS	A	113	9.441	18.329	-0.860	1.00	10.00	A	N
ATOM	1130	HN	LYS	A	113	8.649	18.266	-1.441	1.00	10.00	A	H
ATOM	1131	CA	LYS	A	113	9.362	17.809	0.502	1.00	10.00	A	C
ATOM	1132	CB	LYS	A	113	7.928	17.380	0.829	1.00	10.00	A	C
ATOM	1133	CG	LYS	A	113	6.920	18.521	0.798	1.00	10.00	A	C
ATOM	1134	CD	LYS	A	113	5.499	18.013	0.976	1.00	10.00	A	C
ATOM	1135	CE	LYS	A	113	4.480	19.101	0.685	1.00	10.00	A	C
ATOM	1136	NZ	LYS	A	113	3.085	18.620	0.870	1.00	10.00	A	N
ATOM	1137	HZ1	LYS	A	113	2.989	18.145	1.795	1.00	10.00	A	H
ATOM	1138	HZ2	LYS	A	113	2.831	17.949	0.116	1.00	10.00	A	H
ATOM	1139	HZ3	LYS	A	113	2.425	19.426	0.842	1.00	10.00	A	H
ATOM	1140	C	LYS	A	113	10.340	16.652	0.723	1.00	10.00	A	C
ATOM	1141	O	LYS	A	113	10.610	15.870	-0.195	1.00	10.00	A	O
ATOM	1142	N	PRO	A	114	10.895	16.547	1.940	1.00	10.00	A	N
ATOM	1143	CA	PRO	A	114	11.856	15.494	2.293	1.00	10.00	A	C
ATOM	1144	CB	PRO	A	114	12.427	15.979	3.624	1.00	10.00	A	C
ATOM	1145	CG	PRO	A	114	11.327	16.782	4.222	1.00	10.00	A	C
ATOM	1146	CD	PRO	A	114	10.634	17.455	3.072	1.00	10.00	A	C
ATOM	1147	C	PRO	A	114	11.203	14.128	2.475	1.00	10.00	A	C
ATOM	1148	O	PRO	A	114	10.023	14.025	2.822	1.00	10.00	A	O
ATOM	1149	N	ILE	A	115	11.991	13.084	2.258	1.00	10.00	A	N
ATOM	1150	HN	ILE	A	115	12.926	13.240	2.008	1.00	10.00	A	H
ATOM	1151	CA	ILE	A	115	11.516	11.715	2.383	1.00	10.00	A	C
ATOM	1152	CB	ILE	A	115	11.342	11.061	0.989	1.00	10.00	A	C
ATOM	1153	CG1	ILE	A	115	10.094	11.617	0.298	1.00	10.00	A	C
ATOM	1154	CG2	ILE	A	115	11.275	9.541	1.084	1.00	10.00	A	C
ATOM	1155	CD1	ILE	A	115	9.943	11.182	-1.142	1.00	10.00	A	C
ATOM	1156	C	ILE	A	115	12.470	10.887	3.241	1.00	10.00	A	C
ATOM	1157	O	ILE	A	115	13.685	10.913	3.039	1.00	10.00	A	O
ATOM	1158	N	ARG	A	116	11.909	10.183	4.218	1.00	10.00	A	N
ATOM	1159	HN	ARG	A	116	10.937	10.236	4.340	1.00	10.00	A	H
ATOM	1160	CA	ARG	A	116	12.690	9.336	5.115	1.00	10.00	A	C
ATOM	1161	CB	ARG	A	116	12.537	9.797	6.569	1.00	10.00	A	C
ATOM	1162	CG	ARG	A	116	13.012	11.220	6.824	1.00	10.00	A	C
ATOM	1163	CD	ARG	A	116	13.047	11.534	8.311	1.00	10.00	A	C
ATOM	1164	NE	ARG	A	116	13.314	12.951	8.565	1.00	10.00	A	N
ATOM	1165	HE	ARG	A	116	13.200	13.572	7.812	1.00	10.00	A	H
ATOM	1166	CZ	ARG	A	116	13.710	13.443	9.738	1.00	10.00	A	C
ATOM	1167	NH1	ARG	A	116	13.897	12.644	10.774	1.00	10.00	A	N
ATOM	1168	HH11	ARG	A	116	13.742	11.615	10.678	1.00	10.00	A	H
ATOM	1169	HH12	ARG	A	116	14.206	13.037	11.689	1.00	10.00	A	H
ATOM	1170	NH2	ARG	A	116	13.924	14.743	9.864	1.00	10.00	A	N
ATOM	1171	HH21	ARG	A	116	13.785	15.377	9.040	1.00	10.00	A	H
ATOM	1172	HH22	ARG	A	116	14.234	15.141	10.777	1.00	10.00	A	H
ATOM	1173	C	ARG	A	116	12.250	7.885	4.981	1.00	10.00	A	C
ATOM	1174	O	ARG	A	116	11.067	7.604	4.779	1.00	10.00	A	O
ATOM	1175	N	ALA	A	117	13.198	6.968	5.091	1.00	10.00	A	N
ATOM	1176	HN	ALA	A	117	14.122	7.250	5.259	1.00	10.00	A	H
ATOM	1177	CA	ALA	A	117	12.895	5.549	4.972	1.00	10.00	A	C
ATOM	1178	CB	ALA	A	117	13.119	5.075	3.543	1.00	10.00	A	C
ATOM	1179	C	ALA	A	117	13.718	4.720	5.951	1.00	10.00	A	C
ATOM	1180	O	ALA	A	117	14.875	5.039	6.235	1.00	10.00	A	O
ATOM	1181	N	ALA	A	118	13.110	3.661	6.471	1.00	10.00	A	N
ATOM	1182	HN	ALA	A	118	12.177	3.471	6.213	1.00	10.00	A	H
ATOM	1183	CA	ALA	A	118	13.783	2.772	7.416	1.00	10.00	A	C
ATOM	1184	CB	ALA	A	118	12.762	2.028	8.260	1.00	10.00	A	C
ATOM	1185	C	ALA	A	118	14.708	1.796	6.682	1.00	10.00	A	C
ATOM	1186	O	ALA	A	118	14.835	1.863	5.459	1.00	10.00	A	O
ATOM	1187	N	GLU	A	119	15.338	0.885	7.431	1.00	10.00	A	N

ATOM	1188	HN	GLU	A	119	15.172	0.867	8.395	1.00	10.00	A	H
ATOM	1189	CA	GLU	A	119	16.271	-0.092	6.860	1.00	10.00	A	C
ATOM	1190	CB	GLU	A	119	16.805	-1.034	7.944	1.00	10.00	A	C
ATOM	1191	CG	GLU	A	119	17.927	-1.958	7.480	1.00	10.00	A	C
ATOM	1192	CD	GLU	A	119	19.107	-1.214	6.877	1.00	10.00	A	C
ATOM	1193	OE1	GLU	A	119	19.484	-1.514	5.725	1.00	10.00	A	O
ATOM	1194	OE2	GLU	A	119	19.671	-0.326	7.552	1.00	10.00	A	O
ATOM	1195	C	GLU	A	119	15.658	-0.895	5.717	1.00	10.00	A	C
ATOM	1196	O	GLU	A	119	16.140	-0.839	4.582	1.00	10.00	A	O
ATOM	1197	N	THR	A	120	14.593	-1.629	6.002	1.00	10.00	A	N
ATOM	1198	HN	THR	A	120	14.217	-1.615	6.915	1.00	10.00	A	H
ATOM	1199	CA	THR	A	120	13.948	-2.442	4.978	1.00	10.00	A	C
ATOM	1200	CB	THR	A	120	12.838	-3.328	5.575	1.00	10.00	A	C
ATOM	1201	OG1	THR	A	120	13.283	-3.857	6.833	1.00	10.00	A	O
ATOM	1202	HG1	THR	A	120	13.055	-3.227	7.539	1.00	10.00	A	H
ATOM	1203	CG2	THR	A	120	12.509	-4.480	4.635	1.00	10.00	A	C
ATOM	1204	C	THR	A	120	13.374	-1.560	3.870	1.00	10.00	A	C
ATOM	1205	O	THR	A	120	13.427	-1.912	2.686	1.00	10.00	A	O
ATOM	1206	N	ALA	A	121	12.840	-0.409	4.268	1.00	10.00	A	N
ATOM	1207	HN	ALA	A	121	12.810	-0.209	5.230	1.00	10.00	A	H
ATOM	1208	CA	ALA	A	121	12.269	0.548	3.329	1.00	10.00	A	C
ATOM	1209	CB	ALA	A	121	11.694	1.737	4.074	1.00	10.00	A	C
ATOM	1210	C	ALA	A	121	13.306	1.008	2.308	1.00	10.00	A	C
ATOM	1211	O	ALA	A	121	13.023	1.065	1.109	1.00	10.00	A	O
ATOM	1212	N	VAL	A	122	14.509	1.323	2.787	1.00	10.00	A	N
ATOM	1213	HN	VAL	A	122	14.672	1.254	3.757	1.00	10.00	A	H
ATOM	1214	CA	VAL	A	122	15.591	1.768	1.911	1.00	10.00	A	C
ATOM	1215	CB	VAL	A	122	16.880	2.112	2.701	1.00	10.00	A	C
ATOM	1216	CG1	VAL	A	122	18.066	2.285	1.764	1.00	10.00	A	C
ATOM	1217	CG2	VAL	A	122	16.688	3.376	3.527	1.00	10.00	A	C
ATOM	1218	C	VAL	A	122	15.889	0.700	0.858	1.00	10.00	A	C
ATOM	1219	O	VAL	A	122	16.131	1.015	-0.304	1.00	10.00	A	O
ATOM	1220	N	GLY	A	123	15.834	-0.564	1.271	1.00	10.00	A	N
ATOM	1221	HN	GLY	A	123	15.614	-0.753	2.207	1.00	10.00	A	H
ATOM	1222	CA	GLY	A	123	16.088	-1.661	0.352	1.00	10.00	A	C
ATOM	1223	C	GLY	A	123	15.099	-1.668	-0.797	1.00	10.00	A	C
ATOM	1224	O	GLY	A	123	15.459	-1.957	-1.940	1.00	10.00	A	O
ATOM	1225	N	VAL	A	124	13.852	-1.323	-0.495	1.00	10.00	A	N
ATOM	1226	HN	VAL	A	124	13.634	-1.080	0.431	1.00	10.00	A	H
ATOM	1227	CA	VAL	A	124	12.801	-1.278	-1.505	1.00	10.00	A	C
ATOM	1228	CB	VAL	A	124	11.399	-1.222	-0.860	1.00	10.00	A	C
ATOM	1229	CG1	VAL	A	124	10.312	-1.197	-1.922	1.00	10.00	A	C
ATOM	1230	CG2	VAL	A	124	11.197	-2.402	0.075	1.00	10.00	A	C
ATOM	1231	C	VAL	A	124	12.999	-0.063	-2.406	1.00	10.00	A	C
ATOM	1232	O	VAL	A	124	12.863	-0.148	-3.631	1.00	10.00	A	O
ATOM	1233	N	LEU	A	125	13.349	1.065	-1.789	1.00	10.00	A	N
ATOM	1234	HN	LEU	A	125	13.452	1.065	-0.810	1.00	10.00	A	H
ATOM	1235	CA	LEU	A	125	13.582	2.301	-2.524	1.00	10.00	A	C
ATOM	1236	CB	LEU	A	125	13.856	3.465	-1.566	1.00	10.00	A	C
ATOM	1237	CG	LEU	A	125	12.679	4.400	-1.275	1.00	10.00	A	C
ATOM	1238	CD1	LEU	A	125	11.621	3.698	-0.438	1.00	10.00	A	C
ATOM	1239	CD2	LEU	A	125	13.161	5.666	-0.582	1.00	10.00	A	C
ATOM	1240	C	LEU	A	125	14.739	2.132	-3.499	1.00	10.00	A	C
ATOM	1241	O	LEU	A	125	14.660	2.574	-4.645	1.00	10.00	A	O
ATOM	1242	N	SER	A	126	15.804	1.481	-3.038	1.00	10.00	A	N
ATOM	1243	HN	SER	A	126	15.806	1.167	-2.106	1.00	10.00	A	H
ATOM	1244	CA	SER	A	126	16.977	1.235	-3.864	1.00	10.00	A	C
ATOM	1245	CB	SER	A	126	18.158	0.786	-3.002	1.00	10.00	A	C
ATOM	1246	OG	SER	A	126	18.634	1.861	-2.215	1.00	10.00	A	O
ATOM	1247	HG	SER	A	126	18.714	2.646	-2.776	1.00	10.00	A	H
ATOM	1248	C	SER	A	126	16.691	0.205	-4.951	1.00	10.00	A	C
ATOM	1249	O	SER	A	126	17.232	0.288	-6.052	1.00	10.00	A	O
ATOM	1250	N	GLN	A	127	15.838	-0.766	-4.638	1.00	10.00	A	N
ATOM	1251	HN	GLN	A	127	15.445	-0.788	-3.739	1.00	10.00	A	H
ATOM	1252	CA	GLN	A	127	15.479	-1.804	-5.596	1.00	10.00	A	C
ATOM	1253	CB	GLN	A	127	14.527	-2.817	-4.955	1.00	10.00	A	C
ATOM	1254	CG	GLN	A	127	14.320	-4.081	-5.776	1.00	10.00	A	C
ATOM	1255	CD	GLN	A	127	15.555	-4.957	-5.814	1.00	10.00	A	C
ATOM	1256	OE1	GLN	A	127	16.335	-4.991	-4.864	1.00	10.00	A	O
ATOM	1257	NE2	GLN	A	127	15.746	-5.672	-6.911	1.00	10.00	A	N
ATOM	1258	HE21	GLN	A	127	15.085	-5.602	-7.640	1.00	10.00	A	H
ATOM	1259	HE22	GLN	A	127	16.541	-6.243	-6.957	1.00	10.00	A	H
ATOM	1260	C	GLN	A	127	14.823	-1.191	-6.829	1.00	10.00	A	C
ATOM	1261	O	GLN	A	127	15.150	-1.545	-7.959	1.00	10.00	A	O
ATOM	1262	N	PHE	A	128	13.905	-0.266	-6.595	1.00	10.00	A	N
ATOM	1263	HN	PHE	A	128	13.693	-0.027	-5.666	1.00	10.00	A	H
ATOM	1264	CA	PHE	A	128	13.196	0.395	-7.679	1.00	10.00	A	C
ATOM	1265	CB	PHE	A	128	11.815	0.855	-7.207	1.00	10.00	A	C
ATOM	1266	CG	PHE	A	128	10.890	-0.278	-6.849	1.00	10.00	A	C
ATOM	1267	CD1	PHE	A	128	10.853	-1.432	-7.616	1.00	10.00	A	C
ATOM	1268	CD2	PHE	A	128	10.055	-0.185	-5.749	1.00	10.00	A	C
ATOM	1269	CE1	PHE	A	128	10.002	-2.470	-7.291	1.00	10.00	A	C
ATOM	1270	CE2	PHE	A	128	9.201	-1.219	-5.419	1.00	10.00	A	C
ATOM	1271	CZ	PHE	A	128	9.175	-2.362	-6.191	1.00	10.00	A	C
ATOM	1272	C	PHE	A	128	13.995	1.568	-8.244	1.00	10.00	A	C
ATOM	1273	O	PHE	A	128	14.083	1.741	-9.460	1.00	10.00	A	O
ATOM	1274	N	GLY	A	129	14.575	2.364	-7.356	1.00	10.00	A	N
ATOM	1275	HN	GLY	A	129	14.472	2.173	-6.398	1.00	10.00	A	H
ATOM	1276	CA	GLY	A	129	15.360	3.510	-7.779	1.00	10.00	A	C
ATOM	1277	C	GLY	A	129	14.742	4.830	-7.350	1.00	10.00	A	C
ATOM	1278	O	GLY	A	129	14.454	5.689	-8.188	1.00	10.00	A	O
ATOM	1279	N	GLN	A	130	14.528	4.984	-6.047	1.00	10.00	A	N
ATOM	1280	HN	GLN	A	130	14.779	4.256	-5.436	1.00	10.00	A	H
ATOM	1281	CA	GLN	A	130	13.940	6.202	-5.495	1.00	10.00	A	C
ATOM	1282	CB	GLN	A	130	12.490	5.948	-5.065	1.00	10.00	A	C

ATOM	1283	CG	GLN	A	130	11.500	5.789	-6.211	1.00	10.00	A	C
ATOM	1284	CD	GLN	A	130	11.218	7.091	-6.938	1.00	10.00	A	C
ATOM	1285	OE1	GLN	A	130	11.282	8.173	-6.353	1.00	10.00	A	O
ATOM	1286	NE2	GLN	A	130	10.904	6.993	-8.222	1.00	10.00	A	N
ATOM	1287	HE21	GLN	A	130	10.872	6.101	-8.625	1.00	10.00	A	H
ATOM	1288	HE22	GLN	A	130	10.714	7.818	-8.716	1.00	10.00	A	H
ATOM	1289	C	GLN	A	130	14.744	6.708	-4.296	1.00	10.00	A	C
ATOM	1290	O	GLN	A	130	14.259	7.532	-3.516	1.00	10.00	A	O
ATOM	1291	N	GLU	A	131	15.977	6.228	-4.158	1.00	10.00	A	N
ATOM	1292	HN	GLU	A	131	16.329	5.593	-4.828	1.00	10.00	A	H
ATOM	1293	CA	GLU	A	131	16.828	6.623	-3.038	1.00	10.00	A	C
ATOM	1294	CB	GLU	A	131	17.974	5.635	-2.822	1.00	10.00	A	C
ATOM	1295	CG	GLU	A	131	18.908	5.490	-4.010	1.00	10.00	A	C
ATOM	1296	CD	GLU	A	131	18.464	4.408	-4.966	1.00	10.00	A	C
ATOM	1297	OE1	GLU	A	131	18.992	3.284	-4.870	1.00	10.00	A	O
ATOM	1298	OE2	GLU	A	131	17.582	4.682	-5.803	1.00	10.00	A	O
ATOM	1299	C	GLU	A	131	17.364	8.042	-3.193	1.00	10.00	A	C
ATOM	1300	O	GLU	A	131	18.001	8.578	-2.283	1.00	10.00	A	O
ATOM	1301	N	HIS	A	132	17.095	8.654	-4.339	1.00	10.00	A	N
ATOM	1302	HN	HIS	A	132	16.576	8.178	-5.028	1.00	10.00	A	H
ATOM	1303	CA	HIS	A	132	17.547	10.018	-4.608	1.00	10.00	A	C
ATOM	1304	CB	HIS	A	132	17.403	10.361	-6.093	1.00	10.00	A	C
ATOM	1305	CG	HIS	A	132	16.000	10.277	-6.618	1.00	10.00	A	C
ATOM	1306	ND1	HIS	A	132	15.386	9.064	-6.827	1.00	10.00	A	N
ATOM	1307	CD2	HIS	A	132	15.149	11.276	-6.963	1.00	10.00	A	C
ATOM	1308	CE1	HIS	A	132	14.183	9.345	-7.293	1.00	10.00	A	C
ATOM	1309	NE2	HIS	A	132	13.996	10.668	-7.392	1.00	10.00	A	N
ATOM	1310	HE2	HIS	A	132	13.182	11.120	-7.714	1.00	10.00	A	H
ATOM	1311	C	HIS	A	132	16.788	11.024	-3.740	1.00	10.00	A	C
ATOM	1312	O	HIS	A	132	17.132	12.206	-3.677	1.00	10.00	A	O
ATOM	1313	N	ARG	A	133	15.751	10.544	-3.070	1.00	10.00	A	N
ATOM	1314	HN	ARG	A	133	15.521	9.597	-3.171	1.00	10.00	A	H
ATOM	1315	CA	ARG	A	133	14.946	11.383	-2.198	1.00	10.00	A	C
ATOM	1316	CB	ARG	A	133	13.488	10.929	-2.224	1.00	10.00	A	C
ATOM	1317	CG	ARG	A	133	12.846	10.997	-3.595	1.00	10.00	A	C
ATOM	1318	CD	ARG	A	133	12.894	12.408	-4.155	1.00	10.00	A	C
ATOM	1319	NE	ARG	A	133	12.195	13.366	-3.298	1.00	10.00	A	N
ATOM	1320	HE	ARG	A	133	12.692	13.737	-2.531	1.00	10.00	A	H
ATOM	1321	CZ	ARG	A	133	10.947	13.770	-3.505	1.00	10.00	A	C
ATOM	1322	NH1	ARG	A	133	10.262	13.299	-4.537	1.00	10.00	A	N
ATOM	1323	HH11	ARG	A	133	9.281	13.617	-4.710	1.00	10.00	A	H
ATOM	1324	HH12	ARG	A	133	10.699	12.606	-5.187	1.00	10.00	A	H
ATOM	1325	NH2	ARG	A	133	10.376	14.628	-2.667	1.00	10.00	A	N
ATOM	1326	HH21	ARG	A	133	10.906	14.989	-1.835	1.00	10.00	A	H
ATOM	1327	HH22	ARG	A	133	9.399	14.946	-2.829	1.00	10.00	A	H
ATOM	1328	C	ARG	A	133	15.471	11.333	-0.769	1.00	10.00	A	C
ATOM	1329	O	ARG	A	133	14.985	12.049	0.105	1.00	10.00	A	O
ATOM	1330	N	LEU	A	134	16.462	10.480	-0.538	1.00	10.00	A	N
ATOM	1331	HN	LEU	A	134	16.813	9.941	-1.278	1.00	10.00	A	H
ATOM	1332	CA	LEU	A	134	17.050	10.333	0.788	1.00	10.00	A	C
ATOM	1333	CB	LEU	A	134	17.512	8.890	1.021	1.00	10.00	A	C
ATOM	1334	CG	LEU	A	134	16.441	7.807	0.872	1.00	10.00	A	C
ATOM	1335	CD1	LEU	A	134	17.051	6.421	1.019	1.00	10.00	A	C
ATOM	1336	CD2	LEU	A	134	15.324	8.017	1.883	1.00	10.00	A	C
ATOM	1337	C	LEU	A	134	18.224	11.285	0.969	1.00	10.00	A	C
ATOM	1338	O	LEU	A	134	18.955	11.574	0.018	1.00	10.00	A	O
ATOM	1339	N	SER	A	135	18.405	11.754	2.191	1.00	10.00	A	N
ATOM	1340	HN	SER	A	135	17.799	11.464	2.904	1.00	10.00	A	H
ATOM	1341	CA	SER	A	135	19.483	12.672	2.514	1.00	10.00	A	C
ATOM	1342	CB	SER	A	135	19.051	14.125	2.253	1.00	10.00	A	C
ATOM	1343	OG	SER	A	135	20.063	15.046	2.634	1.00	10.00	A	O
ATOM	1344	HG	SER	A	135	20.388	15.505	1.850	1.00	10.00	A	H
ATOM	1345	C	SER	A	135	19.912	12.497	3.969	1.00	10.00	A	C
ATOM	1346	O	SER	A	135	19.075	12.491	4.876	1.00	10.00	A	O
ATOM	1347	N	PRO	A	136	21.225	12.348	4.211	1.00	10.00	A	N
ATOM	1348	CA	PRO	A	136	21.762	12.191	5.567	1.00	10.00	A	C
ATOM	1349	CB	PRO	A	136	23.222	11.799	5.329	1.00	10.00	A	C
ATOM	1350	CG	PRO	A	136	23.553	12.366	3.991	1.00	10.00	A	C
ATOM	1351	CD	PRO	A	136	22.284	12.304	3.185	1.00	10.00	A	C
ATOM	1352	C	PRO	A	136	21.681	13.504	6.343	1.00	10.00	A	C
ATOM	1353	O	PRO	A	136	21.870	13.535	7.561	1.00	10.00	A	O
ATOM	1354	N	GLU	A	137	21.396	14.584	5.617	1.00	10.00	A	N
ATOM	1355	HN	GLU	A	137	21.262	14.483	4.647	1.00	10.00	A	H
ATOM	1356	CA	GLU	A	137	21.274	15.909	6.209	1.00	10.00	A	C
ATOM	1357	CB	GLU	A	137	21.616	16.986	5.176	1.00	10.00	A	C
ATOM	1358	CG	GLU	A	137	23.095	17.042	4.826	1.00	10.00	A	C
ATOM	1359	CD	GLU	A	137	23.378	17.772	3.531	1.00	10.00	A	C
ATOM	1360	OE1	GLU	A	137	24.094	17.210	2.673	1.00	10.00	A	O
ATOM	1361	OE2	GLU	A	137	22.896	18.910	3.363	1.00	10.00	A	O
ATOM	1362	C	GLU	A	137	19.868	16.116	6.758	1.00	10.00	A	C
ATOM	1363	O	GLU	A	137	19.627	17.025	7.548	1.00	10.00	A	O
ATOM	1364	N	GLU	A	138	18.950	15.258	6.338	1.00	10.00	A	N
ATOM	1365	HN	GLU	A	138	19.210	14.551	5.709	1.00	10.00	A	H
ATOM	1366	CA	GLU	A	138	17.569	15.333	6.790	1.00	10.00	A	C
ATOM	1367	CB	GLU	A	138	16.656	14.594	5.805	1.00	10.00	A	C
ATOM	1368	CG	GLU	A	138	15.194	14.522	6.218	1.00	10.00	A	C
ATOM	1369	CD	GLU	A	138	14.597	15.878	6.517	1.00	10.00	A	C
ATOM	1370	OE1	GLU	A	138	13.797	15.981	7.473	1.00	10.00	A	O
ATOM	1371	OE2	GLU	A	138	14.923	16.848	5.802	1.00	10.00	A	O
ATOM	1372	C	GLU	A	138	17.442	14.738	8.189	1.00	10.00	A	C
ATOM	1373	O	GLU	A	138	16.990	15.403	9.124	1.00	10.00	A	O
ATOM	1374	N	GLY	A	139	17.861	13.491	8.326	1.00	10.00	A	N
ATOM	1375	HN	GLY	A	139	18.219	13.015	7.549	1.00	10.00	A	H
ATOM	1376	CA	GLY	A	139	17.786	12.825	9.604	1.00	10.00	A	C
ATOM	1377	C	GLY	A	139	17.429	11.365	9.452	1.00	10.00	A	C

```
ATOM   1378  O   GLY A 139      17.248  10.882   8.333  1.00 10.00      A    O
ATOM   1379  N   ASP A 140      17.323  10.666  10.573  1.00 10.00      A    N
ATOM   1380  HN  ASP A 140      17.472  11.117  11.432  1.00 10.00      A    H
ATOM   1381  CA  ASP A 140      16.986   9.248  10.569  1.00 10.00      A    C
ATOM   1382  CB  ASP A 140      17.569   8.564  11.813  1.00 10.00      A    C
ATOM   1383  CG  ASP A 140      17.719   7.054  11.678  1.00 10.00      A    C
ATOM   1384  OD1 ASP A 140      17.268   6.482  10.664  1.00 10.00      A    O
ATOM   1385  OD2 ASP A 140      18.299   6.431  12.597  1.00 10.00      A    O
ATOM   1386  C   ASP A 140      15.471   9.067  10.522  1.00 10.00      A    C
ATOM   1387  O   ASP A 140      14.716   9.999  10.807  1.00 10.00      A    O
ATOM   1388  N   ASN A 141      15.035   7.873  10.155  1.00 10.00      A    N
ATOM   1389  HN  ASN A 141      15.696   7.171   9.943  1.00 10.00      A    H
ATOM   1390  CA  ASN A 141      13.610   7.566  10.067  1.00 10.00      A    C
ATOM   1391  CB  ASN A 141      13.363   6.486   9.011  1.00 10.00      A    C
ATOM   1392  CG  ASN A 141      11.890   6.192   8.787  1.00 10.00      A    C
ATOM   1393  OD1 ASN A 141      11.201   6.919   8.069  1.00 10.00      A    O
ATOM   1394  ND2 ASN A 141      11.398   5.116   9.385  1.00 10.00      A    N
ATOM   1395 HD21 ASN A 141      12.005   4.571   9.941  1.00 10.00      A    H
ATOM   1396 HD22 ASN A 141      10.454   4.899   9.242  1.00 10.00      A    H
ATOM   1397  C   ASN A 141      13.058   7.121  11.418  1.00 10.00      A    C
ATOM   1398  O   ASN A 141      11.855   7.238  11.681  1.00 10.00      A    O
END
```

16-bp dsRNA:

```
REMARK FILENAME="/home/enmr/services/HADDOCK/server/run/userrun000001/run1/./"
REMARK ===============================================================
REMARK HADDOCK run for complex
REMARK final NOE weights: unambig 50 amb: 50
REMARK ===============================================================
REMARK            total,bonds,angles,improper,dihe,vdw,elec,air,cdih,coup,sani,vean,dani
REMARK energies: 1550.85, 0, 0, 0, 0, -36.6922, -583.178, 2118.27, 0, 0, 0, 0, 0
REMARK ===============================================================
REMARK            bonds,angles,impropers,dihe,air,cdih,coup,sani,vean,dani
REMARK rms-dev.: 0,0,0,0,0.792854,0.548201,0, 0, 0, 0
REMARK ===============================================================
REMARK               air,cdih,coup,sani,vean,dani
REMARK               >0.3,>5,>1,>0,>5,>0.2
REMARK violations.: 10, 2, 0, 0, 0, 0
REMARK ===============================================================
REMARK                        CVpartition#,violations,rms
REMARK AIRs cross-validation: 2, 9, 1.98977
REMARK ===============================================================
REMARK NCS energy: 0
REMARK ===============================================================
REMARK Symmetry energy: 0
REMARK ===============================================================
REMARK Desolvation energy: 30.8942
REMARK Internal energy free molecules: 15502
REMARK Internal energy complex: -7720.91
REMARK Binding energy: -23811.9
REMARK ===============================================================
REMARK buried surface area: 1287.61
REMARK ===============================================================
REMARK water - chain1: 0 0 0
REMARK water - chain2: 0 0 0
REMARK water - chain3: 0 0 0
REMARK water - chain4: 0 0 0
REMARK water - chain5: 0 0 0
REMARK water - chain6: 0 0 0
REMARK ===============================================================
REMARK water - water: 0 0 0
REMARK ===============================================================
REMARK DATE:15-Jul-2016  01:25:58       created by user: enmr
REMARK VERSION:1.2
ATOM      1  H5T CYT B   1      25.989 -10.188   5.647  1.00 10.00      B    H
ATOM      2  O5' CYT B   1      26.643 -10.727   6.119  1.00 10.00      B    O
ATOM      3  C5' CYT B   1      26.063 -11.035   7.393  1.00 10.00      B    C
ATOM      4  H5' CYT B   1      26.143 -12.106   7.583  1.00 10.00      B    H
ATOM      5 H5'' CYT B   1      25.009 -10.755   7.392  1.00 10.00      B    H
ATOM      6  C4' CYT B   1      26.766 -10.281   8.498  1.00 10.00      B    C
ATOM      7  H4' CYT B   1      26.297 -10.551   9.444  1.00 10.00      B    H
ATOM      8  O4' CYT B   1      28.195 -10.571   8.444  1.00 10.00      B    O
ATOM      9  C1' CYT B   1      28.932  -9.408   8.804  1.00 10.00      B    C
ATOM     10  H1' CYT B   1      29.613  -9.699   9.606  1.00 10.00      B    H
ATOM     11  N1  CYT B   1      29.739  -8.985   7.650  1.00 10.00      B    N
ATOM     12  C6  CYT B   1      29.411  -9.374   6.380  1.00 10.00      B    C
ATOM     13  H6  CYT B   1      28.522  -9.985   6.217  1.00 10.00      B    H
ATOM     14  C2  CYT B   1      30.859  -8.185   7.873  1.00 10.00      B    C
ATOM     15  O2  CYT B   1      31.132  -7.831   9.035  1.00 10.00      B    O
ATOM     16  N3  CYT B   1      31.627  -7.816   6.825  1.00 10.00      B    N
ATOM     17  C4  CYT B   1      31.313  -8.213   5.591  1.00 10.00      B    C
ATOM     18  N4  CYT B   1      32.120  -7.836   4.593  1.00 10.00      B    N
ATOM     19  H41 CYT B   1      31.915  -8.123   3.646  1.00 10.00      B    H
ATOM     20  H42 CYT B   1      32.939  -7.272   4.782  1.00 10.00      B    H
ATOM     21  C5  CYT B   1      30.165  -9.017   5.330  1.00 10.00      B    C
ATOM     22  H5  CYT B   1      29.910  -9.329   4.316  1.00 10.00      B    H
ATOM     23  C2' CYT B   1      27.903  -8.382   9.273  1.00 10.00      B    C
ATOM     24  H2' CYT B   1      28.226  -7.359   9.065  1.00 10.00      B    H
ATOM     25  O2' CYT B   1      27.624  -8.608  10.641  1.00 10.00      B    O
ATOM     26 HO2' CYT B   1      28.326  -9.180  10.964  1.00 10.00      B    H
ATOM     27  C3' CYT B   1      26.727  -8.766   8.392  1.00 10.00      B    C
ATOM     28  H3' CYT B   1      26.840  -8.427   7.362  1.00 10.00      B    H
```

ATOM	29	O3'	CYT	B	1	25.498	-8.230	8.858	1.00	10.00	B	O
ATOM	30	P	CYT	B	2	24.883	-6.938	8.140	1.00	10.00	B	P
ATOM	31	O1P	CYT	B	2	23.446	-6.871	8.498	1.00	10.00	B	O
ATOM	32	O2P	CYT	B	2	25.282	-6.982	6.713	1.00	10.00	B	O
ATOM	33	O5'	CYT	B	2	25.627	-5.723	8.842	1.00	10.00	B	O
ATOM	34	C5'	CYT	B	2	25.730	-5.665	10.258	1.00	10.00	B	C
ATOM	35	H5'	CYT	B	2	25.927	-6.663	10.651	1.00	10.00	B	H
ATOM	36	H5''	CYT	B	2	24.798	-5.295	10.682	1.00	10.00	B	H
ATOM	37	C4'	CYT	B	2	26.853	-4.744	10.661	1.00	10.00	B	C
ATOM	38	H4'	CYT	B	2	26.772	-4.564	11.732	1.00	10.00	B	H
ATOM	39	O4'	CYT	B	2	28.125	-5.332	10.259	1.00	10.00	B	O
ATOM	40	C1'	CYT	B	2	29.018	-4.303	9.852	1.00	10.00	B	C
ATOM	41	H1'	CYT	B	2	29.939	-4.436	10.423	1.00	10.00	B	H
ATOM	42	N1	CYT	B	2	29.331	-4.489	8.428	1.00	10.00	B	N
ATOM	43	C6	CYT	B	2	28.484	-5.174	7.599	1.00	10.00	B	C
ATOM	44	H6	CYT	B	2	27.548	-5.571	7.994	1.00	10.00	B	H
ATOM	45	C2	CYT	B	2	30.519	-3.959	7.932	1.00	10.00	B	C
ATOM	46	O2	CYT	B	2	31.276	-3.325	8.689	1.00	10.00	B	O
ATOM	47	N3	CYT	B	2	30.835	-4.139	6.638	1.00	10.00	B	N
ATOM	48	C4	CYT	B	2	30.019	-4.819	5.835	1.00	10.00	B	C
ATOM	49	N4	CYT	B	2	30.400	-4.983	4.563	1.00	10.00	B	N
ATOM	50	H41	CYT	B	2	29.802	-5.502	3.928	1.00	10.00	B	H
ATOM	51	H42	CYT	B	2	31.274	-4.599	4.234	1.00	10.00	B	H
ATOM	52	C5	CYT	B	2	28.786	-5.363	6.305	1.00	10.00	B	C
ATOM	53	H5	CYT	B	2	28.117	-5.911	5.640	1.00	10.00	B	H
ATOM	54	C2'	CYT	B	2	28.324	-2.985	10.184	1.00	10.00	B	C
ATOM	55	H2'	CYT	B	2	28.611	-2.185	9.498	1.00	10.00	B	H
ATOM	56	O2'	CYT	B	2	28.585	-2.677	11.540	1.00	10.00	B	O
ATOM	57	HO2'	CYT	B	2	28.739	-3.524	11.977	1.00	10.00	B	H
ATOM	58	C3'	CYT	B	2	26.874	-3.387	9.978	1.00	10.00	B	C
ATOM	59	H3'	CYT	B	2	26.596	-3.454	8.926	1.00	10.00	B	H
ATOM	60	O3'	CYT	B	2	25.965	-2.477	10.580	1.00	10.00	B	O
ATOM	61	P	ADE	B	3	25.308	-1.314	9.694	1.00	10.00	B	P
ATOM	62	O1P	ADE	B	3	24.309	-0.633	10.554	1.00	10.00	B	O
ATOM	63	O2P	ADE	B	3	24.889	-1.878	8.390	1.00	10.00	B	O
ATOM	64	O5'	ADE	B	3	26.504	-0.299	9.435	1.00	10.00	B	O
ATOM	65	C5'	ADE	B	3	26.762	0.757	10.350	1.00	10.00	B	C
ATOM	66	H5'	ADE	B	3	27.054	0.342	11.317	1.00	10.00	B	H
ATOM	67	H5''	ADE	B	3	25.863	1.357	10.481	1.00	10.00	B	H
ATOM	68	C4'	ADE	B	3	27.871	1.640	9.832	1.00	10.00	B	C
ATOM	69	H4'	ADE	B	3	28.068	2.409	10.577	1.00	10.00	B	H
ATOM	70	O4'	ADE	B	3	29.035	0.818	9.515	1.00	10.00	B	O
ATOM	71	C1'	ADE	B	3	29.694	1.346	8.372	1.00	10.00	B	C
ATOM	72	H1'	ADE	B	3	30.741	1.489	8.648	1.00	10.00	B	H
ATOM	73	N9	ADE	B	3	29.642	0.359	7.296	1.00	10.00	B	N
ATOM	74	C4	ADE	B	3	30.500	0.303	6.226	1.00	10.00	B	C
ATOM	75	N3	ADE	B	3	31.516	1.139	5.956	1.00	10.00	B	N
ATOM	76	C2	ADE	B	3	32.139	0.775	4.838	1.00	10.00	B	C
ATOM	77	H2	ADE	B	3	32.976	1.408	4.542	1.00	10.00	B	H
ATOM	78	N1	ADE	B	3	31.883	-0.257	4.021	1.00	10.00	B	N
ATOM	79	C6	ADE	B	3	30.857	-1.081	4.322	1.00	10.00	B	C
ATOM	80	N6	ADE	B	3	30.616	-2.113	3.511	1.00	10.00	B	N
ATOM	81	H61	ADE	B	3	29.857	-2.746	3.717	1.00	10.00	B	H
ATOM	82	H62	ADE	B	3	31.200	-2.260	2.696	1.00	10.00	B	H
ATOM	83	C5	ADE	B	3	30.109	-0.798	5.484	1.00	10.00	B	C
ATOM	84	N7	ADE	B	3	29.015	-1.418	6.068	1.00	10.00	B	N
ATOM	85	C8	ADE	B	3	28.774	-0.693	7.135	1.00	10.00	B	C
ATOM	86	H8	ADE	B	3	27.966	-0.900	7.822	1.00	10.00	B	H
ATOM	87	C2'	ADE	B	3	29.004	2.668	8.058	1.00	10.00	B	C
ATOM	88	H2'	ADE	B	3	29.024	2.894	6.989	1.00	10.00	B	H
ATOM	89	O2'	ADE	B	3	29.594	3.681	8.852	1.00	10.00	B	O
ATOM	90	HO2'	ADE	B	3	30.528	3.441	8.940	1.00	10.00	B	H
ATOM	91	C3'	ADE	B	3	27.593	2.348	8.517	1.00	10.00	B	C
ATOM	92	H3'	ADE	B	3	27.049	1.713	7.817	1.00	10.00	B	H
ATOM	93	O3'	ADE	B	3	26.806	3.517	8.696	1.00	10.00	B	O
HETATM	94	P	URI	B	4	25.943	4.089	7.471	1.00	10.00	B	P
HETATM	95	O1P	URI	B	4	25.202	5.264	7.984	1.00	10.00	B	O
HETATM	96	O2P	URI	B	4	25.202	2.972	6.838	1.00	10.00	B	O
HETATM	97	O5'	URI	B	4	27.036	4.599	6.435	1.00	10.00	B	O
HETATM	98	C5'	URI	B	4	27.972	5.604	6.800	1.00	10.00	B	C
HETATM	99	H5'	URI	B	4	28.550	5.272	7.663	1.00	10.00	B	H
HETATM	100	H5''	URI	B	4	27.443	6.522	7.059	1.00	10.00	B	H
HETATM	101	C4'	URI	B	4	28.907	5.884	5.649	1.00	10.00	B	C
HETATM	102	H4'	URI	B	4	29.453	6.799	5.873	1.00	10.00	B	H
HETATM	103	O4'	URI	B	4	29.767	4.725	5.433	1.00	10.00	B	O
HETATM	104	C1'	URI	B	4	30.017	4.567	4.041	1.00	10.00	B	C
HETATM	105	H1'	URI	B	4	31.100	4.514	3.915	1.00	10.00	B	H
HETATM	106	N1	URI	B	4	29.441	3.286	3.608	1.00	10.00	B	N
HETATM	107	C6	URI	B	4	28.404	2.702	4.302	1.00	10.00	B	C
HETATM	108	H6	URI	B	4	27.990	3.227	5.163	1.00	10.00	B	H
HETATM	109	C2	URI	B	4	29.980	2.675	2.488	1.00	10.00	B	C
HETATM	110	O2	URI	B	4	30.882	3.168	1.836	1.00	10.00	B	O
HETATM	111	N3	URI	B	4	29.421	1.465	2.159	1.00	10.00	B	N
HETATM	112	H3	URI	B	4	29.813	0.992	1.353	1.00	10.00	B	H
HETATM	113	C4	URI	B	4	28.396	0.819	2.817	1.00	10.00	B	C
HETATM	114	O4	URI	B	4	28.010	-0.279	2.409	1.00	10.00	B	O
HETATM	115	C5	URI	B	4	27.884	1.521	3.953	1.00	10.00	B	C
HETATM	116	H5	URI	B	4	27.070	1.092	4.537	1.00	10.00	B	H
HETATM	117	C2'	URI	B	4	29.419	5.797	3.364	1.00	10.00	B	C
HETATM	118	H2'	URI	B	4	29.070	5.577	2.352	1.00	10.00	B	H
HETATM	119	O2'	URI	B	4	30.372	6.843	3.408	1.00	10.00	B	O
HETATM	120	HO2'	URI	B	4	31.234	6.418	3.517	1.00	10.00	B	H
HETATM	121	C3'	URI	B	4	28.250	6.070	4.294	1.00	10.00	B	C
HETATM	122	H3'	URI	B	4	27.423	5.375	4.146	1.00	10.00	B	H
HETATM	123	O3'	URI	B	4	27.707	7.372	4.140	1.00	10.00	B	O

ATOM	124	P	CYT	B	5	26.297	7.555	3.404	1.00	10.00	B	P
ATOM	125	O1P	CYT	B	5	25.704	8.822	3.892	1.00	10.00	B	O
ATOM	126	O2P	CYT	B	5	25.535	6.289	3.540	1.00	10.00	B	O
ATOM	127	O5'	CYT	B	5	26.690	7.749	1.875	1.00	10.00	B	O
ATOM	128	C5'	CYT	B	5	27.689	8.692	1.498	1.00	10.00	B	C
ATOM	129	H5'	CYT	B	5	28.465	8.732	2.262	1.00	10.00	B	H
ATOM	130	H5''	CYT	B	5	27.243	9.681	1.391	1.00	10.00	B	H
ATOM	131	C4'	CYT	B	5	28.309	8.289	0.183	1.00	10.00	B	C
ATOM	132	H4'	CYT	B	5	28.925	9.118	-0.164	1.00	10.00	B	H
ATOM	133	O4'	CYT	B	5	29.052	7.048	0.365	1.00	10.00	B	O
ATOM	134	C1'	CYT	B	5	28.934	6.248	-0.804	1.00	10.00	B	C
ATOM	135	H1'	CYT	B	5	29.944	5.967	-1.106	1.00	10.00	B	H
ATOM	136	N1	CYT	B	5	28.200	5.024	-0.451	1.00	10.00	B	N
ATOM	137	C6	CYT	B	5	27.401	4.981	0.659	1.00	10.00	B	C
ATOM	138	H6	CYT	B	5	27.284	5.875	1.272	1.00	10.00	B	H
ATOM	139	C2	CYT	B	5	28.340	3.899	-1.263	1.00	10.00	B	C
ATOM	140	O2	CYT	B	5	29.058	3.973	-2.275	1.00	10.00	B	O
ATOM	141	N3	CYT	B	5	27.693	2.758	-0.930	1.00	10.00	B	N
ATOM	142	C4	CYT	B	5	26.928	2.719	0.164	1.00	10.00	B	C
ATOM	143	N4	CYT	B	5	26.319	1.569	0.463	1.00	10.00	B	N
ATOM	144	H41	CYT	B	5	25.735	1.503	1.286	1.00	10.00	B	H
ATOM	145	H42	CYT	B	5	26.447	0.757	-0.126	1.00	10.00	B	H
ATOM	146	C5	CYT	B	5	26.755	3.859	1.003	1.00	10.00	B	C
ATOM	147	H5	CYT	B	5	26.124	3.820	1.892	1.00	10.00	B	H
ATOM	148	C2'	CYT	B	5	28.237	7.120	-1.846	1.00	10.00	B	C
ATOM	149	H2'	CYT	B	5	27.644	6.528	-2.546	1.00	10.00	B	H
ATOM	150	O2'	CYT	B	5	29.215	7.921	-2.482	1.00	10.00	B	O
ATOM	151	HO2'	CYT	B	5	30.046	7.712	-2.046	1.00	10.00	B	H
ATOM	152	C3'	CYT	B	5	27.345	7.951	-0.940	1.00	10.00	B	C
ATOM	153	H3'	CYT	B	5	26.477	7.397	-0.578	1.00	10.00	B	H
ATOM	154	O3'	CYT	B	5	26.840	9.116	-1.577	1.00	10.00	B	O
ATOM	155	P	CYT	B	6	25.257	9.321	-1.705	1.00	10.00	B	P
ATOM	156	O1P	CYT	B	6	24.975	10.767	-1.534	1.00	10.00	B	O
ATOM	157	O2P	CYT	B	6	24.588	8.336	-0.824	1.00	10.00	B	O
ATOM	158	O5'	CYT	B	6	24.947	8.943	-3.218	1.00	10.00	B	O
ATOM	159	C5'	CYT	B	6	25.808	9.383	-4.261	1.00	10.00	B	C
ATOM	160	H5'	CYT	B	6	26.824	9.488	-3.878	1.00	10.00	B	H
ATOM	161	H5''	CYT	B	6	25.471	10.348	-4.640	1.00	10.00	B	H
ATOM	162	C4'	CYT	B	6	25.808	8.384	-5.390	1.00	10.00	B	C
ATOM	163	H4'	CYT	B	6	26.174	8.886	-6.287	1.00	10.00	B	H
ATOM	164	O4'	CYT	B	6	26.606	7.228	-5.001	1.00	10.00	B	O
ATOM	165	C1'	CYT	B	6	26.026	6.049	-5.542	1.00	10.00	B	C
ATOM	166	H1'	CYT	B	6	26.813	5.518	-6.079	1.00	10.00	B	H
ATOM	167	N1	CYT	B	6	25.560	5.194	-4.441	1.00	10.00	B	N
ATOM	168	C6	CYT	B	6	25.267	5.711	-3.206	1.00	10.00	B	C
ATOM	169	H6	CYT	B	6	25.376	6.782	-3.030	1.00	10.00	B	H
ATOM	170	C2	CYT	B	6	25.417	3.830	-4.681	1.00	10.00	B	C
ATOM	171	O2	CYT	B	6	25.686	3.371	-5.805	1.00	10.00	B	O
ATOM	172	N3	CYT	B	6	24.994	3.027	-3.692	1.00	10.00	B	N
ATOM	173	C4	CYT	B	6	24.713	3.523	-2.491	1.00	10.00	B	C
ATOM	174	N4	CYT	B	6	24.304	2.657	-1.548	1.00	10.00	B	N
ATOM	175	H41	CYT	B	6	24.083	2.988	-0.619	1.00	10.00	B	H
ATOM	176	H42	CYT	B	6	24.206	1.675	-1.762	1.00	10.00	B	H
ATOM	177	C5	CYT	B	6	24.842	4.917	-2.207	1.00	10.00	B	C
ATOM	178	H5	CYT	B	6	24.600	5.322	-1.222	1.00	10.00	B	H
ATOM	179	C2'	CYT	B	6	24.905	6.512	-6.465	1.00	10.00	B	C
ATOM	180	H2'	CYT	B	6	24.094	5.783	-6.521	1.00	10.00	B	H
ATOM	181	O2'	CYT	B	6	25.473	6.815	-7.724	1.00	10.00	B	O
ATOM	182	HO2'	CYT	B	6	26.425	6.684	-7.623	1.00	10.00	B	H
ATOM	183	C3'	CYT	B	6	24.462	7.769	-5.736	1.00	10.00	B	C
ATOM	184	H3'	CYT	B	6	23.877	7.550	-4.842	1.00	10.00	B	H
ATOM	185	O3'	CYT	B	6	23.654	8.622	-6.542	1.00	10.00	B	O
HETATM	186	P	URI	B	7	22.115	8.243	-6.799	1.00	10.00	B	P
HETATM	187	O1P	URI	B	7	21.578	9.215	-7.782	1.00	10.00	B	O
HETATM	188	O2P	URI	B	7	21.452	8.090	-5.481	1.00	10.00	B	O
HETATM	189	O5'	URI	B	7	22.170	6.812	-7.492	1.00	10.00	B	O
HETATM	190	C5'	URI	B	7	22.698	6.664	-8.805	1.00	10.00	B	C
HETATM	191	H5'	URI	B	7	23.780	6.792	-8.782	1.00	10.00	B	H
HETATM	192	H5''	URI	B	7	22.268	7.421	-9.460	1.00	10.00	B	H
HETATM	193	C4'	URI	B	7	22.368	5.294	-9.353	1.00	10.00	B	C
HETATM	194	H4'	URI	B	7	22.544	5.306	-10.428	1.00	10.00	B	H
HETATM	195	O4'	URI	B	7	23.149	4.288	-8.639	1.00	10.00	B	O
HETATM	196	C1'	URI	B	7	22.378	3.101	-8.488	1.00	10.00	B	C
HETATM	197	H1'	URI	B	7	22.980	2.281	-8.887	1.00	10.00	B	H
HETATM	198	N1	URI	B	7	22.162	2.854	-7.055	1.00	10.00	B	N
HETATM	199	C6	URI	B	7	22.178	3.878	-6.133	1.00	10.00	B	C
HETATM	200	H6	URI	B	7	22.336	4.899	-6.482	1.00	10.00	B	H
HETATM	201	C2	URI	B	7	21.949	1.544	-6.661	1.00	10.00	B	C
HETATM	202	O2	URI	B	7	21.912	0.617	-7.450	1.00	10.00	B	O
HETATM	203	N3	URI	B	7	21.778	1.363	-5.313	1.00	10.00	B	N
HETATM	204	H3	URI	B	7	21.620	0.409	-5.012	1.00	10.00	B	H
HETATM	205	C4	URI	B	7	21.793	2.335	-4.335	1.00	10.00	B	C
HETATM	206	O4	URI	B	7	21.641	2.011	-3.155	1.00	10.00	B	O
HETATM	207	C5	URI	B	7	22.006	3.664	-4.823	1.00	10.00	B	C
HETATM	208	H5	URI	B	7	22.027	4.503	-4.126	1.00	10.00	B	H
HETATM	209	C2'	URI	B	7	21.100	3.321	-9.292	1.00	10.00	B	C
HETATM	210	H2'	URI	B	7	20.249	2.790	-8.856	1.00	10.00	B	H
HETATM	211	O2'	URI	B	7	21.347	2.962	-10.641	1.00	10.00	B	O
HETATM	212	HO2'	URI	B	7	22.303	2.845	-10.723	1.00	10.00	B	H
HETATM	213	C3'	URI	B	7	20.942	4.823	-9.132	1.00	10.00	B	C
HETATM	214	H3'	URI	B	7	20.571	5.107	-8.147	1.00	10.00	B	H
HETATM	215	O3'	URI	B	7	20.041	5.383	-10.077	1.00	10.00	B	O
ATOM	216	P	CYT	B	8	18.508	5.612	-9.667	1.00	10.00	B	P
ATOM	217	O1P	CYT	B	8	17.892	6.437	-10.734	1.00	10.00	B	O
ATOM	218	O2P	CYT	B	8	18.454	6.075	-8.263	1.00	10.00	B	O

ATOM	219	O5'	CYT	B	8	17.878	4.153	-9.735	1.00	10.00	B	O
ATOM	220	C5'	CYT	B	8	18.135	3.313	-10.852	1.00	10.00	B	C
ATOM	221	H5'	CYT	B	8	19.210	3.267	-11.039	1.00	10.00	B	H
ATOM	222	H5''	CYT	B	8	17.639	3.715	-11.735	1.00	10.00	B	H
ATOM	223	C4'	CYT	B	8	17.616	1.920	-10.593	1.00	10.00	B	C
ATOM	224	H4'	CYT	B	8	17.485	1.420	-11.553	1.00	10.00	B	H
ATOM	225	O4'	CYT	B	8	18.527	1.225	-9.687	1.00	10.00	B	O
ATOM	226	C1'	CYT	B	8	17.782	0.378	-8.819	1.00	10.00	B	C
ATOM	227	H1'	CYT	B	8	18.213	-0.622	-8.901	1.00	10.00	B	H
ATOM	228	N1	CYT	B	8	17.945	0.833	-7.429	1.00	10.00	B	N
ATOM	229	C6	CYT	B	8	18.443	2.073	-7.134	1.00	10.00	B	C
ATOM	230	H6	CYT	B	8	18.710	2.754	-7.942	1.00	10.00	B	H
ATOM	231	C2	CYT	B	8	17.582	-0.039	-6.405	1.00	10.00	B	C
ATOM	232	O2	CYT	B	8	17.118	-1.154	-6.696	1.00	10.00	B	O
ATOM	233	N3	CYT	B	8	17.739	0.337	-5.118	1.00	10.00	B	N
ATOM	234	C4	CYT	B	8	18.239	1.541	-4.833	1.00	10.00	B	C
ATOM	235	N4	CYT	B	8	18.389	1.862	-3.543	1.00	10.00	B	N
ATOM	236	H41	CYT	B	8	18.769	2.771	-3.299	1.00	10.00	B	H
ATOM	237	H42	CYT	B	8	18.149	1.217	-2.803	1.00	10.00	B	H
ATOM	238	C5	CYT	B	8	18.607	2.466	-5.859	1.00	10.00	B	C
ATOM	239	H5	CYT	B	8	19.010	3.450	-5.618	1.00	10.00	B	H
ATOM	240	C2'	CYT	B	8	16.341	0.423	-9.318	1.00	10.00	B	C
ATOM	241	H2'	CYT	B	8	15.623	0.284	-8.505	1.00	10.00	B	H
ATOM	242	O2'	CYT	B	8	16.199	-0.530	-10.355	1.00	10.00	B	O
ATOM	243	HO2'	CYT	B	8	16.748	-1.283	-10.097	1.00	10.00	B	H
ATOM	244	C3'	CYT	B	8	16.290	1.841	-9.857	1.00	10.00	B	C
ATOM	245	H3'	CYT	B	8	16.220	2.590	-9.067	1.00	10.00	B	H
ATOM	246	O3'	CYT	B	8	15.179	2.060	-10.713	1.00	10.00	B	O
HETATM	247	P	URI	B	9	13.745	2.383	-10.074	1.00	10.00	B	P
HETATM	248	O1P	URI	B	9	12.797	2.538	-11.204	1.00	10.00	B	O
HETATM	249	O2P	URI	B	9	13.920	3.495	-9.106	1.00	10.00	B	O
HETATM	250	O5'	URI	B	9	13.365	1.061	-9.276	1.00	10.00	B	O
HETATM	251	C5'	URI	B	9	13.109	-0.156	-9.970	1.00	10.00	B	C
HETATM	252	H5'	URI	B	9	14.014	-0.481	-10.486	1.00	10.00	B	H
HETATM	253	H5''	URI	B	9	12.319	-0.002	-10.704	1.00	10.00	B	H
HETATM	254	C4'	URI	B	9	12.675	-1.228	-9.001	1.00	10.00	B	C
HETATM	255	H4'	URI	B	9	12.370	-2.100	-9.579	1.00	10.00	B	H
HETATM	256	O4'	URI	B	9	13.756	-1.497	-8.059	1.00	10.00	B	O
HETATM	257	C1'	URI	B	9	13.211	-1.782	-6.776	1.00	10.00	B	C
HETATM	258	H1'	URI	B	9	13.638	-2.734	-6.453	1.00	10.00	B	H
HETATM	259	N1	URI	B	9	13.652	-0.742	-5.836	1.00	10.00	B	N
HETATM	260	C6	URI	B	9	13.981	0.526	-6.264	1.00	10.00	B	C
HETATM	261	H6	URI	B	9	13.883	0.764	-7.323	1.00	10.00	B	H
HETATM	262	C2	URI	B	9	13.738	-1.083	-4.499	1.00	10.00	B	C
HETATM	263	O2	URI	B	9	13.441	-2.187	-4.079	1.00	10.00	B	O
HETATM	264	N3	URI	B	9	14.181	-0.084	-3.670	1.00	10.00	B	N
HETATM	265	H3	URI	B	9	14.257	-0.324	-2.689	1.00	10.00	B	H
HETATM	266	C4	URI	B	9	14.540	1.195	-4.026	1.00	10.00	B	C
HETATM	267	O4	URI	B	9	14.939	1.977	-3.159	1.00	10.00	B	O
HETATM	268	C5	URI	B	9	14.414	1.477	-5.425	1.00	10.00	B	C
HETATM	269	H5	URI	B	9	14.668	2.466	-5.807	1.00	10.00	B	H
HETATM	270	C2'	URI	B	9	11.698	-1.866	-6.968	1.00	10.00	B	C
HETATM	271	H2'	URI	B	9	11.157	-1.552	-6.072	1.00	10.00	B	H
HETATM	272	O2'	URI	B	9	11.354	-3.171	-7.395	1.00	10.00	B	O
HETATM	273	HO2'	URI	B	9	12.186	-3.628	-7.574	1.00	10.00	B	H
HETATM	274	C3'	URI	B	9	11.514	-0.861	-8.092	1.00	10.00	B	C
HETATM	275	H3'	URI	B	9	11.572	0.172	-7.751	1.00	10.00	B	H
HETATM	276	O3'	URI	B	9	10.261	-1.001	-8.749	1.00	10.00	B	O
ATOM	277	P	ADE	B	10	9.050	-0.026	-8.357	1.00	10.00	B	P
ATOM	278	O1P	ADE	B	10	7.985	-0.194	-9.375	1.00	10.00	B	O
ATOM	279	O2P	ADE	B	10	9.597	1.325	-8.089	1.00	10.00	B	O
ATOM	280	O5'	ADE	B	10	8.497	-0.627	-6.993	1.00	10.00	B	O
ATOM	281	C5'	ADE	B	10	7.564	-1.702	-7.004	1.00	10.00	B	C
ATOM	282	H5'	ADE	B	10	7.856	-2.435	-7.757	1.00	10.00	B	H
ATOM	283	H5''	ADE	B	10	6.571	-1.325	-7.242	1.00	10.00	B	H
ATOM	284	C4'	ADE	B	10	7.523	-2.369	-5.651	1.00	10.00	B	C
ATOM	285	H4'	ADE	B	10	6.942	-3.285	-5.747	1.00	10.00	B	H
ATOM	286	O4'	ADE	B	10	8.887	-2.589	-5.182	1.00	10.00	B	O
ATOM	287	C1'	ADE	B	10	8.936	-2.413	-3.772	1.00	10.00	B	C
ATOM	288	H1'	ADE	B	10	9.413	-3.299	-3.351	1.00	10.00	B	H
ATOM	289	N9	ADE	B	10	9.769	-1.252	-3.468	1.00	10.00	B	N
ATOM	290	C4	ADE	B	10	10.306	-0.947	-2.240	1.00	10.00	B	C
ATOM	291	N3	ADE	B	10	10.169	-1.640	-1.096	1.00	10.00	B	N
ATOM	292	C2	ADE	B	10	10.829	-1.042	-0.105	1.00	10.00	B	C
ATOM	293	H2	ADE	B	10	10.764	-1.536	0.866	1.00	10.00	B	H
ATOM	294	N1	ADE	B	10	11.556	0.082	-0.131	1.00	10.00	B	N
ATOM	295	C6	ADE	B	10	11.677	0.750	-1.297	1.00	10.00	B	C
ATOM	296	N6	ADE	B	10	12.413	1.861	-1.325	1.00	10.00	B	N
ATOM	297	H61	ADE	B	10	12.516	2.366	-2.193	1.00	10.00	B	H
ATOM	298	H62	ADE	B	10	12.865	2.195	-0.483	1.00	10.00	B	H
ATOM	299	C5	ADE	B	10	11.018	0.223	-2.421	1.00	10.00	B	C
ATOM	300	N7	ADE	B	10	10.930	0.654	-3.737	1.00	10.00	B	N
ATOM	301	C8	ADE	B	10	10.179	-0.253	-4.315	1.00	10.00	B	C
ATOM	302	H8	ADE	B	10	9.903	-0.213	-5.360	1.00	10.00	B	H
ATOM	303	C2'	ADE	B	10	7.491	-2.255	-3.312	1.00	10.00	B	C
ATOM	304	H2'	ADE	B	10	7.411	-1.627	-2.421	1.00	10.00	B	H
ATOM	305	O2'	ADE	B	10	6.937	-3.547	-3.135	1.00	10.00	B	O
ATOM	306	HO2'	ADE	B	10	7.455	-4.136	-3.690	1.00	10.00	B	H
ATOM	307	C3'	ADE	B	10	6.904	-1.560	-4.526	1.00	10.00	B	C
ATOM	308	H3'	ADE	B	10	7.187	-0.508	-4.583	1.00	10.00	B	H
ATOM	309	O3'	ADE	B	10	5.484	-1.586	-4.552	1.00	10.00	B	O
ATOM	310	P	CYT	B	11	4.667	-0.284	-4.091	1.00	10.00	B	P
ATOM	311	O1P	CYT	B	11	3.664	0.020	-5.141	1.00	10.00	B	O
ATOM	312	O2P	CYT	B	11	5.657	0.749	-3.706	1.00	10.00	B	O
ATOM	313	O5'	CYT	B	11	3.905	-0.757	-2.779	1.00	10.00	B	O

ATOM	314	C5'	CYT	B	11	4.397	-1.844	-2.004	1.00	10.00	B	C
ATOM	315	H5'	CYT	B	11	5.398	-2.113	-2.345	1.00	10.00	B	H
ATOM	316	H5''	CYT	B	11	3.739	-2.704	-2.118	1.00	10.00	B	H
ATOM	317	C4'	CYT	B	11	4.453	-1.460	-0.544	1.00	10.00	B	C
ATOM	318	H4'	CYT	B	11	3.826	-2.160	0.008	1.00	10.00	B	H
ATOM	319	O4'	CYT	B	11	5.841	-1.445	-0.097	1.00	10.00	B	O
ATOM	320	C1'	CYT	B	11	6.025	-0.398	0.847	1.00	10.00	B	C
ATOM	321	H1'	CYT	B	11	6.494	-0.839	1.729	1.00	10.00	B	H
ATOM	322	N1	CYT	B	11	6.955	0.587	0.276	1.00	10.00	B	N
ATOM	323	C6	CYT	B	11	7.076	0.737	-1.078	1.00	10.00	B	C
ATOM	324	H6	CYT	B	11	6.456	0.135	-1.743	1.00	10.00	B	H
ATOM	325	C2	CYT	B	11	7.723	1.365	1.140	1.00	10.00	B	C
ATOM	326	O2	CYT	B	11	7.579	1.224	2.368	1.00	10.00	B	O
ATOM	327	N3	CYT	B	11	8.601	2.256	0.625	1.00	10.00	B	N
ATOM	328	C4	CYT	B	11	8.725	2.386	-0.696	1.00	10.00	B	C
ATOM	329	N4	CYT	B	11	9.619	3.267	-1.155	1.00	10.00	B	N
ATOM	330	H41	CYT	B	11	9.738	3.384	-2.149	1.00	10.00	B	H
ATOM	331	H42	CYT	B	11	10.181	3.812	-0.511	1.00	10.00	B	H
ATOM	332	C5	CYT	B	11	7.941	1.615	-1.604	1.00	10.00	B	C
ATOM	333	H5	CYT	B	11	8.041	1.735	-2.682	1.00	10.00	B	H
ATOM	334	C2'	CYT	B	11	4.634	0.152	1.148	1.00	10.00	B	C
ATOM	335	H2'	CYT	B	11	4.660	1.210	1.409	1.00	10.00	B	H
ATOM	336	O2'	CYT	B	11	4.053	-0.657	2.155	1.00	10.00	B	O
ATOM	337	HO2'	CYT	B	11	4.213	-1.563	1.885	1.00	10.00	B	H
ATOM	338	C3'	CYT	B	11	3.965	-0.065	-0.199	1.00	10.00	B	C
ATOM	339	H3'	CYT	B	11	4.275	0.667	-0.947	1.00	10.00	B	H
ATOM	340	O3'	CYT	B	11	2.548	0.012	-0.133	1.00	10.00	B	O
ATOM	341	P	ADE	B	12	1.809	1.329	-0.671	1.00	10.00	B	P
ATOM	342	O1P	ADE	B	12	0.629	0.913	-1.468	1.00	10.00	B	O
ATOM	343	O2P	ADE	B	12	2.841	2.193	-1.288	1.00	10.00	B	O
ATOM	344	O5'	ADE	B	12	1.299	2.053	0.650	1.00	10.00	B	O
ATOM	345	C5'	ADE	B	12	1.185	1.336	1.874	1.00	10.00	B	C
ATOM	346	H5'	ADE	B	12	1.856	0.476	1.859	1.00	10.00	B	H
ATOM	347	H5''	ADE	B	12	0.162	0.986	2.002	1.00	10.00	B	H
ATOM	348	C4'	ADE	B	12	1.548	2.229	3.035	1.00	10.00	B	C
ATOM	349	H4'	ADE	B	12	0.952	1.919	3.893	1.00	10.00	B	H
ATOM	350	O4'	ADE	B	12	2.987	2.160	3.269	1.00	10.00	B	O
ATOM	351	C1'	ADE	B	12	3.465	3.436	3.678	1.00	10.00	B	C
ATOM	352	H1'	ADE	B	12	4.031	3.287	4.599	1.00	10.00	B	H
ATOM	353	N9	ADE	B	12	4.378	3.939	2.652	1.00	10.00	B	N
ATOM	354	C4	ADE	B	12	5.339	4.911	2.815	1.00	10.00	B	C
ATOM	355	N3	ADE	B	12	5.624	5.601	3.933	1.00	10.00	B	N
ATOM	356	C2	ADE	B	12	6.623	6.460	3.714	1.00	10.00	B	C
ATOM	357	H2	ADE	B	12	6.913	7.070	4.572	1.00	10.00	B	H
ATOM	358	N1	ADE	B	12	7.317	6.683	2.590	1.00	10.00	B	N
ATOM	359	C6	ADE	B	12	7.006	5.969	1.486	1.00	10.00	B	C
ATOM	360	N6	ADE	B	12	7.702	6.183	0.368	1.00	10.00	B	N
ATOM	361	H61	ADE	B	12	7.472	5.650	-0.458	1.00	10.00	B	H
ATOM	362	H62	ADE	B	12	8.452	6.862	0.338	1.00	10.00	B	H
ATOM	363	C5	ADE	B	12	5.962	5.033	1.585	1.00	10.00	B	C
ATOM	364	N7	ADE	B	12	5.401	4.163	0.660	1.00	10.00	B	N
ATOM	365	C8	ADE	B	12	4.466	3.543	1.339	1.00	10.00	B	C
ATOM	366	H8	ADE	B	12	3.820	2.790	0.906	1.00	10.00	B	H
ATOM	367	C2'	ADE	B	12	2.227	4.302	3.895	1.00	10.00	B	C
ATOM	368	H2'	ADE	B	12	2.427	5.358	3.701	1.00	10.00	B	H
ATOM	369	O2'	ADE	B	12	1.741	4.056	5.201	1.00	10.00	B	O
ATOM	370	HO2'	ADE	B	12	2.022	3.167	5.417	1.00	10.00	B	H
ATOM	371	C3'	ADE	B	12	1.306	3.717	2.839	1.00	10.00	B	C
ATOM	372	H3'	ADE	B	12	1.565	4.038	1.830	1.00	10.00	B	H
ATOM	373	O3'	ADE	B	12	-0.057	4.077	3.034	1.00	10.00	B	O
ATOM	374	P	GUA	B	13	-0.677	5.303	2.202	1.00	10.00	B	P
ATOM	375	O1P	GUA	B	13	-2.135	5.087	2.069	1.00	10.00	B	O
ATOM	376	O2P	GUA	B	13	0.136	5.544	0.987	1.00	10.00	B	O
ATOM	377	O5'	GUA	B	13	-0.485	6.545	3.175	1.00	10.00	B	O
ATOM	378	C5'	GUA	B	13	-0.390	6.351	4.580	1.00	10.00	B	C
ATOM	379	H5'	GUA	B	13	0.121	5.410	4.787	1.00	10.00	B	H
ATOM	380	H5''	GUA	B	13	-1.386	6.317	5.018	1.00	10.00	B	H
ATOM	381	C4'	GUA	B	13	0.385	7.483	5.206	1.00	10.00	B	C
ATOM	382	H4'	GUA	B	13	0.044	7.598	6.234	1.00	10.00	B	H
ATOM	383	O4'	GUA	B	13	1.813	7.214	5.088	1.00	10.00	B	O
ATOM	384	C1'	GUA	B	13	2.510	8.433	4.877	1.00	10.00	B	C
ATOM	385	H1'	GUA	B	13	3.291	8.489	5.638	1.00	10.00	B	H
ATOM	386	N9	GUA	B	13	3.156	8.382	3.570	1.00	10.00	B	N
ATOM	387	C4	GUA	B	13	4.219	9.152	3.162	1.00	10.00	B	C
ATOM	388	N3	GUA	B	13	4.839	10.101	3.895	1.00	10.00	B	N
ATOM	389	C2	GUA	B	13	5.834	10.667	3.231	1.00	10.00	B	C
ATOM	390	N2	GUA	B	13	6.545	11.641	3.812	1.00	10.00	B	N
ATOM	391	H21	GUA	B	13	6.321	11.940	4.750	1.00	10.00	B	H
ATOM	392	H22	GUA	B	13	7.307	12.089	3.313	1.00	10.00	B	H
ATOM	393	N1	GUA	B	13	6.199	10.322	1.951	1.00	10.00	B	N
ATOM	394	H1	GUA	B	13	6.983	10.795	1.519	1.00	10.00	B	H
ATOM	395	C6	GUA	B	13	5.574	9.352	1.176	1.00	10.00	B	C
ATOM	396	O6	GUA	B	13	5.979	9.127	0.027	1.00	10.00	B	O
ATOM	397	C5	GUA	B	13	4.499	8.738	1.875	1.00	10.00	B	C
ATOM	398	N7	GUA	B	13	3.623	7.736	1.479	1.00	10.00	B	N
ATOM	399	C8	GUA	B	13	2.845	7.561	2.513	1.00	10.00	B	C
ATOM	400	H8	GUA	B	13	2.040	6.841	2.536	1.00	10.00	B	H
ATOM	401	C2'	GUA	B	13	1.477	9.545	5.036	1.00	10.00	B	C
ATOM	402	H2'	GUA	B	13	1.713	10.412	4.415	1.00	10.00	B	H
ATOM	403	O2'	GUA	B	13	1.366	9.861	6.412	1.00	10.00	B	O
ATOM	404	HO2'	GUA	B	13	2.124	9.460	6.842	1.00	10.00	B	H
ATOM	405	C3'	GUA	B	13	0.235	8.833	4.529	1.00	10.00	B	C
ATOM	406	H3'	GUA	B	13	0.209	8.746	3.443	1.00	10.00	B	H
ATOM	407	O3'	GUA	B	13	-0.973	9.482	4.910	1.00	10.00	B	O
ATOM	408	P	GUA	B	14	-1.882	10.189	3.792	1.00	10.00	B	P

ATOM	409	O1P	GUA	B	14	-3.274	10.172	4.305	1.00	10.00	B	O
ATOM	410	O2P	GUA	B	14	-1.581	9.571	2.479	1.00	10.00	B	O
ATOM	411	O5'	GUA	B	14	-1.368	11.694	3.775	1.00	10.00	B	O
ATOM	412	C5'	GUA	B	14	-1.160	12.402	4.991	1.00	10.00	B	C
ATOM	413	H5'	GUA	B	14	-0.989	11.693	5.803	1.00	10.00	B	H
ATOM	414	H5''	GUA	B	14	-2.037	13.002	5.224	1.00	10.00	B	H
ATOM	415	C4'	GUA	B	14	0.038	13.311	4.865	1.00	10.00	B	C
ATOM	416	H4'	GUA	B	14	0.089	13.932	5.759	1.00	10.00	B	H
ATOM	417	O4'	GUA	B	14	1.235	12.508	4.636	1.00	10.00	B	O
ATOM	418	C1'	GUA	B	14	2.109	13.203	3.759	1.00	10.00	B	C
ATOM	419	H1'	GUA	B	14	3.084	13.255	4.251	1.00	10.00	B	H
ATOM	420	N9	GUA	B	14	2.263	12.438	2.526	1.00	10.00	B	N
ATOM	421	C4	GUA	B	14	3.148	12.714	1.514	1.00	10.00	B	C
ATOM	422	N3	GUA	B	14	4.018	13.747	1.485	1.00	10.00	B	N
ATOM	423	C2	GUA	B	14	4.740	13.753	0.375	1.00	10.00	B	C
ATOM	424	N2	GUA	B	14	5.645	14.720	0.182	1.00	10.00	B	N
ATOM	425	H21	GUA	B	14	5.777	15.439	0.878	1.00	10.00	B	H
ATOM	426	H22	GUA	B	14	6.171	14.769	-0.683	1.00	10.00	B	H
ATOM	427	N1	GUA	B	14	4.625	12.816	-0.623	1.00	10.00	B	N
ATOM	428	H1	GUA	B	14	5.225	12.899	-1.438	1.00	10.00	B	H
ATOM	429	C6	GUA	B	14	3.740	11.742	-0.616	1.00	10.00	B	C
ATOM	430	O6	GUA	B	14	3.723	10.952	-1.575	1.00	10.00	B	O
ATOM	431	C5	GUA	B	14	2.948	11.727	0.570	1.00	10.00	B	C
ATOM	432	N7	GUA	B	14	1.953	10.850	0.981	1.00	10.00	B	N
ATOM	433	C8	GUA	B	14	1.575	11.313	2.142	1.00	10.00	B	C
ATOM	434	H8	GUA	B	14	0.795	10.861	2.736	1.00	10.00	B	H
ATOM	435	C2'	GUA	B	14	1.498	14.585	3.548	1.00	10.00	B	C
ATOM	436	H2'	GUA	B	14	1.726	14.986	2.558	1.00	10.00	B	H
ATOM	437	O2'	GUA	B	14	1.918	15.432	4.601	1.00	10.00	B	O
ATOM	438	HO2'	GUA	B	14	2.073	14.864	5.370	1.00	10.00	B	H
ATOM	439	C3'	GUA	B	14	0.025	14.243	3.665	1.00	10.00	B	C
ATOM	440	H3'	GUA	B	14	-0.367	13.750	2.775	1.00	10.00	B	H
ATOM	441	O3'	GUA	B	14	-0.781	15.396	3.870	1.00	10.00	B	O
ATOM	442	P	CYT	B	15	-1.099	16.365	2.631	1.00	10.00	B	P
ATOM	443	O1P	CYT	B	15	-2.111	17.349	3.079	1.00	10.00	B	O
ATOM	444	O2P	CYT	B	15	-1.380	15.520	1.450	1.00	10.00	B	O
ATOM	445	O5'	CYT	B	15	0.265	17.138	2.366	1.00	10.00	B	O
ATOM	446	C5'	CYT	B	15	0.327	18.555	2.479	1.00	10.00	B	C
ATOM	447	H5'	CYT	B	15	0.816	18.828	3.415	1.00	10.00	B	H
ATOM	448	H5''	CYT	B	15	-0.680	18.969	2.473	1.00	10.00	B	H
ATOM	449	C4'	CYT	B	15	1.105	19.137	1.323	1.00	10.00	B	C
ATOM	450	H4'	CYT	B	15	1.407	20.147	1.598	1.00	10.00	B	H
ATOM	451	O4'	CYT	B	15	2.226	18.259	1.002	1.00	10.00	B	O
ATOM	452	C1'	CYT	B	15	2.442	18.262	-0.405	1.00	10.00	B	C
ATOM	453	H1'	CYT	B	15	3.495	18.496	-0.568	1.00	10.00	B	H
ATOM	454	N1	CYT	B	15	2.187	16.913	-0.931	1.00	10.00	B	N
ATOM	455	C6	CYT	B	15	1.588	15.952	-0.165	1.00	10.00	B	C
ATOM	456	H6	CYT	B	15	1.280	16.189	0.852	1.00	10.00	B	H
ATOM	457	C2	CYT	B	15	2.574	16.631	-2.238	1.00	10.00	B	C
ATOM	458	O2	CYT	B	15	3.109	17.526	-2.904	1.00	10.00	B	O
ATOM	459	N3	CYT	B	15	2.357	15.397	-2.747	1.00	10.00	B	N
ATOM	460	C4	CYT	B	15	1.775	14.460	-1.994	1.00	10.00	B	C
ATOM	461	N4	CYT	B	15	1.579	13.254	-2.536	1.00	10.00	B	N
ATOM	462	H41	CYT	B	15	1.143	12.515	-2.004	1.00	10.00	B	H
ATOM	463	H42	CYT	B	15	1.885	13.062	-3.486	1.00	10.00	B	H
ATOM	464	C5	CYT	B	15	1.367	14.719	-0.650	1.00	10.00	B	C
ATOM	465	H5	CYT	B	15	0.897	13.947	-0.040	1.00	10.00	B	H
ATOM	466	C2'	CYT	B	15	1.519	19.332	-0.977	1.00	10.00	B	C
ATOM	467	H2'	CYT	B	15	1.193	19.088	-1.990	1.00	10.00	B	H
ATOM	468	O2'	CYT	B	15	2.171	20.586	-0.891	1.00	10.00	B	O
ATOM	469	HO2'	CYT	B	15	3.110	20.395	-0.750	1.00	10.00	B	H
ATOM	470	C3'	CYT	B	15	0.361	19.238	0.002	1.00	10.00	B	C
ATOM	471	H3'	CYT	B	15	-0.272	18.369	-0.176	1.00	10.00	B	H
ATOM	472	O3'	CYT	B	15	-0.491	20.375	-0.057	1.00	10.00	B	O
ATOM	473	P	GUA	B	16	-1.634	20.452	-1.182	1.00	10.00	B	P
ATOM	474	O1P	GUA	B	16	-2.242	21.802	-1.113	1.00	10.00	B	O
ATOM	475	O2P	GUA	B	16	-2.499	19.256	-1.050	1.00	10.00	B	O
ATOM	476	O5'	GUA	B	16	-0.843	20.344	-2.558	1.00	10.00	B	O
ATOM	477	C5'	GUA	B	16	-0.098	21.452	-3.053	1.00	10.00	B	C
ATOM	478	H5'	GUA	B	16	0.618	21.781	-2.299	1.00	10.00	B	H
ATOM	479	H5''	GUA	B	16	-0.774	22.277	-3.280	1.00	10.00	B	H
ATOM	480	C4'	GUA	B	16	0.647	21.071	-4.312	1.00	10.00	B	C
ATOM	481	H4'	GUA	B	16	1.313	21.891	-4.572	1.00	10.00	B	H
ATOM	482	O4'	GUA	B	16	1.332	19.797	-4.110	1.00	10.00	B	O
ATOM	483	C1'	GUA	B	16	1.315	19.047	-5.320	1.00	10.00	B	C
ATOM	484	H1'	GUA	B	16	2.351	18.780	-5.541	1.00	10.00	B	H
ATOM	485	N9	GUA	B	16	0.566	17.815	-5.102	1.00	10.00	B	N
ATOM	486	C4	GUA	B	16	0.575	16.705	-5.913	1.00	10.00	B	C
ATOM	487	N3	GUA	B	16	1.264	16.572	-7.067	1.00	10.00	B	N
ATOM	488	C2	GUA	B	16	1.082	15.383	-7.618	1.00	10.00	B	C
ATOM	489	N2	GUA	B	16	1.695	15.090	-8.774	1.00	10.00	B	N
ATOM	490	H21	GUA	B	16	2.297	15.769	-9.228	1.00	10.00	B	H
ATOM	491	H22	GUA	B	16	1.566	14.185	-9.211	1.00	10.00	B	H
ATOM	492	N1	GUA	B	16	0.286	14.401	-7.083	1.00	10.00	B	N
ATOM	493	H1	GUA	B	16	0.218	13.522	-7.580	1.00	10.00	B	H
ATOM	494	C6	GUA	B	16	-0.437	14.513	-5.900	1.00	10.00	B	C
ATOM	495	O6	GUA	B	16	-1.128	13.559	-5.509	1.00	10.00	B	O
ATOM	496	C5	GUA	B	16	-0.251	15.790	-5.292	1.00	10.00	B	C
ATOM	497	N7	GUA	B	16	-0.778	16.319	-4.121	1.00	10.00	B	N
ATOM	498	C8	GUA	B	16	-0.267	17.518	-4.051	1.00	10.00	B	C
ATOM	499	H8	GUA	B	16	-0.476	18.210	-3.245	1.00	10.00	B	H
ATOM	500	C2'	GUA	B	16	0.725	19.969	-6.383	1.00	10.00	B	C
ATOM	501	H2'	GUA	B	16	0.175	19.412	-7.144	1.00	10.00	B	H
ATOM	502	O2'	GUA	B	16	1.761	20.770	-6.922	1.00	10.00	B	O
ATOM	503	HO2'	GUA	B	16	2.583	20.300	-6.758	1.00	10.00	B	H

ATOM	504	C3'	GUA	B	16	-0.222	20.794	-5.528	1.00	10.00	B	C
ATOM	505	H3'	GUA	B	16	-1.135	20.257	-5.265	1.00	10.00	B	H
ATOM	506	O3'	GUA	B	16	-0.631	21.997	-6.167	1.00	10.00	B	O
ATOM	507	P	CYT	B	17	4.226	6.504	-9.080	1.00	10.00	B	P
ATOM	508	O1P	CYT	B	17	5.434	5.777	-9.552	1.00	10.00	B	O
ATOM	509	O2P	CYT	B	17	4.363	7.542	-8.031	1.00	10.00	B	O
ATOM	510	O5'	CYT	B	17	3.543	7.175	-10.351	1.00	10.00	B	O
ATOM	511	C5'	CYT	B	17	4.274	7.346	-11.560	1.00	10.00	B	C
ATOM	512	H5'	CYT	B	17	3.796	6.785	-12.365	1.00	10.00	B	H
ATOM	513	H5''	CYT	B	17	5.292	6.979	-11.430	1.00	10.00	B	H
ATOM	514	C4'	CYT	B	17	4.323	8.809	-11.935	1.00	10.00	B	C
ATOM	515	H4'	CYT	B	17	4.775	8.884	-12.924	1.00	10.00	B	H
ATOM	516	O4'	CYT	B	17	2.981	9.377	-11.862	1.00	10.00	B	O
ATOM	517	C1'	CYT	B	17	3.055	10.720	-11.398	1.00	10.00	B	C
ATOM	518	H1'	CYT	B	17	2.515	11.335	-12.120	1.00	10.00	B	H
ATOM	519	N1	CYT	B	17	2.354	10.815	-10.107	1.00	10.00	B	N
ATOM	520	C6	CYT	B	17	2.503	9.852	-9.146	1.00	10.00	B	C
ATOM	521	H6	CYT	B	17	3.177	9.013	-9.325	1.00	10.00	B	H
ATOM	522	C2	CYT	B	17	1.517	11.906	-9.883	1.00	10.00	B	C
ATOM	523	O2	CYT	B	17	1.422	12.778	-10.759	1.00	10.00	B	O
ATOM	524	N3	CYT	B	17	0.834	11.992	-8.717	1.00	10.00	B	N
ATOM	525	C4	CYT	B	17	0.974	11.041	-7.789	1.00	10.00	B	C
ATOM	526	N4	CYT	B	17	0.270	11.162	-6.657	1.00	10.00	B	N
ATOM	527	H41	CYT	B	17	0.346	10.463	-5.930	1.00	10.00	B	H
ATOM	528	H42	CYT	B	17	-0.345	11.950	-6.503	1.00	10.00	B	H
ATOM	529	C5	CYT	B	17	1.838	9.923	-7.983	1.00	10.00	B	C
ATOM	530	H5	CYT	B	17	1.956	9.157	-7.216	1.00	10.00	B	H
ATOM	531	C2'	CYT	B	17	4.538	11.069	-11.347	1.00	10.00	B	C
ATOM	532	H2'	CYT	B	17	4.761	11.798	-10.566	1.00	10.00	B	H
ATOM	533	O2'	CYT	B	17	4.934	11.496	-12.637	1.00	10.00	B	O
ATOM	534	HO2'	CYT	B	17	4.562	10.856	-13.250	1.00	10.00	B	H
ATOM	535	C3'	CYT	B	17	5.124	9.709	-11.009	1.00	10.00	B	C
ATOM	536	H3'	CYT	B	17	4.987	9.439	-9.962	1.00	10.00	B	H
ATOM	537	O3'	CYT	B	17	6.520	9.647	-11.259	1.00	10.00	B	O
ATOM	538	P	GUA	B	18	7.546	9.694	-10.025	1.00	10.00	B	P
ATOM	539	O1P	GUA	B	18	8.413	8.494	-10.117	1.00	10.00	B	O
ATOM	540	O2P	GUA	B	18	6.772	9.948	-8.787	1.00	10.00	B	O
ATOM	541	O5'	GUA	B	18	8.448	10.972	-10.312	1.00	10.00	B	O
ATOM	542	C5'	GUA	B	18	8.058	11.939	-11.280	1.00	10.00	B	C
ATOM	543	H5'	GUA	B	18	7.074	11.686	-11.676	1.00	10.00	B	H
ATOM	544	H5''	GUA	B	18	8.777	11.953	-12.100	1.00	10.00	B	H
ATOM	545	C4'	GUA	B	18	8.005	13.311	-10.652	1.00	10.00	B	C
ATOM	546	H4'	GUA	B	18	8.583	13.990	-11.279	1.00	10.00	B	H
ATOM	547	O4'	GUA	B	18	6.613	13.715	-10.481	1.00	10.00	B	O
ATOM	548	C1'	GUA	B	18	6.480	14.468	-9.281	1.00	10.00	B	C
ATOM	549	H1'	GUA	B	18	5.984	15.405	-9.544	1.00	10.00	B	H
ATOM	550	N9	GUA	B	18	5.613	13.735	-8.364	1.00	10.00	B	N
ATOM	551	C4	GUA	B	18	4.948	14.254	-7.278	1.00	10.00	B	C
ATOM	552	N3	GUA	B	18	4.992	15.536	-6.859	1.00	10.00	B	N
ATOM	553	C2	GUA	B	18	4.246	15.730	-5.784	1.00	10.00	B	C
ATOM	554	N2	GUA	B	18	4.192	16.948	-5.235	1.00	10.00	B	N
ATOM	555	H21	GUA	B	18	4.712	17.721	-5.629	1.00	10.00	B	H
ATOM	556	H22	GUA	B	18	3.650	17.104	-4.390	1.00	10.00	B	H
ATOM	557	N1	GUA	B	18	3.507	14.748	-5.173	1.00	10.00	B	N
ATOM	558	H1	GUA	B	18	2.962	14.993	-4.352	1.00	10.00	B	H
ATOM	559	C6	GUA	B	18	3.441	13.422	-5.591	1.00	10.00	B	C
ATOM	560	O6	GUA	B	18	2.734	12.616	-4.974	1.00	10.00	B	O
ATOM	561	C5	GUA	B	18	4.245	13.196	-6.739	1.00	10.00	B	C
ATOM	562	N7	GUA	B	18	4.471	12.035	-7.465	1.00	10.00	B	N
ATOM	563	C8	GUA	B	18	5.290	12.402	-8.412	1.00	10.00	B	C
ATOM	564	H8	GUA	B	18	5.686	11.722	-9.154	1.00	10.00	B	H
ATOM	565	C2'	GUA	B	18	7.895	14.696	-8.763	1.00	10.00	B	C
ATOM	566	H2'	GUA	B	18	7.924	14.766	-7.673	1.00	10.00	B	H
ATOM	567	O2'	GUA	B	18	8.434	15.833	-9.410	1.00	10.00	B	O
ATOM	568	HO2'	GUA	B	18	7.744	16.167	-9.995	1.00	10.00	B	H
ATOM	569	C3'	GUA	B	18	8.563	13.421	-9.243	1.00	10.00	B	C
ATOM	570	H3'	GUA	B	18	8.306	12.552	-8.636	1.00	10.00	B	H
ATOM	571	O3'	GUA	B	18	9.983	13.512	-9.230	1.00	10.00	B	O
ATOM	572	P	CYT	B	19	10.787	13.165	-7.885	1.00	10.00	B	P
ATOM	573	O1P	CYT	B	19	12.194	13.581	-8.092	1.00	10.00	B	O
ATOM	574	O2P	CYT	B	19	10.489	11.770	-7.484	1.00	10.00	B	O
ATOM	575	O5'	CYT	B	19	10.161	14.141	-6.797	1.00	10.00	B	O
ATOM	576	C5'	CYT	B	19	10.816	15.360	-6.467	1.00	10.00	B	C
ATOM	577	H5'	CYT	B	19	10.929	15.970	-7.364	1.00	10.00	B	H
ATOM	578	H5''	CYT	B	19	11.804	15.147	-6.060	1.00	10.00	B	H
ATOM	579	C4'	CYT	B	19	10.018	16.127	-5.443	1.00	10.00	B	C
ATOM	580	H4'	CYT	B	19	10.327	17.172	-5.487	1.00	10.00	B	H
ATOM	581	O4'	CYT	B	19	8.593	15.926	-5.686	1.00	10.00	B	O
ATOM	582	C1'	CYT	B	19	7.899	15.884	-4.444	1.00	10.00	B	C
ATOM	583	H1'	CYT	B	19	7.096	16.621	-4.502	1.00	10.00	B	H
ATOM	584	N1	CYT	B	19	7.290	14.555	-4.279	1.00	10.00	B	N
ATOM	585	C6	CYT	B	19	7.509	13.554	-5.186	1.00	10.00	B	C
ATOM	586	H6	CYT	B	19	8.152	13.739	-6.046	1.00	10.00	B	H
ATOM	587	C2	CYT	B	19	6.473	14.333	-3.171	1.00	10.00	B	C
ATOM	588	O2	CYT	B	19	6.297	15.256	-2.366	1.00	10.00	B	O
ATOM	589	N3	CYT	B	19	5.896	13.121	-3.001	1.00	10.00	B	N
ATOM	590	C4	CYT	B	19	6.109	12.150	-3.893	1.00	10.00	B	C
ATOM	591	N4	CYT	B	19	5.509	10.973	-3.690	1.00	10.00	B	N
ATOM	592	H41	CYT	B	19	5.649	10.218	-4.351	1.00	10.00	B	H
ATOM	593	H42	CYT	B	19	4.906	10.833	-2.885	1.00	10.00	B	H
ATOM	594	C5	CYT	B	19	6.943	12.346	-5.034	1.00	10.00	B	C
ATOM	595	H5	CYT	B	19	7.113	11.547	-5.755	1.00	10.00	B	H
ATOM	596	C2'	CYT	B	19	8.926	16.236	-3.370	1.00	10.00	B	C
ATOM	597	H2'	CYT	B	19	8.709	15.735	-2.424	1.00	10.00	B	H
ATOM	598	O2'	CYT	B	19	9.006	17.644	-3.244	1.00	10.00	B	O

ATOM	599	HO2'	CYT	B	19	8.163	17.992	-3.568	1.00	10.00	B	H
ATOM	600	C3'	CYT	B	19	10.183	15.668	-4.005	1.00	10.00	B	C
ATOM	601	H3'	CYT	B	19	10.237	14.580	-3.932	1.00	10.00	B	H
ATOM	602	O3'	CYT	B	19	11.379	16.168	-3.419	1.00	10.00	B	O
ATOM	603	P	CYT	B	20	12.611	15.172	-3.170	1.00	10.00	B	P
ATOM	604	O1P	CYT	B	20	13.851	15.884	-3.555	1.00	10.00	B	O
ATOM	605	O2P	CYT	B	20	12.291	13.869	-3.797	1.00	10.00	B	O
ATOM	606	O5'	CYT	B	20	12.644	14.989	-1.590	1.00	10.00	B	O
ATOM	607	C5'	CYT	B	20	12.719	16.124	-0.736	1.00	10.00	B	C
ATOM	608	H5'	CYT	B	20	12.246	16.980	-1.219	1.00	10.00	B	H
ATOM	609	H5''	CYT	B	20	13.764	16.366	-0.534	1.00	10.00	B	H
ATOM	610	C4'	CYT	B	20	12.021	15.843	0.572	1.00	10.00	B	C
ATOM	611	H4'	CYT	B	20	12.256	16.655	1.260	1.00	10.00	B	H
ATOM	612	O4'	CYT	B	20	10.592	15.676	0.328	1.00	10.00	B	O
ATOM	613	C1'	CYT	B	20	10.071	14.690	1.211	1.00	10.00	B	C
ATOM	614	H1'	CYT	B	20	9.221	15.142	1.727	1.00	10.00	B	H
ATOM	615	N1	CYT	B	20	9.571	13.557	0.415	1.00	10.00	B	N
ATOM	616	C6	CYT	B	20	9.971	13.372	-0.881	1.00	10.00	B	C
ATOM	617	H6	CYT	B	20	10.693	14.060	-1.326	1.00	10.00	B	H
ATOM	618	C2	CYT	B	20	8.666	12.672	1.006	1.00	10.00	B	C
ATOM	619	O2	CYT	B	20	8.338	12.851	2.187	1.00	10.00	B	O
ATOM	620	N3	CYT	B	20	8.173	11.643	0.277	1.00	10.00	B	N
ATOM	621	C4	CYT	B	20	8.557	11.480	-0.991	1.00	10.00	B	C
ATOM	622	N4	CYT	B	20	8.032	10.460	-1.673	1.00	10.00	B	N
ATOM	623	H41	CYT	B	20	8.295	10.306	-2.635	1.00	10.00	B	H
ATOM	624	H42	CYT	B	20	7.361	9.849	-1.219	1.00	10.00	B	H
ATOM	625	C5	CYT	B	20	9.493	12.356	-1.615	1.00	10.00	B	C
ATOM	626	H5	CYT	B	20	9.808	12.207	-2.648	1.00	10.00	B	H
ATOM	627	C2'	CYT	B	20	11.204	14.337	2.172	1.00	10.00	B	C
ATOM	628	H2'	CYT	B	20	11.144	13.301	2.512	1.00	10.00	B	H
ATOM	629	O2'	CYT	B	20	11.193	15.273	3.234	1.00	10.00	B	O
ATOM	630	HO2'	CYT	B	20	10.305	15.652	3.234	1.00	10.00	B	H
ATOM	631	C3'	CYT	B	20	12.404	14.546	1.264	1.00	10.00	B	C
ATOM	632	H3'	CYT	B	20	12.549	13.730	0.555	1.00	10.00	B	H
ATOM	633	O3'	CYT	B	20	13.622	14.678	1.984	1.00	10.00	B	O
HETATM	634	P	URI	B	21	14.365	13.370	2.537	1.00	10.00	B	P
HETATM	635	O1P	URI	B	21	15.528	13.841	3.325	1.00	10.00	B	O
HETATM	636	O2P	URI	B	21	14.579	12.425	1.416	1.00	10.00	B	O
HETATM	637	O5'	URI	B	21	13.323	12.719	3.544	1.00	10.00	B	O
HETATM	638	C5'	URI	B	21	13.237	13.170	4.890	1.00	10.00	B	C
HETATM	639	H5'	URI	B	21	12.723	14.131	4.923	1.00	10.00	B	H
HETATM	640	H5''	URI	B	21	14.238	13.290	5.303	1.00	10.00	B	H
HETATM	641	C4'	URI	B	21	12.477	12.170	5.726	1.00	10.00	B	C
HETATM	642	H4'	URI	B	21	12.498	12.509	6.762	1.00	10.00	B	H
HETATM	643	O4'	URI	B	21	11.131	12.020	5.186	1.00	10.00	B	O
HETATM	644	C1'	URI	B	21	10.709	10.670	5.324	1.00	10.00	B	C
HETATM	645	H1'	URI	B	21	9.739	10.687	5.824	1.00	10.00	B	H
HETATM	646	N1	URI	B	21	10.527	10.101	3.981	1.00	10.00	B	N
HETATM	647	C6	URI	B	21	11.315	10.494	2.922	1.00	10.00	B	C
HETATM	648	H6	URI	B	21	12.100	11.233	3.094	1.00	10.00	B	H
HETATM	649	C2	URI	B	21	9.529	9.159	3.818	1.00	10.00	B	C
HETATM	650	O2	URI	B	21	8.824	8.775	4.738	1.00	10.00	B	O
HETATM	651	N3	URI	B	21	9.388	8.681	2.540	1.00	10.00	B	N
HETATM	652	H3	URI	B	21	8.657	7.994	2.397	1.00	10.00	B	H
HETATM	653	C4	URI	B	21	10.132	9.032	1.434	1.00	10.00	B	C
HETATM	654	O4	URI	B	21	9.862	8.535	0.338	1.00	10.00	B	O
HETATM	655	C5	URI	B	21	11.155	10.001	1.689	1.00	10.00	B	C
HETATM	656	H5	URI	B	21	11.802	10.335	0.879	1.00	10.00	B	H
HETATM	657	C2'	URI	B	21	11.782	9.977	6.162	1.00	10.00	B	C
HETATM	658	H2'	URI	B	21	11.871	8.916	5.915	1.00	10.00	B	H
HETATM	659	O2'	URI	B	21	11.508	10.208	7.531	1.00	10.00	B	O
HETATM	660	HO2'	URI	B	21	10.940	10.989	7.569	1.00	10.00	B	H
HETATM	661	C3'	URI	B	21	13.009	10.747	5.710	1.00	10.00	B	C
HETATM	662	H3'	URI	B	21	13.354	10.453	4.719	1.00	10.00	B	H
HETATM	663	O3'	URI	B	21	14.116	10.579	6.588	1.00	10.00	B	O
ATOM	664	P	GUA	B	22	15.032	9.271	6.458	1.00	10.00	B	P
ATOM	665	O1P	GUA	B	22	16.119	9.373	7.459	1.00	10.00	B	O
ATOM	666	O2P	GUA	B	22	15.372	9.091	5.029	1.00	10.00	B	O
ATOM	667	O5'	GUA	B	22	14.067	8.084	6.891	1.00	10.00	B	O
ATOM	668	C5'	GUA	B	22	13.690	7.909	8.253	1.00	10.00	B	C
ATOM	669	H5'	GUA	B	22	13.249	8.832	8.635	1.00	10.00	B	H
ATOM	670	H5''	GUA	B	22	14.567	7.662	8.850	1.00	10.00	B	H
ATOM	671	C4'	GUA	B	22	12.683	6.790	8.372	1.00	10.00	B	C
ATOM	672	H4'	GUA	B	22	12.421	6.682	9.424	1.00	10.00	B	H
ATOM	673	O4'	GUA	B	22	11.541	7.080	7.512	1.00	10.00	B	O
ATOM	674	C1'	GUA	B	22	11.045	5.871	6.956	1.00	10.00	B	C
ATOM	675	H1'	GUA	B	22	9.975	5.837	7.167	1.00	10.00	B	H
ATOM	676	N9	GUA	B	22	11.221	5.928	5.509	1.00	10.00	B	N
ATOM	677	C4	GUA	B	22	10.529	5.201	4.568	1.00	10.00	B	C
ATOM	678	N3	GUA	B	22	9.573	4.277	4.821	1.00	10.00	B	N
ATOM	679	C2	GUA	B	22	9.080	3.760	3.705	1.00	10.00	B	C
ATOM	680	N2	GUA	B	22	8.113	2.824	3.767	1.00	10.00	B	N
ATOM	681	H21	GUA	B	22	7.750	2.499	4.651	1.00	10.00	B	H
ATOM	682	H22	GUA	B	22	7.713	2.484	2.909	1.00	10.00	B	H
ATOM	683	N1	GUA	B	22	9.495	4.118	2.446	1.00	10.00	B	N
ATOM	684	H1	GUA	B	22	9.065	3.665	1.648	1.00	10.00	B	H
ATOM	685	C6	GUA	B	22	10.473	5.063	2.161	1.00	10.00	B	C
ATOM	686	O6	GUA	B	22	10.764	5.311	0.980	1.00	10.00	B	O
ATOM	687	C5	GUA	B	22	11.012	5.628	3.348	1.00	10.00	B	C
ATOM	688	N7	GUA	B	22	11.998	6.592	3.519	1.00	10.00	B	N
ATOM	689	C8	GUA	B	22	12.093	6.730	4.813	1.00	10.00	B	C
ATOM	690	H8	GUA	B	22	12.789	7.405	5.291	1.00	10.00	B	H
ATOM	691	C2'	GUA	B	22	11.804	4.743	7.651	1.00	10.00	B	C
ATOM	692	H2'	GUA	B	22	11.920	3.871	7.004	1.00	10.00	B	H
ATOM	693	O2'	GUA	B	22	11.150	4.447	8.873	1.00	10.00	B	O

ATOM	694	HO2'	GUA	B	22	10.227	4.698	8.752	1.00	10.00	B	H
ATOM	695	C3'	GUA	B	22	13.140	5.428	7.884	1.00	10.00	B	C
ATOM	696	H3'	GUA	B	22	13.745	5.498	6.981	1.00	10.00	B	H
ATOM	697	O3'	GUA	B	22	13.941	4.769	8.858	1.00	10.00	B	O
HETATM	698	P	URI	B	23	14.934	3.595	8.406	1.00	10.00	B	P
HETATM	699	O1P	URI	B	23	15.527	3.030	9.639	1.00	10.00	B	O
HETATM	700	O2P	URI	B	23	15.824	4.095	7.332	1.00	10.00	B	O
HETATM	701	O5'	URI	B	23	13.968	2.498	7.783	1.00	10.00	B	O
HETATM	702	C5'	URI	B	23	12.950	1.894	8.572	1.00	10.00	B	C
HETATM	703	H5'	URI	B	23	12.130	2.599	8.722	1.00	10.00	B	H
HETATM	704	H5''	URI	B	23	13.354	1.610	9.544	1.00	10.00	B	H
HETATM	705	C4'	URI	B	23	12.428	0.661	7.882	1.00	10.00	B	C
HETATM	706	H4'	URI	B	23	11.994	0.007	8.638	1.00	10.00	B	H
HETATM	707	O4'	URI	B	23	11.490	1.053	6.836	1.00	10.00	B	O
HETATM	708	C1'	URI	B	23	11.618	0.174	5.726	1.00	10.00	B	C
HETATM	709	H1'	URI	B	23	10.622	-0.209	5.503	1.00	10.00	B	H
HETATM	710	N1	URI	B	23	12.084	0.948	4.568	1.00	10.00	B	N
HETATM	711	C6	URI	B	23	12.794	2.120	4.723	1.00	10.00	B	C
HETATM	712	H6	URI	B	23	13.026	2.466	5.730	1.00	10.00	B	H
HETATM	713	C2	URI	B	23	11.781	0.461	3.311	1.00	10.00	B	C
HETATM	714	O2	URI	B	23	11.166	-0.578	3.133	1.00	10.00	B	O
HETATM	715	N3	URI	B	23	12.226	1.233	2.267	1.00	10.00	B	N
HETATM	716	H3	URI	B	23	12.010	0.885	1.341	1.00	10.00	B	H
HETATM	717	C4	URI	B	23	12.930	2.415	2.344	1.00	10.00	B	C
HETATM	718	O4	URI	B	23	13.253	2.998	1.306	1.00	10.00	B	O
HETATM	719	C5	URI	B	23	13.211	2.850	3.678	1.00	10.00	B	C
HETATM	720	H5	URI	B	23	13.764	3.776	3.843	1.00	10.00	B	H
HETATM	721	C2'	URI	B	23	12.569	-0.934	6.175	1.00	10.00	B	C
HETATM	722	H2'	URI	B	23	13.145	-1.343	5.341	1.00	10.00	B	H
HETATM	723	O2'	URI	B	23	11.812	-1.908	6.865	1.00	10.00	B	O
HETATM	724	HO2'	URI	B	23	11.101	-1.431	7.295	1.00	10.00	B	H
HETATM	725	C3'	URI	B	23	13.461	-0.149	7.121	1.00	10.00	B	C
HETATM	726	H3'	URI	B	23	14.175	0.490	6.599	1.00	10.00	B	H
HETATM	727	O3'	URI	B	23	14.223	-0.976	7.992	1.00	10.00	B	O
ATOM	728	P	ADE	B	24	15.544	-1.698	7.444	1.00	10.00	B	P
ATOM	729	O1P	ADE	B	24	16.058	-2.548	8.544	1.00	10.00	B	O
ATOM	730	O2P	ADE	B	24	16.422	-0.668	6.843	1.00	10.00	B	O
ATOM	731	O5'	ADE	B	24	15.022	-2.640	6.275	1.00	10.00	B	O
ATOM	732	C5'	ADE	B	24	14.573	-3.959	6.555	1.00	10.00	B	C
ATOM	733	H5'	ADE	B	24	13.620	-3.920	7.084	1.00	10.00	B	H
ATOM	734	H5''	ADE	B	24	15.303	-4.473	7.177	1.00	10.00	B	H
ATOM	735	C4'	ADE	B	24	14.397	-4.728	5.270	1.00	10.00	B	C
ATOM	736	H4'	ADE	B	24	14.050	-5.728	5.521	1.00	10.00	B	H
ATOM	737	O4'	ADE	B	24	13.491	-3.995	4.396	1.00	10.00	B	O
ATOM	738	C1'	ADE	B	24	13.902	-4.153	3.049	1.00	10.00	B	C
ATOM	739	H1'	ADE	B	24	13.031	-4.499	2.489	1.00	10.00	B	H
ATOM	740	N9	ADE	B	24	14.290	-2.846	2.524	1.00	10.00	B	N
ATOM	741	C4	ADE	B	24	14.249	-2.467	1.204	1.00	10.00	B	C
ATOM	742	N3	ADE	B	24	13.878	-3.218	0.154	1.00	10.00	B	N
ATOM	743	C2	ADE	B	24	13.958	-2.514	-0.975	1.00	10.00	B	C
ATOM	744	H2	ADE	B	24	13.680	-3.051	-1.883	1.00	10.00	B	H
ATOM	745	N1	ADE	B	24	14.332	-1.240	-1.154	1.00	10.00	B	N
ATOM	746	C6	ADE	B	24	14.694	-0.512	-0.077	1.00	10.00	B	C
ATOM	747	N6	ADE	B	24	15.051	0.761	-0.259	1.00	10.00	B	N
ATOM	748	H61	ADE	B	24	15.316	1.318	0.541	1.00	10.00	B	H
ATOM	749	H62	ADE	B	24	15.053	1.170	-1.183	1.00	10.00	B	H
ATOM	750	C5	ADE	B	24	14.661	-1.146	1.179	1.00	10.00	B	C
ATOM	751	N7	ADE	B	24	14.974	-0.703	2.457	1.00	10.00	B	N
ATOM	752	C8	ADE	B	24	14.741	-1.749	3.216	1.00	10.00	B	C
ATOM	753	H8	ADE	B	24	14.896	-1.747	4.287	1.00	10.00	B	H
ATOM	754	C2'	ADE	B	24	15.019	-5.192	3.069	1.00	10.00	B	C
ATOM	755	H2'	ADE	B	24	15.734	-5.044	2.257	1.00	10.00	B	H
ATOM	756	O2'	ADE	B	24	14.420	-6.476	3.059	1.00	10.00	B	O
ATOM	757	HO2'	ADE	B	24	13.583	-6.363	2.590	1.00	10.00	B	H
ATOM	758	C3'	ADE	B	24	15.649	-4.888	4.417	1.00	10.00	B	C
ATOM	759	H3'	ADE	B	24	16.255	-3.981	4.409	1.00	10.00	B	H
ATOM	760	O3'	ADE	B	24	16.483	-5.930	4.921	1.00	10.00	B	O
ATOM	761	P	GUA	B	25	17.709	-6.500	4.043	1.00	10.00	B	P
ATOM	762	O1P	GUA	B	25	17.922	-7.894	4.496	1.00	10.00	B	O
ATOM	763	O2P	GUA	B	25	18.822	-5.526	4.122	1.00	10.00	B	O
ATOM	764	O5'	GUA	B	25	17.202	-6.562	2.535	1.00	10.00	B	O
ATOM	765	C5'	GUA	B	25	16.837	-7.807	1.949	1.00	10.00	B	C
ATOM	766	H5'	GUA	B	25	15.848	-8.102	2.300	1.00	10.00	B	H
ATOM	767	H5''	GUA	B	25	17.556	-8.574	2.236	1.00	10.00	B	H
ATOM	768	C4'	GUA	B	25	16.815	-7.697	0.443	1.00	10.00	B	C
ATOM	769	H4'	GUA	B	25	16.478	-8.653	0.042	1.00	10.00	B	H
ATOM	770	O4'	GUA	B	25	15.968	-6.573	0.056	1.00	10.00	B	O
ATOM	771	C1'	GUA	B	25	16.512	-5.944	-1.097	1.00	10.00	B	C
ATOM	772	H1'	GUA	B	25	15.711	-5.874	-1.835	1.00	10.00	B	H
ATOM	773	N9	GUA	B	25	16.932	-4.591	-0.749	1.00	10.00	B	N
ATOM	774	C4	GUA	B	25	17.057	-3.540	-1.622	1.00	10.00	B	C
ATOM	775	N3	GUA	B	25	16.816	-3.583	-2.949	1.00	10.00	B	N
ATOM	776	C2	GUA	B	25	17.017	-2.411	-3.526	1.00	10.00	B	C
ATOM	777	N2	GUA	B	25	16.823	-2.274	-4.845	1.00	10.00	B	N
ATOM	778	H21	GUA	B	25	16.525	-3.050	-5.417	1.00	10.00	B	H
ATOM	779	H22	GUA	B	25	16.969	-1.376	-5.274	1.00	10.00	B	H
ATOM	780	N1	GUA	B	25	17.423	-1.286	-2.855	1.00	10.00	B	N
ATOM	781	H1	GUA	B	25	17.540	-0.445	-3.403	1.00	10.00	B	H
ATOM	782	C6	GUA	B	25	17.683	-1.215	-1.491	1.00	10.00	B	C
ATOM	783	O6	GUA	B	25	18.050	-0.141	-0.990	1.00	10.00	B	O
ATOM	784	C5	GUA	B	25	17.468	-2.470	-0.854	1.00	10.00	B	C
ATOM	785	N7	GUA	B	25	17.602	-2.844	0.478	1.00	10.00	B	N
ATOM	786	C8	GUA	B	25	17.278	-4.108	0.490	1.00	10.00	B	C
ATOM	787	H8	GUA	B	25	17.288	-4.719	1.383	1.00	10.00	B	H
ATOM	788	C2'	GUA	B	25	17.653	-6.836	-1.568	1.00	10.00	B	C

ATOM	789	H2'	GUA	B	25	18.439	-6.266	-2.072	1.00	10.00	B	H
ATOM	790	O2'	GUA	B	25	17.108	-7.867	-2.373	1.00	10.00	B	O
ATOM	791	HO2'	GUA	B	25	16.186	-7.951	-2.112	1.00	10.00	B	H
ATOM	792	C3'	GUA	B	25	18.137	-7.372	-0.234	1.00	10.00	B	C
ATOM	793	H3'	GUA	B	25	18.711	-6.636	0.332	1.00	10.00	B	H
ATOM	794	O3'	GUA	B	25	18.978	-8.508	-0.378	1.00	10.00	B	O
ATOM	795	P	ADE	B	26	20.570	-8.314	-0.361	1.00	10.00	B	P
ATOM	796	O1P	ADE	B	26	21.170	-9.615	0.024	1.00	10.00	B	O
ATOM	797	O2P	ADE	B	26	20.862	-7.108	0.446	1.00	10.00	B	O
ATOM	798	O5'	ADE	B	26	20.940	-8.010	-1.878	1.00	10.00	B	O
ATOM	799	C5'	ADE	B	26	20.791	-9.013	-2.874	1.00	10.00	B	C
ATOM	800	H5'	ADE	B	26	19.860	-9.557	-2.708	1.00	10.00	B	H
ATOM	801	H5''	ADE	B	26	21.624	-9.714	-2.820	1.00	10.00	B	H
ATOM	802	C4'	ADE	B	26	20.764	-8.389	-4.250	1.00	10.00	B	C
ATOM	803	H4'	ADE	B	26	20.606	-9.186	-4.974	1.00	10.00	B	H
ATOM	804	O4'	ADE	B	26	19.731	-7.362	-4.285	1.00	10.00	B	O
ATOM	805	C1'	ADE	B	26	20.161	-6.283	-5.103	1.00	10.00	B	C
ATOM	806	H1'	ADE	B	26	19.362	-6.082	-5.817	1.00	10.00	B	H
ATOM	807	N9	ADE	B	26	20.328	-5.101	-4.258	1.00	10.00	B	N
ATOM	808	C4	ADE	B	26	20.463	-3.800	-4.684	1.00	10.00	B	C
ATOM	809	N3	ADE	B	26	20.480	-3.352	-5.953	1.00	10.00	B	N
ATOM	810	C2	ADE	B	26	20.624	-2.025	-5.980	1.00	10.00	B	C
ATOM	811	H2	ADE	B	26	20.644	-1.579	-6.974	1.00	10.00	B	H
ATOM	812	N1	ADE	B	26	20.742	-1.163	-4.960	1.00	10.00	B	N
ATOM	813	C6	ADE	B	26	20.719	-1.646	-3.699	1.00	10.00	B	C
ATOM	814	N6	ADE	B	26	20.838	-0.788	-2.683	1.00	10.00	B	N
ATOM	815	H61	ADE	B	26	20.824	-1.142	-1.736	1.00	10.00	B	H
ATOM	816	H62	ADE	B	26	20.944	0.204	-2.844	1.00	10.00	B	H
ATOM	817	C5	ADE	B	26	20.573	-3.036	-3.534	1.00	10.00	B	C
ATOM	818	N7	ADE	B	26	20.513	-3.840	-2.405	1.00	10.00	B	N
ATOM	819	C8	ADE	B	26	20.374	-5.053	-2.887	1.00	10.00	B	C
ATOM	820	H8	ADE	B	26	20.309	-5.932	-2.263	1.00	10.00	B	H
ATOM	821	C2'	ADE	B	26	21.439	-6.759	-5.786	1.00	10.00	B	C
ATOM	822	H2'	ADE	B	26	22.109	-5.932	-6.023	1.00	10.00	B	H
ATOM	823	O2'	ADE	B	26	21.013	-7.481	-6.926	1.00	10.00	B	O
ATOM	824	HO2'	ADE	B	26	20.094	-7.723	-6.762	1.00	10.00	B	H
ATOM	825	C3'	ADE	B	26	22.014	-7.639	-4.683	1.00	10.00	B	C
ATOM	826	H3'	ADE	B	26	22.400	-7.038	-3.856	1.00	10.00	B	H
ATOM	827	O3'	ADE	B	26	23.067	-8.568	-5.000	1.00	10.00	B	O
ATOM	828	P	GUA	B	27	23.700	-8.657	-6.480	1.00	10.00	B	P
ATOM	829	O1P	GUA	B	27	22.745	-9.393	-7.341	1.00	10.00	B	O
ATOM	830	O2P	GUA	B	27	25.079	-9.183	-6.322	1.00	10.00	B	O
ATOM	831	O5'	GUA	B	27	23.830	-7.162	-7.013	1.00	10.00	B	O
ATOM	832	C5'	GUA	B	27	23.732	-6.903	-8.411	1.00	10.00	B	C
ATOM	833	H5'	GUA	B	27	22.682	-6.899	-8.707	1.00	10.00	B	H
ATOM	834	H5''	GUA	B	27	24.250	-7.683	-8.966	1.00	10.00	B	H
ATOM	835	C4'	GUA	B	27	24.349	-5.569	-8.761	1.00	10.00	B	C
ATOM	836	H4'	GUA	B	27	24.493	-5.539	-9.840	1.00	10.00	B	H
ATOM	837	O4'	GUA	B	27	23.498	-4.497	-8.257	1.00	10.00	B	O
ATOM	838	C1'	GUA	B	27	24.307	-3.413	-7.824	1.00	10.00	B	C
ATOM	839	H1'	GUA	B	27	23.932	-2.517	-8.320	1.00	10.00	B	H
ATOM	840	N9	GUA	B	27	24.148	-3.237	-6.386	1.00	10.00	B	N
ATOM	841	C4	GUA	B	27	24.424	-2.092	-5.685	1.00	10.00	B	C
ATOM	842	N3	GUA	B	27	24.900	-0.943	-6.210	1.00	10.00	B	N
ATOM	843	C2	GUA	B	27	25.070	-0.012	-5.289	1.00	10.00	B	C
ATOM	844	N2	GUA	B	27	25.550	1.192	-5.651	1.00	10.00	B	N
ATOM	845	H21	GUA	B	27	25.784	1.389	-6.615	1.00	10.00	B	H
ATOM	846	H22	GUA	B	27	25.670	1.926	-4.969	1.00	10.00	B	H
ATOM	847	N1	GUA	B	27	24.783	-0.195	-3.955	1.00	10.00	B	N
ATOM	848	H1	GUA	B	27	24.934	0.546	-3.294	1.00	10.00	B	H
ATOM	849	C6	GUA	B	27	24.286	-1.363	-3.393	1.00	10.00	B	C
ATOM	850	O6	GUA	B	27	24.055	-1.407	-2.174	1.00	10.00	B	O
ATOM	851	C5	GUA	B	27	24.110	-2.378	-4.373	1.00	10.00	B	C
ATOM	852	N7	GUA	B	27	23.654	-3.684	-4.251	1.00	10.00	B	N
ATOM	853	C8	GUA	B	27	23.695	-4.153	-5.470	1.00	10.00	B	C
ATOM	854	H8	GUA	B	27	23.407	-5.162	-5.731	1.00	10.00	B	H
ATOM	855	C2'	GUA	B	27	25.730	-3.749	-8.248	1.00	10.00	B	C
ATOM	856	H2'	GUA	B	27	26.468	-3.318	-7.570	1.00	10.00	B	H
ATOM	857	O2'	GUA	B	27	25.909	-3.348	-9.593	1.00	10.00	B	O
ATOM	858	HO2'	GUA	B	27	25.042	-3.103	-9.929	1.00	10.00	B	H
ATOM	859	C3'	GUA	B	27	25.695	-5.261	-8.124	1.00	10.00	B	C
ATOM	860	H3'	GUA	B	27	25.745	-5.602	-7.091	1.00	10.00	B	H
ATOM	861	O3'	GUA	B	27	26.781	-5.880	-8.805	1.00	10.00	B	O
ATOM	862	P	GUA	B	28	28.201	-6.027	-8.067	1.00	10.00	B	P
ATOM	863	O1P	GUA	B	28	29.046	-6.893	-8.923	1.00	10.00	B	O
ATOM	864	O2P	GUA	B	28	27.970	-6.400	-6.648	1.00	10.00	B	O
ATOM	865	O5'	GUA	B	28	28.816	-4.560	-8.104	1.00	10.00	B	O
ATOM	866	C5'	GUA	B	28	29.614	-4.136	-9.207	1.00	10.00	B	C
ATOM	867	H5'	GUA	B	28	28.992	-4.054	-10.100	1.00	10.00	B	H
ATOM	868	H5''	GUA	B	28	30.404	-4.864	-9.392	1.00	10.00	B	H
ATOM	869	C4'	GUA	B	28	30.244	-2.796	-8.917	1.00	10.00	B	C
ATOM	870	H4'	GUA	B	28	30.804	-2.492	-9.801	1.00	10.00	B	H
ATOM	871	O4'	GUA	B	28	29.202	-1.849	-8.534	1.00	10.00	B	O
ATOM	872	C1'	GUA	B	28	29.704	-0.966	-7.539	1.00	10.00	B	C
ATOM	873	H1'	GUA	B	28	29.494	0.053	-7.871	1.00	10.00	B	H
ATOM	874	N9	GUA	B	28	28.980	-1.205	-6.295	1.00	10.00	B	N
ATOM	875	C4	GUA	B	28	28.965	-0.392	-5.188	1.00	10.00	B	C
ATOM	876	N3	GUA	B	28	29.623	0.779	-5.056	1.00	10.00	B	N
ATOM	877	C2	GUA	B	28	29.416	1.333	-3.873	1.00	10.00	B	C
ATOM	878	N2	GUA	B	28	30.007	2.502	-3.579	1.00	10.00	B	N
ATOM	879	H21	GUA	B	28	30.603	2.942	-4.266	1.00	10.00	B	H
ATOM	880	H22	GUA	B	28	29.902	2.921	-2.669	1.00	10.00	B	H
ATOM	881	N1	GUA	B	28	28.616	0.784	-2.899	1.00	10.00	B	N
ATOM	882	H1	GUA	B	28	28.502	1.280	-2.026	1.00	10.00	B	H
ATOM	883	C6	GUA	B	28	27.930	-0.419	-3.012	1.00	10.00	B	C

ATOM	884	O6	GUA	B	28	27.238	-0.823	-2.068	1.00	10.00	B	O
ATOM	885	C5	GUA	B	28	28.150	-1.029	-4.276	1.00	10.00	B	C
ATOM	886	N7	GUA	B	28	27.663	-2.220	-4.800	1.00	10.00	B	N
ATOM	887	C8	GUA	B	28	28.182	-2.280	-5.996	1.00	10.00	B	C
ATOM	888	H8	GUA	B	28	28.006	-3.096	-6.682	1.00	10.00	B	H
ATOM	889	C2'	GUA	B	28	31.198	-1.250	-7.436	1.00	10.00	B	C
ATOM	890	H2'	GUA	B	28	31.583	-1.054	-6.433	1.00	10.00	B	H
ATOM	891	O2'	GUA	B	28	31.863	-0.508	-8.443	1.00	10.00	B	O
ATOM	892	HO2'	GUA	B	28	31.173	-0.164	-9.020	1.00	10.00	B	H
ATOM	893	C3'	GUA	B	28	31.202	-2.737	-7.741	1.00	10.00	B	C
ATOM	894	H3'	GUA	B	28	30.846	-3.338	-6.903	1.00	10.00	B	H
ATOM	895	O3'	GUA	B	28	32.493	-3.230	-8.062	1.00	10.00	B	O
ATOM	896	P	ADE	B	29	33.297	-4.087	-6.972	1.00	10.00	B	P
ATOM	897	O1P	ADE	B	29	34.326	-4.869	-7.697	1.00	10.00	B	O
ATOM	898	O2P	ADE	B	29	32.314	-4.788	-6.116	1.00	10.00	B	O
ATOM	899	O5'	ADE	B	29	34.034	-2.987	-6.092	1.00	10.00	B	O
ATOM	900	C5'	ADE	B	29	35.049	-2.170	-6.661	1.00	10.00	B	C
ATOM	901	H5'	ADE	B	29	34.743	-1.842	-7.656	1.00	10.00	B	H
ATOM	902	H5''	ADE	B	29	35.974	-2.739	-6.745	1.00	10.00	B	H
ATOM	903	C4'	ADE	B	29	35.297	-0.958	-5.793	1.00	10.00	B	C
ATOM	904	H4'	ADE	B	29	36.061	-0.346	-6.273	1.00	10.00	B	H
ATOM	905	O4'	ADE	B	29	34.036	-0.258	-5.572	1.00	10.00	B	O
ATOM	906	C1'	ADE	B	29	34.018	0.285	-4.257	1.00	10.00	B	C
ATOM	907	H1'	ADE	B	29	33.785	1.346	-4.353	1.00	10.00	B	H
ATOM	908	N9	ADE	B	29	32.943	-0.350	-3.497	1.00	10.00	B	N
ATOM	909	C4	ADE	B	29	32.455	0.098	-2.293	1.00	10.00	B	C
ATOM	910	N3	ADE	B	29	32.874	1.166	-1.592	1.00	10.00	B	N
ATOM	911	C2	ADE	B	29	32.164	1.301	-0.472	1.00	10.00	B	C
ATOM	912	H2	ADE	B	29	32.446	2.141	0.162	1.00	10.00	B	H
ATOM	913	N1	ADE	B	29	31.155	0.548	-0.011	1.00	10.00	B	N
ATOM	914	C6	ADE	B	29	30.758	-0.516	-0.741	1.00	10.00	B	C
ATOM	915	N6	ADE	B	29	29.748	-1.258	-0.285	1.00	10.00	B	N
ATOM	916	H61	ADE	B	29	29.447	-2.052	-0.832	1.00	10.00	B	H
ATOM	917	H62	ADE	B	29	29.286	-1.039	0.586	1.00	10.00	B	H
ATOM	918	C5	ADE	B	29	31.437	-0.773	-1.950	1.00	10.00	B	C
ATOM	919	N7	ADE	B	29	31.292	-1.762	-2.914	1.00	10.00	B	N
ATOM	920	C8	ADE	B	29	32.209	-1.468	-3.805	1.00	10.00	B	C
ATOM	921	H8	ADE	B	29	32.373	-2.054	-4.699	1.00	10.00	B	H
ATOM	922	C2'	ADE	B	29	35.411	0.052	-3.682	1.00	10.00	B	C
ATOM	923	H2'	ADE	B	29	35.386	-0.082	-2.598	1.00	10.00	B	H
ATOM	924	O2'	ADE	B	29	36.254	1.114	-4.091	1.00	10.00	B	O
ATOM	925	HO2'	ADE	B	29	35.746	1.921	-3.936	1.00	10.00	B	H
ATOM	926	C3'	ADE	B	29	35.774	-1.247	-4.381	1.00	10.00	B	C
ATOM	927	H3'	ADE	B	29	35.269	-2.111	-3.951	1.00	10.00	B	H
ATOM	928	O3'	ADE	B	29	37.166	-1.536	-4.343	1.00	10.00	B	O
HETATM	929	P	URI	B	30	37.763	-2.398	-3.129	1.00	10.00	B	P
HETATM	930	O1P	URI	B	30	39.122	-2.834	-3.530	1.00	10.00	B	O
HETATM	931	O2P	URI	B	30	36.758	-3.415	-2.733	1.00	10.00	B	O
HETATM	932	O5'	URI	B	30	37.911	-1.350	-1.942	1.00	10.00	B	O
HETATM	933	C5'	URI	B	30	38.394	-0.032	-2.184	1.00	10.00	B	C
HETATM	934	H5'	URI	B	30	37.806	0.438	-2.977	1.00	10.00	B	H
HETATM	935	H5''	URI	B	30	39.438	-0.070	-2.492	1.00	10.00	B	H
HETATM	936	C4'	URI	B	30	38.284	0.793	-0.927	1.00	10.00	B	C
HETATM	937	H4'	URI	B	30	38.972	1.634	-1.009	1.00	10.00	B	H
HETATM	938	O4'	URI	B	30	36.893	1.183	-0.734	1.00	10.00	B	O
HETATM	939	C1'	URI	B	30	36.593	1.191	0.653	1.00	10.00	B	C
HETATM	940	H1'	URI	B	30	36.183	2.178	0.879	1.00	10.00	B	H
HETATM	941	N1	URI	B	30	35.544	0.195	0.910	1.00	10.00	B	N
HETATM	942	C6	URI	B	30	35.344	-0.875	0.063	1.00	10.00	B	C
HETATM	943	H6	URI	B	30	36.002	-0.994	-0.797	1.00	10.00	B	H
HETATM	944	C2	URI	B	30	34.748	0.374	2.028	1.00	10.00	B	C
HETATM	945	O2	URI	B	30	34.904	1.295	2.812	1.00	10.00	B	O
HETATM	946	N3	URI	B	30	33.762	-0.563	2.193	1.00	10.00	B	N
HETATM	947	H3	URI	B	30	33.151	-0.449	2.992	1.00	10.00	B	H
HETATM	948	C4	URI	B	30	33.492	-1.642	1.383	1.00	10.00	B	C
HETATM	949	O4	URI	B	30	32.528	-2.366	1.645	1.00	10.00	B	O
HETATM	950	C5	URI	B	30	34.369	-1.774	0.260	1.00	10.00	B	C
HETATM	951	H5	URI	B	30	34.246	-2.609	-0.431	1.00	10.00	B	H
HETATM	952	C2'	URI	B	30	37.916	0.946	1.374	1.00	10.00	B	C
HETATM	953	H2'	URI	B	30	37.772	0.420	2.322	1.00	10.00	B	H
HETATM	954	O2'	URI	B	30	38.572	2.190	1.523	1.00	10.00	B	O
HETATM	955	HO2'	URI	B	30	37.895	2.869	1.430	1.00	10.00	B	H
HETATM	956	C3'	URI	B	30	38.617	0.056	0.359	1.00	10.00	B	C
HETATM	957	H3'	URI	B	30	38.235	-0.965	0.354	1.00	10.00	B	H
HETATM	958	O3'	URI	B	30	40.035	-0.040	0.519	1.00	10.00	B	O
ATOM	959	P	GUA	B	31	40.667	-0.613	1.885	1.00	10.00	B	P
ATOM	960	O1P	GUA	B	31	42.009	0.001	2.024	1.00	10.00	B	O
ATOM	961	O2P	GUA	B	31	40.541	-2.089	1.849	1.00	10.00	B	O
ATOM	962	O5'	GUA	B	31	39.726	-0.077	3.049	1.00	10.00	B	O
ATOM	963	C5'	GUA	B	31	40.210	0.839	4.029	1.00	10.00	B	C
ATOM	964	H5'	GUA	B	31	40.109	1.859	3.659	1.00	10.00	B	H
ATOM	965	H5''	GUA	B	31	41.259	0.637	4.239	1.00	10.00	B	H
ATOM	966	C4'	GUA	B	31	39.415	0.690	5.302	1.00	10.00	B	C
ATOM	967	H4'	GUA	B	31	39.751	1.456	5.998	1.00	10.00	B	H
ATOM	968	O4'	GUA	B	31	37.995	0.772	4.986	1.00	10.00	B	O
ATOM	969	C1'	GUA	B	31	37.270	-0.107	5.832	1.00	10.00	B	C
ATOM	970	H1'	GUA	B	31	36.464	0.471	6.285	1.00	10.00	B	H
ATOM	971	N9	GUA	B	31	36.679	-1.149	5.001	1.00	10.00	B	N
ATOM	972	C4	GUA	B	31	35.552	-1.878	5.285	1.00	10.00	B	C
ATOM	973	N3	GUA	B	31	34.800	-1.767	6.401	1.00	10.00	B	N
ATOM	974	C2	GUA	B	31	33.773	-2.599	6.387	1.00	10.00	B	C
ATOM	975	N2	GUA	B	31	32.926	-2.624	7.430	1.00	10.00	B	N
ATOM	976	H21	GUA	B	31	33.069	-2.013	8.221	1.00	10.00	B	H
ATOM	977	H22	GUA	B	31	32.133	-3.248	7.421	1.00	10.00	B	H
ATOM	978	N1	GUA	B	31	33.504	-3.467	5.353	1.00	10.00	B	N

```
ATOM    979  H1  GUA B  31      32.705  -4.071   5.403  1.00 10.00      B    H
ATOM    980  C6  GUA B  31      34.261  -3.597   4.196  1.00 10.00      B    C
ATOM    981  O6  GUA B  31      33.918  -4.411   3.324  1.00 10.00      B    O
ATOM    982  C5  GUA B  31      35.372  -2.713   4.202  1.00 10.00      B    C
ATOM    983  N7  GUA B  31      36.374  -2.521   3.261  1.00 10.00      B    N
ATOM    984  C8  GUA B  31      37.126  -1.590   3.780  1.00 10.00      B    C
ATOM    985  H8  GUA B  31      38.017  -1.207   3.302  1.00 10.00      B    H
ATOM    986  C2' GUA B  31      38.267  -0.623   6.864  1.00 10.00      B    C
ATOM    987  H2' GUA B  31      38.011  -1.627   7.210  1.00 10.00      B    H
ATOM    988  O2' GUA B  31      38.360   0.319   7.914  1.00 10.00      B    O
ATOM    989 HO2' GUA B  31      38.367   1.189   7.499  1.00 10.00      B    H
ATOM    990  C3' GUA B  31      39.527  -0.645   6.020  1.00 10.00      B    C
ATOM    991  H3' GUA B  31      39.561  -1.483   5.327  1.00 10.00      B    H
ATOM    992  O3' GUA B  31      40.706  -0.725   6.811  1.00 10.00      B    O
ATOM    993  P   GUA B  32      41.193  -2.147   7.365  1.00 10.00      B    P
ATOM    994  O1P GUA B  32      42.472  -1.919   8.079  1.00 10.00      B    O
ATOM    995  O2P GUA B  32      41.144  -3.117   6.246  1.00 10.00      B    O
ATOM    996  O5' GUA B  32      40.087  -2.557   8.434  1.00 10.00      B    O
ATOM    997  C5' GUA B  32      40.262  -2.249   9.812  1.00 10.00      B    C
ATOM    998  H5' GUA B  32      40.089  -1.186   9.977  1.00 10.00      B    H
ATOM    999 H5'' GUA B  32      41.278  -2.494  10.120  1.00 10.00      B    H
ATOM   1000  C4' GUA B  32      39.294  -3.047  10.650  1.00 10.00      B    C
ATOM   1001  H4' GUA B  32      39.439  -2.761  11.692  1.00 10.00      B    H
ATOM   1002  O4' GUA B  32      37.940  -2.817  10.164  1.00 10.00      B    O
ATOM   1003  C1' GUA B  32      37.185  -4.012  10.284  1.00 10.00      B    C
ATOM   1004  H1' GUA B  32      36.269  -3.760  10.824  1.00 10.00      B    H
ATOM   1005  N9  GUA B  32      36.819  -4.458   8.944  1.00 10.00      B    N
ATOM   1006  C4  GUA B  32      35.810  -5.329   8.614  1.00 10.00      B    C
ATOM   1007  N3  GUA B  32      34.978  -5.944   9.481  1.00 10.00      B    N
ATOM   1008  C2  GUA B  32      34.109  -6.726   8.861  1.00 10.00      B    C
ATOM   1009  N2  GUA B  32      33.207  -7.416   9.576  1.00 10.00      B    N
ATOM   1010  H21 GUA B  32      33.189  -7.341  10.583  1.00 10.00      B    H
ATOM   1011  H22 GUA B  32      32.563  -8.045   9.119  1.00 10.00      B    H
ATOM   1012  N1  GUA B  32      34.059  -6.887   7.501  1.00 10.00      B    N
ATOM   1013  H1  GUA B  32      33.350  -7.503   7.121  1.00 10.00      B    H
ATOM   1014  C6  GUA B  32      34.903  -6.268   6.587  1.00 10.00      B    C
ATOM   1015  O6  GUA B  32      34.763  -6.489   5.374  1.00 10.00      B    O
ATOM   1016  C5  GUA B  32      35.845  -5.427   7.237  1.00 10.00      B    C
ATOM   1017  N7  GUA B  32      36.859  -4.635   6.714  1.00 10.00      B    N
ATOM   1018  C8  GUA B  32      37.406  -4.083   7.762  1.00 10.00      B    C
ATOM   1019  H8  GUA B  32      38.249  -3.405   7.708  1.00 10.00      B    H
ATOM   1020  C2' GUA B  32      38.062  -4.993  11.058  1.00 10.00      B    C
ATOM   1021  H2' GUA B  32      37.861  -6.029  10.779  1.00 10.00      B    H
ATOM   1022  O2' GUA B  32      37.921  -4.755  12.446  1.00 10.00      B    O
ATOM   1023 HO2' GUA B  32      37.342  -3.986  12.524  1.00 10.00      B    H
ATOM   1024  H3' GUA B  32      39.650  -4.897   9.564  1.00 10.00      B    H
ATOM   1025  C3' GUA B  32      39.439  -4.561  10.578  1.00 10.00      B    C
ATOM   1026  O3' GUA B  32      40.454  -5.055  11.450  1.00 10.00      B    O
ATOM   1027  H3T GUA B  32      40.078  -5.831  11.896  1.00 10.00      B    H
CONECT   29   27   30
CONECT   60   61   58
CONECT   30   33   29   31   32
CONECT   93   94   91
CONECT   61   63   60   62   64
CONECT  104  103  106  117  105
CONECT  109  106  111  110
CONECT  117  104  121  118  119
CONECT  121  101  117  123  122
CONECT  113  111  114  115
CONECT  101  102  103   98  121
CONECT  115  116  107  113
CONECT   98   97   99  100  101
CONECT  107  106  108  115
CONECT  105  104
CONECT  118  117
CONECT  112  111
CONECT  122  121
CONECT  102  101
CONECT  116  115
CONECT   99   98
CONECT  100   98
CONECT  108  107
CONECT  120  119
CONECT  106  104  107  109
CONECT  111  112  109  113
CONECT   95   94
CONECT  110  109
CONECT  119  117  120
CONECT   96   94
CONECT  123  121  124
CONECT  114  113
CONECT  103  101  104
CONECT   97   94   98
CONECT   94   93   95   96   97
CONECT  154  152  155
CONECT  124  123  127  126  125
CONECT  185  183  186
CONECT  155  157  154  156  158
CONECT  196  195  197  209  198
CONECT  201  203  202  198
CONECT  209  196  213  211  210
CONECT  213  214  193  215  209
CONECT  205  206  207  203
CONECT  193  195  190  194  213
CONECT  207  205  199  208
```

```
CONECT  190  189  193  191  192
CONECT  199  200  207  198
CONECT  197  196
CONECT  210  209
CONECT  204  203
CONECT  214  213
CONECT  194  193
CONECT  208  207
CONECT  191  190
CONECT  192  190
CONECT  200  199
CONECT  212  211
CONECT  198  196  201  199
CONECT  203  204  205  201
CONECT  187  186
CONECT  202  201
CONECT  211  209  212
CONECT  188  186
CONECT  215  216  213
CONECT  206  205
CONECT  195  196  193
CONECT  189  190  186
CONECT  186  188  189  187  185
CONECT  246  247  244
CONECT  216  219  215  218  217
CONECT  257  259  256  258  270
CONECT  262  259  263  264
CONECT  270  274  257  271  272
CONECT  274  275  270  276  254
CONECT  266  264  267  268
CONECT  254  274  255  256  251
CONECT  268  266  260  269
CONECT  251  252  250  253  254
CONECT  260  259  261  268
CONECT  258  257
CONECT  271  270
CONECT  265  264
CONECT  275  274
CONECT  255  254
CONECT  269  268
CONECT  252  251
CONECT  253  251
CONECT  261  260
CONECT  273  272
CONECT  259  257  262  260
CONECT  264  265  262  266
CONECT  248  247
CONECT  263  262
CONECT  272  273  270
CONECT  249  247
CONECT  276  274  277
CONECT  267  266
CONECT  256  257  254
CONECT  250  247  251
CONECT  247  248  249  250  246
CONECT  309  307  310
CONECT  277  280  278  276  279
CONECT  340  338  341
CONECT  310  312  309  313  311
CONECT  373  371  374
CONECT  341  340  343  344  342
CONECT  407  408  405
CONECT  374  373  377  376  375
CONECT  441  439  442
CONECT  408  411  409  410  407
CONECT  472  470  473
CONECT  442  445  444  441  443
CONECT  492  488  493  494  524
CONECT  473  475  472  474  476
CONECT  524  492  525  522
CONECT  537  535  538
CONECT  571  572  569
CONECT  538  539  541  537  540
CONECT  602  600  603
CONECT  572  575  573  571  574
CONECT  633  631  634
CONECT  603  602  606  604  605
CONECT  644  645  657  646  643
CONECT  649  650  651  646
CONECT  657  644  658  661  659
CONECT  661  663  657  662  641
CONECT  653  651  654  655
CONECT  641  661  638  642  643
CONECT  655  656  653  647
CONECT  638  639  640  637  641
CONECT  647  646  648  655
CONECT  645  644
CONECT  658  657
CONECT  652  651
CONECT  662  661
CONECT  642  641
CONECT  656  655
CONECT  639  638
CONECT  640  638
CONECT  648  647
```

```
CONECT  660  659
CONECT  646  644  647  649
CONECT  651  652  653  649
CONECT  635  634
CONECT  650  649
CONECT  659  657  660
CONECT  636  634
CONECT  663  661  664
CONECT  654  653
CONECT  643  644  641
CONECT  637  638  634
CONECT  634  636  635  633  637
CONECT  697  695  698
CONECT  664  667  666  665  663
CONECT  708  707  710  709  721
CONECT  713  715  714  710
CONECT  721  725  722  723  708
CONECT  725  726  705  727  721
CONECT  717  715  718  719
CONECT  705  702  725  707  706
CONECT  719  717  720  711
CONECT  702  703  704  705  701
CONECT  711  710  719  712
CONECT  709  708
CONECT  722  721
CONECT  716  715
CONECT  726  725
CONECT  706  705
CONECT  720  719
CONECT  703  702
CONECT  704  702
CONECT  712  711
CONECT  724  723
CONECT  710  713  708  711
CONECT  715  717  716  713
CONECT  699  698
CONECT  714  713
CONECT  723  724  721
CONECT  700  698
CONECT  727  725  728
CONECT  718  717
CONECT  707  705  708
CONECT  701  698  702
CONECT  698  699  697  700  701
CONECT  760  758  761
CONECT  728  729  727  731  730
CONECT  794  795  792
CONECT  761  760  762  763  764
CONECT  827  825  828
CONECT  795  796  797  794  798
CONECT  861  859  862
CONECT  828  827  829  830  831
CONECT  895  893  896
CONECT  862  864  861  865  863
CONECT  928  926  929
CONECT  896  895  898  897  899
CONECT  939  941  938  940  952
CONECT  944  941  946  945
CONECT  952  953  939  954  956
CONECT  956  936  952  957  958
CONECT  948  946  949  950
CONECT  936  933  937  938  956
CONECT  950  951  948  942
CONECT  933  936  932  934  935
CONECT  942  941  943  950
CONECT  940  939
CONECT  953  952
CONECT  947  946
CONECT  957  956
CONECT  937  936
CONECT  951  950
CONECT  934  933
CONECT  935  933
CONECT  943  942
CONECT  955  954
CONECT  941  944  939  942
CONECT  946  947  944  948
CONECT  930  929
CONECT  945  944
CONECT  954  952  955
CONECT  931  929
CONECT  958  956  959
CONECT  949  948
CONECT  938  936  939
CONECT  932  933  929
CONECT  929  931  932  928  930
CONECT  992  993  990
CONECT  959  958  960  962  961
CONECT  993  992  994  995  996
END
```

3P-5’-hpRNA:

ATOM	1	O5'	GUA	B	1	-0.954	-9.110	8.904	1.00	10.00	B	O
ATOM	2	C5'	GUA	B	1	-1.166	-8.376	7.685	1.00	10.00	B	C
ATOM	3	H5'	GUA	B	1	-1.014	-7.312	7.868	1.00	10.00	B	H
ATOM	4	H5''	GUA	B	1	-2.187	-8.528	7.340	1.00	10.00	B	H
ATOM	5	C4'	GUA	B	1	-0.213	-8.833	6.602	1.00	10.00	B	C
ATOM	6	H4'	GUA	B	1	0.607	-8.115	6.571	1.00	10.00	B	H
ATOM	7	O4'	GUA	B	1	0.217	-10.186	6.871	1.00	10.00	B	O
ATOM	8	C1'	GUA	B	1	0.421	-10.870	5.655	1.00	10.00	B	C
ATOM	9	H1'	GUA	B	1	1.487	-11.105	5.608	1.00	10.00	B	H
ATOM	10	N9	GUA	B	1	-0.300	-12.132	5.731	1.00	10.00	B	N
ATOM	11	C4	GUA	B	1	-0.531	-13.030	4.714	1.00	10.00	B	C
ATOM	12	N3	GUA	B	1	-0.160	-12.885	3.423	1.00	10.00	B	N
ATOM	13	C2	GUA	B	1	-0.515	-13.927	2.688	1.00	10.00	B	C
ATOM	14	N2	GUA	B	1	-0.235	-13.942	1.380	1.00	10.00	B	N
ATOM	15	H21	GUA	B	1	0.245	-13.163	0.949	1.00	10.00	B	H
ATOM	16	H22	GUA	B	1	-0.508	-14.733	0.806	1.00	10.00	B	H
ATOM	17	N1	GUA	B	1	-1.172	-15.027	3.183	1.00	10.00	B	N
ATOM	18	H1	GUA	B	1	-1.405	-15.780	2.547	1.00	10.00	B	H
ATOM	19	C6	GUA	B	1	-1.557	-15.200	4.507	1.00	10.00	B	C
ATOM	20	O6	GUA	B	1	-2.134	-16.239	4.855	1.00	10.00	B	O
ATOM	21	C5	GUA	B	1	-1.194	-14.087	5.302	1.00	10.00	B	C
ATOM	22	N7	GUA	B	1	-1.399	-13.848	6.653	1.00	10.00	B	N
ATOM	23	C8	GUA	B	1	-0.862	-12.678	6.857	1.00	10.00	B	C
ATOM	24	H8	GUA	B	1	-0.863	-12.182	7.820	1.00	10.00	B	H
ATOM	25	C2'	GUA	B	1	0.002	-9.964	4.494	1.00	10.00	B	C
ATOM	26	H2'	GUA	B	1	-0.623	-10.498	3.775	1.00	10.00	B	H
ATOM	27	O2'	GUA	B	1	1.179	-9.442	3.910	1.00	10.00	B	O
ATOM	28	HO2'	GUA	B	1	1.132	-8.485	4.012	1.00	10.00	B	H
ATOM	29	C3'	GUA	B	1	-0.806	-8.870	5.197	1.00	10.00	B	C
ATOM	30	H3'	GUA	B	1	-1.870	-9.082	5.216	1.00	10.00	B	H
ATOM	31	O3'	GUA	B	1	-0.607	-7.625	4.542	1.00	10.00	B	O
ATOM	32	P	ADE	B	2	-1.860	-6.855	3.903	1.00	10.00	B	P
ATOM	33	O1P	ADE	B	2	-1.613	-5.398	4.016	1.00	10.00	B	O
ATOM	34	O2P	ADE	B	2	-3.103	-7.429	4.463	1.00	10.00	B	O
ATOM	35	O5'	ADE	B	2	-1.807	-7.230	2.358	1.00	10.00	B	O
ATOM	36	C5'	ADE	B	2	-0.564	-7.372	1.678	1.00	10.00	B	C
ATOM	37	H5'	ADE	B	2	0.235	-7.546	2.402	1.00	10.00	B	H
ATOM	38	H5''	ADE	B	2	-0.343	-6.464	1.115	1.00	10.00	B	H
ATOM	39	C4'	ADE	B	2	-0.634	-8.538	0.726	1.00	10.00	B	C
ATOM	40	H4'	ADE	B	2	0.185	-8.431	0.013	1.00	10.00	B	H
ATOM	41	O4'	ADE	B	2	-0.585	-9.773	1.485	1.00	10.00	B	O
ATOM	42	C1'	ADE	B	2	-1.407	-10.744	0.865	1.00	10.00	B	C
ATOM	43	H1'	ADE	B	2	-0.784	-11.620	0.683	1.00	10.00	B	H
ATOM	44	N9	ADE	B	2	-2.452	-11.119	1.818	1.00	10.00	B	N
ATOM	45	C4	ADE	B	2	-3.266	-12.226	1.762	1.00	10.00	B	C
ATOM	46	N3	ADE	B	2	-3.290	-13.178	0.814	1.00	10.00	B	N
ATOM	47	C2	ADE	B	2	-4.206	-14.104	1.100	1.00	10.00	B	C
ATOM	48	H2	ADE	B	2	-4.297	-14.914	0.375	1.00	10.00	B	H
ATOM	49	N1	ADE	B	2	-5.035	-14.178	2.152	1.00	10.00	B	N
ATOM	50	C6	ADE	B	2	-4.986	-13.207	3.086	1.00	10.00	B	C
ATOM	51	N6	ADE	B	2	-5.809	-13.287	4.132	1.00	10.00	B	N
ATOM	52	H61	ADE	B	2	-5.799	-12.582	4.856	1.00	10.00	B	H
ATOM	53	H62	ADE	B	2	-6.447	-14.070	4.211	1.00	10.00	B	H
ATOM	54	C5	ADE	B	2	-4.060	-12.166	2.896	1.00	10.00	B	C
ATOM	55	N7	ADE	B	2	-3.762	-11.041	3.647	1.00	10.00	B	N
ATOM	56	C8	ADE	B	2	-2.811	-10.449	2.964	1.00	10.00	B	C
ATOM	57	H8	ADE	B	2	-2.359	-9.514	3.268	1.00	10.00	B	H
ATOM	58	C2'	ADE	B	2	-1.940	-10.132	-0.432	1.00	10.00	B	C
ATOM	59	H2'	ADE	B	2	-2.956	-10.466	-0.650	1.00	10.00	B	H
ATOM	60	O2'	ADE	B	2	-1.029	-10.419	-1.477	1.00	10.00	B	O
ATOM	61	HO2'	ADE	B	2	-0.335	-10.973	-1.102	1.00	10.00	B	H
ATOM	62	C3'	ADE	B	2	-1.917	-8.647	-0.087	1.00	10.00	B	C
ATOM	63	H3'	ADE	B	2	-2.778	-8.351	0.504	1.00	10.00	B	H
ATOM	64	O3'	ADE	B	2	-1.873	-7.839	-1.254	1.00	10.00	B	O
ATOM	65	P	ADE	B	3	-3.242	-7.292	-1.884	1.00	10.00	B	P
ATOM	66	O1P	ADE	B	3	-2.919	-6.302	-2.939	1.00	10.00	B	O
ATOM	67	O2P	ADE	B	3	-4.145	-6.908	-0.773	1.00	10.00	B	O
ATOM	68	O5'	ADE	B	3	-3.878	-8.562	-2.600	1.00	10.00	B	O
ATOM	69	C5'	ADE	B	3	-3.143	-9.295	-3.574	1.00	10.00	B	C
ATOM	70	H5'	ADE	B	3	-2.152	-9.535	-3.185	1.00	10.00	B	H
ATOM	71	H5''	ADE	B	3	-3.033	-8.700	-4.479	1.00	10.00	B	H
ATOM	72	C4'	ADE	B	3	-3.869	-10.575	-3.911	1.00	10.00	B	C
ATOM	73	H4'	ADE	B	3	-3.362	-11.020	-4.767	1.00	10.00	B	H
ATOM	74	O4'	ADE	B	3	-3.891	-11.433	-2.743	1.00	10.00	B	O
ATOM	75	C1'	ADE	B	3	-5.094	-12.179	-2.727	1.00	10.00	B	C
ATOM	76	H1'	ADE	B	3	-4.818	-13.234	-2.705	1.00	10.00	B	H
ATOM	77	N9	ADE	B	3	-5.785	-11.869	-1.478	1.00	10.00	B	N
ATOM	78	C4	ADE	B	3	-6.803	-12.578	-0.887	1.00	10.00	B	C
ATOM	79	N3	ADE	B	3	-7.395	-13.695	-1.344	1.00	10.00	B	N
ATOM	80	C2	ADE	B	3	-8.336	-14.107	-0.495	1.00	10.00	B	C
ATOM	81	H2	ADE	B	3	-8.873	-15.010	-0.792	1.00	10.00	B	H
ATOM	82	N1	ADE	B	3	-8.718	-13.570	0.673	1.00	10.00	B	N
ATOM	83	C6	ADE	B	3	-8.099	-12.451	1.104	1.00	10.00	B	C
ATOM	84	N6	ADE	B	3	-8.466	-11.923	2.272	1.00	10.00	B	N
ATOM	85	H61	ADE	B	3	-8.005	-11.089	2.608	1.00	10.00	B	H
ATOM	86	H62	ADE	B	3	-9.178	-12.366	2.837	1.00	10.00	B	H
ATOM	87	C5	ADE	B	3	-7.090	-11.910	0.291	1.00	10.00	B	C
ATOM	88	N7	ADE	B	3	-6.280	-10.792	0.433	1.00	10.00	B	N
ATOM	89	C8	ADE	B	3	-5.531	-10.810	-0.643	1.00	10.00	B	C
ATOM	90	H8	ADE	B	3	-4.785	-10.057	-0.857	1.00	10.00	B	H
ATOM	91	C2'	ADE	B	3	-5.885	-11.815	-3.985	1.00	10.00	B	C
ATOM	92	H2'	ADE	B	3	-6.958	-11.768	-3.787	1.00	10.00	B	H
ATOM	93	O2'	ADE	B	3	-5.556	-12.738	-5.007	1.00	10.00	B	O

```
ATOM      94 HO2' ADE B   3      -4.593 -12.815  -5.021  1.00 10.00      B    H
ATOM      95  C3' ADE B   3      -5.334 -10.427  -4.297  1.00 10.00      B    C
ATOM      96  H3' ADE B   3      -5.824  -9.645  -3.723  1.00 10.00      B    H
ATOM      97  O3' ADE B   3      -5.462 -10.126  -5.680  1.00 10.00      B    O
TER       98      ADE B   3
HETATM    99  P   URI B   4      -9.158  -7.547  -4.716  1.00 10.00      B    P
HETATM   100  O1P URI B   4      -9.038  -6.723  -5.944  1.00 10.00      B    O
HETATM   101  O2P URI B   4      -8.687  -6.992  -3.425  1.00 10.00      B    O
HETATM   102  O5' URI B   4      -8.337  -8.886  -4.973  1.00 10.00      B    O
HETATM   103  C5' URI B   4      -8.681  -9.762  -6.044  1.00 10.00      B    C
HETATM   104  H5' URI B   4      -7.773 -10.126  -6.528  1.00 10.00      B    H
HETATM   105 H5'' URI B   4      -9.284  -9.229  -6.778  1.00 10.00      B    H
HETATM   106  C4' URI B   4      -9.470 -10.937  -5.521  1.00 10.00      B    C
HETATM   107  H4' URI B   4      -9.444 -11.720  -6.279  1.00 10.00      B    H
HETATM   108  O4' URI B   4      -8.932 -11.352  -4.238  1.00 10.00      B    O
HETATM   109  C1' URI B   4      -9.979 -11.860  -3.429  1.00 10.00      B    C
HETATM   110  H1' URI B   4      -9.718 -12.887  -3.175  1.00 10.00      B    H
HETATM   111  N1  URI B   4     -10.020 -11.081  -2.186  1.00 10.00      B    N
HETATM   112  C6  URI B   4      -9.257  -9.944  -2.024  1.00 10.00      B    C
HETATM   113  H6  URI B   4      -8.621  -9.617  -2.846  1.00 10.00      B    H
HETATM   114  C2  URI B   4     -10.851 -11.532  -1.177  1.00 10.00      B    C
HETATM   115  O2  URI B   4     -11.544 -12.530  -1.289  1.00 10.00      B    O
HETATM   116  N3  URI B   4     -10.839 -10.772  -0.035  1.00 10.00      B    N
HETATM   117  H3  URI B   4     -11.433 -11.074   0.727  1.00 10.00      B    H
HETATM   118  C4  URI B   4     -10.100  -9.632   0.200  1.00 10.00      B    C
HETATM   119  O4  URI B   4     -10.184  -9.069   1.294  1.00 10.00      B    O
HETATM   120  C5  URI B   4      -9.271  -9.227  -0.893  1.00 10.00      B    C
HETATM   121  H5  URI B   4      -8.652  -8.334  -0.806  1.00 10.00      B    H
HETATM   122  C2' URI B   4     -11.272 -11.778  -4.247  1.00 10.00      B    C
HETATM   123  H2' URI B   4     -12.125 -11.504  -3.622  1.00 10.00      B    H
HETATM   124  O2' URI B   4     -11.470 -12.995  -4.939  1.00 10.00      B    O
HETATM   125 HO2' URI B   4     -10.937 -13.661  -4.499  1.00 10.00      B    H
HETATM   126  C3' URI B   4     -10.935 -10.657  -5.222  1.00 10.00      B    C
HETATM   127  H3' URI B   4     -11.074  -9.671  -4.786  1.00 10.00      B    H
HETATM   128  O3' URI B   4     -11.719 -10.746  -6.401  1.00 10.00      B    O
ATOM     129  P   ADE B   5     -12.898  -9.690  -6.646  1.00 10.00      B    P
ATOM     130  O1P ADE B   5     -13.297  -9.789  -8.069  1.00 10.00      B    O
ATOM     131  O2P ADE B   5     -12.477  -8.382  -6.095  1.00 10.00      B    O
ATOM     132  O5' ADE B   5     -14.097 -10.236  -5.755  1.00 10.00      B    O
ATOM     133  C5' ADE B   5     -15.021 -11.182  -6.279  1.00 10.00      B    C
ATOM     134  H5' ADE B   5     -14.478 -12.009  -6.740  1.00 10.00      B    H
ATOM     135 H5'' ADE B   5     -15.650 -10.706  -7.030  1.00 10.00      B    H
ATOM     136  C4' ADE B   5     -15.896 -11.719  -5.172  1.00 10.00      B    C
ATOM     137  H4' ADE B   5     -16.468 -12.555  -5.576  1.00 10.00      B    H
ATOM     138  O4' ADE B   5     -15.063 -12.080  -4.040  1.00 10.00      B    O
ATOM     139  C1' ADE B   5     -15.745 -11.786  -2.837  1.00 10.00      B    C
ATOM     140  H1' ADE B   5     -15.778 -12.709  -2.257  1.00 10.00      B    H
ATOM     141  N9  ADE B   5     -14.957 -10.810  -2.086  1.00 10.00      B    N
ATOM     142  C4  ADE B   5     -15.146 -10.455  -0.773  1.00 10.00      B    C
ATOM     143  N3  ADE B   5     -16.083 -10.922   0.067  1.00 10.00      B    N
ATOM     144  C2  ADE B   5     -15.965 -10.354   1.264  1.00 10.00      B    C
ATOM     145  H2  ADE B   5     -16.691 -10.681   2.007  1.00 10.00      B    H
ATOM     146  N1  ADE B   5     -15.078  -9.439   1.687  1.00 10.00      B    N
ATOM     147  C6  ADE B   5     -14.147  -8.992   0.818  1.00 10.00      B    C
ATOM     148  N6  ADE B   5     -13.261  -8.087   1.239  1.00 10.00      B    N
ATOM     149  H61 ADE B   5     -12.559  -7.751   0.595  1.00 10.00      B    H
ATOM     150  H62 ADE B   5     -13.281  -7.744   2.188  1.00 10.00      B    H
ATOM     151  C5  ADE B   5     -14.169  -9.517  -0.491  1.00 10.00      B    C
ATOM     152  N7  ADE B   5     -13.379  -9.280  -1.607  1.00 10.00      B    N
ATOM     153  C8  ADE B   5     -13.889 -10.067  -2.526  1.00 10.00      B    C
ATOM     154  H8  ADE B   5     -13.510 -10.121  -3.538  1.00 10.00      B    H
ATOM     155  C2' ADE B   5     -17.143 -11.287  -3.203  1.00 10.00      B    C
ATOM     156  H2' ADE B   5     -17.482 -10.501  -2.525  1.00 10.00      B    H
ATOM     157  O2' ADE B   5     -18.025 -12.395  -3.246  1.00 10.00      B    O
ATOM     158 HO2' ADE B   5     -17.472 -13.188  -3.257  1.00 10.00      B    H
ATOM     159  C3' ADE B   5     -16.905 -10.730  -4.601  1.00 10.00      B    C
ATOM     160  H3' ADE B   5     -16.501  -9.719  -4.581  1.00 10.00      B    H
ATOM     161  O3' ADE B   5     -18.103 -10.721  -5.361  1.00 10.00      B    O
HETATM   162  P   URI B   6     -18.822  -9.324  -5.686  1.00 10.00      B    P
HETATM   163  O1P URI B   6     -19.667  -9.544  -6.884  1.00 10.00      B    O
HETATM   164  O2P URI B   6     -17.795  -8.259  -5.702  1.00 10.00      B    O
HETATM   165  O5' URI B   6     -19.778  -9.082  -4.439  1.00 10.00      B    O
HETATM   166  C5' URI B   6     -20.985  -9.822  -4.301  1.00 10.00      B    C
HETATM   167  H5' URI B   6     -20.844 -10.831  -4.687  1.00 10.00      B    H
HETATM   168 H5'' URI B   6     -21.783  -9.338  -4.863  1.00 10.00      B    H
HETATM   169  C4' URI B   6     -21.391  -9.899  -2.848  1.00 10.00      B    C
HETATM   170  H4' URI B   6     -22.164 -10.660  -2.757  1.00 10.00      B    H
HETATM   171  O4' URI B   6     -20.216 -10.156  -2.034  1.00 10.00      B    O
HETATM   172  C1' URI B   6     -20.344  -9.483  -0.794  1.00 10.00      B    C
HETATM   173  H1' URI B   6     -20.287 -10.246  -0.016  1.00 10.00      B    H
HETATM   174  N1  URI B   6     -19.196  -8.585  -0.622  1.00 10.00      B    N
HETATM   175  C6  URI B   6     -18.338  -8.304  -1.661  1.00 10.00      B    C
HETATM   176  H6  URI B   6     -18.528  -8.754  -2.635  1.00 10.00      B    H
HETATM   177  C2  URI B   6     -19.007  -8.036   0.628  1.00 10.00      B    C
HETATM   178  O2  URI B   6     -19.755  -8.259   1.565  1.00 10.00      B    O
HETATM   179  N3  URI B   6     -17.916  -7.215   0.741  1.00 10.00      B    N
HETATM   180  H3  URI B   6     -17.749  -6.803   1.653  1.00 10.00      B    H
HETATM   181  C4  URI B   6     -17.013  -6.891  -0.247  1.00 10.00      B    C
HETATM   182  O4  URI B   6     -16.072  -6.140   0.016  1.00 10.00      B    O
HETATM   183  C5  URI B   6     -17.281  -7.496  -1.516  1.00 10.00      B    C
HETATM   184  H5  URI B   6     -16.622  -7.300  -2.364  1.00 10.00      B    H
HETATM   185  C2' URI B   6     -21.693  -8.768  -0.786  1.00 10.00      B    C
HETATM   186  H2' URI B   6     -21.629  -7.793  -0.300  1.00 10.00      B    H
HETATM   187  O2' URI B   6     -22.638  -9.624  -0.173  1.00 10.00      B    O
HETATM   188 HO2' URI B   6     -22.130 -10.252   0.351  1.00 10.00      B    H
```

```
HETATM  189  C3' URI B   6     -21.962  -8.610  -2.279  1.00 10.00      B    C
HETATM  190  H3' URI B   6     -21.466  -7.739  -2.697  1.00 10.00      B    H
HETATM  191  O3' URI B   6     -23.350  -8.511  -2.550  1.00 10.00      B    O
ATOM    192  P   ADE B   7     -23.971  -7.104  -3.003  1.00 10.00      B    P
ATOM    193  O1P ADE B   7     -25.301  -7.394  -3.589  1.00 10.00      B    O
ATOM    194  O2P ADE B   7     -22.955  -6.383  -3.806  1.00 10.00      B    O
ATOM    195  O5' ADE B   7     -24.190  -6.310  -1.642  1.00 10.00      B    O
ATOM    196  C5' ADE B   7     -25.448  -6.341  -0.974  1.00 10.00      B    C
ATOM    197  H5' ADE B   7     -25.831  -7.363  -0.958  1.00 10.00      B    H
ATOM    198 H5'' ADE B   7     -26.160  -5.705  -1.500  1.00 10.00      B    H
ATOM    199  C4' ADE B   7     -25.300  -5.843   0.442  1.00 10.00      B    C
ATOM    200  H4' ADE B   7     -26.197  -6.135   0.986  1.00 10.00      B    H
ATOM    201  O4' ADE B   7     -24.078  -6.379   1.012  1.00 10.00      B    O
ATOM    202  C1' ADE B   7     -23.505  -5.425   1.887  1.00 10.00      B    C
ATOM    203  H1' ADE B   7     -23.395  -5.907   2.859  1.00 10.00      B    H
ATOM    204  N9  ADE B   7     -22.170  -5.103   1.386  1.00 10.00      B    N
ATOM    205  C4  ADE B   7     -21.163  -4.473   2.078  1.00 10.00      B    C
ATOM    206  N3  ADE B   7     -21.205  -4.014   3.341  1.00 10.00      B    N
ATOM    207  C2  ADE B   7     -20.038  -3.465   3.680  1.00 10.00      B    C
ATOM    208  H2  ADE B   7     -19.989  -3.062   4.692  1.00 10.00      B    H
ATOM    209  N1  ADE B   7     -18.918  -3.335   2.952  1.00 10.00      B    N
ATOM    210  C6  ADE B   7     -18.911  -3.807   1.687  1.00 10.00      B    C
ATOM    211  N6  ADE B   7     -17.795  -3.682   0.963  1.00 10.00      B    N
ATOM    212  H61 ADE B   7     -17.774  -4.033   0.016  1.00 10.00      B    H
ATOM    213  H62 ADE B   7     -16.970  -3.248   1.353  1.00 10.00      B    H
ATOM    214  C5  ADE B   7     -20.089  -4.409   1.206  1.00 10.00      B    C
ATOM    215  N7  ADE B   7     -20.415  -4.980  -0.017  1.00 10.00      B    N
ATOM    216  C8  ADE B   7     -21.657  -5.372   0.142  1.00 10.00      B    C
ATOM    217  H8  ADE B   7     -22.227  -5.859  -0.637  1.00 10.00      B    H
ATOM    218  C2' ADE B   7     -24.448  -4.221   1.942  1.00 10.00      B    C
ATOM    219  H2' ADE B   7     -23.899  -3.280   2.012  1.00 10.00      B    H
ATOM    220  O2' ADE B   7     -25.351  -4.413   3.013  1.00 10.00      B    O
ATOM    221 HO2' ADE B   7     -24.877  -4.954   3.657  1.00 10.00      B    H
ATOM    222  C3' ADE B   7     -25.165  -4.336   0.601  1.00 10.00      B    C
ATOM    223  H3' ADE B   7     -24.587  -3.903  -0.211  1.00 10.00      B    H
ATOM    224  O3' ADE B   7     -26.437  -3.705   0.636  1.00 10.00      B    O
ATOM    225  P   ADE B   8     -26.659  -2.333  -0.165  1.00 10.00      B    P
ATOM    226  O1P ADE B   8     -28.058  -2.318  -0.655  1.00 10.00      B    O
ATOM    227  O2P ADE B   8     -25.545  -2.179  -1.129  1.00 10.00      B    O
ATOM    228  O5' ADE B   8     -26.510  -1.205   0.946  1.00 10.00      B    O
ATOM    229  C5' ADE B   8     -27.100  -1.369   2.229  1.00 10.00      B    C
ATOM    230  H5' ADE B   8     -27.186  -2.431   2.459  1.00 10.00      B    H
ATOM    231 H5'' ADE B   8     -28.092  -0.923   2.240  1.00 10.00      B    H
ATOM    232  C4' ADE B   8     -26.252  -0.702   3.282  1.00 10.00      B    C
ATOM    233  H4' ADE B   8     -26.851  -0.634   4.190  1.00 10.00      B    H
ATOM    234  O4' ADE B   8     -25.027  -1.461   3.455  1.00 10.00      B    O
ATOM    235  C1' ADE B   8     -23.946  -0.577   3.674  1.00 10.00      B    C
ATOM    236  H1' ADE B   8     -23.451  -0.901   4.591  1.00 10.00      B    H
ATOM    237  N9  ADE B   8     -23.003  -0.739   2.572  1.00 10.00      B    N
ATOM    238  C4  ADE B   8     -21.669  -0.408   2.565  1.00 10.00      B    C
ATOM    239  N3  ADE B   8     -20.960   0.148   3.564  1.00 10.00      B    N
ATOM    240  C2  ADE B   8     -19.691   0.319   3.198  1.00 10.00      B    C
ATOM    241  H2  ADE B   8     -19.042   0.767   3.952  1.00 10.00      B    H
ATOM    242  N1  ADE B   8     -19.096   0.019   2.036  1.00 10.00      B    N
ATOM    243  C6  ADE B   8     -19.837  -0.539   1.054  1.00 10.00      B    C
ATOM    244  N6  ADE B   8     -19.246  -0.840  -0.101  1.00 10.00      B    N
ATOM    245  H61 ADE B   8     -19.785  -1.258  -0.844  1.00 10.00      B    H
ATOM    246  H62 ADE B   8     -18.255  -0.668  -0.225  1.00 10.00      B    H
ATOM    247  C5  ADE B   8     -21.198  -0.770   1.315  1.00 10.00      B    C
ATOM    248  N7  ADE B   8     -22.217  -1.311   0.545  1.00 10.00      B    N
ATOM    249  C8  ADE B   8     -23.264  -1.265   1.333  1.00 10.00      B    C
ATOM    250  H8  ADE B   8     -24.245  -1.607   1.034  1.00 10.00      B    H
ATOM    251  C2' ADE B   8     -24.520   0.835   3.795  1.00 10.00      B    C
ATOM    252  H2' ADE B   8     -23.846   1.583   3.369  1.00 10.00      B    H
ATOM    253  O2' ADE B   8     -24.830   1.083   5.153  1.00 10.00      B    O
ATOM    254 HO2' ADE B   8     -24.731   0.231   5.602  1.00 10.00      B    H
ATOM    255  C3' ADE B   8     -25.788   0.713   2.957  1.00 10.00      B    C
ATOM    256  H3' ADE B   8     -25.596   0.835   1.893  1.00 10.00      B    H
ATOM    257  O3' ADE B   8     -26.760   1.668   3.352  1.00 10.00      B    O
HETATM  258  P   URI B   9     -26.879   3.049   2.549  1.00 10.00      B    P
HETATM  259  O1P URI B   9     -27.939   3.851   3.206  1.00 10.00      B    O
HETATM  260  O2P URI B   9     -26.989   2.736   1.106  1.00 10.00      B    O
HETATM  261  O5' URI B   9     -25.488   3.772   2.821  1.00 10.00      B    O
HETATM  262  C5' URI B   9     -25.227   4.386   4.080  1.00 10.00      B    C
HETATM  263  H5' URI B   9     -25.473   3.690   4.884  1.00 10.00      B    H
HETATM  264 H5'' URI B   9     -25.837   5.281   4.187  1.00 10.00      B    H
HETATM  265  C4' URI B   9     -23.772   4.769   4.185  1.00 10.00      B    C
HETATM  266  H4' URI B   9     -23.609   5.174   5.186  1.00 10.00      B    H
HETATM  267  O4' URI B   9     -22.947   3.614   3.888  1.00 10.00      B    O
HETATM  268  C1' URI B   9     -21.771   4.029   3.219  1.00 10.00      B    C
HETATM  269  H1' URI B   9     -20.925   3.672   3.808  1.00 10.00      B    H
HETATM  270  N1  URI B   9     -21.727   3.356   1.915  1.00 10.00      B    N
HETATM  271  C6  URI B   9     -22.863   2.823   1.353  1.00 10.00      B    C
HETATM  272  H6  URI B   9     -23.808   2.919   1.889  1.00 10.00      B    H
HETATM  273  C2  URI B   9     -20.506   3.272   1.273  1.00 10.00      B    C
HETATM  274  O2  URI B   9     -19.483   3.742   1.738  1.00 10.00      B    O
HETATM  275  N3  URI B   9     -20.528   2.618   0.067  1.00 10.00      B    N
HETATM  276  H3  URI B   9     -19.636   2.556  -0.408  1.00 10.00      B    H
HETATM  277  C4  URI B   9     -21.625   2.055  -0.551  1.00 10.00      B    C
HETATM  278  O4  URI B   9     -21.485   1.482  -1.635  1.00 10.00      B    O
HETATM  279  C5  URI B   9     -22.851   2.193   0.175  1.00 10.00      B    C
HETATM  280  H5  URI B   9     -23.776   1.781  -0.233  1.00 10.00      B    H
HETATM  281  C2' URI B   9     -21.803   5.556   3.128  1.00 10.00      B    C
HETATM  282  H2' URI B   9     -21.388   5.916   2.186  1.00 10.00      B    H
HETATM  283  O2' URI B   9     -21.136   6.083   4.260  1.00 10.00      B    O
```

HETATM	284	HO2'	URI	B	9	-21.056	5.358	4.893	1.00	10.00	B	H
HETATM	285	C3'	URI	B	9	-23.302	5.832	3.200	1.00	10.00	B	C
HETATM	286	H3'	URI	B	9	-23.788	5.721	2.233	1.00	10.00	B	H
HETATM	287	O3'	URI	B	9	-23.577	7.132	3.697	1.00	10.00	B	O
ATOM	288	P	ADE	B	10	-24.448	8.149	2.814	1.00	10.00	B	P
ATOM	289	O1P	ADE	B	10	-24.878	9.248	3.711	1.00	10.00	B	O
ATOM	290	O2P	ADE	B	10	-25.468	7.379	2.064	1.00	10.00	B	O
ATOM	291	O5'	ADE	B	10	-23.403	8.735	1.767	1.00	10.00	B	O
ATOM	292	C5'	ADE	B	10	-22.913	10.065	1.899	1.00	10.00	B	C
ATOM	293	H5'	ADE	B	10	-22.894	10.348	2.954	1.00	10.00	B	H
ATOM	294	H5''	ADE	B	10	-23.566	10.751	1.361	1.00	10.00	B	H
ATOM	295	C4'	ADE	B	10	-21.520	10.168	1.330	1.00	10.00	B	C
ATOM	296	H4'	ADE	B	10	-21.004	10.966	1.862	1.00	10.00	B	H
ATOM	297	O4'	ADE	B	10	-20.861	8.878	1.436	1.00	10.00	B	O
ATOM	298	C1'	ADE	B	10	-19.995	8.696	0.331	1.00	10.00	B	C
ATOM	299	H1'	ADE	B	10	-18.991	8.538	0.732	1.00	10.00	B	H
ATOM	300	N9	ADE	B	10	-20.395	7.482	-0.375	1.00	10.00	B	N
ATOM	301	C4	ADE	B	10	-19.700	6.877	-1.393	1.00	10.00	B	C
ATOM	302	N3	ADE	B	10	-18.532	7.274	-1.925	1.00	10.00	B	N
ATOM	303	C2	ADE	B	10	-18.157	6.448	-2.898	1.00	10.00	B	C
ATOM	304	H2	ADE	B	10	-17.216	6.701	-3.388	1.00	10.00	B	H
ATOM	305	N1	ADE	B	10	-18.773	5.350	-3.361	1.00	10.00	B	N
ATOM	306	C6	ADE	B	10	-19.943	4.978	-2.799	1.00	10.00	B	C
ATOM	307	N6	ADE	B	10	-20.550	3.884	-3.256	1.00	10.00	B	N
ATOM	308	H61	ADE	B	10	-21.427	3.584	-2.848	1.00	10.00	B	H
ATOM	309	H62	ADE	B	10	-20.132	3.356	-4.011	1.00	10.00	B	H
ATOM	310	C5	ADE	B	10	-20.449	5.774	-1.759	1.00	10.00	B	C
ATOM	311	N7	ADE	B	10	-21.598	5.683	-0.986	1.00	10.00	B	N
ATOM	312	C8	ADE	B	10	-21.519	6.717	-0.182	1.00	10.00	B	C
ATOM	313	H8	ADE	B	10	-22.271	6.951	0.559	1.00	10.00	B	H
ATOM	314	C2'	ADE	B	10	-20.078	9.950	-0.541	1.00	10.00	B	C
ATOM	315	H2'	ADE	B	10	-20.049	9.706	-1.603	1.00	10.00	B	H
ATOM	316	O2'	ADE	B	10	-19.041	10.827	-0.154	1.00	10.00	B	O
ATOM	317	HO2'	ADE	B	10	-18.410	10.304	0.358	1.00	10.00	B	H
ATOM	318	C3'	ADE	B	10	-21.444	10.508	-0.152	1.00	10.00	B	C
ATOM	319	H3'	ADE	B	10	-22.254	10.040	-0.706	1.00	10.00	B	H
ATOM	320	O3'	ADE	B	10	-21.511	11.910	-0.361	1.00	10.00	B	O
ATOM	321	P	GUA	B	11	-22.376	12.487	-1.584	1.00	10.00	B	P
ATOM	322	O1P	GUA	B	11	-22.597	13.933	-1.347	1.00	10.00	B	O
ATOM	323	O2P	GUA	B	11	-23.538	11.596	-1.795	1.00	10.00	B	O
ATOM	324	O5'	GUA	B	11	-21.414	12.347	-2.841	1.00	10.00	B	O
ATOM	325	C5'	GUA	B	11	-20.210	13.103	-2.919	1.00	10.00	B	C
ATOM	326	H5'	GUA	B	11	-19.727	13.131	-1.942	1.00	10.00	B	H
ATOM	327	H5''	GUA	B	11	-20.434	14.123	-3.231	1.00	10.00	B	H
ATOM	328	C4'	GUA	B	11	-19.274	12.482	-3.922	1.00	10.00	B	C
ATOM	329	H4'	GUA	B	11	-18.382	13.104	-3.971	1.00	10.00	B	H
ATOM	330	O4'	GUA	B	11	-19.006	11.105	-3.547	1.00	10.00	B	O
ATOM	331	C1'	GUA	B	11	-18.868	10.314	-4.715	1.00	10.00	B	C
ATOM	332	H1'	GUA	B	11	-17.888	9.840	-4.664	1.00	10.00	B	H
ATOM	333	N9	GUA	B	11	-19.878	9.262	-4.677	1.00	10.00	B	N
ATOM	334	C4	GUA	B	11	-19.890	8.112	-5.429	1.00	10.00	B	C
ATOM	335	N3	GUA	B	11	-18.964	7.754	-6.344	1.00	10.00	B	N
ATOM	336	C2	GUA	B	11	-19.247	6.593	-6.908	1.00	10.00	B	C
ATOM	337	N2	GUA	B	11	-18.427	6.099	-7.850	1.00	10.00	B	N
ATOM	338	H21	GUA	B	11	-17.600	6.611	-8.129	1.00	10.00	B	H
ATOM	339	H22	GUA	B	11	-18.619	5.205	-8.288	1.00	10.00	B	H
ATOM	340	N1	GUA	B	11	-20.351	5.835	-6.592	1.00	10.00	B	N
ATOM	341	H1	GUA	B	11	-20.483	4.956	-7.069	1.00	10.00	B	H
ATOM	342	C6	GUA	B	11	-21.321	6.183	-5.655	1.00	10.00	B	C
ATOM	343	O6	GUA	B	11	-22.283	5.423	-5.449	1.00	10.00	B	O
ATOM	344	C5	GUA	B	11	-21.029	7.434	-5.044	1.00	10.00	B	C
ATOM	345	N7	GUA	B	11	-21.719	8.145	-4.068	1.00	10.00	B	N
ATOM	346	C8	GUA	B	11	-21.001	9.220	-3.888	1.00	10.00	B	C
ATOM	347	H8	GUA	B	11	-21.264	10.004	-3.191	1.00	10.00	B	H
ATOM	348	C2'	GUA	B	11	-18.990	11.247	-5.920	1.00	10.00	B	C
ATOM	349	H2'	GUA	B	11	-19.510	10.770	-6.754	1.00	10.00	B	H
ATOM	350	O2'	GUA	B	11	-17.697	11.706	-6.267	1.00	10.00	B	O
ATOM	351	HO2'	GUA	B	11	-17.060	11.156	-5.793	1.00	10.00	B	H
ATOM	352	C3'	GUA	B	11	-19.822	12.384	-5.338	1.00	10.00	B	C
ATOM	353	H3'	GUA	B	11	-20.885	12.155	-5.335	1.00	10.00	B	H
ATOM	354	O3'	GUA	B	11	-19.625	13.602	-6.041	1.00	10.00	B	O
HETATM	355	P	URI	B	12	-20.776	14.147	-7.013	1.00	10.00	B	P
HETATM	356	O1P	URI	B	12	-20.195	15.248	-7.818	1.00	10.00	B	O
HETATM	357	O2P	URI	B	12	-21.982	14.401	-6.191	1.00	10.00	B	O
HETATM	358	O5'	URI	B	12	-21.070	12.916	-7.977	1.00	10.00	B	O
HETATM	359	C5'	URI	B	12	-22.309	12.808	-8.667	1.00	10.00	B	C
HETATM	360	H5'	URI	B	12	-22.784	13.788	-8.728	1.00	10.00	B	H
HETATM	361	H5''	URI	B	12	-22.971	12.126	-8.133	1.00	10.00	B	H
HETATM	362	C4'	URI	B	12	-22.075	12.278	-10.064	1.00	10.00	B	C
HETATM	363	H4'	URI	B	12	-23.044	12.210	-10.557	1.00	10.00	B	H
HETATM	364	O4'	URI	B	12	-21.133	13.144	-10.749	1.00	10.00	B	O
HETATM	365	C1'	URI	B	12	-20.319	12.371	-11.613	1.00	10.00	B	C
HETATM	366	H1'	URI	B	12	-20.460	12.771	-12.620	1.00	10.00	B	H
HETATM	367	N1	URI	B	12	-18.915	12.596	-11.237	1.00	10.00	B	N
HETATM	368	C6	URI	B	12	-18.585	13.147	-10.019	1.00	10.00	B	C
HETATM	369	H6	URI	B	12	-19.385	13.390	-9.317	1.00	10.00	B	H
HETATM	370	C2	URI	B	12	-17.938	12.249	-12.149	1.00	10.00	B	C
HETATM	371	O2	URI	B	12	-18.191	11.738	-13.226	1.00	10.00	B	O
HETATM	372	N3	URI	B	12	-16.649	12.519	-11.751	1.00	10.00	B	N
HETATM	373	H3	URI	B	12	-15.913	12.284	-12.400	1.00	10.00	B	H
HETATM	374	C4	URI	B	12	-16.249	13.080	-10.557	1.00	10.00	B	C
HETATM	375	O4	URI	B	12	-15.049	13.291	-10.356	1.00	10.00	B	O
HETATM	376	C5	URI	B	12	-17.319	13.393	-9.662	1.00	10.00	B	C
HETATM	377	H5	URI	B	12	-17.103	13.835	-8.689	1.00	10.00	B	H
HETATM	378	C2'	URI	B	12	-20.777	10.914	-11.509	1.00	10.00	B	C

```
HETATM  379  H2' URI B  12     -19.932  10.223 -11.537  1.00 10.00      B    H
HETATM  380  O2' URI B  12     -21.720  10.664 -12.537  1.00 10.00      B    O
HETATM  381 HO2' URI B  12     -22.007  11.527 -12.860  1.00 10.00      B    H
HETATM  382  C3' URI B  12     -21.444  10.896 -10.136  1.00 10.00      B    C
HETATM  383  H3' URI B  12     -20.733  10.738  -9.330  1.00 10.00      B    H
HETATM  384  O3' URI B  12     -22.441   9.888 -10.065  1.00 10.00      B    O
ATOM    385  P   GUA B  13     -22.238   8.642  -9.079  1.00 10.00      B    P
ATOM    386  O1P GUA B  13     -23.458   7.808  -9.181  1.00 10.00      B    O
ATOM    387  O2P GUA B  13     -21.818   9.167  -7.758  1.00 10.00      B    O
ATOM    388  O5' GUA B  13     -21.025   7.831  -9.714  1.00 10.00      B    O
ATOM    389  C5' GUA B  13     -21.252   6.800 -10.675  1.00 10.00      B    C
ATOM    390  H5' GUA B  13     -22.164   7.012 -11.234  1.00 10.00      B    H
ATOM    391 H5'' GUA B  13     -21.359   5.842 -10.168  1.00 10.00      B    H
ATOM    392  C4' GUA B  13     -20.085   6.725 -11.629  1.00 10.00      B    C
ATOM    393  H4' GUA B  13     -20.456   6.313 -12.567  1.00 10.00      B    H
ATOM    394  O4' GUA B  13     -19.515   8.050 -11.768  1.00 10.00      B    O
ATOM    395  C1' GUA B  13     -18.112   7.952 -11.906  1.00 10.00      B    C
ATOM    396  H1' GUA B  13     -17.837   8.471 -12.823  1.00 10.00      B    H
ATOM    397  N9  GUA B  13     -17.502   8.659 -10.787  1.00 10.00      B    N
ATOM    398  C4  GUA B  13     -16.214   9.131 -10.709  1.00 10.00      B    C
ATOM    399  N3  GUA B  13     -15.267   9.018 -11.665  1.00 10.00      B    N
ATOM    400  C2  GUA B  13     -14.124   9.578 -11.297  1.00 10.00      B    C
ATOM    401  N2  GUA B  13     -13.072   9.550 -12.122  1.00 10.00      B    N
ATOM    402  H21 GUA B  13     -13.136   9.104 -13.028  1.00 10.00      B    H
ATOM    403  H22 GUA B  13     -12.201   9.992 -11.852  1.00 10.00      B    H
ATOM    404  N1  GUA B  13     -13.928  10.203 -10.089  1.00 10.00      B    N
ATOM    405  H1  GUA B  13     -13.017  10.607  -9.913  1.00 10.00      B    H
ATOM    406  C6  GUA B  13     -14.887  10.327  -9.089  1.00 10.00      B    C
ATOM    407  O6  GUA B  13     -14.605  10.907  -8.030  1.00 10.00      B    O
ATOM    408  C5  GUA B  13     -16.118   9.730  -9.469  1.00 10.00      B    C
ATOM    409  N7  GUA B  13     -17.317   9.631  -8.779  1.00 10.00      B    N
ATOM    410  C8  GUA B  13     -18.106   8.988  -9.596  1.00 10.00      B    C
ATOM    411  H8  GUA B  13     -19.132   8.738  -9.359  1.00 10.00      B    H
ATOM    412  C2' GUA B  13     -17.745   6.467 -11.941  1.00 10.00      B    C
ATOM    413  H2' GUA B  13     -16.806   6.268 -11.423  1.00 10.00      B    H
ATOM    414  O2' GUA B  13     -17.727   6.047 -13.294  1.00 10.00      B    O
ATOM    415 HO2' GUA B  13     -18.414   6.551 -13.754  1.00 10.00      B    H
ATOM    416  C3' GUA B  13     -18.921   5.844 -11.193  1.00 10.00      B    C
ATOM    417  H3' GUA B  13     -18.786   5.880 -10.115  1.00 10.00      B    H
ATOM    418  O3' GUA B  13     -19.103   4.487 -11.573  1.00 10.00      B    O
ATOM    419  P   ADE B  14     -18.522   3.323 -10.635  1.00 10.00      B    P
ATOM    420  O1P ADE B  14     -19.090   2.036 -11.108  1.00 10.00      B    O
ATOM    421  O2P ADE B  14     -18.731   3.738  -9.230  1.00 10.00      B    O
ATOM    422  O5' ADE B  14     -16.957   3.325 -10.927  1.00 10.00      B    O
ATOM    423  C5' ADE B  14     -16.414   2.546 -11.990  1.00 10.00      B    C
ATOM    424  H5' ADE B  14     -17.093   2.566 -12.844  1.00 10.00      B    H
ATOM    425 H5'' ADE B  14     -16.287   1.514 -11.664  1.00 10.00      B    H
ATOM    426  C4' ADE B  14     -15.071   3.099 -12.410  1.00 10.00      B    C
ATOM    427  H4' ADE B  14     -14.889   2.781 -13.438  1.00 10.00      B    H
ATOM    428  O4' ADE B  14     -15.076   4.539 -12.239  1.00 10.00      B    O
ATOM    429  C1' ADE B  14     -13.790   4.976 -11.845  1.00 10.00      B    C
ATOM    430  H1' ADE B  14     -13.456   5.702 -12.590  1.00 10.00      B    H
ATOM    431  N9  ADE B  14     -13.916   5.675 -10.569  1.00 10.00      B    N
ATOM    432  C4  ADE B  14     -12.999   6.535 -10.013  1.00 10.00      B    C
ATOM    433  N3  ADE B  14     -11.809   6.896 -10.519  1.00 10.00      B    N
ATOM    434  C2  ADE B  14     -11.191   7.750  -9.703  1.00 10.00      B    C
ATOM    435  H2  ADE B  14     -10.214   8.094 -10.043  1.00 10.00      B    H
ATOM    436  N1  ADE B  14     -11.599   8.245  -8.525  1.00 10.00      B    N
ATOM    437  C6  ADE B  14     -12.801   7.860  -8.046  1.00 10.00      B    C
ATOM    438  N6  ADE B  14     -13.213   8.353  -6.879  1.00 10.00      B    N
ATOM    439  H61 ADE B  14     -14.114   8.073  -6.511  1.00 10.00      B    H
ATOM    440  H62 ADE B  14     -12.641   9.009  -6.369  1.00 10.00      B    H
ATOM    441  C5  ADE B  14     -13.555   6.956  -8.820  1.00 10.00      B    C
ATOM    442  N7  ADE B  14     -14.798   6.371  -8.623  1.00 10.00      B    N
ATOM    443  C8  ADE B  14     -14.963   5.620  -9.686  1.00 10.00      B    C
ATOM    444  H8  ADE B  14     -15.840   5.010  -9.851  1.00 10.00      B    H
ATOM    445  C2' ADE B  14     -12.875   3.751 -11.786  1.00 10.00      B    C
ATOM    446  H2' ADE B  14     -12.180   3.804 -10.945  1.00 10.00      B    H
ATOM    447  O2' ADE B  14     -12.219   3.624 -13.035  1.00 10.00      B    O
ATOM    448 HO2' ADE B  14     -12.535   4.357 -13.583  1.00 10.00      B    H
ATOM    449  C3' ADE B  14     -13.884   2.622 -11.587  1.00 10.00      B    C
ATOM    450  H3' ADE B  14     -14.156   2.493 -10.540  1.00 10.00      B    H
ATOM    451  O3' ADE B  14     -13.391   1.385 -12.077  1.00 10.00      B    O
HETATM  452  P   URI B  15     -13.362   0.108 -11.108  1.00 10.00      B    P
HETATM  453  O1P URI B  15     -12.755  -1.016 -11.860  1.00 10.00      B    O
HETATM  454  O2P URI B  15     -14.711  -0.054 -10.511  1.00 10.00      B    O
HETATM  455  O5' URI B  15     -12.345   0.528  -9.960  1.00 10.00      B    O
HETATM  456  C5' URI B  15     -12.744   0.541  -8.593  1.00 10.00      B    C
HETATM  457  H5' URI B  15     -12.183  -0.210  -8.037  1.00 10.00      B    H
HETATM  458 H5'' URI B  15     -13.807   0.315  -8.517  1.00 10.00      B    H
HETATM  459  C4' URI B  15     -12.485   1.902  -7.993  1.00 10.00      B    C
HETATM  460  H4' URI B  15     -11.517   2.244  -8.362  1.00 10.00      B    H
HETATM  461  O4' URI B  15     -13.580   2.790  -8.336  1.00 10.00      B    O
HETATM  462  C1' URI B  15     -13.822   3.681  -7.264  1.00 10.00      B    C
HETATM  463  H1' URI B  15     -13.738   4.692  -7.668  1.00 10.00      B    H
HETATM  464  N1  URI B  15     -15.205   3.492  -6.810  1.00 10.00      B    N
HETATM  465  C6  URI B  15     -16.002   2.498  -7.335  1.00 10.00      B    C
HETATM  466  H6  URI B  15     -15.586   1.841  -8.097  1.00 10.00      B    H
HETATM  467  C2  URI B  15     -15.683   4.348  -5.840  1.00 10.00      B    C
HETATM  468  O2  URI B  15     -15.004   5.237  -5.355  1.00 10.00      B    O
HETATM  469  N3  URI B  15     -16.984   4.126  -5.458  1.00 10.00      B    N
HETATM  470  H3  URI B  15     -17.372   4.727  -4.743  1.00 10.00      B    H
HETATM  471  C4  URI B  15     -17.838   3.159  -5.939  1.00 10.00      B    C
HETATM  472  O4  URI B  15     -18.992   3.101  -5.512  1.00 10.00      B    O
HETATM  473  C5  URI B  15     -17.268   2.311  -6.941  1.00 10.00      B    C
```

HETATM	474	H5	URI	B	15	-17.866	1.514	-7.385	1.00	10.00	B	H
HETATM	475	C2'	URI	B	15	-12.777	3.405	-6.182	1.00	10.00	B	C
HETATM	476	H2'	URI	B	15	-13.198	3.506	-5.179	1.00	10.00	B	H
HETATM	477	O2'	URI	B	15	-11.680	4.272	-6.407	1.00	10.00	B	O
HETATM	478	HO2'	URI	B	15	-12.034	5.162	-6.408	1.00	10.00	B	H
HETATM	479	C3'	URI	B	15	-12.415	1.951	-6.471	1.00	10.00	B	C
HETATM	480	H3'	URI	B	15	-13.118	1.254	-6.020	1.00	10.00	B	H
HETATM	481	O3'	URI	B	15	-11.109	1.639	-6.003	1.00	10.00	B	O
ATOM	482	P	ADE	B	16	-10.888	0.371	-5.044	1.00	10.00	B	P
ATOM	483	O1P	ADE	B	16	-9.502	-0.113	-5.254	1.00	10.00	B	O
ATOM	484	O2P	ADE	B	16	-12.022	-0.560	-5.233	1.00	10.00	B	O
ATOM	485	O5'	ADE	B	16	-10.987	0.965	-3.572	1.00	10.00	B	O
ATOM	486	C5'	ADE	B	16	-9.952	1.792	-3.045	1.00	10.00	B	C
ATOM	487	H5'	ADE	B	16	-9.375	2.222	-3.862	1.00	10.00	B	H
ATOM	488	H5''	ADE	B	16	-9.291	1.200	-2.415	1.00	10.00	B	H
ATOM	489	C4'	ADE	B	16	-10.554	2.904	-2.219	1.00	10.00	B	C
ATOM	490	H4'	ADE	B	16	-9.755	3.606	-1.981	1.00	10.00	B	H
ATOM	491	O4'	ADE	B	16	-11.646	3.504	-2.960	1.00	10.00	B	O
ATOM	492	C1'	ADE	B	16	-12.667	3.894	-2.062	1.00	10.00	B	C
ATOM	493	H1'	ADE	B	16	-12.861	4.954	-2.231	1.00	10.00	B	H
ATOM	494	N9	ADE	B	16	-13.875	3.151	-2.411	1.00	10.00	B	N
ATOM	495	C4	ADE	B	16	-15.128	3.311	-1.873	1.00	10.00	B	C
ATOM	496	N3	ADE	B	16	-15.499	4.180	-0.919	1.00	10.00	B	N
ATOM	497	C2	ADE	B	16	-16.796	4.051	-0.647	1.00	10.00	B	C
ATOM	498	H2	ADE	B	16	-17.179	4.718	0.124	1.00	10.00	B	H
ATOM	499	N1	ADE	B	16	-17.696	3.215	-1.186	1.00	10.00	B	N
ATOM	500	C6	ADE	B	16	-17.289	2.356	-2.145	1.00	10.00	B	C
ATOM	501	N6	ADE	B	16	-18.185	1.527	-2.684	1.00	10.00	B	N
ATOM	502	H61	ADE	B	16	-17.884	0.882	-3.404	1.00	10.00	B	H
ATOM	503	H62	ADE	B	16	-19.151	1.539	-2.390	1.00	10.00	B	H
ATOM	504	C5	ADE	B	16	-15.936	2.392	-2.519	1.00	10.00	B	C
ATOM	505	N7	ADE	B	16	-15.205	1.663	-3.445	1.00	10.00	B	N
ATOM	506	C8	ADE	B	16	-13.991	2.148	-3.339	1.00	10.00	B	C
ATOM	507	H8	ADE	B	16	-13.156	1.786	-3.922	1.00	10.00	B	H
ATOM	508	C2'	ADE	B	16	-12.171	3.611	-0.643	1.00	10.00	B	C
ATOM	509	H2'	ADE	B	16	-12.980	3.275	0.010	1.00	10.00	B	H
ATOM	510	O2'	ADE	B	16	-11.519	4.769	-0.158	1.00	10.00	B	O
ATOM	511	HO2'	ADE	B	16	-11.393	5.354	-0.910	1.00	10.00	B	H
ATOM	512	C3'	ADE	B	16	-11.175	2.483	-0.895	1.00	10.00	B	C
ATOM	513	H3'	ADE	B	16	-11.665	1.515	-0.978	1.00	10.00	B	H
ATOM	514	O3'	ADE	B	16	-10.196	2.403	0.135	1.00	10.00	B	O
HETATM	515	P	URI	B	17	-10.154	1.110	1.085	1.00	10.00	B	P
HETATM	516	O1P	URI	B	17	-8.735	0.740	1.308	1.00	10.00	B	O
HETATM	517	O2P	URI	B	17	-11.086	0.111	0.512	1.00	10.00	B	O
HETATM	518	O5'	URI	B	17	-10.750	1.624	2.467	1.00	10.00	B	O
HETATM	519	C5'	URI	B	17	-10.466	2.937	2.943	1.00	10.00	B	C
HETATM	520	H5'	URI	B	17	-10.119	3.562	2.118	1.00	10.00	B	H
HETATM	521	H5''	URI	B	17	-9.691	2.893	3.706	1.00	10.00	B	H
HETATM	522	C4'	URI	B	17	-11.709	3.550	3.540	1.00	10.00	B	C
HETATM	523	H4'	URI	B	17	-11.410	4.461	4.061	1.00	10.00	B	H
HETATM	524	O4'	URI	B	17	-12.687	3.774	2.493	1.00	10.00	B	O
HETATM	525	C1'	URI	B	17	-13.990	3.576	3.009	1.00	10.00	B	C
HETATM	526	H1'	URI	B	17	-14.543	4.500	2.837	1.00	10.00	B	H
HETATM	527	N1	URI	B	17	-14.629	2.514	2.220	1.00	10.00	B	N
HETATM	528	C6	URI	B	17	-13.890	1.742	1.353	1.00	10.00	B	C
HETATM	529	H6	URI	B	17	-12.812	1.905	1.294	1.00	10.00	B	H
HETATM	530	C2	URI	B	17	-15.991	2.322	2.362	1.00	10.00	B	C
HETATM	531	O2	URI	B	17	-16.674	2.969	3.138	1.00	10.00	B	O
HETATM	532	N3	URI	B	17	-16.523	1.340	1.563	1.00	10.00	B	N
HETATM	533	H3	URI	B	17	-17.516	1.165	1.647	1.00	10.00	B	H
HETATM	534	C4	URI	B	17	-15.847	0.547	0.658	1.00	10.00	B	C
HETATM	535	O4	URI	B	17	-16.475	-0.268	-0.020	1.00	10.00	B	O
HETATM	536	C5	URI	B	17	-14.442	0.796	0.587	1.00	10.00	B	C
HETATM	537	H5	URI	B	17	-13.820	0.215	-0.096	1.00	10.00	B	H
HETATM	538	C2'	URI	B	17	-13.850	3.263	4.499	1.00	10.00	B	C
HETATM	539	H2'	URI	B	17	-14.585	2.526	4.829	1.00	10.00	B	H
HETATM	540	O2'	URI	B	17	-13.929	4.481	5.217	1.00	10.00	B	O
HETATM	541	HO2'	URI	B	17	-13.395	5.098	4.709	1.00	10.00	B	H
HETATM	542	C3'	URI	B	17	-12.441	2.682	4.551	1.00	10.00	B	C
HETATM	543	H3'	URI	B	17	-12.413	1.633	4.269	1.00	10.00	B	H
HETATM	544	O3'	URI	B	17	-11.866	2.820	5.840	1.00	10.00	B	O
HETATM	545	P	URI	B	18	-11.308	1.525	6.600	1.00	10.00	B	P
HETATM	546	O1P	URI	B	18	-10.548	1.997	7.782	1.00	10.00	B	O
HETATM	547	O2P	URI	B	18	-10.655	0.628	5.616	1.00	10.00	B	O
HETATM	548	O5'	URI	B	18	-12.619	0.810	7.144	1.00	10.00	B	O
HETATM	549	C5'	URI	B	18	-13.192	1.211	8.383	1.00	10.00	B	C
HETATM	550	H5'	URI	B	18	-13.075	2.289	8.511	1.00	10.00	B	H
HETATM	551	H5''	URI	B	18	-12.690	0.699	9.204	1.00	10.00	B	H
HETATM	552	C4'	URI	B	18	-14.656	0.864	8.413	1.00	10.00	B	C
HETATM	553	H4'	URI	B	18	-15.105	1.387	9.258	1.00	10.00	B	H
HETATM	554	O4'	URI	B	18	-15.255	1.200	7.136	1.00	10.00	B	O
HETATM	555	C1'	URI	B	18	-16.283	0.272	6.840	1.00	10.00	B	C
HETATM	556	H1'	URI	B	18	-17.203	0.842	6.702	1.00	10.00	B	H
HETATM	557	N1	URI	B	18	-15.960	-0.388	5.568	1.00	10.00	B	N
HETATM	558	C6	URI	B	18	-14.698	-0.312	5.020	1.00	10.00	B	C
HETATM	559	H6	URI	B	18	-13.926	0.251	5.551	1.00	10.00	B	H
HETATM	560	C2	URI	B	18	-16.969	-1.095	4.940	1.00	10.00	B	C
HETATM	561	O2	URI	B	18	-18.095	-1.184	5.398	1.00	10.00	B	O
HETATM	562	N3	URI	B	18	-16.609	-1.695	3.761	1.00	10.00	B	N
HETATM	563	H3	URI	B	18	-17.340	-2.217	3.289	1.00	10.00	B	H
HETATM	564	C4	URI	B	18	-15.370	-1.664	3.156	1.00	10.00	B	C
HETATM	565	O4	URI	B	18	-15.196	-2.277	2.100	1.00	10.00	B	O
HETATM	566	C5	URI	B	18	-14.382	-0.909	3.865	1.00	10.00	B	C
HETATM	567	H5	URI	B	18	-13.373	-0.822	3.465	1.00	10.00	B	H
HETATM	568	C2'	URI	B	18	-16.375	-0.708	8.012	1.00	10.00	B	C

HETATM	569	H2'	URI	B	18	-16.590	-1.723	7.675	1.00	10.00	B	H
HETATM	570	O2'	URI	B	18	-17.333	-0.217	8.933	1.00	10.00	B	O
HETATM	571	HO2'	URI	B	18	-17.842	0.458	8.461	1.00	10.00	B	H
HETATM	572	C3'	URI	B	18	-14.967	-0.613	8.590	1.00	10.00	B	C
HETATM	573	H3'	URI	B	18	-14.258	-1.229	8.041	1.00	10.00	B	H
HETATM	574	O3'	URI	B	18	-14.926	-0.992	9.955	1.00	10.00	B	O
ATOM	575	P	ADE	B	19	-14.183	-2.349	10.370	1.00	10.00	B	P
ATOM	576	O1P	ADE	B	19	-13.869	-2.248	11.816	1.00	10.00	B	O
ATOM	577	O2P	ADE	B	19	-13.090	-2.595	9.398	1.00	10.00	B	O
ATOM	578	O5'	ADE	B	19	-15.297	-3.467	10.176	1.00	10.00	B	O
ATOM	579	C5'	ADE	B	19	-16.417	-3.532	11.052	1.00	10.00	B	C
ATOM	580	H5'	ADE	B	19	-16.838	-2.535	11.182	1.00	10.00	B	H
ATOM	581	H5''	ADE	B	19	-16.105	-3.912	12.023	1.00	10.00	B	H
ATOM	582	C4'	ADE	B	19	-17.473	-4.447	10.483	1.00	10.00	B	C
ATOM	583	H4'	ADE	B	19	-18.265	-4.542	11.226	1.00	10.00	B	H
ATOM	584	O4'	ADE	B	19	-17.928	-3.916	9.212	1.00	10.00	B	O
ATOM	585	C1'	ADE	B	19	-18.234	-4.985	8.335	1.00	10.00	B	C
ATOM	586	H1'	ADE	B	19	-19.276	-4.865	8.035	1.00	10.00	B	H
ATOM	587	N9	ADE	B	19	-17.400	-4.850	7.143	1.00	10.00	B	N
ATOM	588	C4	ADE	B	19	-17.578	-5.493	5.941	1.00	10.00	B	C
ATOM	589	N3	ADE	B	19	-18.544	-6.372	5.622	1.00	10.00	B	N
ATOM	590	C2	ADE	B	19	-18.402	-6.787	4.365	1.00	10.00	B	C
ATOM	591	H2	ADE	B	19	-19.145	-7.508	4.024	1.00	10.00	B	H
ATOM	592	N1	ADE	B	19	-17.475	-6.445	3.456	1.00	10.00	B	N
ATOM	593	C6	ADE	B	19	-16.520	-5.559	3.808	1.00	10.00	B	C
ATOM	594	N6	ADE	B	19	-15.600	-5.215	2.902	1.00	10.00	B	N
ATOM	595	H61	ADE	B	19	-14.881	-4.552	3.149	1.00	10.00	B	H
ATOM	596	H62	ADE	B	19	-15.627	-5.602	1.966	1.00	10.00	B	H
ATOM	597	C5	ADE	B	19	-16.557	-5.046	5.119	1.00	10.00	B	C
ATOM	598	N7	ADE	B	19	-15.746	-4.144	5.791	1.00	10.00	B	N
ATOM	599	C8	ADE	B	19	-16.286	-4.063	6.984	1.00	10.00	B	C
ATOM	600	H8	ADE	B	19	-15.890	-3.435	7.770	1.00	10.00	B	H
ATOM	601	C2'	ADE	B	19	-17.999	-6.295	9.089	1.00	10.00	B	C
ATOM	602	H2'	ADE	B	19	-17.567	-7.061	8.443	1.00	10.00	B	H
ATOM	603	O2'	ADE	B	19	-19.220	-6.698	9.678	1.00	10.00	B	O
ATOM	604	HO2'	ADE	B	19	-19.903	-6.133	9.298	1.00	10.00	B	H
ATOM	605	C3'	ADE	B	19	-17.001	-5.858	10.156	1.00	10.00	B	C
ATOM	606	H3'	ADE	B	19	-15.981	-5.853	9.784	1.00	10.00	B	H
ATOM	607	O3'	ADE	B	19	-17.053	-6.701	11.296	1.00	10.00	B	O
HETATM	608	P	URI	B	20	-15.910	-7.807	11.507	1.00	10.00	B	P
HETATM	609	O1P	URI	B	20	-16.059	-8.346	12.877	1.00	10.00	B	O
HETATM	610	O2P	URI	B	20	-14.615	-7.220	11.087	1.00	10.00	B	O
HETATM	611	O5'	URI	B	20	-16.301	-8.958	10.484	1.00	10.00	B	O
HETATM	612	C5'	URI	B	20	-17.537	-9.646	10.615	1.00	10.00	B	C
HETATM	613	H5'	URI	B	20	-18.301	-8.960	10.981	1.00	10.00	B	H
HETATM	614	H5''	URI	B	20	-17.428	-10.465	11.325	1.00	10.00	B	H
HETATM	615	C4'	URI	B	20	-17.970	-10.206	9.283	1.00	10.00	B	C
HETATM	616	H4'	URI	B	20	-18.969	-10.628	9.402	1.00	10.00	B	H
HETATM	617	O4'	URI	B	20	-17.886	-9.170	8.267	1.00	10.00	B	O
HETATM	618	C1'	URI	B	20	-17.539	-9.756	7.025	1.00	10.00	B	C
HETATM	619	H1'	URI	B	20	-18.361	-9.535	6.340	1.00	10.00	B	H
HETATM	620	N1	URI	B	20	-16.337	-9.092	6.502	1.00	10.00	B	N
HETATM	621	C6	URI	B	20	-15.591	-8.226	7.270	1.00	10.00	B	C
HETATM	622	H6	URI	B	20	-15.870	-8.072	8.313	1.00	10.00	B	H
HETATM	623	C2	URI	B	20	-15.990	-9.357	5.191	1.00	10.00	B	C
HETATM	624	O2	URI	B	20	-16.604	-10.147	4.498	1.00	10.00	B	O
HETATM	625	N3	URI	B	20	-14.897	-8.671	4.724	1.00	10.00	B	N
HETATM	626	H3	URI	B	20	-14.643	-8.836	3.758	1.00	10.00	B	H
HETATM	627	C4	URI	B	20	-14.121	-7.774	5.424	1.00	10.00	B	C
HETATM	628	O4	URI	B	20	-13.188	-7.202	4.852	1.00	10.00	B	O
HETATM	629	C5	URI	B	20	-14.525	-7.573	6.782	1.00	10.00	B	C
HETATM	630	H5	URI	B	20	-13.967	-6.886	7.419	1.00	10.00	B	H
HETATM	631	C2'	URI	B	20	-17.388	-11.261	7.251	1.00	10.00	B	C
HETATM	632	H2'	URI	B	20	-16.562	-11.676	6.670	1.00	10.00	B	H
HETATM	633	O2'	URI	B	20	-18.629	-11.878	6.962	1.00	10.00	B	O
HETATM	634	HO2'	URI	B	20	-19.249	-11.583	7.639	1.00	10.00	B	H
HETATM	635	C3'	URI	B	20	-17.080	-11.316	8.745	1.00	10.00	B	C
HETATM	636	H3'	URI	B	20	-16.032	-11.128	8.963	1.00	10.00	B	H
HETATM	637	O3'	URI	B	20	-17.450	-12.566	9.313	1.00	10.00	B	O
ATOM	638	P	ADE	B	21	-16.317	-13.641	9.684	1.00	10.00	B	P
ATOM	639	O1P	ADE	B	21	-16.901	-14.553	10.698	1.00	10.00	B	O
ATOM	640	O2P	ADE	B	21	-15.061	-12.922	9.994	1.00	10.00	B	O
ATOM	641	O5'	ADE	B	21	-16.100	-14.467	8.343	1.00	10.00	B	O
ATOM	642	C5'	ADE	B	21	-17.088	-15.377	7.872	1.00	10.00	B	C
ATOM	643	H5'	ADE	B	21	-18.081	-14.951	8.019	1.00	10.00	B	H
ATOM	644	H5''	ADE	B	21	-17.022	-16.315	8.421	1.00	10.00	B	H
ATOM	645	C4'	ADE	B	21	-16.875	-15.651	6.402	1.00	10.00	B	C
ATOM	646	H4'	ADE	B	21	-17.643	-16.357	6.086	1.00	10.00	B	H
ATOM	647	O4'	ADE	B	21	-16.911	-14.399	5.673	1.00	10.00	B	O
ATOM	648	C1'	ADE	B	21	-16.025	-14.471	4.571	1.00	10.00	B	C
ATOM	649	H1'	ADE	B	21	-16.607	-14.262	3.676	1.00	10.00	B	H
ATOM	650	N9	ADE	B	21	-15.030	-13.412	4.728	1.00	10.00	B	N
ATOM	651	C4	ADE	B	21	-14.215	-12.881	3.758	1.00	10.00	B	C
ATOM	652	N3	ADE	B	21	-14.150	-13.231	2.461	1.00	10.00	B	N
ATOM	653	C2	ADE	B	21	-13.244	-12.493	1.821	1.00	10.00	B	C
ATOM	654	H2	ADE	B	21	-13.124	-12.714	0.759	1.00	10.00	B	H
ATOM	655	N1	ADE	B	21	-12.457	-11.517	2.295	1.00	10.00	B	N
ATOM	656	C6	ADE	B	21	-12.549	-11.187	3.599	1.00	10.00	B	C
ATOM	657	N6	ADE	B	21	-11.771	-10.206	4.063	1.00	10.00	B	N
ATOM	658	H61	ADE	B	21	-11.823	-9.934	5.038	1.00	10.00	B	H
ATOM	659	H62	ADE	B	21	-11.129	-9.741	3.435	1.00	10.00	B	H
ATOM	660	C5	ADE	B	21	-13.470	-11.899	4.389	1.00	10.00	B	C
ATOM	661	N7	ADE	B	21	-13.799	-11.820	5.733	1.00	10.00	B	N
ATOM	662	C8	ADE	B	21	-14.722	-12.738	5.884	1.00	10.00	B	C
ATOM	663	H8	ADE	B	21	-15.195	-12.951	6.832	1.00	10.00	B	H

ATOM	664	C2'	ADE	B	21	-15.421	-15.876	4.555	1.00	10.00	B	C
ATOM	665	H2'	ADE	B	21	-14.377	-15.869	4.229	1.00	10.00	B	H
ATOM	666	O2'	ADE	B	21	-16.247	-16.700	3.751	1.00	10.00	B	O
ATOM	667	HO2'	ADE	B	21	-17.114	-16.273	3.702	1.00	10.00	B	H
ATOM	668	C3'	ADE	B	21	-15.533	-16.265	6.025	1.00	10.00	B	C
ATOM	669	H3'	ADE	B	21	-14.726	-15.851	6.623	1.00	10.00	B	H
ATOM	670	O3'	ADE	B	21	-15.539	-17.675	6.185	1.00	10.00	B	O
HETATM	671	P	URI	B	22	-14.234	-18.414	6.751	1.00	10.00	B	P
HETATM	672	O1P	URI	B	22	-14.703	-19.619	7.473	1.00	10.00	B	O
HETATM	673	O2P	URI	B	22	-13.388	-17.420	7.457	1.00	10.00	B	O
HETATM	674	O5'	URI	B	22	-13.441	-18.882	5.453	1.00	10.00	B	O
HETATM	675	C5'	URI	B	22	-13.999	-19.836	4.555	1.00	10.00	B	C
HETATM	676	H5'	URI	B	22	-15.088	-19.818	4.629	1.00	10.00	B	H
HETATM	677	H5''	URI	B	22	-13.642	-20.834	4.806	1.00	10.00	B	H
HETATM	678	C4'	URI	B	22	-13.592	-19.512	3.139	1.00	10.00	B	C
HETATM	679	H4'	URI	B	22	-14.209	-20.119	2.475	1.00	10.00	B	H
HETATM	680	O4'	URI	B	22	-13.733	-18.087	2.912	1.00	10.00	B	O
HETATM	681	C1'	URI	B	22	-12.745	-17.657	1.995	1.00	10.00	B	C
HETATM	682	H1'	URI	B	22	-13.269	-17.207	1.150	1.00	10.00	B	H
HETATM	683	N1	URI	B	22	-11.959	-16.603	2.655	1.00	10.00	B	N
HETATM	684	C6	URI	B	22	-12.048	-16.413	4.017	1.00	10.00	B	C
HETATM	685	H6	URI	B	22	-12.693	-17.072	4.597	1.00	10.00	B	H
HETATM	686	C2	URI	B	22	-11.136	-15.806	1.875	1.00	10.00	B	C
HETATM	687	O2	URI	B	22	-11.019	-15.949	0.669	1.00	10.00	B	O
HETATM	688	N3	URI	B	22	-10.453	-14.833	2.564	1.00	10.00	B	N
HETATM	689	H3	URI	B	22	-9.841	-14.241	2.016	1.00	10.00	B	H
HETATM	690	C4	URI	B	22	-10.505	-14.581	3.920	1.00	10.00	B	C
HETATM	691	O4	URI	B	22	-9.855	-13.643	4.389	1.00	10.00	B	O
HETATM	692	C5	URI	B	22	-11.367	-15.454	4.653	1.00	10.00	B	C
HETATM	693	H5	URI	B	22	-11.470	-15.336	5.732	1.00	10.00	B	H
HETATM	694	C2'	URI	B	22	-11.924	-18.884	1.587	1.00	10.00	B	C
HETATM	695	H2'	URI	B	22	-10.866	-18.641	1.472	1.00	10.00	B	H
HETATM	696	O2'	URI	B	22	-12.492	-19.445	0.416	1.00	10.00	B	O
HETATM	697	HO2'	URI	B	22	-13.091	-18.775	0.059	1.00	10.00	B	H
HETATM	698	C3'	URI	B	22	-12.144	-19.809	2.779	1.00	10.00	B	C
HETATM	699	H3'	URI	B	22	-11.474	-19.584	3.607	1.00	10.00	B	H
HETATM	700	O3'	URI	B	22	-11.977	-21.172	2.417	1.00	10.00	B	O
HETATM	701	P	URI	B	23	-10.584	-21.908	2.722	1.00	10.00	B	P
HETATM	702	O1P	URI	B	23	-10.780	-23.361	2.493	1.00	10.00	B	O
HETATM	703	O2P	URI	B	23	-10.087	-21.437	4.036	1.00	10.00	B	O
HETATM	704	O5'	URI	B	23	-9.600	-21.360	1.600	1.00	10.00	B	O
HETATM	705	C5'	URI	B	23	-9.764	-21.737	0.235	1.00	10.00	B	C
HETATM	706	H5'	URI	B	23	-10.825	-21.858	0.012	1.00	10.00	B	H
HETATM	707	H5''	URI	B	23	-9.253	-22.682	0.050	1.00	10.00	B	H
HETATM	708	C4'	URI	B	23	-9.183	-20.674	-0.667	1.00	10.00	B	C
HETATM	709	H4'	URI	B	23	-9.547	-20.865	-1.678	1.00	10.00	B	H
HETATM	710	O4'	URI	B	23	-9.548	-19.366	-0.156	1.00	10.00	B	O
HETATM	711	C1'	URI	B	23	-8.494	-18.453	-0.394	1.00	10.00	B	C
HETATM	712	H1'	URI	B	23	-8.912	-17.635	-0.984	1.00	10.00	B	H
HETATM	713	N1	URI	B	23	-8.073	-17.906	0.904	1.00	10.00	B	N
HETATM	714	C6	URI	B	23	-8.639	-18.359	2.074	1.00	10.00	B	C
HETATM	715	H6	URI	B	23	-9.395	-19.143	2.023	1.00	10.00	B	H
HETATM	716	C2	URI	B	23	-7.100	-16.924	0.917	1.00	10.00	B	C
HETATM	717	O2	URI	B	23	-6.568	-16.511	-0.096	1.00	10.00	B	O
HETATM	718	N3	URI	B	23	-6.770	-16.448	2.163	1.00	10.00	B	N
HETATM	719	H3	URI	B	23	-6.067	-15.719	2.199	1.00	10.00	B	H
HETATM	720	C4	URI	B	23	-7.298	-16.851	3.371	1.00	10.00	B	C
HETATM	721	O4	URI	B	23	-6.905	-16.325	4.415	1.00	10.00	B	O
HETATM	722	C5	URI	B	23	-8.291	-17.876	3.272	1.00	10.00	B	C
HETATM	723	H5	URI	B	23	-8.765	-18.266	4.173	1.00	10.00	B	H
HETATM	724	C2'	URI	B	23	-7.389	-19.198	-1.147	1.00	10.00	B	C
HETATM	725	H2'	URI	B	23	-6.396	-18.888	-0.816	1.00	10.00	B	H
HETATM	726	O2'	URI	B	23	-7.588	-19.007	-2.536	1.00	10.00	B	O
HETATM	727	HO2'	URI	B	23	-8.000	-18.140	-2.622	1.00	10.00	B	H
HETATM	728	C3'	URI	B	23	-7.665	-20.646	-0.746	1.00	10.00	B	C
HETATM	729	H3'	URI	B	23	-7.213	-20.905	0.207	1.00	10.00	B	H
HETATM	730	O3'	URI	B	23	-7.189	-21.550	-1.734	1.00	10.00	B	O
ATOM	731	P	CYT	B	24	-5.747	-22.225	-1.562	1.00	10.00	B	P
ATOM	732	O1P	CYT	B	24	-5.581	-23.220	-2.647	1.00	10.00	B	O
ATOM	733	O2P	CYT	B	24	-5.594	-22.650	-0.153	1.00	10.00	B	O
ATOM	734	O5'	CYT	B	24	-4.724	-21.037	-1.830	1.00	10.00	B	O
ATOM	735	C5'	CYT	B	24	-4.236	-20.779	-3.143	1.00	10.00	B	C
ATOM	736	H5'	CYT	B	24	-5.070	-20.539	-3.805	1.00	10.00	B	H
ATOM	737	H5''	CYT	B	24	-3.722	-21.660	-3.524	1.00	10.00	B	H
ATOM	738	C4'	CYT	B	24	-3.273	-19.617	-3.117	1.00	10.00	B	C
ATOM	739	H4'	CYT	B	24	-3.047	-19.352	-4.151	1.00	10.00	B	H
ATOM	740	O4'	CYT	B	24	-3.864	-18.535	-2.358	1.00	10.00	B	O
ATOM	741	C1'	CYT	B	24	-2.854	-17.850	-1.643	1.00	10.00	B	C
ATOM	742	H1'	CYT	B	24	-2.907	-16.805	-1.940	1.00	10.00	B	H
ATOM	743	N1	CYT	B	24	-3.182	-17.933	-0.214	1.00	10.00	B	N
ATOM	744	C6	CYT	B	24	-4.120	-18.820	0.237	1.00	10.00	B	C
ATOM	745	H6	CYT	B	24	-4.615	-19.486	-0.473	1.00	10.00	B	H
ATOM	746	C2	CYT	B	24	-2.524	-17.089	0.678	1.00	10.00	B	C
ATOM	747	O2	CYT	B	24	-1.666	-16.307	0.244	1.00	10.00	B	O
ATOM	748	N3	CYT	B	24	-2.837	-17.144	1.993	1.00	10.00	B	N
ATOM	749	C4	CYT	B	24	-3.763	-18.005	2.424	1.00	10.00	B	C
ATOM	750	N4	CYT	B	24	-4.052	-18.009	3.726	1.00	10.00	B	N
ATOM	751	H41	CYT	B	24	-4.754	-18.644	4.083	1.00	10.00	B	H
ATOM	752	H42	CYT	B	24	-3.545	-17.394	4.351	1.00	10.00	B	H
ATOM	753	C5	CYT	B	24	-4.440	-18.890	1.536	1.00	10.00	B	C
ATOM	754	H5	CYT	B	24	-5.183	-19.602	1.899	1.00	10.00	B	H
ATOM	755	C2'	CYT	B	24	-1.510	-18.489	-2.000	1.00	10.00	B	C
ATOM	756	H2'	CYT	B	24	-0.844	-18.539	-1.136	1.00	10.00	B	H
ATOM	757	O2'	CYT	B	24	-0.932	-17.817	-3.101	1.00	10.00	B	O
ATOM	758	HO2'	CYT	B	24	-1.373	-16.959	-3.168	1.00	10.00	B	H

```
ATOM    759  H3' CYT B  24      -2.047 -20.570  -1.592  1.00 10.00      B    H
ATOM    760  C3' CYT B  24      -1.941 -19.887  -2.430  1.00 10.00      B    C
ATOM    761  O3' CYT B  24      -0.969 -20.401  -3.325  1.00 10.00      B    O
ATOM    762  H3T CYT B  24      -0.551 -19.607  -3.688  1.00 10.00      B    H
TER     763      CYT B  24
HETATM  764  O2G GTP B   0      -2.802 -12.813  10.036  1.00 10.00      B    O
HETATM  765  PG  GTP B   0      -3.511 -11.414  10.396  1.00 10.00      B    P
HETATM  766  O3G GTP B   0      -2.735 -10.303   9.530  1.00 10.00      B    O
HETATM  767  O1G GTP B   0      -4.957 -11.447  10.086  1.00 10.00      B    O
HETATM  768  O3B GTP B   0      -3.212 -11.127  11.956  1.00 10.00      B    O
HETATM  769  PB  GTP B   0      -1.850 -10.452  12.486  1.00 10.00      B    P
HETATM  770  O1B GTP B  0      -1.886 -10.512  13.966  1.00 10.00      B    O
HETATM  771  O2B GTP B   0     -0.692 -11.061  11.802  1.00 10.00      B    O
HETATM  772  O3A GTP B   0      -2.000  -8.913  12.030  1.00 10.00      B    O
HETATM  773  PA  GTP B   0      -3.019  -7.942  12.810  1.00 10.00      B    P
HETATM  774  O2A GTP B   0      -2.456  -6.573  12.768  1.00 10.00      B    O
HETATM  775  O1A GTP B   0      -4.382  -8.157  12.281  1.00 10.00      B    O
CONECT   31   32   29
CONECT   64   62   65
CONECT   32   33   34   31   35
CONECT   65   68   67   64   66
CONECT  109  111  108  110  122
CONECT  114  111  116  115
CONECT  122  109  123  124  126
CONECT  126  106  122  127  128
CONECT  118  116  119  120
CONECT  106  103  108  107  126
CONECT  120  112  118  121
CONECT  103  102  105  104  106
CONECT  112  111  113  120
CONECT  110  109
CONECT  123  122
CONECT  117  116
CONECT  127  126
CONECT  107  106
CONECT  121  120
CONECT  104  103
CONECT  105  103
CONECT  113  112
CONECT  125  124
CONECT  111  112  114  109
CONECT  116  114  117  118
CONECT  100   99
CONECT  115  114
CONECT  124  122  125
CONECT  101   99
CONECT  128  126  129
CONECT  119  118
CONECT  108  109  106
CONECT  102  103   99
CONECT   99  101  102  100
CONECT  161  159  162
CONECT  129  130  128  131  132
CONECT  172  174  171  173  185
CONECT  177  179  174  178
CONECT  185  172  189  186  187
CONECT  189  169  185  190  191
CONECT  181  179  182  183
CONECT  169  171  166  170  189
CONECT  183  181  175  184
CONECT  166  165  169  167  168
CONECT  175  183  174  176
CONECT  173  172
CONECT  186  185
CONECT  180  179
CONECT  190  189
CONECT  170  169
CONECT  184  183
CONECT  167  166
CONECT  168  166
CONECT  176  175
CONECT  188  187
CONECT  174  177  175  172
CONECT  179  181  177  180
CONECT  163  162
CONECT  178  177
CONECT  187  185  188
CONECT  164  162
CONECT  191  189  192
CONECT  182  181
CONECT  171  169  172
CONECT  165  166  162
CONECT  162  165  161  163  164
CONECT  224  225  222
CONECT  192  195  191  194  193
CONECT  257  258  255
CONECT  225  224  227  226  228
CONECT  268  267  269  270  281
CONECT  273  274  275  270
CONECT  281  268  285  283  282
CONECT  285  265  287  286  281
CONECT  277  278  275  279
CONECT  265  266  267  262  285
CONECT  279  277  271  280
CONECT  262  265  261  264  263
```

```
CONECT  271  272  279  270
CONECT  269  268
CONECT  282  281
CONECT  276  275
CONECT  286  285
CONECT  266  265
CONECT  280  279
CONECT  263  262
CONECT  264  262
CONECT  272  271
CONECT  284  283
CONECT  270  268  273  271
CONECT  275  276  277  273
CONECT  259  258
CONECT  274  273
CONECT  283  284  281
CONECT  260  258
CONECT  287  285  288
CONECT  278  277
CONECT  267  265  268
CONECT  261  258  262
CONECT  258  259  261  260  257
CONECT  320  318  321
CONECT  288  287  289  290  291
CONECT  354  352  355
CONECT  321  323  322  320  324
CONECT  365  366  367  378  364
CONECT  370  367  372  371
CONECT  378  379  382  365  380
CONECT  382  378  383  362  384
CONECT  374  372  375  376
CONECT  362  363  359  364  382
CONECT  376  374  368  377
CONECT  359  362  358  361  360
CONECT  368  367  369  376
CONECT  366  365
CONECT  379  378
CONECT  373  372
CONECT  383  382
CONECT  363  362
CONECT  377  376
CONECT  360  359
CONECT  361  359
CONECT  369  368
CONECT  381  380
CONECT  367  370  365  368
CONECT  372  373  374  370
CONECT  356  355
CONECT  371  370
CONECT  380  378  381
CONECT  357  355
CONECT  384  385  382
CONECT  375  374
CONECT  364  362  365
CONECT  358  355  359
CONECT  355  356  354  357  358
CONECT  418  416  419
CONECT  385  386  388  387  384
CONECT  451  449  452
CONECT  419  418  421  422  420
CONECT  462  464  463  461  475
CONECT  467  469  464  468
CONECT  475  462  479  476  477
CONECT  479  459  480  475  481
CONECT  471  469  472  473
CONECT  459  456  460  461  479
CONECT  473  471  465  474
CONECT  456  457  459  458  455
CONECT  465  466  464  473
CONECT  463  462
CONECT  476  475
CONECT  470  469
CONECT  480  479
CONECT  460  459
CONECT  474  473
CONECT  457  456
CONECT  458  456
CONECT  466  465
CONECT  478  477
CONECT  464  467  462  465
CONECT  469  467  470  471
CONECT  453  452
CONECT  468  467
CONECT  477  478  475
CONECT  454  452
CONECT  481  479  482
CONECT  472  471
CONECT  461  462  459
CONECT  455  456  452
CONECT  452  453  454  451  455
CONECT  514  512  515
CONECT  482  484  485  481  483
CONECT  525  527  526  538  524
CONECT  530  531  532  527
CONECT  538  525  539  542  540
```

```
CONECT  542  538  522  544  543
CONECT  534  532  535  536
CONECT  522  523  524  519  542
CONECT  536  528  534  537
CONECT  519  520  521  522  518
CONECT  528  536  527  529
CONECT  526  525
CONECT  539  538
CONECT  533  532
CONECT  543  542
CONECT  523  522
CONECT  537  536
CONECT  520  519
CONECT  521  519
CONECT  529  528
CONECT  541  540
CONECT  527  528  530  525
CONECT  532  533  534  530
CONECT  516  515
CONECT  531  530
CONECT  540  538  541
CONECT  517  515
CONECT  544  545  542
CONECT  535  534
CONECT  524  525  522
CONECT  518  519  515
CONECT  515  517  514  516  518
CONECT  555  568  554  557  556
CONECT  560  562  557  561
CONECT  568  570  569  572  555
CONECT  572  574  568  552  573
CONECT  564  562  565  566
CONECT  552  549  554  553  572
CONECT  566  564  567  558
CONECT  549  548  551  552  550
CONECT  558  557  566  559
CONECT  556  555
CONECT  569  568
CONECT  563  562
CONECT  573  572
CONECT  553  552
CONECT  567  566
CONECT  550  549
CONECT  551  549
CONECT  559  558
CONECT  571  570
CONECT  557  555  558  560
CONECT  562  564  560  563
CONECT  546  545
CONECT  561  560
CONECT  570  568  571
CONECT  547  545
CONECT  574  575  572
CONECT  565  564
CONECT  554  552  555
CONECT  548  545  549
CONECT  545  544  548  547  546
CONECT  607  605  608
CONECT  575  574  577  578  576
CONECT  618  617  620  631  619
CONECT  623  625  624  620
CONECT  631  632  618  633  635
CONECT  635  637  636  631  615
CONECT  627  629  625  628
CONECT  615  616  635  617  612
CONECT  629  621  630  627
CONECT  612  613  614  611  615
CONECT  621  629  622  620
CONECT  619  618
CONECT  632  631
CONECT  626  625
CONECT  636  635
CONECT  616  615
CONECT  630  629
CONECT  613  612
CONECT  614  612
CONECT  622  621
CONECT  634  633
CONECT  620  621  623  618
CONECT  625  626  623  627
CONECT  609  608
CONECT  624  623
CONECT  633  634  631
CONECT  610  608
CONECT  637  638  635
CONECT  628  627
CONECT  617  618  615
CONECT  611  608  612
CONECT  608  609  610  611  607
CONECT  670  668  671
CONECT  638  637  639  640  641
CONECT  681  680  682  694  683
CONECT  686  688  683  687
CONECT  694  698  695  681  696
CONECT  698  699  694  700  678
```

```
CONECT  690  692  691  688
CONECT  678  680  698  675  679
CONECT  692  690  684  693
CONECT  675  676  677  674  678
CONECT  684  692  685  683
CONECT  682  681
CONECT  695  694
CONECT  689  688
CONECT  699  698
CONECT  679  678
CONECT  693  692
CONECT  676  675
CONECT  677  675
CONECT  685  684
CONECT  697  696
CONECT  683  684  681  686
CONECT  688  690  686  689
CONECT  672  671
CONECT  687  686
CONECT  696  694  697
CONECT  673  671
CONECT  700  698  701
CONECT  691  690
CONECT  680  681  678
CONECT  674  675  671
CONECT  671  670  673  672  674
CONECT  711  710  724  713  712
CONECT  716  717  713  718
CONECT  724  726  725  728  711
CONECT  728  708  724  729  730
CONECT  720  722  721  718
CONECT  708  710  728  705  709
CONECT  722  714  720  723
CONECT  705  708  704  706  707
CONECT  714  715  722  713
CONECT  712  711
CONECT  725  724
CONECT  719  718
CONECT  729  728
CONECT  709  708
CONECT  723  722
CONECT  706  705
CONECT  707  705
CONECT  715  714
CONECT  727  726
CONECT  713  714  711  716
CONECT  718  719  720  716
CONECT  702  701
CONECT  717  716
CONECT  726  724  727
CONECT  703  701
CONECT  730  728  731
CONECT  721  720
CONECT  710  708  711
CONECT  704  701  705
CONECT  701  703  702  704  700
CONECT  731  730  732  733  734
CONECT  775  773
CONECT  770  769
CONECT  767  765
CONECT  774  773
CONECT  771  769
CONECT  764  765
CONECT  772  773  769
CONECT  768  765  769
CONECT  766  765
CONECT  773  774  772  775
CONECT  769  771  772  770  768
CONECT  765  764  767  768  766
END
```

Constraints to prevent triphosphate floating 5’-hpRNA (CNS format):

ASSIGN (resid 0 and atomtype PG) (resid 1 and atomtype O5’) 3.5 3.0 4.0

Chapter 6: NS1B Competes for Influenza Panhandle RNA to Suppress Activation of RIG-I

Introduction:

RIG-I and innate immune system activation:

RIG-I is one of the first proteins to detect infection from certain classes of RNA viruses. Once RIG-I recognizes viral infection, it begins a cascading pathway involving conformational changes, RIG-I ATPase activity, phosphorylation of IRF3, transcription of IFN, and ultimately activation of the immune system (Figure 1.9, 1.10, 1.11). RIG-I binds to and is activated by 3P-5' dsRNA (4). Human cells add a methyl modification on the first nucleotide of human RNA to prevent binding/activation of RIG-I. His830 in the RNA binding site of RIG-I clashes with this modification, significantly reducing the affinity for modified host RNA (15). RIG-I is activated by vRNA which has a signature 3P-5' end, a pathogen-associated molecular pattern (PAMP) that is a product of the process of vRNA synthesis (5). Interestingly, due to sequence conservation of the influenza's genome at the 3' and 5' ends and these highly conserved regions are able to base pair, it is theorized that the influenza genome forms 3P-5' panhandle RNA (Figure 1.2) (3). This means every RNA chromosome would begin and terminate in a 3P-5'-stem, a PAMP signal that activates RIG-I (4). In fact, RIG-I and the innate immune system are specifically activated in the presence of the Influenza A genomic RNA (48).

RIG-I ATPase activity and NS1B RNA binding affinities:

Our NS1B:RNA blunt-end binding model suggests that NS1 might function to complete with RIG-I for binding 3P-5' panhandle RNA PAMPs, like those presented by influenza vRNA. Specifically, our blunt-end binding model is similar to the way that RIG-I binds its dsRNA substrates. This hypothesis leads to the corollary hypothesis that 5'-

triphophorylated modification of dsRNA substrate blunt ends would change their binding affinity for NS1B-CTD. RIG-I is activated by 3P-5'-hpRNA and turns on its ATPase activity. Our model further suggests that NS1B-CTD can inhibit the dsRNA-activated RIG-I. This can be measured by monitoring ATPase activity (Chapter 1).

Virology:

To gain the biological relevance of NS1B binding RNA in the proposed model (Chapter 5) we collaborated with R. Krug (University of Texas) to carry out virology experiments. Using distinct antibodies to unphosphorylated and phosphorylated IRF-3, the relative p-IRF3 intensities in the Western blot provides an assay measuring the amount of innate immune system activation (Chapter 1). To test NS1B-FL model bound to dsRNA we decided to mutate one amino acid essential for RNA binding on each domain that would result in a loss of function. R208A is a mutation in NS1B-CTD resulting in the loss of RNA binding function for the CTD whereas R50A is a mutation in NS1B-NTD resulting in the loss of RNA binding function for the NTD. Relative total IRF3, RIG-I and NS1B is measured as a control to confirm that the proteins are present. Actin is also used as a loading control to confirm that the same relative amount of protein is loaded in each sample. This experiment is reproducing the study presented in Ma et al. (2) (Figure 1.14), but in the current study M.O.I was reduced from 5 to 2. In Ma et al. (2), it was concluded that NS1B did in fact have the ability to inhibit the immune system. This function was located in NS1B-CTD, but it was not related to the NS1B-CTD RNA binding function (2). This conclusion was made because virus expressing wild-type NS1B-FL is able to suppress phosphorylation of IRF3, and activation of RIG-I. But when the NS1B-CTD is removed it no longer has this function, IRF3 is phosphorylated, and RIG-I is activated by viral infection. However, when single mutations were made in the RNA

binding site of NS1B-CTD which suppress dsRNA binding, the virus was still able to prevent phosphorylation of IRF3 with efficiency similar to that of the NS1B-FL.

In this work, we discovered, based on structural and biochemical evidence, that the function of RNA binding site in the NS1B-CTD is in fact to suppress the function of dsRNA-activated RIG-I. Using lower M.O.I. in these viral assays, we observe that mutations in the NS1-CTD which suppress dsRNA binding do in fact also reduce the virus's ability to suppress phosphorylation of IRF3. Thus, to properly test NS1B RNA binding inhibiting RIG-I, in future studies multiple point mutations must be performed to fully eliminate the RNA binding function or a lower viral M.O.I. must be used.

Methods**:**

ATPase activity:

ATPase inhibition experiments were performed by Brandon Schweibenz under conditions described previously (14) with the exception that we used constant RIG-I concentrations (10 nM) and varied NS1B-CTD concentration.

Measuring binding affinities:

RNA binding studies were performed using a 5' hydroxyl 24-mer hpRNA (OH-5'-hpRNA) and a 5' triphosphorylated 24-mer hpRNA (3P-5'-hpRNA). Both substrates have a GAAUAUAAUAGUGAUAUUAUAUUC sequence. This RNA forms a 10 base paired stem with 4 nucleotide loop (10-bp-S-GUGA-L) structure. The binding studies were mostly carried out as described previously (14), with exception of the fluorophore in this current studying being fluorescein. The major change in this is the excitation and emission are now at 494 nm and 516 nm respectively. Another change in the protocol to note is the way we measured change in the NS1B-NTD experiment. In this experiment

we measured change in anisotropy rather than change in intensity. The implications of this will be described in the discussion.

Virology: Experiments were performed as described previously in Ma et al. 2016 (2) but with a M.O.I reduction from 5 to 2 in our current study.

Results:

With the blunt-end binding mechanism proposed by the SAXS results of the 16-bp dsRNA, experiments were performed to determine whether R238A-NS1B-CTD has the ability to bind RIG-I substrate RNA tightly enough to inhibit the dsRNA-activated ATPase activity of RIG-I. Note that the R238A mutant suppresses dimerization of NS1B-CTD, but has little effect on the dsRNA binding affinity. If RIG-I ATPase activity is affected by the presence of R238A-NS1B-CTD, this would provide evidence that not only does the NS1B-CTD have the ability to bind RNA, but it also has the ability to directly compete for RIG-I substrate. Figure 6.1 clearly shows that NS1B-CTD has this ability to inhibit RIG-I's ATPase activity at a competing concentration of 100X the concentration of RIG-I

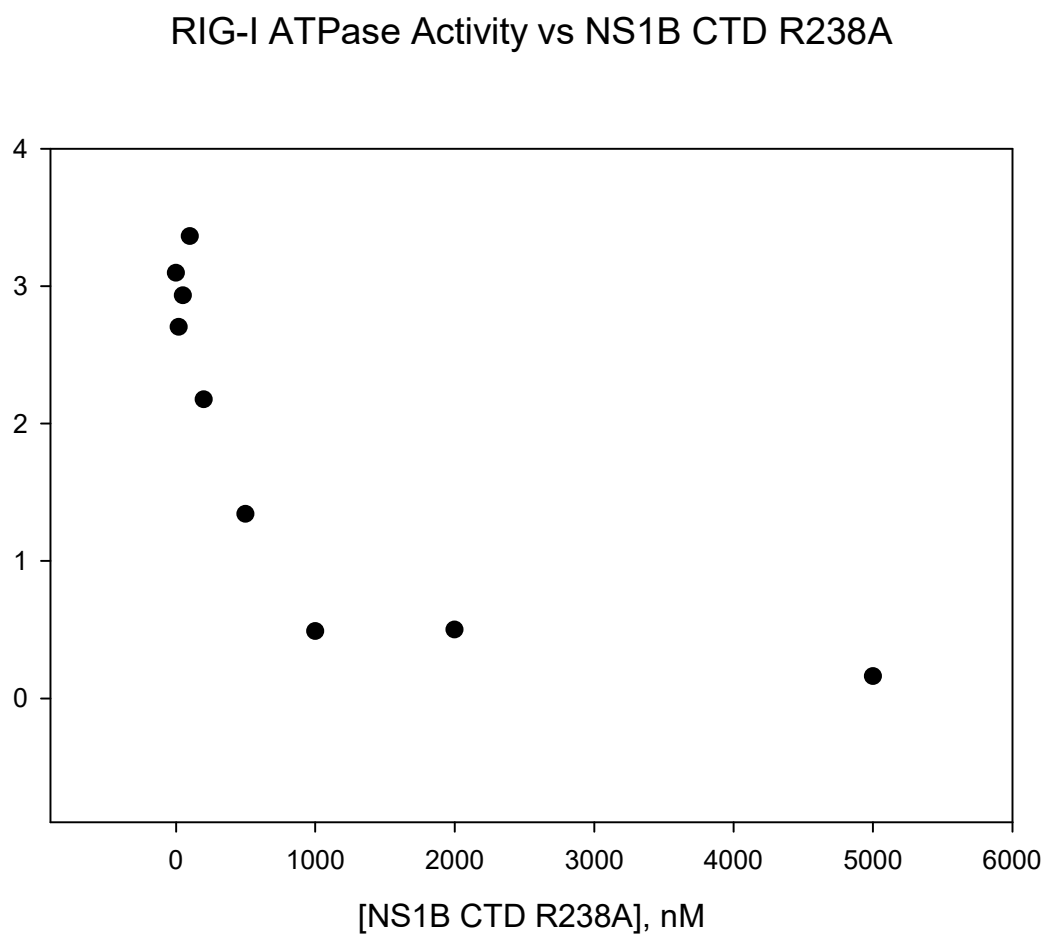

Figure 6.1: RIG-I ATPase activity decreases when titrated with NS1B-CTD R238A

This data demonstrates that R238A-NS1B-CTD, which can bind dsRNA in a blunt-end mode based on combine NMR and SAXS studies, also has the ability to compete for PAMP-containing dsRNA substrates of RIG-I, and to inhibit RIG-I ATPase activity.

Measuring binding affinities:

Fluorescence polarization measurements were next used to determine if R238A-NS1B-CTD can bind 3P-5'-hpRNA, the canonical substrate of RIG-I, and if this triphosphate modification makes a difference in the binding affinity. Figure 6.2 shows

that R238A-NS1B-CTD binds 3P-5'-hpRNA ~8-fold more tightly than the corresponding OH-5'-hpRNA. This data demonstrate that NS1B-CTD does have a significant preference for 5' triphosphorylated dsRNA, the signature PAMP modification for vRNA.

Figure 6.3 shows that this preference for triphosphorylated dsRNA substrates is also preserved in the NS1B-FL protein. However, the NS1B-NTD is not affected by the 3P-5' RNA modification (Figure 6.4), which was expected. The residues of NS1B-CTD involved in the 16-bp dsRNA binding (2) also had similar changes in affinity for the 3P-5'-hpRNA substrate (Table 6.1). These results are in agreement with what was expected; that the R208A or K221A mutations would be the most disruptive. R160A also had a disruption of the affinity for RNA but it was not as drastic as R208A or K221A mutations.

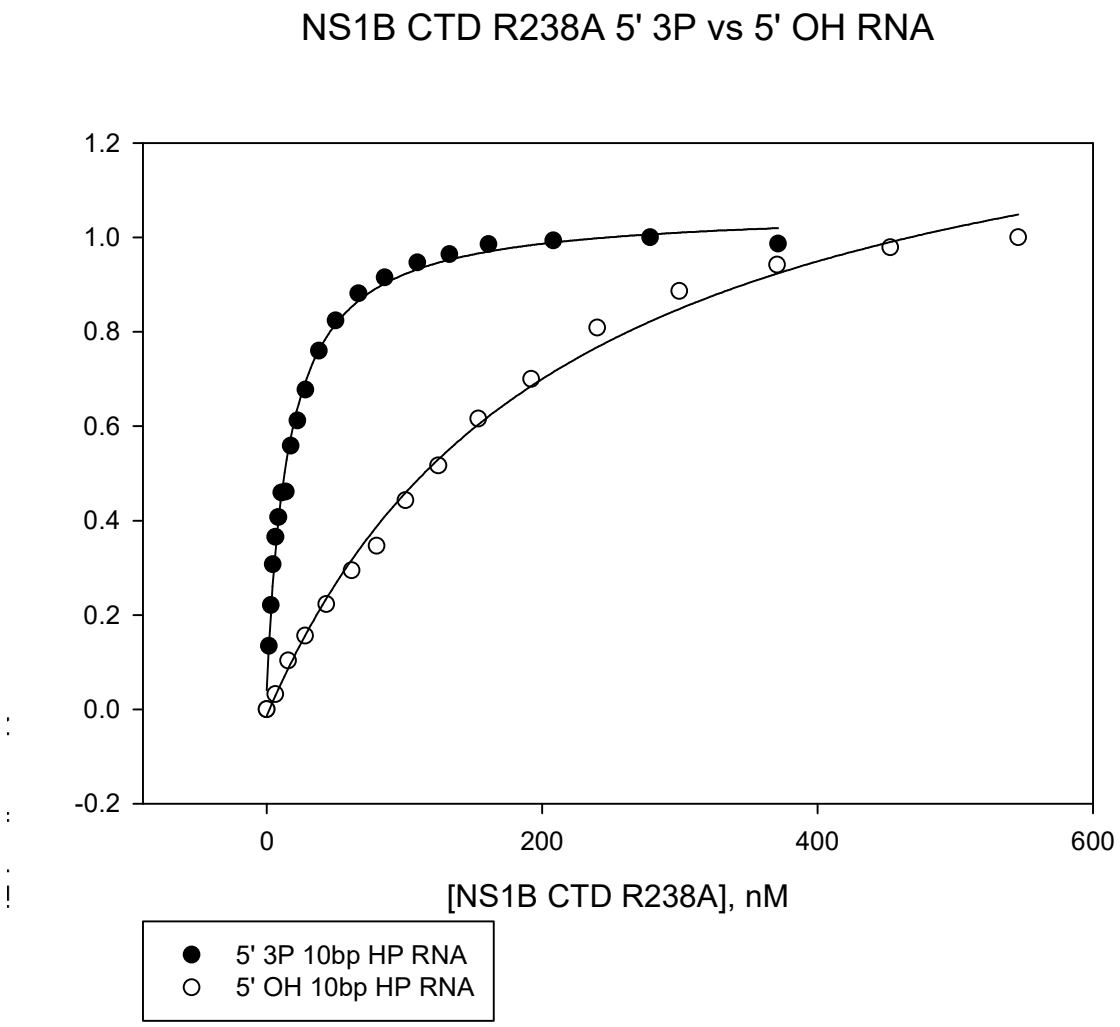

Figure 6.2: R238A has a higher affinity for 3P-5'-hpRNA vs OH-5'-hpRNA

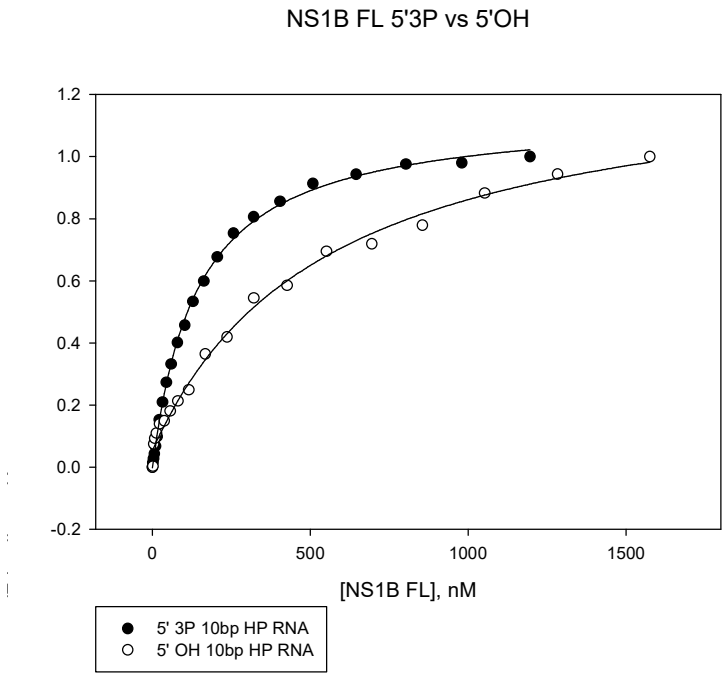

Figure 6.3: NS1B-FL has a higher affinity for 3P-5'-hpRNA vs OH-5'-hpRNA

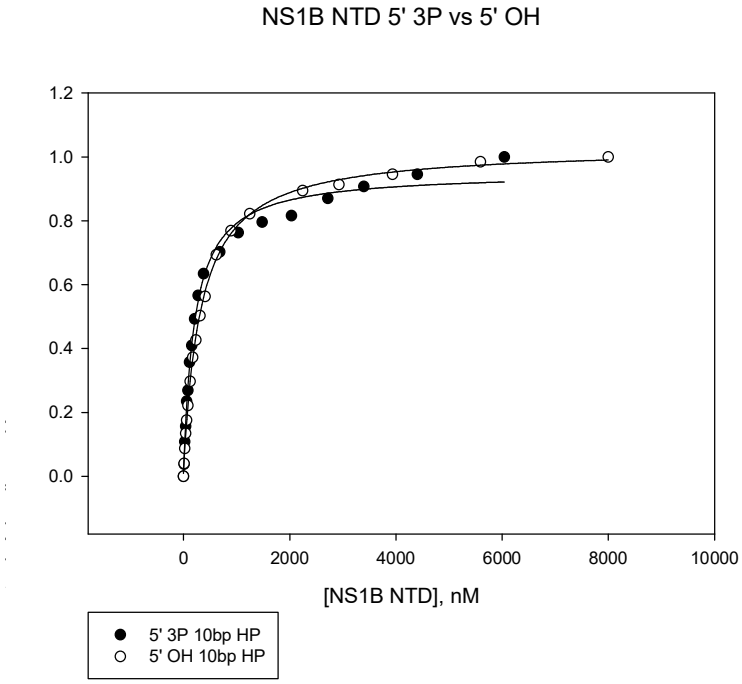

Figure 6.4: NS1B-NTD has no affinity change for 3P-5'-hpRNA vs OH-5'-hpRNA

NS1B Construct	10-bp HP PPP K_d	10-bp HP OH K_d
NS1B FL	142 ± 4 nM	1290 ± 680 nM
NS1B CTD	34 ± 4 nM	Not done
NS1B CTD R238K	16 ± 1 nM	215 ± 22 nM
NS1B CTD K160A	117 ± 11 nM	NA
NS1B CTD R208A	650 ± 73 nM	NA
NS1B CTD K221A	2800 ± 1000 nM	NA
NS1B NTD	205 ± 19 nM	323 ± 10 nM

Table 6.1: Binding K_d's for different NS1B constructs and 3P-5'-hpRNA and OH-5'-hpRNA

Virology:

Phosphorylation of IRF3 (p-IRF3) is a cellular marker to see when the innate immune system is being activated (Chapter 1). Since NS1B is produced after viral infection and is not present in large quantities in the viral particle, NS1B requires time to be produced and be active in its function. This is why the NS1B protein band builds up over time and after it begins to build up p-IRF3 levels drop. Since total IRF3 amounts are staying the same it is suggesting that NS1B is preventing the phosphorylation of IRF3,

this is typically done by acrivated RIG-I. RIG-I also does not change in concentration. The conclusion is that NS1B is preventing RIG-I phosphorylation of IRF3 without changing the amount of the proteins, which means it is either changing one of these proteins to prevent the activation or it is interacting with RIG-I substrates (3P-5' RNA or vRNA). When a mutation is made in NS1B-CTD to weaken its ability to bind RNA (R208A) the virus no longer maintains the ability to prevent the phosphorylation of IRF3. This makes the connection that if the RNA binding function in the NS1B-CTD is lost NS1B will also lose the ability to prevent innate immune system activation.

To see if this connection also is held true in NS1B-NTD we also mutated NS1B-NTD (R50A) to weaken this domain's abiltiy to bind RNA. However, when the NS1B-NTD is mutated it still retains its ability to prevent phosphorylation of IRF3. Albeit the starting amount of p-IRF3 is very low, p-IRF3 still decreased when NS1B is produced (Figure 6.5). This suggests that the virus's ability to prevent innate immune system activation is restricted to NS1B-CTD.

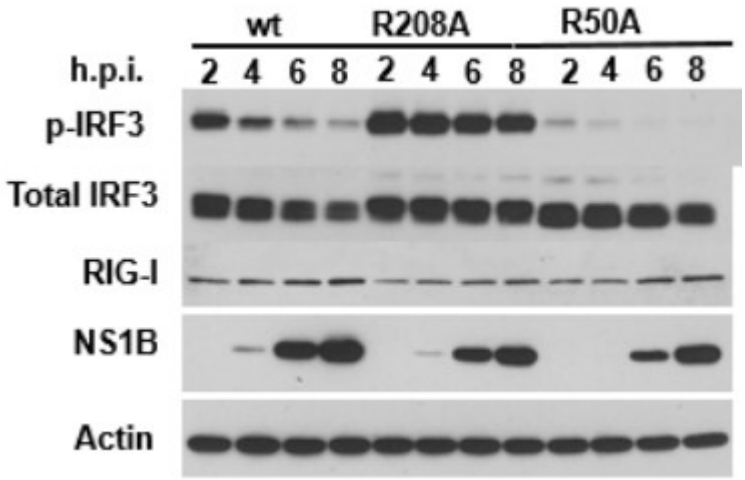

Figure 6.5: Western blot determines prevention of the activation of the innate immune system is lost when NS1B-CTD loses RNA binding function. p-IRF3 is an indicator of innate immune system activation. h.p.i. is hours post infection. p-IRF3 decreases as h.p.i increases due to NS1B ability to compete for RIG-I substrates. R208A mutates NS1B-CTD ability to bind RNA resulting in the loss of function of preventing innate immune system activation. R50A mutates NS1B-NTD RNA binding function, however, when this function is lost the innate immune system can still be activated and the results are similar to WT. This data was kindly provided by Dr. Chen Zhao; data interpretation was a collaborative effort between Dr. Gaetano Montelione, Dr. Chen Zhao, and myself.

Discussion:

While the results here followed expectations, there were a few unusual results that are worth mentioning. First is the decrease in affinity for the substrate from the NS1B-CTD compared to NS1B-FL. This can be explained by the size of the substrate being very small. While NS1B-CTD is small enough to bind comfortably on this hairpin substrate, NS1B-FL would have trouble binding such a small substrate (see Chapters 5 and 7). Another expected result was the way that the NS1B-NTD affinity was measured. For all other constructs we were able to measure intensity change of the fluorescein. This can be done because when the environment surrounding the fluorescein changes (i.e. a protein binding at that site) the intensity will change. For NS1B-NTD binding experiment there was no change in intensity, however, when we repeated the experiment this time measuring anisotropy, we were able to detect changes. Because no environmental changes occurred, no changes around the fluorescein were detected but changes in rotational speed was detected. This gives further evidence for the model proposed in Chapter 5 where NS1B-CTD binds the blunt end and is affected by

triphosphorylated modifications but NS1B-NTD binds the RNA backbone and is not affected by this modification.

Virology:

While these results directly run contrary to previously reported results (2), these differences can be explained. Multiplicity of infection (M.O.I.) is a way to quantify the amount of initial virus. In Ma LC. et al. the experiments with an M.O.I. of 5, whereas we replicated these experiments with a M.O.I. of 2. We conjecture that the results in Ma et al. (2) were performed at a viral concentration that saturated the cells with NS1B, and because the mutations tested did not knockout RNA binding function completely, NS1B still had enough RNA binding activity and concentration to perform its function. When these studies were done with a construct in which the NS1B-CTD domain was completely deleted, the ability to prevent phosphorylation of IRF3, and to suppress RIG-I activation, was lost. Li et al (2) concluded erroneously that the ability to prevent phosphorylation of IRF3 was located in NS1B-CTD but not related to its RNA binding function. However, when we repeated these experiments with a lower M.O.I., we observed that this RNA binding function of the NS1B-CTD is in fact responsible for phosphorylation of IRF3. In addition to this we also showed that NS1B still retains its ability to prevent phosphorylation of IRF3 if NS1B-NTD has a significantly reduced binding activity. This suggests the main purpose of NS1B-CTD binding activity is to prevent phosphorylation of IRF3 and this function is restricted to this domain.

Chapter 7: Overall Discussion and Future Direction

While assembling data for this report there is one concluding theory that I have developed for the future of this project. NS1B-CTD acts as a sensory domain to detect vRNA, binding the vRNA and hiding this substrate from RIG-I. While NS1B-NTD has been studied more, my model suggests that NS1B-NTD acts to increase the affinity to all RNAs, but NS1B-CTD would be the domain that increases NS1B's specificity for vRNA.

It is important to identify the weaknesses of this study and the strengths. While the NS1B-FL model bound to dsRNA I developed for this study was adjusted by hand and has clashes between the NTD and CTD domain, there are a few conclusions that can be made. First the residue – nucleic acid interactions for each domain was preserved, thus if NS1B-FL did bind to a single piece of RNA it would have maintained these interactions. Second if NS1B-FL would bind a single piece of RNA, it would most likely prefer a much larger RNA. The box model in Figure 7.1 shows how I predict this would occur. It is also of note that the NS1B-FL model was developed early on in the study, and was a major reason for attempting the experiments with 3P-5'-hpRNA. Despite the NS1B-FL model being developed early on we have yet to collect data to disprove it.

This is also why I think this study is very strong, all of the major assumptions we had at the beginning were incorrect. The three major assumptions we originally had: i) the RNA bound to NS1B-CTD in the same way the NS1B-NTD bound RNA (along the phosphate backbone), ii) because NS1B-NTD bound as a dimer NS1B-CTD also binds as a dimer, iii) the RNA binding activity of NS1B-CTD did not play a role in preventing activation of the innate immune system, were all shown to be incorrect. Try as I might, I could not prove the model proposed here wrong and the original assumptions correct. As data became reproducible it became clear that our blunt-end binding model was

actually correct, and our original assumptions were incorrect. This is brought up because a study is usually made stronger when the attempts to prove it wrong fail.

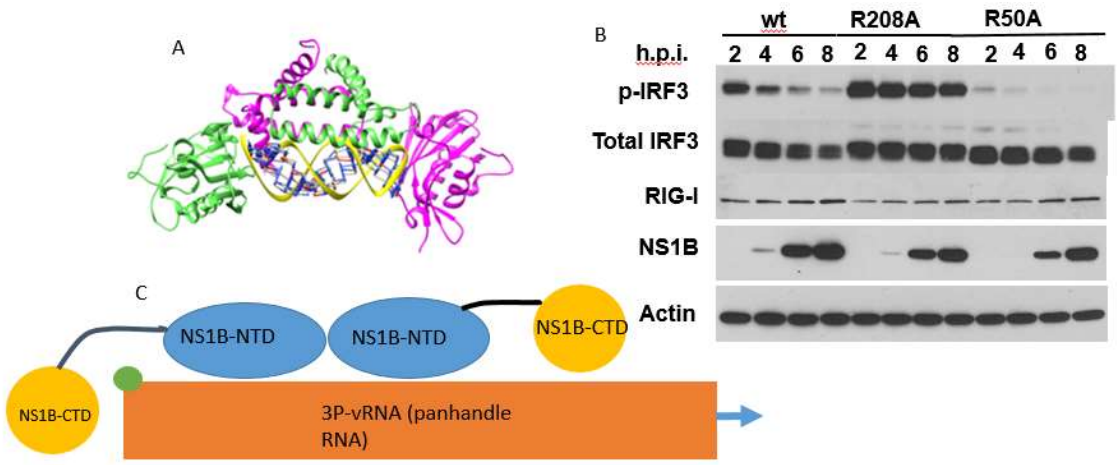

Figure 7.1. Proposed model of how NS1B-FL binds and interacts with vRNA. A) NS1B-FL model proposed in chapter 5. B) Virology result presented in chapter 6. C) Box diagram of how we propose the NS1B-FL protein binds and hides vRNA.

It was also observed by Ma et al. (2) that there are acidic residues on the surface of the NS1B-CTD that have CSPs upon binding to dsRNA. This is slightly surprising as it would be expected that acidic residues would repulse the negative RNA. It should be pointed out that a CSP does not necessarily mean that the RNA is bound, it simply means there is a change in the chemical environment. Therefore, a CSP could be generated by the negative RNA repulsing the acidic amino acids into a different environment. However, it is also noticed that while RNA is highly negative, there are positively charged atoms that the acidic amino acids could bind to if it is forced into that position. In fact, RIG-I has acidic amino acids close in proximity to the RNA (15), as discussed in Chapter 1.

It is also important to identify where the battle for vRNA is happening between RIG-I and NS1B. Based on the data here, I predict that RIG-I binds vRNA very early in the viral infection. This is evident by the presence of pIRF3 before any NS1B is even detected (Figure 7.1). However, the location of NS1B throughout the time of viral infection is interesting. In early stages of infection NS1B forms beads and locates to the nucleus and by late viral infection it is exported to the cytoplasm. This indicates that NS1B is co-locatlizing with an undetermined biomolecule. Given its new-found ability to bind vRNA, NS1B's ability to inhibit RIG-I (which is located in the cytoplasm) in late infection, viral life cycle (Figure 1.8), and location in the cell I propose that it is following vRNA until it is packaged. There is a problem with this theory, which is NS1 has not been detected in viral particles. However, this was done with NS1A which has a different mechanism (34). It also assumes that NS1B does not degrade in the virus or that the amount of NS1B is above the detection threshold. Performing experiments to see if NS1B is detectable in viral particles would be a logical test. In addition, co-localization experiments should be done to see if RIG-I and NS1B co-localize in the cell and if so at what time points. Does the location of RIG-I change with wt NS1B and NS1B-CTD RNA

binding mutant? A lot of interesting and important questions have been generated from this study.

Future Work:

In addition to the NMR studies that should be completed as outlined in Chapter 4, there are some new questions this study created. Crystallization will be attempted again in the near future to try to crystallize NS1B-CTD/FL with the 3P-5'-hpRNA. This study has made connections with data about the viral genome that has been public for almost 40 years (3). Now that we know the first 11 nucleotides of the 5' end and 3' end of viral genome is high conserved between all types of influenza and all genes, it would be interesting to investigate these sequences and see if they bind with a higher affinity. In addition, binding studies with single phosphorylated RNA would give greater insight into the affect that phosphorylation of RNAs has on the binding. We also recognize that the ATPase inhibition experiment is not fully complete as there are no controls for the experiment. We would also like to repeat these experiments with a variety of NS1B-CTD mutants that weaken or delete the RNA binding activity. In addition since we can also use NS1A as a control. NS1A inhibits the immune system but it performs this by binding to various proteins and can inhibit the immune system in two different steps of the activation pathway. However, NS1A does have RNA binding affinity so it would be a surprise to get a positive result. If this happens, we would revisit this question and see if we could rescue RIG-I ATPase activity by flooding the system with 5'-OH-hpRNA that would not activate RIG-I but it would block NS1A from binding the 3P-5'-hpRNA since NS1A is not sensitive to phosphorylated RNA. This would be a difficult experiment and ratios would need to be optimize empirically.

It would also be of great interest to do mutational studies of His207 and the effect on RNA binding. In the RIG-I structure it was shown that a Phe853 pi-stacks with the nucleotide at the blunt end of dsRNA and that His830 makes a tight pocket around the triphosphate of the 5' end. Loss of this His830 results in loss of the ability to differentiate between vRNA and cap-1,2 host RNA. In my model His207 pi-stacks with the blunt end of dsRNA and points away from the triphosphate. To test the resolution and residue accuracy of the NS1B-CTD : 3P-5'-hpRNA SAXS model mutating this residue will result in a loss of affinity but not the loss of specificity. In Chapter 6 it was mentioned that the virology study performed in collaboration with this project was done at a much lower M.O.I. than the Ma et al. (2) study, eluding to a specific time point in the infection at which NS1B-CTD is most critical. It would be interesting to test out the effect of varying M.O.I. and mutating the NS1B RNA binding functions. Discussions of why higher M.O.I. would give the result in Ma LC. (2) and lower M.O.I. gave the results presented here with the R208A mutant. Theoretically if the virus is making NS1B in too high of a concentration to be affected by the weakening of RNA binding function, as we argue, there would be also more vRNA for RIG-I to bind. This is under the assumption that RIG-I and NS1B and vRNA are kept at constant ratios, which may not be the case. However, if the ratios do stay constant, it does raise the question whether there is another mechanism that inhibits RIG-I at a higher concentration. It would be advantageous to test this by generating an even weaker RNA binding NS1B-CTD by performing double mutants or even mutating a basic to an acidic amino acid. If the RNA binding affinity is completely deleted and phosphorylation of IRF3 was not inhibited, this question would be addressed. These results can give us key insights into the different stages of influenza infection and the role of NS1B at those stages. Ma LC. (2) also showed evidence for binding of ssRNA. It would be interesting to investigate this and whether NS1B-CTD can force structural changes to ssRNA. One final experiment that can be

done is a through bioinformatics study looking at the evolution of influenza virus and if we can see a point where influenza A and influenza B diverges, and whether NS1-CTD contained the basic residues that were essential for RNA binding in both strains before this divergent point. Are the conserved basic residues a gain of function for influenza B or is it a loss of function for influenza A? If Influenza A lost this function, what is the mechanism for inhibiting the innate immune response that replaced it? If we mutate NS1A-CTD to contain the basic residues at the same positions on the structure does it gain the ability to bind RNA and select triphosphorylated RNA? Can the mechanism from NS1B-CTD be seen in any other RNA virus? Do viruses other than RNA viruses contain a similar mechanism or is this mechanism specific to RNA viruses (or even influenza B)?

It is also worth discussing the possibility of NS1B-CTD binding the loop of the hpRNA. In the RNA binding studies, a second binding event was observed. However, this second binding event was decreased with the sample that contained a mutation weakening the dimerization, implying it could be NS1B-CTD dimerizing and not actually binding the hpRNA. This second binding event in conjunction with the SAXS from Chapter 5 does not rule out the loop binding models. Additionally, the NMR from chapter 4, suggesting slowing of the exchange rate for the non-base paired nucleotides means that we cannot rule out binding of the loop. Trying to identify this as an artifact or if NS1B-CTD actually binds the loop would really be helpful in including or excluding possible models, thus, giving the modeling less degrees of freedom. If the loop binding is real, studies into the biological relevance of this event would also be very interesting.

With all the directions this study could go there are a few suggestions for following up this study. Buffers, filters, sample homogeneity, and cleanliness are key. While this seems like common knowledge, extra special attention was given to buffers that were

used for structural studies. SAXS requires buffer blanks from the same stock that the sample is in. If you do a buffer exchange and run out of the stock, you will not be able to make a buffer that will be close enough and another stock must be made. When doing structural studies buffers were always made and used within a week. Buffers and samples for structural studies were also filtered using the 0.02 nm filter. Buffer exchanges for structural studies was always done with a desalting column. Centrifuging NS1B-CTD and paying special attention to the UV scan of a nanodrop can tell you a lot about the aggregation state of a protein. Aggregation can kill a SAXS sample, as scattering is correlated with mass[2]. This means a dimer will scatter 4 times as much as a monomer. Even if you have 1% of your sample aggregated it can destroy a SAXS sample whereas it will not affect NMR or biochemical studies. NS1B-CTD is a very delicate and sensitive sample, but if proper care and emphasis is put on quality control of samples, filtration of samples, and buffer optimization you can get very nice reproducible data. Finally, buffer optimization was performed for NS1B-CTD, this is how the 2K buffer was developed. I highly recommend optimizing the buffer for the NS1B-CTD:RNA complex. This is something I realized very late in the study and did not have time to complete. It is my expectation that if the NS1B-CTD:RNA is sent to a buffer screening center and the conditions were optimized, the structure could be crystallized. This would also significantly increase sample stability and longevity.

Bibliography

1. Acton T.B. Xiao R. Anderson S. Aramini J. Buchwald W.A. Ciccosanti C. Conover K. Everett J. Hamilton K. Huang Y.J. et al. **Preparation of Protein Samples for NMR Structure, Function, and Small-Molecule Screening Studies.** *Methods Enzymology* 2011; **493**: 21-60
2. Ma LC, Guan R, Hamilton K, Aramini JM, Mao L, Wang S, Krug RM, Montelione GT. **A Second RNA-Binding Site in the NS1 Protein of Influenza B Virus.** *Structure.* 2016; **24(9);** 1562-1572.
3. Desselberger U, Racaniello VR, Zazra JJ, Palese P. **The 3'and 5'-Terminal Sequences of Influenza A, B and C Virus RNA Segments are Highly Conserved and Show Partial Inverted Complementarity**. *Gene*. 1980; 8(3): 315-28.
4. Rehwinkel J, e Sousa CR. **Targeting the Viral Achilles' Heel: Recognition of 5′-Triphosphate RNA in Innate Anti-Viral Defence**. *Current opinion in microbiology*. 2013; 16(4):485-92.
5. te Velthuis AJ, Fodor E. **Influenza Virus RNA Polymerase: Insights into the Mechanisms of Viral RNA Synthesis**. *Nature Reviews Microbiology*. 2016;14(8): 479.
6. Chauca-Diaz AM, Jung Choi Y, Resendiz MJ**. Biophysical Properties and Thermal Stability of Oligonucleotides of RNA Containing 7, 8-Dihydro-8-Hydroxyadenosine**. *Biopolymers*. 2015; 103(3): 167-74.
7. Greenfield NJ. **Using Circular Dichroism Spectra to Estimate Protein Secondary Structure**. *Nature protocols*. 2006; 1(6):2876.
8. Baker ES, Bowers MT. **B-DNA Helix Stability in a Solvent-Free Environment**. *American Society for Mass Spectrometry*. 2007; 18(7):1188-95.
9. Pettersen EF, Goddard TD, Huang CC, Couch GS, Greenblatt DM, Meng EC, Ferrin TE. **UCSF Chimera—a Visualization System for Exploratory Research and Analysis.** *computational chemistry.* 2004;25(13):1605-12.
10. Bonneau R, Strauss CE, Baker D. **Improving the Performance of Rosetta Using Multiple Sequence Alignment Information and Global Measures of Hydrophobic Core Formation.** *Proteins: Structure, Function, and Bioinformatics*. 2001; 43(1):1-1.
11. Schneidman-Duhovny D, Hammel M, Tainer JA, Sali A. **FoXS, FoXSDock and MultiFoXS: Single-State and Multi-State Structural Modeling of Proteins and Their Complexes Based on SAXS Profiles.** *Nucleic acids*. 2016; 44(W1):W424-9.
12. Hopkins JB, Gillilan RE, Skou S. **BioXTAS RAW: Improvements to a Free Open-Source Program for Small-Angle X-ray Scattering Data Reduction and Analysis.** Applied *crystallography*. 2017; 50(5):1545-53.
13. Konarev PV, Volkov VV, Sokolova AV, Koch MH, Svergun DI. **PRIMUS: a Windows PC-Based System for Small-Angle Scattering Data Analysis**. Applied *crystallography*. 2003; 36(5):1277-82.
14. Devarkar SC, Schweibenz B, Wang C, Marcotrigiano J, Patel SS. **RIG-I Uses an ATPase-Powered Translocation-Throttling Mechanism for Kinetic Proofreading of RNAs and Oligomerization**. *cell.* 2018; 72(2):355-68.
15. Devarkar SC, Wang C, Miller MT, Ramanathan A, Jiang F, Khan AG, Patel SS, Marcotrigiano J. **Structural Basis for m7G Recognition and 2′-O-methyl Discrimination in Capped RNAs by the Innate Immune Receptor RIG-I**. *PNAS*. 2016; 113(3):596-601.
16. Van Zundert GC, Rodrigues JP, Trellet M, Schmitz C, Kastritis PL, Karaca E, Melquiond AS, van Dijk M, De Vries SJ, Bonvin AM. **The HADDOCK2. 2 Web Server: User-Friendly Integrative Modeling of Biomolecular Complexes.** *molecular biology.* 2016; 428(4):720-5.

17. van Dijk M, Bonvin AM. **Pushing the Limits of What is Achievable in Protein–DNA Docking: Benchmarking HADDOCK's Performance**. *Nucleic acids.* 2010; 38(17):5634-47.
18. Franke D, Jeffries CM, Svergun DI. **Correlation Map, a Goodness-of-Fit Test for One-Dimensional X-ray Scattering Spectra.** *Nature Methods*. 2015; 12(5):419.
19. Franke, D. Jeffries, C.M. Svergun, D.I. **Correlation Map, a Goodness-of-Fit Test for One-Dimensional X-Ray Scattering Spectra**. *Nature Methods* 2015, 12, 419.
20. Dyer KN, Hammel M, Rambo RP, Tsutakawa SE, Rodic I, Classen S, Tainer JA, Hura GL. **High-Throughput SAXS For the Characterization of Biomolecules in Solution: A Practical Approach.** *Methods Mol. Biol.* 2014; (pp. 245-258).
21. Classen S, Hura GL, Holton JM, Rambo RP, Rodic I, McGuire PJ, Dyer K, Hammel M, Meigs G, Frankel KA, Tainer JA. **Implementation and Performance of SIBYLS: A Dual Endstation Small-Angle X-Ray Scattering and Macromolecular Crystallography Beamline at the Advanced Light**. *applied crystallography*. 2013; 1;46(1):1-3.
22. Hura GL, Menon AL, Hammel M, Rambo RP, Poole Ii FL, Tsutakawa SE, Jenney Jr FE, Classen S, Frankel KA, Hopkins RC, Yang SJ. **Robust, High-Throughput Solution Structural Analyses by Small Angle X-ray Scattering (SAXS).** *Nature.* 2009; 20;6(8):606.
23. Putnam CD, Hammel M, Hura GL, Tainer JA. **X-ray Solution Scattering (SAXS) Combined with Crystallography and Computation: Defining Accurate Macromolecular Structures, Conformations and Assemblies in Solution**. *Quarterly reviews of biophysics*. 2007; 40(3):191-285.
24. **Scatter Java-Based SAXS Analysis Tool**. https://bl1231.als.lbl.gov/scatter/
25. Yin C, Khan JA, Swapna GV, Ertekin A, Krug RM, Tong L, Montelione GT. **Conserved Surface Features Form the Double-Stranded RNA Binding Site of Non-Structural Protein 1 (NS1) From Influenza A and B Viruses**. *Journal of Biological Chemistry*. 2007; 282(28):20584-92.
26. Cheng A, Wong SM, Yuan YA. **Structural Basis for dsRNA Recognition by NS1 Protein of Influenza A Virus**. *Cell*. 2009; 19(2):187.
27. Vorobiev, S.M., Ma, L.-C., Montelione, G.T. **Crystal Structure of the 16-mer doublestranded RNA. Northeast Structural Genomics Consortium (NESG) Target RNA1.** PDB: 5KVJ. 2016.
28. Delaglio F, Grzesiek S, Vuister GW, Zhu G, Pfeifer J, Bax AD. **NMRPipe: A Multidimensional Spectral Processing System Based on UNIX Pipes**. *biomolecular NMR*. 1995; 6(3):277-93.
29. T. D. Goddard and D. G. Kneller, **SPARKY 3**, University of California, San Francisco
30. **Summary of the 2017-2018 Influenza Seasonal [Internet].** CDC. 2018. [cited 24 December 2018]. Available from: https://www.cdc.gov/flu/about/season/flu-season-2017-2018.htm.
31. Nagaswamy U, Gao X, Martinis SA, Fox GE**. NMR Structure of a Ribosomal RNA Hairpin Containing a Conserved CUCAA Pentaloop.** *Nucleic acids*. 2001. 15;29(24):5129-39.
32. Krug RM, Aramini JM. **Emerging Antiviral Targets for Influenza A Virus.** *pharmacological sciences*. 2009; 30(6):269-77.
33. Levene R, Gaglia M. **Host Shutoff in Influenza A Virus: Many Means to an End.** *Viruses.* 2018; 10(9):475.
34. Krug RM. **Functions of the Influenza A Virus NS1 Protein in Antiviral Defense.** *virology*. 2015; 12:1-6.
35. Schneider J, Wolff T. **Nuclear Functions of the Influenza A and B Viruses NS1 Proteins: Do They Play a Role in Viral mRNA Export?.** *Vaccine*. 2009; 27(45):6312-6.
36. Yin C, Khan JA, Swapna GV, Ertekin A, Krug RM, Tong L, Montelione GT. **Conserved Surface Features Form the Double-Stranded RNA Binding Site of Non-Structural**

Protein 1 (NS1) From Influenza A and B Viruses. *Biological Chemistry*. 2007; 282(28):20584-92.
37. Cheng A, Wong SM, Yuan YA. **Structural Basis for dsRNA Recognition by NS1 Protein of Influenza A Virus.** Cell research. 2009; (2):187.
38. Bornholdt ZA, Prasad BV. **X-ray Structure of NS1 From a Highly Pathogenic H5N1 Influenza Virus.** *Nature*. 2008; 456(7224):985.
39. Amano R, Aoki K, Miyakawa S, Nakamura Y, Kozu T, Kawai G, Sakamoto T. **NMR Monitoring of the SELEX Process to Confirm Enrichment of Structured RNA.** *Scientific*. 2017; 7(1):283.
40. Yadav DK, Lukavsky PJ. **NMR Solution Structure Determination of Large RNA-Protein Complexes.** *Progress in nuclear magnetic resonance spectroscopy*. 2016; 97:57-81.
41. Stefl R, Oberstrass FC, Hood JL, Jourdan M, Zimmermann M, Skrisovska L, Maris C, Peng L, Hofr C, Emeson RB, Allain FH. **The Solution Structure of the ADAR2 dsRBM-RNA Complex Reveals a Sequence-Specific Readout of the Minor Groove.** *Cell.* 2010; 143(2):225-37.
42. Turner DH (ed), Mathews DH (ed). **RNA Structural Determination.** New York NY: Springer Nature; 2016.
43. Rambo RP, Tainer JA. **Accurate Assessment of Mass, Models and Resolution by Small-Angle Scattering.** *Nature*. 2013; 496(7446):477.
44. Hannoush RN, Damha MJ. **Remarkable Stability of Hairpins Containing 2 ‘, 5 ‘-Linked RNA Loops.** *American Chemical Society*. 2001; 123(49):12368-74.
45. Wüthrich K. **Protein Structure Determination in Solution by NMR Spectroscopy.** *Biological Chemistry.* 1990; 265(36):22059-62.
46. Belorusova AY, Osz J, Petoukhov MV, Peluso-Iltis C, Kieffer B, Svergun DI, Rochel N. **Solution Behavior of the Intrinsically Disordered N-Terminal Domain of Retinoid X Receptor α in the Context of the Full-Length Protein.** *Biochemistry*. 2016; 15;55(12):1741-8.
47. Boldon L, Laliberte F, Liu L. **Review of the Fundamental Theories Behind Small Angle X-Ray Scattering, Molecular Dynamics Simulations, and Relevant Integrated Application.** *Nano.* 2015; 6(1):25661.
48. Liu G, Park HS, Pyo HM, Liu Q, Zhou Y. **Influenza A Virus Panhandle Structure is Directly Involved in RIG-I Activation and IFN Induction.** *Journal of virology*. 2015 25:JVI-00232.
49. **Types of Influenza Viruses [Internet].** CDC. 2018. [cited 20 March 2019]. Available from: https://www.cdc.gov/flu/about/viruses/types.htm
50. **Influenza (flu) Past Pandemics [Internet].** CDC. 2018. [cited 20 March 2019]. Available from: https://www.cdc.gov/flu/pandemic-resources/basics/past-pandemics.html
51. **Influenza (flu) 1918 Pandemic [Internet].** CDC. 2018. [cited 20 March 2019]. Available from: https://www.cdc.gov/flu/pandemic-resources/1918-pandemic-h1n1.html
52. Krug R.M. (ed), Alonso-Caplen,F.V., Julkunen,I. Katze,M. **The Influenza Viruses.** *Chapter: Expression and replication of the influenza virus genome.* New York, NY, pp. 89–152.. Plenum Press, 1989.
53. Young CL, Britton ZT, Robinson AS. **Recombinant protein expression and purification: a comprehensive review of affinity tags and microbial applications.** *Biotechnology*. 2012; 7(5):620-34.
54. Voet D, Voet JG. **Biochemistry, 4-th Edition**. NewYork: John Wiley & SonsInc. 2011
55. **Nucleic Acid Quantitation: Sample Purity (260/280 : 260/230 Ratios) [Internet].** Wikipedia. 2019. [cited 04 April 2019]. Available from: https://en.wikipedia.org/wiki/Nucleic_acid_quantitation#cite_note-6
56. **An introduction to Extinction Coefficients and Molecular Weights of Oligonucleotides [Internet]**. Ngo J. Trilink. 2019 (cited 04 April 2019). www.trilinkbiotech.com/tech/extinction_intro.asp

57. N.R. Krishna (ed), L.J. Berliner (ed), Montelione, G.T., Rios, C.B., Swapna, G.V.T., Zimmerman, D.E. **NMR pulse sequences and computational approaches for automated analysis of sequence-specific backbone resonance assignments of proteins.** *Biological magnetic resonance***.** New York, NY volume 17, pp, 81–130. Kluwer Academic/Plenum. 1999.
58. Li, Y.-C. Montelione, G.T. **Solvent saturation-transfer effects in pulsed-field-gradient heteronuclear single-quantum-coherence (PFGHSQC) spectra of polypeptides and proteins**. *Magnetic Resonance*. 1993. 101: 315–319.
59. Case D.A., Ben-Shalom I.Y., Brozell S.R., Cerutti D.S., Cheatham, III T.E., . Cruzeiro V.W.D, Darden T.A., Duke R.E., Ghoreishi D., Gilson M.K., Gohlke H., Goetz A.W., Greene D., Harris R, Homeyer N., Izadi S., Kovalenko A., Kurtzman T., Lee T.S., LeGrand S., Li P., Lin C., Liu J., Luchko T., Luo R., Mermelstein D.J., Merz K.M., Miao Y., Monard G., Nguyen C., Nguyen H., Omelyan I., Onufriev A., Pan F., Qi R., Roe D.R., Roitberg A., Sagui C., Schott-Verdugo S., Shen J., Simmerling C.L., Smith J., Salomon-Ferrer R., Swails J., Walker R.C., Wang J., Wei H., Wolf R.M., Wu X., Xiao L., York D.M. Kollman P.A. **AMBER 2014**, 2014, University of California, San Francisco.